The Thesis Committee for Jenna Kromann
Certifies that this is the approved version of the following thesis:

Surface Water Recharge in Karst:
Edwards-Trinity Aquifers-Nueces River System

APPROVED BY

SUPERVISING COMMITTEE:

Supervisor:

John M. Sharp Jr., Supervisor

Marcus O. Gary, Co-Supervisor

Joel P. Johnson

Surface Water Recharge in Karst:

Edwards-Trinity Aquifers-Nueces River System

by

Jenna Kromann, B.S.

Thesis

Presented to the Faculty of the Graduate School of

The University of Texas at Austin

in Partial Fulfillment

of the Requirements

for the Degree of

Master of Science in Geological Sciences

The University of Texas at Austin

May 2015

Dedication

To my family and friends

“Be the change you wish to see in the world” ~Mahatma Gandhi

Acknowledgements

Thanks to everyone, professors, family, and friends, who provided support in completing my thesis, I would not have been able to do it without you. Special thanks to my family, I could not have done this without your endless support and love: Mary Parsons, Gary Kromann, and Laura Kromann. Thank you for your edits, comments, support, and feedback, this research would not be the same without your guidance: Jack Sharp, Marcus Gary and Joel Johnson. I would also like to thank the landowners and ranchers who allowed me to have access to their property, which was invaluable in being able to collect data: Ron Sprouse, Willie Edwards, Bill Luce, Archie, Sky Lewey, and John Rogers. A special thanks to Scott Osborne and Patricia Bobeck for their help with my data collection and thesis writing.

I would never have been interested in hydrogeology if it was not for my science teacher and science fair advocate, Jill Harding. Thank you for helping me find what I am passionate about. Thank you to the Barton Springs Edwards Aquifer Conservation District for comprehensive training in hydrogeology and mentoring by Brian Hunt and Brian Smith. It was such a privilege to work, train, and learn from all of you.

This research would not have been completed without the financial support from the: Edwards Aquifer Authority, National Science Foundation, Geological Society of America, University of Texas at Austin-Jackson School of Geosciences and the Nueces River Authority.

Abstract

Surface Water Recharge in Karst:

Edwards-Trinity Aquifers-Nueces River System

by

Jenna Kromann, M.S.Geo.Sci.

The University of Texas at Austin, 2015

Supervisor: John M. Sharp Jr. and Marcus O. Gary

The karstic Edwards Aquifer is a primary source of water in south-central Texas for domestic, agriculture, and industrial uses. Significant recharge into the aquifer occurs as surface water streams, including the Nueces River, cross the Recharge Zone (RZ). Recharge models use data from two stream gauges, located above and below the RZ. These gauges are used to compute recharge into the aquifer; this may underestimate recharge volume because the actual water balance is complex. Synoptic gain/loss studies show that: flow rates change significantly as the river passes through extensive unconsolidated alluvium, gain/loss in reaches varies temporally, and recharge may be occurring in the Contributing Zone (CZ). From these synoptic studies, a 10-km reach of the Nueces River near Montell, TX, was identified that loses 100% of flow over the CZ during low stream flows. In this study reach, Candelaria Creek runs parallel to the dry segment of the Nueces River for 2.5 km; the creek contributes 52-64% of flow measured at the USGS recharge index gauge. The main sources of flow to the creek are two springs, hypothesized as possibly being sourced from: underflow from the Nueces River,

a combination of Trinity Aquifer groundwater and river underflow, or solely groundwater from the Trinity Aquifer. To investigate recharge in the CZ and the source water for springs that contribute flow to Candelaria Creek, a variety of methods were used including: hydrograph and gain/loss analyses, potential evapotranspiration calculations, and interpretation of specific conductance, temperature, chemical, isotopic, and near surface geophysical data. The data suggest that the springs are likely sourced from both Nueces River underflow and Trinity Aquifer groundwater. Defining the source of the springs that contribute to Candelaria Creek is important to understand the complex water balance in the Nueces River and the role of underflow/storage in this system. It was found that underflow was a significant source of spring flow, but could not account for the total amount of spring flow; this suggests the Trinity Aquifer also contributes flow to the springs. A water balance estimates that recharge in the CZ at 6,213,048-9,814,814 m^3 per year, which is between 0.9 to 2% of total recharge to the Edwards Aquifer and 4 to 11% of Nueces Basin recharge may be unaccounted for over the CZ during low hydrologic flow conditions. This water balance suggests that there is significant recharge occurring over the CZ and some recharge may be unaccounted for based on the current method used to calculate recharge.

Table of Contents

Dedication iv

Acknowledgements v

Abstract v

Table of Contents viii

List of Tables xi

List of Figures xii

INDEX OF TERMS XVIII

1. INTRODUCTION AND BACKGROUND 1

Introduction 1

Previous Work 11

Background 13

Hydrologic Setting 13

Geologic Setting 15

Site Description 18

Problem Statement 18

Ch. 1 Figures 21

2. METHODS OF INVESTIGATION 33

Methods 33

Sites Monitored 33

Geologic Mapping 37

Flow Gain/Loss Study 37

Streamflow Hydrographs 38

Evapotranspiration and Weather Stations 39

Specific Conductance Measurements 43
Temperature Measurements 44
Chemical Analysis 44
Near Surface Geophysical Methods 47
Volumetric Flow Calculations and Hydrograph Analysis 49
Water Balance Calculations 51
Flow Calculation 53

Ch. 2 Figures 56

3. RESULTS AND DISSCUSSION 59

Results 59
Flow Gain/Loss Studies 59
Evapotranspiration Results 60
Specific conductance Results 61
Temperature Results 67
Chemical Results 68
Near Surface Geophysical Results 70
Flow Studies/Volume Calculations Results 70
Water Balance Calculation Results 73
Flow Calculation Results 74
Comparison of Recharge Estimates 77

Discussion 80
Recharge is Occurring in the EACZ 80
Candelaria Springs Is Sourced From The Nueces River and Trinity Aquifer 82

Ch. 3 Figures 86

4. CONCLUSIONS 118

A. APPENDIX: ENDANGERED SPECIES 121

A.1. List of endangered & threatened Species covered by EAA-HCP.......121

B. APPENDIX: GAIN/LOSS STUDY **122**

C. APPENDIX: STRATIGRAPHY OF UVALDE COUNTY **124**

D. APPENDIX: METHODOLOGIES USED **125**

E. APPENDIX: TEMPERATURE AND RAIN **130**

Tidbit Probes 132

Comparison of Hobo Temperature To Tidbit 141

Hobo probes 142

F. APPENDIX: THERMAL INFRARED **144**

G. APPENDIX: GEOPHYSICAL STUDIES: EM **147**

H. APPENDIX: ET **156**

I. WATER CHEMISTRY **171**

J. HYDROGRAPHS **173**

NUE010 174

CAN012 177

Laguna 180

CR414 183

REFERENCES **184**

List of Tables

Table 1.1. Estimated mean annual recharge from 1934-2013 and total recharge for 2013 (a dry year) in river basins crossing the San Antonio Segment of the Edwards Aquifer and percentage of total recharge (EAA, 2013). 4
Table 1.2. Estimated mean annual recharge from 1934-2007 and total recharge for 2007 (a wet year) in river basins crossing the San Antonio Segment of the Edwards Aquifer and percentage of total recharge (EAA, 2007). 5
Table 1.3. Estimated mean annual recharge from 1934-2014 and total recharge for 2014 (a dry year) in river basins crossing the San Antonio Segment of the Edwards Aquifer and percentage of total recharge (EAA, 2014). 6
Table 1.4. General hydrostratigraphy of the study area. Hydraulic conductivity and effective porosity values estimated from (1) Green, 2004; (2) Freeze and Cherry, 1979; (3) Clark, 2003. The composition was estimated based on observed crossection and soil investigation. 17
Table 2.1. Sites monitored on the Nueces River and Candelaria Creek 36
Table 2.2. Average leaf porometer readings gathered with a Decagon SC-1 Leaf Porometer 42
Table 3.1 Specific conductance statistics from four different sites in the Nueces River and springs feeding Candelaria Creek at various high and low flow conditions over the period of record most from June 2013 to January 2015. 65
Table 3.2. Time lag associated with peak flow or peak precipitation events and lower specific conductance values. 66
Table 3.3. Hydraulic conductivity values calculated with flow calculation methods for different sites along the Nueces River and for springs that feed Candelaria Creek. These were estimated from NUE010 to the site found in the column “Site Name”. See Table 1.4 for a comparison of hydraulic conductivity values from literature and estimated effective porosity of different geologic units in the area. 76
Table 3.4. Table showing the average recharge estimates calculated in three different ways and the percentage of total recharge and recharge in the Nueces River Basin.. 79
Table C.1. Stratigraphy of Uvalde county modeled after Clark, 2003 124
Table D.1. Instrumentation used at various sites in performing the research for this thesis. 125
Table H.1. Monthly estimated PET values, converted to mm/day to compare PET values estimated on the Nueces River to values from Texas A&M Agrilife Extension and TWDB in Quad 808 (Texas A&M AgriLife Extension, 2013 and TWDB, 2013)... 156

List of Figures

Figure 1.1. Spatially divided segments of the Edwards Aquifer, the Recharge Zone is green Contributing Zone is pink. 21
Figure 1.2. Two USGS gauges (USGS Laguna and USGS Below Uvalde) used to calculate recharge over the Recharge Zone of the Edwards Aquifer. Permanent gauge locations and synoptic locations used in this study are shown as well. 22
Figure 1.3. Location of Trinity Aquifer in Texas outlined in green (TWDB, 2015a). 23
Figure 1.4. Gain/Loss study conducted in January 2012 on the Nueces River over the EACZ and EARZ (EAA and University of Texas at Austin). 24
Figure 1.5. Gain/Loss study conducted in March 2013 on the Nueces River over the EACZ and EARZ (EAA). 25
Figure 1.6. Gain/Loss study conducted in March 2014 on the Nueces River over the EACZ and EARZ (EAA). 26
Figure 1.7. The area of study for this thesis near Montell, Texas including Candelaria Creek and part of the Nueces River outlined in the black box. 27
Figure 1.8. Conceptual model of geology near the Nueces River (terrace, gravel deposits, and bedrock). 28
Figure 1.9. Geology near the Nueces River from NUE010 to CR414 modified from Geologic Atlas of Texas (TWDB, 2015b; TNRIS, 2014). 29
Figure 1.10. Location of cross sections see Figure 1.11 for detailed cross sections. Geology modified from Geologic Atlas of Texas (TWDB, 2015b; TNRIS, 2014) ... 30
Figure 1.11. Conceptual cross sections from NUE010 to CR 414 depicting terrace, bedrock, and alluvial deposits 31
Figure 1.12. Conceptual Model of the water balance in the Nueces River over the Contributing Zone 32
Figure 2.1. Spring and gauge site locations near Candelaria Creek and the Nueces River used as part of this study. 56
Figure 2.2. Rating Curve NUE010, equation and R^2 value seen in graph. Flood flow in the Nueces River near NUE010 was estimated using indirect measurement techniques (see red triangle). 57
Figure 2.3. Rating Curve CAN012, equation and R^2 value seen in graph. 58
Figure 3.1. Gain/loss study of Candelaria Creek in May 2014, red segments are losing streams and blue segments are gaining streams. The black dots are the gauging locations. Flow is in cfs and the amount of gain (green) or loss (red) is also in cfs... 86
Figure 3.2. Shows the average potential evapotranspiration from the Nueces River near Durnell and NUE010. The fifteen minute data is displayed in green, daily average in purple, and monthly PET from the TWDB for the Uvalde area is displayed with red dots (TWDB, 2013). The black inset box shows where the green and purple PET values were collected at ET 1 Weather Station and the red dots were collected from the larger area cross-hatched in red. 87

Figure 3.3. Specific conductance measured in the Nueces River near NUE010 and the springs that contribute to Candelaria Creek noted in the graph as orange, green, red, and purple lines. The blue line is flow from CAN012 in the top graph and NUE010 in the bottom graph. The red boxes outline times of high flow. 88
Figure 3.4. Specific conductance measured in the Nueces River near NUE010 and springs that contribute to Candelaria Creek noted in the graph as orange, green, red, and purple lines. The blue line is rain near NUE010 in the upper plot and the lower plot shows specific conductance. The red boxes outlines times of high flow. 89
Figure 3.5. Candelaria Springs specific conductance shown with precipitation and flow (blue lines). The red box outlines an event of large precipitation and high flow. More detail on the time periods are shown in the lower two boxes. 90
Figure 3.6. Candelaria Headwater Springs A specific conductance shown with precipitation and flow (blue lines). The red box outlines an event of large precipitation and high flow. More detail on the time periods are shown in the lower two boxes. 91
Figure 3.7. Candelaria Headwater Springs B specific conductance shown with precipitation and flow (blue lines). The red box outlines an event of large precipitation and high flow. These time periods are shown in the lower two boxes in more detail. 92
Figure 3.8. Nueces River near NUE010 specific conductance shown with precipitation and flow (blue lines). The red box outlines an event of large precipitation and high flow. More detail on the time periods are shown in the lower two boxes. 93
Figure 3.9. The graph shows the response of the Nueces River and springs that contribute flow to Candelaria Creek during a large precipitation event in May 2014 (blue line). This shows the propagation of a flood in this system and associated time lag from upstream to downstream (top to bottom). 94
Figure 3.10. The graph shows the response of the Nueces River and springs that contribute flow to Candelaria Creek during a large flow event in May 2014 (blue line). This shows the propagation of a flood in this system and associated time lag from upstream to downstream (top to bottom). 95
Figure 3.11. Synoptic specific conductance in April 2014. Low specific conductance signature is green, mid-level specific conductance is orange, and high specific conductance signature is red. 96
Figure 3.12. Synoptic specific conductance in May 2014. Low specific conductance signature is green, mid-level specific conductance is orange, and high specific conductance signature is red. 97
Figure 3.13. Synoptic specific conductance in August 2013. Low specific conductance signature is green, mid-level specific conductance is orange, and high specific conductance signature is red. 98
Figure 3.14. Temperature response to precipitation (blue lines) recorded in the springs that contribute flow to Candelaria Creek and the Nueces River near NUE010 (red, green, purple, and orange lines). 99

Figure 3.15. Piper diagrams of general water chemistry collected in June and July 2013 and July 2014 of springs, surface water, and wells... 100
Figure 3.16. Oxygen isotopic chemistry for surface water, wells, and springs collected in July 2014. The inset hydrographs show flow conditions at CAN012 and NUE010 at the sampling time. The black line is the local meteoritic water line from Pape, 2010. The red box denotes where the majority of samples fall. 101
Figure 3.17. Shows the range of isotopic signatures for different source waters groundwater springs, groundwater wells, and surface water sources for samples collected in July 2014. The red box shows that the main springs that feed Candelaria Creek are very similar to the surface water sources. The Edwards and Trinity groundwater are significantly different from the general Sr isotopic signature. 102
Figure 3.18. Range of Sr isotopic signatures compared to Edwards Aquifer Springs, Rocks, and Trinity Aquifer Rocks (BSEACD, 2011; Musgrove, 2010; Musgrove and Banner, 2004; Oetting, 1996; Christian et al., 2010; Wong, 2012; Koepnick, 1995). The red box highlights where the Nueces River Basin samples fall........................ 103
Figure 3.19. Strontium isotopic signature v. 1/Sr concentration. This shows that there are two end members: Trinity Groundwater and Edwards Groundwater. The black line is a linear regression showing a good correlation, which suggests that mixing between these two end members, is occurring. 104
Figure 3.20. Location of ER lines near Candelaria Creek, ER lines depicted as red lines, data were gathered in October 2014. 105
Figure 3.21. Interpreted Inverted Resistivity Sections near Candelaria Creek using the dipole-dipole array. Black dashed lines represent different contacts. 106
Figure 3.22. ER Line 1 Inverted Resistivity Section shown with an outcrop near where ER Line 1 data was collected, this shows the method used to ground truth the data. 107
Figure 3.23. Volumetric amount of water moving through the system during high flow conditions noted as ΔV. The hydrographs on the right side of the figure illustrate how the amount of loss (ΔV) is found, as the area under the rising and falling limb (time is not necessarily aligned for each graph, but each graph covers the same time period). For more detailed hydrographs see Appendix J... 108
Figure 3.24. Hydrographs from left to right (upstream to downstream) shows response of flow (blue lines) to precipitation events (red lines). 109
Figure 3.25. Hydrographs from the Nueces River from NUE010 to Laguna. CR414, the purple line, is typically 0 but has increased flow during precipitation or high-flow events. The red boxes outline high flow events. 110
Figure 3.26. More detailed hydrographs of flood events and how they propagate through the system. The red boxes highlight the order of peak flow in the system. (Sometimes there is no peak flow at certain gauges). 111
Figure 3.27. More detailed hydrographs of flood events and how they propagate through the system. The red boxes highlight the order of peak flow in the system. (Sometimes there is no peak flow at certain gauges). 112

Figure 3.28. Location and intensity of precipitation shown with NexRad data obtained from the EAA in the storm on May 2013. Rain is daily total in inches. The areas that had the most rain are red and the areas with little to no precipitation are blue. 113
Figure 3.29. Location and intensity of precipitation shown with NexRad data obtained from the EAA in the storm on May 2014. Rain is daily total in inches. The areas that had the most rain are red and the areas with little to no precipitation are blue. 114
Figure 3.30. Location and intensity of precipitation shown with NexRad data obtained from the EAA in the storm on September 2014. Rain is daily total in inches. The areas that had the most rain are red and the areas with little to no precipitation are blue... 115
Figure 3.31. Water balance of the Nueces River system in the area of study includes the main outflows and inflows in this system on a daily basis. Note volumes are estimated daily averages in ac-ft and cfs in parentheses. The annual amount of recharge is outlined in the red box. 116
Figure 3.32. This figure shows the location of Candelaria Springs, Candelaria Headwater Springs, and a conceptual model of the springs and their location relative to the Nueces River. 117
Figure B.1. The gain/loss study conducted in 2014 was the most comprehensive gain loss study. Gains are in blue, loss in red. Also shown are the locations of springs known or found in the area. There is some correlation between the location of springs and gaining streams. In general there is likely a spring source in the gaining segment of the river or some source of underflow. 123
Figure E.1. Temperature response to rain at springs that feed Candelaria Creek and at the Nueces River, temperature measurements gathered with Hobo probes displayed as red lines and rain data from PET 1 displayed as blue lines. 131
Figure E.2. Temperature in green at NUE040 compared to precipitation events in blue from ET 1. 133
Figure E.3. Temperature in green at NUE020 compared to precipitation events in blue from PET 1.. 134
Figure E.4. Temperature in green on the Nueces River near Durnell compared to precipitation events in blue from PET 1 135
Figure E.5. . Temperature in green on the Nueces River near Candelaria Springs compared to precipitation events in blue from PET 1. 136
Figure E.6. Temperature in green in Durnell Pool near Durnell Springs compared to precipitation events in blue from PET 1. 137
Figure E.7 . Temperature in green in Candelaria Creek near Candelaria Springs compared to precipitation events in blue from PET 1. 138
Figure E.8 . Temperature in green on the Nueces River near Archies Spring compared to precipitation events in blue from PET 1. 139
Figure E.9. Temperature in green at Candelaria Headwater Springs B compared to precipitation events in blue from PET 1. 140

Figure E.10 . Two different Tiddbit probes were used at each site; the figure shows a comparison of the different probes at NUE040. This comparison was completed for each site to make sure the temperature readings were accurate............................... 141
Figure E.11. Temperature data collected for Bird Springs (red) a spring over the EARZ. The blue is precipitation from PET 1... 142
Figure E.12. Temperature data collected for Durnell Springs (red) near NUE010 and Durnell Pool. The blue is precipitation data from PET 1. 143
Figure F.1. Locations of thermal infrared shot near Nueces River by NUE010, numbers correspond to sites where thermal infrared images were taken. See Figure F.2 for thermal infrared images. 145
Figure F.2. Thermal infrared images, numbers correspond to the figure above showing the location of the image... 146
Figure G.1. Results from EM 34 spaced 40 m measured in the vertical orientation. These measurements were gathered along ER lines near Candelaria Creek and the Nueces River. Colored points shown represent the range of conductivity in the subsurface.148
Figure G.2. Results from EM 34 spaced 40 m measured in the horizontal orientation. These measurements were gathered along ER lines near Candelaria Creek and the Nueces River. Colored points shown represent the range of conductivity in the subsurface. 149
Figure G.3. Results from EM 34 spaced 20 m measured in the vertical orientation. These measurements were gathered along ER lines near Candelaria Creek and the Nueces River. Colored points shown represent the range of conductivity in the subsurface.150
Figure G.4. Results from EM 34 spaced 20 m measured in the horizontal orientation. These measurements were gathered along ER lines near Candelaria Creek and the Nueces River. Colored points shown represent the range of conductivity in the subsurface. 151
Figure G.5. Results from EM 34 spaced 10 m measured in the vertical orientation. These measurements were gathered along ER lines near Candelaria Creek and the Nueces River. Colored points shown represent the range of conductivity in the subsurface.152
Figure G.6. Results from EM 34 spaced 10 m measured in the horizontal orientation. These measurements were gathered along ER lines near Candelaria Creek and the Nueces River. Colored points shown represent the range of conductivity in the subsurface. 153
Figure G.7. Results from EM 31 gathered in the horizontal orientation near Candelaria Creek and the Nueces River. Colored points shown represent the range of conductivity in the subsurface. 154
Figure G.8. Results from EM 31 gathered in the vertical orientation near Candelaria Creek and the Nueces River. Colored points shown represent the range of conductivity in the subsurface. 155
Figure H.1. Comparison of PET values for two different PET stations near the Nueces River , 15 minute in green and daily averaged values in red................................... 157
Figure H.2. PET and flow at NUE010 in the fall... 159

Figure H.3. PET and flow at NUE010 in the late fall. 160
Figure H.4. PET and flow at NUE010 in the winter. 161
Figure H.5. PET and flow at NUE010 in the spring. 162
Figure H.6. PET and flow at NUE010 in the spring during a shorter time period. 163
Figure H.7. PET and flow at NUE010 in the summer. 164
Figure H.8. PET and flow at CAN012 in the late fall.. 165
Figure H.9. PET and flow at CAN012 in the early fall. 166
Figure H.10. PET and flow at CAN012 in the winter. 167
Figure H.11. PET and flow at CAN012 in the spring.. 168
Figure H.12. PET and flow at CAN012 in the spring during a shorter time period. 169
Figure H.13. PET and flow at CAN012 in the summer. 170
Figure I.1. Schoeller Diagram for general chemistry of samples collected in July 2014. The springs are in blue, the surface water sources are in red, and the groundwater sources are in green. This diagram shows sulfate, magnesium and Na+K vary the most at each site. 172
Figure J.1. Flow at NUE010 in blue and daily mean flow values in red. 174
Figure J.2. The top graph shows 15 minute flow data for NUE010, the middle graph shows the daily average flow, and the bottom graph shows the difference from the mean (15 minute flow data subtracted from the daily average flow). These graphs display the amplitude of cyclic fluctuations. 175
Figure J.3. Peridogram analysis results for NUE010. The peak shows a daily reoccurrence in cyclic fluctuations at NUE010. 176
Figure J.4. Flow at CAN012 in blue and daily mean flow values in red. 177
Figure J.5. The top graph shows 15 minute flow data for CAN012, the middle graph shows the daily average flow, and the bottom graph shows the difference from the mean (15 minute flow data subtracted from the daily average flow). These graphs display the amplitude of cyclic fluctuations. 178
Figure J.6. Peridogram analysis performed for CAN012. This shows daily cyclic fluctuations... 179
Figure J.7. Flow at Laguna in blue and daily mean flow values in red. 180
Figure J.8. The top graph shows 15 minute flow data for Laguna, the middle graph shows the daily average flow, and the bottom graph shows the difference from the mean (15 minute flow data subtracted from the daily average flow). These graphs display the amplitude of cyclic fluctuations. 181
Figure J.9. Peridogram analysis results for Laguna gauge. The peak shows a daily reoccurrence in cyclic fluctuations at Laguna gauge. 182
Figure J.10. Flow at CR414 in blue and daily mean flow values in red. 183

INDEX OF TERMS

ac-ft.-acre feet

cfs-cubic feet per second

Contributing Zone (EACZ) - segment of the Edwards Aquifer classified by the EAA as an area where runoff flows directly into streams and surface water bodies.

EAA-Edwards Aquifer Authority

EAHCP-Edwards Aquifer Habit Conservation Plan

EPA-Environmental Protection Agency

ER-Electrical resistivity

EM-Electromagnetic

HSPF- Hydrologic Simulation Program-Fortran

Recharge Zone (EARZ)- segment of the aquifer classified by the EAA, where units of the Edwards Group at the surface and are faulted and karstified, allowing runoff and surface water bodies to recharge the Edwards Aquifer.

RMS-Average Root Mean Square Error

SAWS-San Antonio Water Systems

PET-Potential Evapotranspiration

TWDB-Texas Water Development Board

1. INTRODUCTION AND BACKGROUND

Introduction

Many investigations have been conducted on the relation between rivers and alluvial channel beds, including hyporheic exchange (Cardenas et al. 2008, 2009, 2012; Burkholder et al., 2008), but studies typically have not consider sites where alluvium overlies a karst aquifer. The complex interactions of these systems are important because 25 percent of the world's population relies on karst aquifers for their water supply (Ford and Williams, 2007). The Nueces River is characterized by extensive alluvial gravel deposits in the riverbed, Trinity and Edwards Group limestone beneath the riverbed and adjacent to the river channel, and terrace deposits along the banks. These three factors make the Nueces River an ideal site to study these interactions.

The Edwards Aquifer is composed of Cretaceous carbonate rocks, and is subdivided spatially into three segments: San Antonio, Barton Springs, and Northern segments (Figure 1.1). It is a major water source in central Texas, and one of the largest karst aquifers in the United States (Rose, 1972; McClay and Small, 1976). It covers an area of 108,779 km^2 (42,000 mi^2) and is heavily faulted/fractured due to activity along Balcones Fault Zone (Barker and Ardis, 1994; Jordan, 1977). The faulting and subsequent karstification (sinkholes, dolines, and fissures) provide pathways of discrete infiltration for recharge (Ford and Williams, 2007).

The San Antonio segment of the Edwards Aquifer is the focus of this study. Over two million people rely on this aquifer as their primary water source; many others use this water for irrigation and other agricultural uses. The water in the Edwards Aquifer available for municipal use is expected to decline between 2010 and 2060 with future predicted droughts and groundwater pumping being reduced in certain areas. The south-central Texas region will need more water in the future for agriculture and municipal use (TWDB, 2012). The aquifer is also the sole habitat for a number of federally-listed endangered species (EAA, 2015a; Appendix A). Discrete recharge occurring in rivers and creeks is an important component of flow to Comal and San Marcos Springs. These two springs have endangered species that are protected under the Edwards Aquifer Habit Conservation Plan (EAHCP). The EAHCP includes different protection measures, such as: habitat restoration, pumping limitations, and flow protection measures (EAA, 2015a). Flow protection measures include: the Voluntary Irrigation Suspension Program Option, the Regional Water Conservation Program, the Stage V Critical Management Period, and the use of San Antonio Water System (SAWS) Aquifer Storage and Recovery. Flow protection measures are designed to ensure that there is adequate flow and a healthy habitat for endangered species in the springs.

Most recharge to the Edwards Aquifer occurs in a region (termed the Recharge Zone (EARZ) where rock units of the aquifer are exposed at the surface. The Edward Aquifer Authority (EAA) estimated mean annual recharge from the Nueces Basin to the Edwards Aquifer between: 1934 and 2014 at 152,335,007 m^3/yr. (123,500 acre-feet/yr.; dry year), 1934 and 2013 at 122,978,139 m^3/yr. (97,700 acre-feet/yr.; dry year), and 1934 and 2007 159,612,550 m^3/yr. (1,294,000 acre-feet/yr.; wet year) (Table 1.1, Table 1.2,

Table 1.3). The hydrologic conditions during 2013 and 2014 were dry and during 2007 very wet; these years were picked to show the variability in the amount of recharge under various hydrologic conditions (wet v. dry). This study also took place from 2013 to 2014 during dry conditions. The total recharge in the Nueces River Basin in 2013 was estimated at 83,506,720 m^3/yr. (67,700 ac-ft.) and 24,422,940 m^3/yr. (19,800 ac-ft.) in 2014 (EAA, 2013, EAA, 2014). This was estimated based on the USGS Puente method, which is the method used by the EAA to estimate annual recharge into the San Antonio segment of the Edwards Aquifer (Puente, 1978). This method uses a water balance to calculate direct recharge in the river, using the difference between streamflow above and below the Recharge Zone (Figure 1.2).

Table 1.1. Estimated mean annual recharge from 1934-2013 and total recharge for 2013 (a dry year) in river basins crossing the San Antonio Segment of the Edwards Aquifer and percentage of total recharge (EAA, 2013).

River Basins	**Estimated Mean Value for Period of Record (1934-2013) m^3 (ac-ft.)**	**Percentage of Total Recharge (%)**	**Total Recharge for 2013 m^3 (ac-ft.)**	**Percentage of Total Recharge (%)**
Nueces/West Nueces	153,938,533 (124,800)	18	83,506,720 (67,700)	37
Frio-Dry Frio	167,260,137 (135,600)	19	32,933,965 (26,700)	15
Sabinal River	50,819,452 (41,200)	5	616,741 (500)	1
Area between Sabinal River and Medina River	135,066,261 (109,500)	16	3,453,749 (2,800)	3
Medina River	76,352,526 (61,900)	8	13,321,604 (10,800)	6
Area between Medina River and Cibolo Creek/Dry Comal	86,713,773 (70,300)	10	4,070,490 (3,300)	2
Cibolo Creek and Dry Comal Creek	585,163,784 (109,300)	18	585,163,784 (28,700)	14
Blanco River	57,480,254 (46,600)	6	51,929,585 (42,100)	22
Total recharge for all surface water basins	862,697,197 (699,400)		225,233,784 (182,600)	

Table 1.2. Estimated mean annual recharge from 1934-2007 and total recharge for 2007 (a wet year) in river basins crossing the San Antonio Segment of the Edwards Aquifer and percentage of total recharge (EAA, 2007).

River Basins	Estimated Mean Value for Period of Record (1934-2007) m^3 (ac-ft.)	Percentage of Total Recharge (%)	Total Recharge for 2007 m^3 (ac-ft.)	Percentage of Total Recharge (%)
Nueces/West Nueces	159,612,550 (129,400)	18	581,956,731 (471,800)	22
Frio-Dry Frio	175,771,162 (142,500)	21	585,163,784 (474,400)	22
Sabinal River	54,149,853 (43,900)	6	128,282,111 (104,000)	5
Area between Sabinal River and Medina River	142,343,804 (115,400)	12	501,287,019 (406,400)	19
Medina River	78,202,749 (63,400)	10	92,757,834 (75,200)	3
Area between Medina River and Cibolo/Dry Comal Creek	92,017,745 (74,600)	10	280,740,466 (227,600)	11
Cibolo Creek and Dry Comal Creek	585,163,784 (114,400)	17	585,163,784 (306,100)	14
Blanco River	58,590,387 (47,500)	6	119,524,390 (96,900	4
Total recharge for all surface water basins	901,921,920 (731,200)		2,667,157,777 (2,162,300)	

Table 1.3. Estimated mean annual recharge from 1934-2014 and total recharge for 2014 (a dry year) in river basins crossing the San Antonio Segment of the Edwards Aquifer and percentage of total recharge (EAA, 2014).

River Basins	Estimated Mean Value for Period of Record (1934-2014) m^3 (ac-ft.)	Percentage of Total Recharge (%)	Total Recharge for 2014 m^3 (ac-ft.)	Percentage of Total Recharge (%)
Nueces/West Nueces	152,335,007 (123,500)	18	24,422,940 (19,800)	18
Frio-Dry Frio	165,656,611 (134,300)	19	40,458,204 (32,800)	31
Sabinal River	50,326,059 (40,800)	5	6,044,061 (4,900)	3
Area between Sabinal River and Medina River	133,709,431 (108,400)	16	17,762,138 (14,400)	5
Medina River	75,612,437 (61,300)	8	10,977,988 (8,900)	10
Area between Medina River Basin and Cibolo-Dry Comal Creek	85,726,988 (69,500)	10	493,393 (400)	2
Cibolo Creek and Dry Comal Creek	585,163,784 (108,000)	18	585,163,784 (9,500)	15
Blanco River	57,110,209 (46,300)	6	20,352,450 (16,500)	16
Total recharge for all surface water basins	855,049,610 (693,200)		132,229,253 (107,200)	

This calculation is completed for nine of the basins that cross the Edwards Aquifer on monthly time scales (Puente, 1978). The Puente method uses the equation below:

Error! Bookmark not defined.

$$R = (Q_U + SI - Q_L) \qquad \textbf{(1-1)}$$

Where:

R= the monthly recharge [L^3]; Q_U=the volume of flow at the upper gauge [L^3/t]; SI=the estimated volume of runoff (including infiltration) resulting from precipitation in the intervening area [L^3-t]; and Q_L=the volume of flow at the lower gauge [L^3/t]

Equation 1-2 is used to estimate recharge in the Nueces-West Nueces River basin:

$$R_{nwn} = (Q_n + Q_{wn} + (SI_n)(RF_n - Q_{nbu}) \qquad \textbf{(1-2)}$$

Where:

R_{nwn}=the monthly recharge to the aquifer in the basin [L^3]; Q_n=the total monthly flow at the gauging station Nueces River at Laguna [L^3/t]; Q_{wn}=the total monthly flow at the gauging station West Nueces River near Brackettville [L^3/t]; SI_n=the estimated monthly runoff [L^3-t] in the area between the two upper gauges and the lower gauge; Q_{nbu}=the total monthly flow at the gauging station Nueces River below Uvalde [L^3/t] and RF_n=the rainfall ratio which is obtained by:

$$RF_n = \frac{LP}{UP} \qquad \textbf{(1-3)}$$

Where:

LP= average monthly precipitation in the area; UP=average monthly precipitation in the drainage area above the upper gauge (RF_n usually set to 0.8-1.2). Runoff is assumed to be proportional to the runoff in the drainage area above the Laguna gauge (Puente, 1978).

Another method used to estimate recharge for the Edwards Aquifer in the Nueces River basin is the Hydrologic Simulation Program-Fortran (HSPF), which was developed by a series of consulting companies (LBG-Guyton, HDR, and Clear Creek Solutions) to simulate the hydrologic cycle using rainfall and other meteorological records. The program can represent one or many river reaches; it can conduct frequency duration analysis from 1 minute to 1 day; and the simulation period can last for a few minutes to hundreds of years (USGS, 2014). HSPF requires meteorological data, watershed characteristics (land area), and channel size. It runs different application and utility models to simulate runoff and water quality from pervious and impervious areas, and to simulate the movement of runoff into stream channels and reservoirs. This is a two-dimensional model that can provide a more detailed way to calculate recharge than the Puente method.

Data gathered in this thesis can be used to improve recharge estimates as inputs to the HSPF model and the Puente method to estimate recharge. For example, the HSPF model could be refined with data gathered in this thesis using: climatic conditions (data from weather stations in Recharge and Contributing Zone, currently weather data is estimated with limited stations), stream flow/recharge (data from multiple gauges in the

Contributing Zone, currently there are limited streamflow gauges), alluvial cover (geologic maps created from field investigation and electrical resistivity data), spring flow (gauged data), and hydraulic conductivity (estimated in Water Balance). The calibration of the HSPF model can be improved with field-based data inputs, which were gathered as a part of this thesis, with improved model calibration recharge can be estimated more accurately. The methods used in this study can be applied to other surface water basins in the San Antonio segment of the Edwards Aquifer.

Data from this thesis will aid in determining if there are enough gauges present to estimate recharge accurately using the Puente Method. Currently, the Puente Method only uses one gauge below the Contributing Zone to estimate recharge (Figure 1.2). This gauge may not capture all of the flood flow and recharge over the Contributing Zone. Recharge from the Contributing Zone (Trinity Aquifer) could flow to the Edwards Aquifer through interformational flow. The Puente method was developed under the main assumption that all recharge to the Edwards Aquifer occurs as rivers cross the Recharge Zone, but this assumption may not be correct. This thesis tests that assumption and determines if recharge could be occurring over the Contributing Zone. The research described in this thesis provides improved recharge estimates and understanding of recharge from the Nueces River.

Streams crossing the EARZ are the primary source of recharge to the aquifer; water is lost through channel beds. Another source of recharge to the Edwards Aquifer is direct infiltration from precipitation. Flow rates in the Nueces River and streams near

Uvalde, Texas, decrease as the streams cross the EARZ; water lost in the rivers and streams recharges the Uvalde Pool of the Edwards Aquifer. Recharge from the Uvalde County area provides approximately 45 percent of total recharge in the Edwards Aquifer (Clark, 2003; Table 1.1, Table 1.2). Recharge estimates from other basins in the San Antonio segment of the Edwards are shown in Table 1.1 to Table 1.3 during dry and wet hydrologic conditions. These recharge values were estimated by the EAA and USGS using the Puente method.

Watersheds north of the Recharge Zone comprise the Contributing Zone (EACZ), which may also contribute to Edwards recharge. In the EARZ, spring-fed baseflow sustains most rivers; most springs in the area originate from the Trinity or Edwards Aquifers. Rivers or streams that originate in the EACZ flow to the Recharge Zone, where they provide the majority of Edwards recharge. Geologic units exposed at the surface in the EACZ are predominantly Upper Glen Rose (Trinity Group) Limestone. The Upper Glen Rose Limestone makes up the Upper Trinity Aquifer. The Trinity Aquifer spans through central Texas towards the northeastern part of the state (Figure 1.3). The Trinity Aquifer supplies water to numerous users in the Hill Country. The freshwater thickness ranges from 183 m (600 ft.) to 579 m. (1,900 ft.). Water in the Trinity Aquifer tends to be hard with total dissolved solids ranging from less than 1,000 up to 5,000 mg/L (TWDB, 2015a). The connection in recharge between the Trinity and Edwards aquifers has been investigated with multiple studies (e.g. Gary et al., 2011). Some studies found the Trinity Aquifer may contribute recharge to the Edwards Aquifer through interformational flow;

if the Trinity Aquifer is recharging the Edwards it could modify how the Trinity Aquifer is managed (TWDB, 2011; Jones et al., 2011; Johnson et al., 2010).

Recharge is a key input parameter for resource management in groundwater models of the Edwards Aquifer, but recharge via surface water streams can be difficult to quantify. Models that calculate recharge based on gauging station data may underestimate recharge because of the complexity of the actual water balance in the Nueces River (Figure 1.2 (see gauges); Puente, 1978; Gary et al., 2011; Green et al., 2009). This thesis improves recharge estimation by providing more data and knowledge of the recharge process over the EACZ.

Previous Work

Numerous rivers throughout the world and Untied States are similar to the Nueces River, in that they recharge underlying karst aquifers. In the Dinaric karst area of Bosnia and Herzegovina, the Trebisnjica River, Zalomka River, Neretva River, and Bregava River, all recharge underlying karst aquifers (Milanovic, 2004). Flow in these rivers is intermittent due to surface water loss through karst features. The Trebisnjica River is characterized by intermittent alluvial and bare rock deposits, similar to the Nueces River. The Peace River in Florida, USA is also similar to the Nueces River system. On the Peace River, Lewelling et al. (1998) conducted a diffuse recharge study to determine the hydrologic connection between groundwater and surface water in the river. Using seismic refraction and seepage investigations, they identified diffuse groundwater discharge and discrete features where recharge and discharge could occur.

A recent gain/loss study (Banta et al., 2012) conducted over the Nueces Basin by the USGS estimated the spatial dynamics of recharge in the basin. This study used gauging station data and synoptic measurements collected between 2008 and 2010 in the Upper Nueces Basin, upstream and downstream of the Edwards Aquifer Recharge Zone. This study identified gains and losses in the Upper Nueces Basin, both temporally and spatially. Although the study was a useful overall estimate of spatial recharge dynamics, the study used a limited number of gauging stations, conducted only three synoptic measurements, and did not quantify recharge to the Edwards Aquifer. Slade et al. (2002) conducted a broad study to investigate how many gain/loss studies had been conducted on streams crossing major aquifer outcrops. They found 126 gain/loss studies had been conducted in the Edwards Aquifer, but few of these gain/loss studies were on the Nueces River. They also noted that the amount of gain or loss changed significantly based on hydrologic conditions. Gain/loss studies in this thesis assess possible recharge in the EACZ and determine a focused area of study.

Over a three-year period, a series of synoptic flow measurements (gain/loss studies) were taken to understand the spatial dynamics of recharge under various flow conditions on the Nueces River as it crosses the EACZ and EARZ. These measurements were taken in cooperation with the Edwards Aquifer Authority (EAA) staff and students at The University of Texas. Flow measurements were taken periodically over several days in: January 2012, March 2013, and March 2014 (Figure 1.4, Figure 1.5, Figure 1.6). These were taken at locations where access could be gained. Most gauging locations were situated where roads intersected the Nueces River. These gain/loss studies showed that there was a significant amount of loss over the EACZ and gain/loss varies temporally and spatially. The most comprehensive study was completed in March 2014; this gain/loss study incorporated 13 reaches: two (2) losing and five (5) gaining reaches over the Contributing Zone, and three (3) losing and three (3) gaining reaches over the Recharge Zone. In the Contributing Zone, the average loss was 0.34 m^3/s (12.14 cfs.) and the average gain was 0.19 m^3/s (6.58 cfs.). In the Recharge Zone, the average loss was 0.31 m^3/s (10.9 cfs.) and the average gain was 0.084 m^3/s (3 cfs.) (Figure 1.6; Appendix B). This gain/loss study was useful in determining where to conduct further site investigation for this thesis over the EACZ.

Background

HYDROLOGIC SETTING

There are nine major drainage basins that intersect the San Antonio segment of the Edwards Aquifer. The major river basins are: Nueces-West Nueces, Frio-Dry Frio, Sabinal, Medina, Guadalupe, Blanco, Cibolo and Dry Comal River. These river basins are a significant source of surface water recharge to the Edwards Aquifer. The Nueces Basin is the furthest west and is one of the largest river basins in the San Antonio segment of the Edwards Aquifer. The Nueces River basin contributes 14 to 22% of total recharge to the Edwards Aquifer depending upon hydrologic conditions (EAA, 2011; EAA, 2007; Table 1.1,Table 1.2, Table 1.3). Spring input and runoff from large precipitation events are the main sources that sustain streamflow in these rivers.

The Nueces River originates from springs at the base of the Edwards Aquifer located in northwestern Real County and northeastern Edwards County and flows through Edwards, Uvalde, Zavala, Dimmit, La Salle, McMullen, Live Oak, San Patricio, and Nueces Counties to the Gulf of Mexico. The drainage area of the Nueces is 42,994 km^2 (16,600 mi^2). Flow in the Nueces River is sustained by many springfed creeks or springs along the Nueces River. The Nueces River runs approximately 510 km (315 miles) across southwest Texas from the headwaters to the Nueces Bay. Lake Corpus Christi, which provides water for Corpus Christi, is located 64 km (40 miles) upstream of the Nueces Bay.

The Nueces River was named by the Spaniards; it had many pecan trees in the riparian zone, and nueces is Spanish for nut or pecan. Today, the main vegetation along the Nueces River is pecan, hackberry, oak, cedar, and sycamore trees. The Upper Nueces River, the focus of this study, has substantial gains and loses throughout the river, water managers are interested in determining what impacts gain/loss and if the majority of the loss is recharge. Historically, earlier settlers documented the disappearing nature of the Nueces. They noted streamflow at the headwaters, a dry streambed a few miles downstream, then streamflow would resurface a few more miles downstream. The Upper Nueces River Basin has a drainage area of 5,574 km^2 (2,152 mi^2) where elevation varies 305 m (1,000 ft.) from lowest to highest land surface. The Nueces River is characterized by extensive terrace and alluvial gravel deposits in and adjacent to the stream channel.

During the study time period for this thesis the Nueces River has been in drought conditions. The 2011 drought was one of the worst droughts on record in Texas with record low precipitation and high temperatures. The Nueces River is still recovering from loss that happened during this drought; during the study time period from 2013 to 2014 there were some significant precipitation events, but not enough to return the river to "normal" flow conditions.

GEOLOGIC SETTING

The general geology of the Uvalde area is characterized by Cretaceous carbonate rocks. One of the main formations in this area is the Devils River Formation; it was formed in a carbonate bank in an open marine environment with high energy. The Devils River trend, part of the Edwards Aquifer, was formed in seas during the Cretaceous. The Balcones Fault Zone is a prominent structural feature in the area with high-angle normal faults striking southwest to northeast (Clark, 2003; Rose, 1972). Porosity in the Edwards and Trinity Aquifers is a result of depositional, diagnetic effects, and development from structural and solutional features; porosity is influenced by fracturing, dissolution and chemical weathering. The general hydostratigraphy of the site (from top to bottom) is: Devils River Formation and Upper Glen Rose (confining unit) (Table 1.4; Clark, 2003, Rose, 1972; Appendix C). The Devils River Formation is 158-183m (520-600 ft.) thick and the Upper Glen Rose is 244 m (800ft) or more thick (Clark, 2003; Rose, 1972; Appendix C).

The focus of this study is Candelaria Creek and a short segment of the Nueces River as it crosses the EACZ. The Contributing Zone is composed of Upper Glen Rose Limestone, which is part of the Trinity Aquifer (Figure 1.7). Downstream of the Contributing Zone is the EARZ, the Recharge Zone is composed of units in the Edwards Group (Devils River Formation) part of the Edwards Aquifer. The Edwards Aquifer is located above the Upper Glen Rose limestone (Trinity Aquifer). The Upper Glen Rose Limestone is bedrock under the Nueces River in the study area (Figure 1.7) and there are outcrops of the Devils River Formation in the hills located 1-2 km (0.6-1.24 mi.) from the main river channel (Table 1.4). Two terrace and two gravel units have been identified. The Quaternary terraces are divided by age and lithology, T4 and T3 from oldest to youngest respectively. The Holocene gravels are also divided by age and lithology, G2 and G1, oldest to youngest respectively (Figure 1.8-Figure 1.11). The most permeable unit is G1 and the least permeable units are T4 and Upper Glen Rose Limestone. Four different conceptual cross sections were developed Figure 1.10 and Figure 1.11, based on field observations. A conceptual model of the geology near the Nueces River of the different terraces and gravels units is shown in Figure 1.8 displaying how the Nueces River meandered over time, creating the terraces and gravel deposits present today. The units described in Figure 1.8 conceptually were then used to create a more detailed geologic map near the Nueces River (Figure 1.9). The geology of the Nueces River in map view shows there is a greater area of terrace deposits near Candelaria Creek with a limited area of gravel deposits; and near NUE010 there is a larger area of gravel deposits with less terrace deposits located further from the main stream channel (Figure 1.9).

Table 1.4. General hydrostratigraphy of the study area. Hydraulic conductivity and effective porosity values estimated from (1) Green, 2004; (2) Freeze and Cherry, 1979; (3) Clark, 2003. The composition was estimated based on observed crossection and soil investigation.

Unit Name	Characteristics	Locations	Estimated Composition	Hydraulic Conductivity (K) (cm/s)	Estimated Effective Porosity (%)	Unit Thickness (m)
G1 (Gravel Unit 1)	Youngest unit, active gravel, little to no vegetation	In river bed throughout study area	Mainly gravels with some sands and fines	2-4.5[1]	24[2]	0-3
G2 (Gravel Unit 2)	Pleistocene, Older gravel unit, more stable less active, supports trees and larger vegetation (small sycamores and grasses) growing in gravels, typically elevated above active river channel unit	In river beds throughout study area	Mixture of gravel with silts, sand, and fines	0.5-1.5[2]	20[2]	0-3
T3 (Terrace Unit 3)	More recently deposited terrace contains gravel lenses within the silt matrix, lower elevation, supports larger trees and plants	Cliffs along river bank	Mixture of mainly silt, with some gravel lenses, sand and clayey sand	0.2-0.4[2]	15[2]	1-15
T4 (Terrace Unit 4)	Older terrace, terrace more compacted, no gravel lenses, typically located at higher elevations	Elevated near river channel	Mixture of mainly silt and caliche, and a mixture of sand and clayey sand	0.01-0.03[2]	10[2]	1-15
Limestone Kdvr	Low Cretaceous series, part of the Edwards Group Devils River Trend, composed of mudstones, wacke stones, grainstones, and sparry limestone[3]	Only present at high elevations, top of mountains, most eroded	Limestone	9.93E-03[3]	2-5[3]	1-25[3]
Bedrock-Glen Rose Limestone	Low Cretaceous series, formed in shallow marine environments, limestone[3]	Throughout the river, exposed sites at Candelaria Creek and near NUE 10	Limestone	3.35E-05[3]	0.5-1.5[3]	2-10[3]

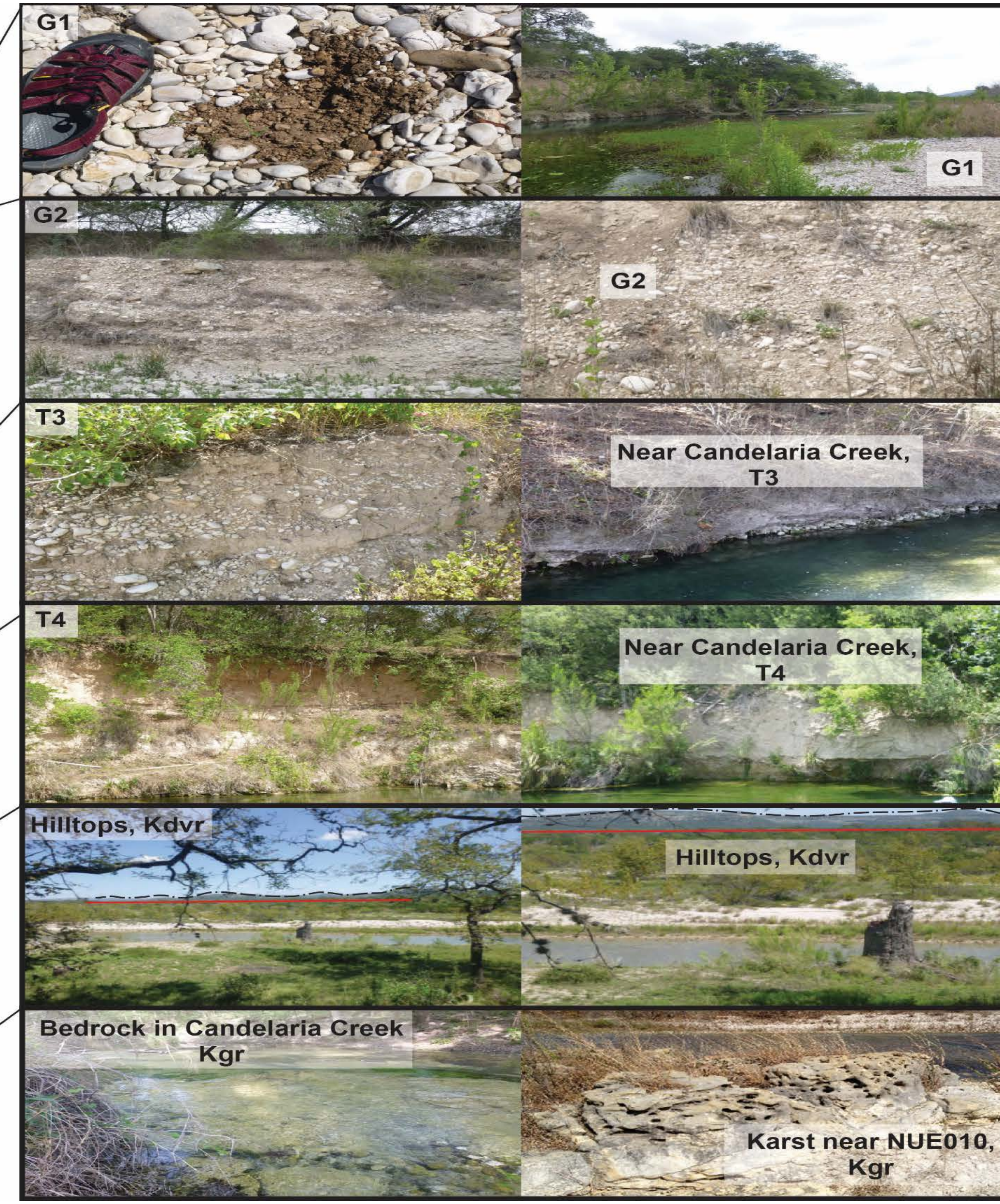

Site Description

The Trinity-Edwards Aquifers are an ideal site to study the interactions of karst, streams, and alluvium. This study investigates these interactions and their impact on recharge and streamflow. There are many outputs and inputs in this system, which are quantified so that recharge over the EACZ can be estimated (Figure 1.12). The focus of this study is Candelaria Creek and the Nueces River from NUE010 to CR414 (Figure 1.2). This segment of the Nueces River has significant loss over the EACZ. This area was selected to further investigate if this loss could be recharge.

The study area is in central Texas on the Edwards Plateau in the EPA ecoregion called the Balcones Canyonland and Northern Nueces Alluvial Plains (EPA, 2003). The climate is semi-arid; most precipitation is in the form of storms moving northeastward from Mexico (Diebel and Norda, 2014). Average annual precipitation is 533 mm (23 in) and the average temperature is 20.5˚C (69˚F) with a low of -1.1˚C (30˚F) to a high of 36.1˚C (97˚F) (Diebel and Norda, 2014). The average potential evapotranspiration (PET) in Uvalde, Texas, is 4.05 mm/day (58.24 inches/yr.); the highest PET, 6.3 mm/day (7.5 in/month) in July and the low 1.96 mm/day (2.36 in/month) in December (Texas A&M AgriLife Extension, 2013, TWDB, 2013).

Problem Statement

Gain/loss studies conducted previously in a larger area of the Upper Nueces over the EARZ and EACZ, led to a more focused study of a smaller area near Montell (Figure

1.7), which is a segment (10 km/6 mi) of the Nueces River where significant loss occurs across the EACZ (NUE010 to CAN012; Figure 1.2). Here the Nueces River loses 100% of flow over the EACZ upstream of the EARZ (17-22 cfs) (Figure 1.4, Figure 1.5, Figure 1.6). Candelaria Creek (1.5 km/1 mile), which runs parallel to the dry segment of the Nueces River, is a gaining stream that provides a significant amount of water to the river. Candelaria Creek contributes 52-64% of the flow measured at the USGS recharge index gauge (Laguna gauge) located downstream of the junction of Candelaria Creek and the Nueces River (Figure 1.2). The primary sources of flow to the creek are two headwater springs (Candelaria Headwater Springs A and B) and Candelaria Springs. This thesis addresses the following question:

Does recharge occur over the Contributing Zone of the Edwards Aquifer (EACZ) (Trinity Aquifer/Upper Glen Rose Limestone) in the Nueces River Basin?

It is hypothesized that recharge is occurring over the EACZ, based on a series of gain/loss studies that show significant flow loss over the Contributing Zone (Figure 1.4-Figure 1.6). To understand if the loss in the gain/loss studies was direct recharge to the Trinity Aquifer or underflow though alluvial material, a water balance was calculated. Multiple methods were used in this research: geologic mapping, geophysical studies, gain/loss studies, streamflow analysis, potential evapotranspiration measurements, specific conductance, temperature, and volumetric calculations of flood pulses. Data gathered from these methods were then used to create a water balance for this system.

The main input to the Nueces River is spring flow and rainfall. Determining the source water for springs in Candelaria Creek is significant, as the springs provide a substantial amount of flow measured at the USGS recharge index gauge (Laguna).

This led to the secondary hypothesis. These springs can be sourced from:

(a) underflow from the Nueces River,

(b) a combination of Trinity Aquifer groundwater and Nueces River underflow, or

(c) solely groundwater from the Trinity Aquifer.

Geologic mapping, geophysical studies, temperature, specific conductance and chemical analysis were used to test these hypotheses and determine source water location for the springs that feed Candelaria Creek. Determining the source water location of the springs was significant as it aided in understanding the hydrologic role of storage and underflow in this system.

The following chapters describe the methods (Ch. 2), results (Ch. 3), discussion (Ch. 3) and conclusions (Ch. 4).

Ch. 1 Figures

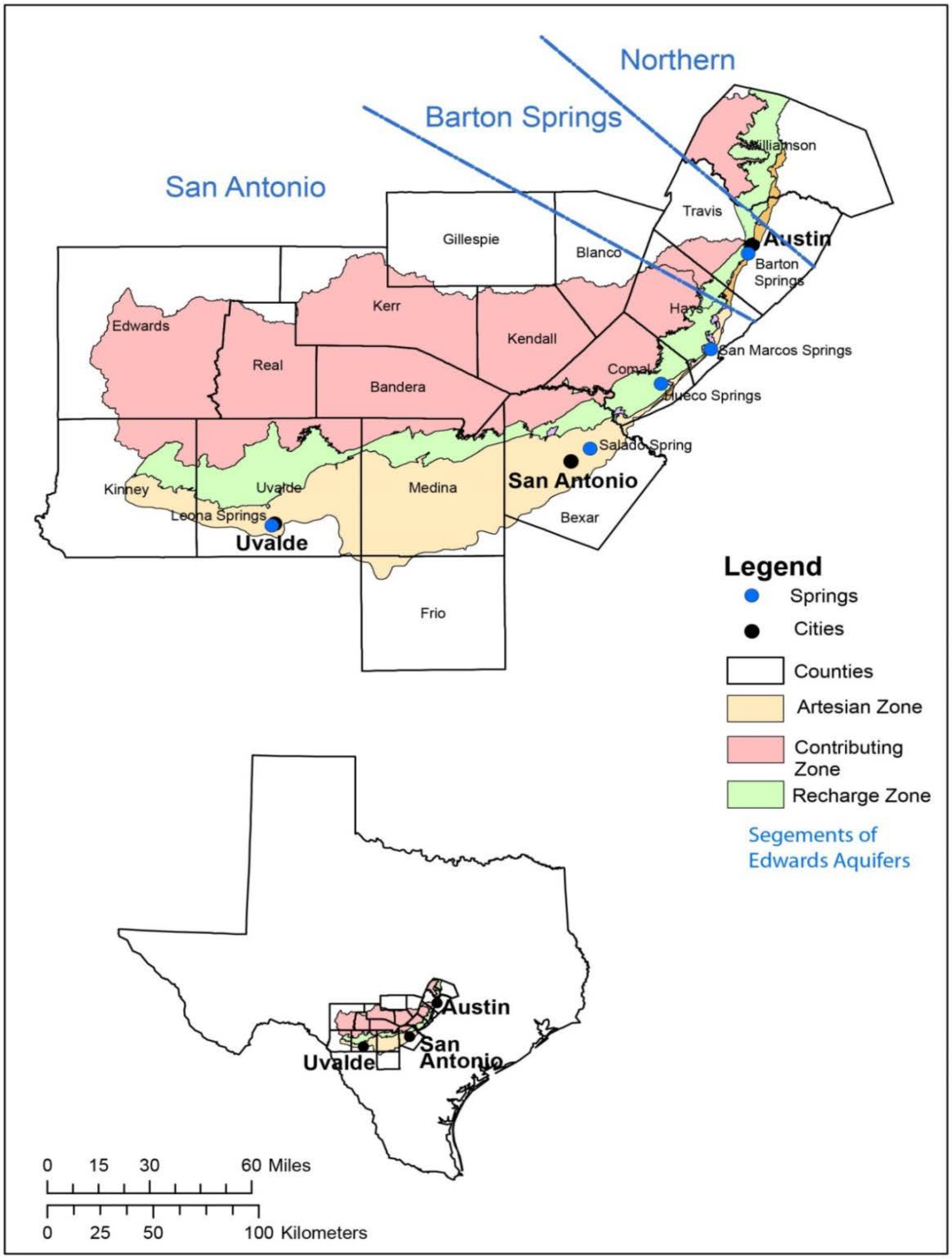

Figure 1.1. Spatially divided segments of the Edwards Aquifer, the Recharge Zone is green Contributing Zone is pink.

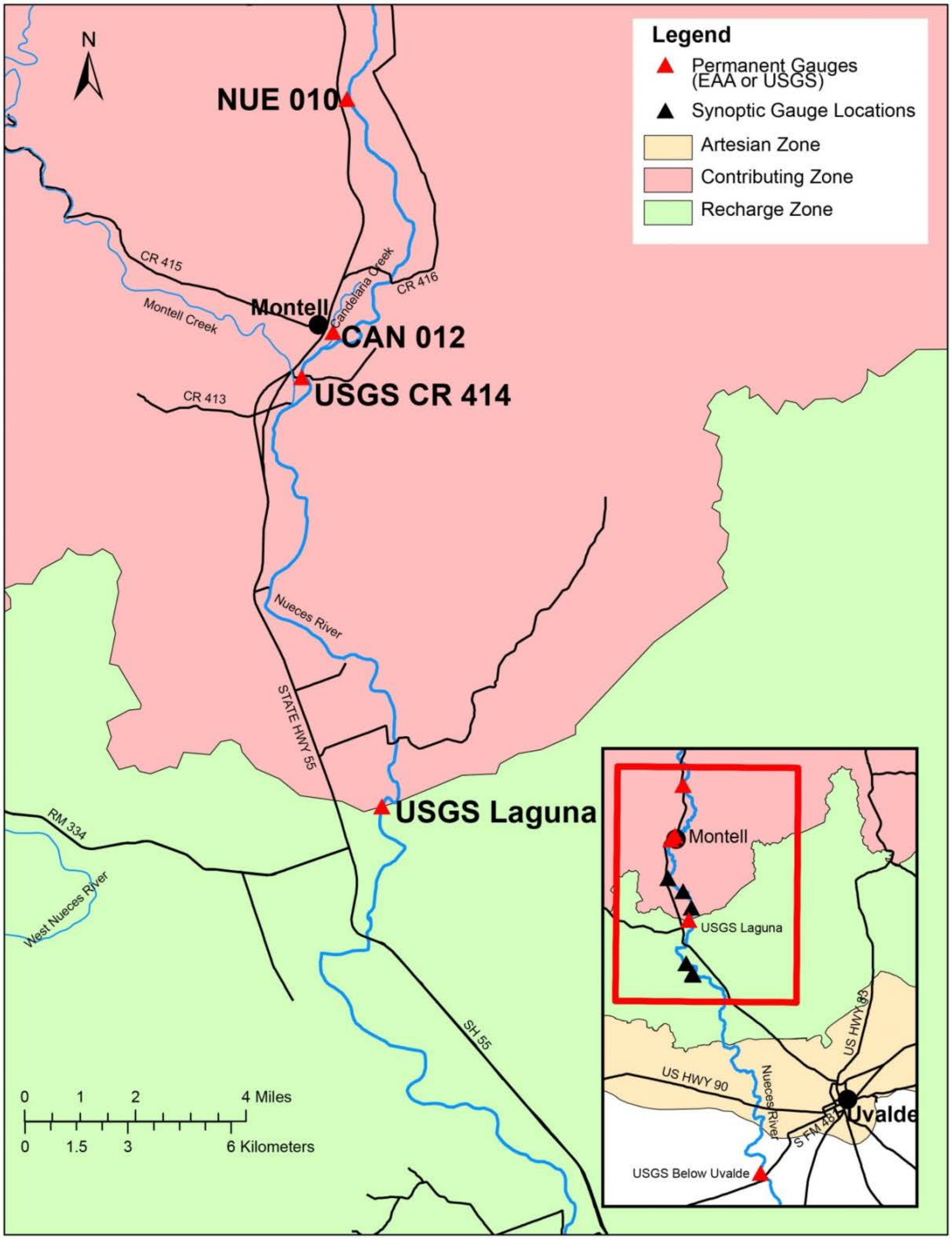

Figure 1.2. Two USGS gauges (USGS Laguna and USGS Below Uvalde) used to calculate recharge over the Recharge Zone of the Edwards Aquifer. Permanent gauge locations and synoptic locations used in this study are shown as well.

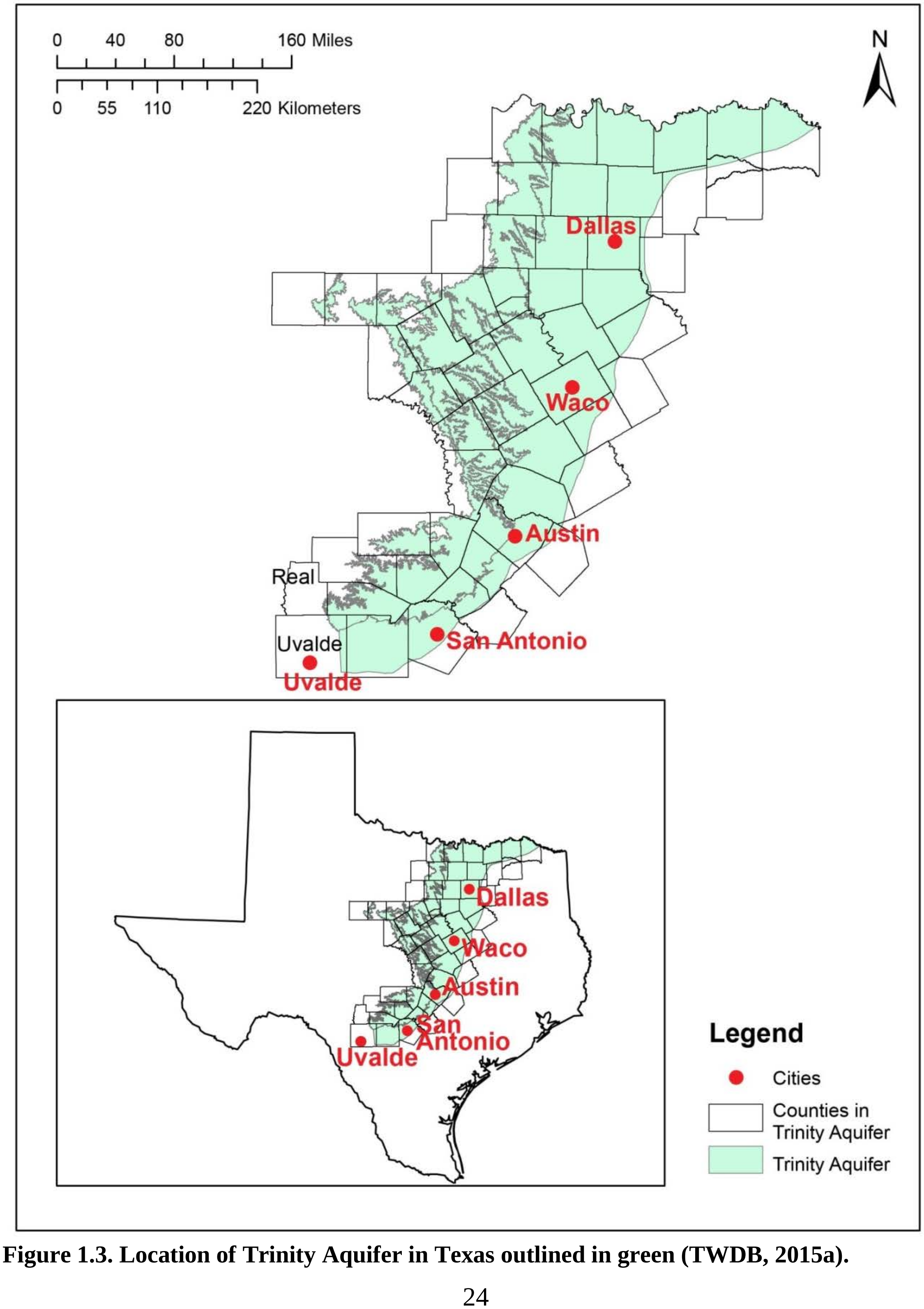

Figure 1.3. Location of Trinity Aquifer in Texas outlined in green (TWDB, 2015a).

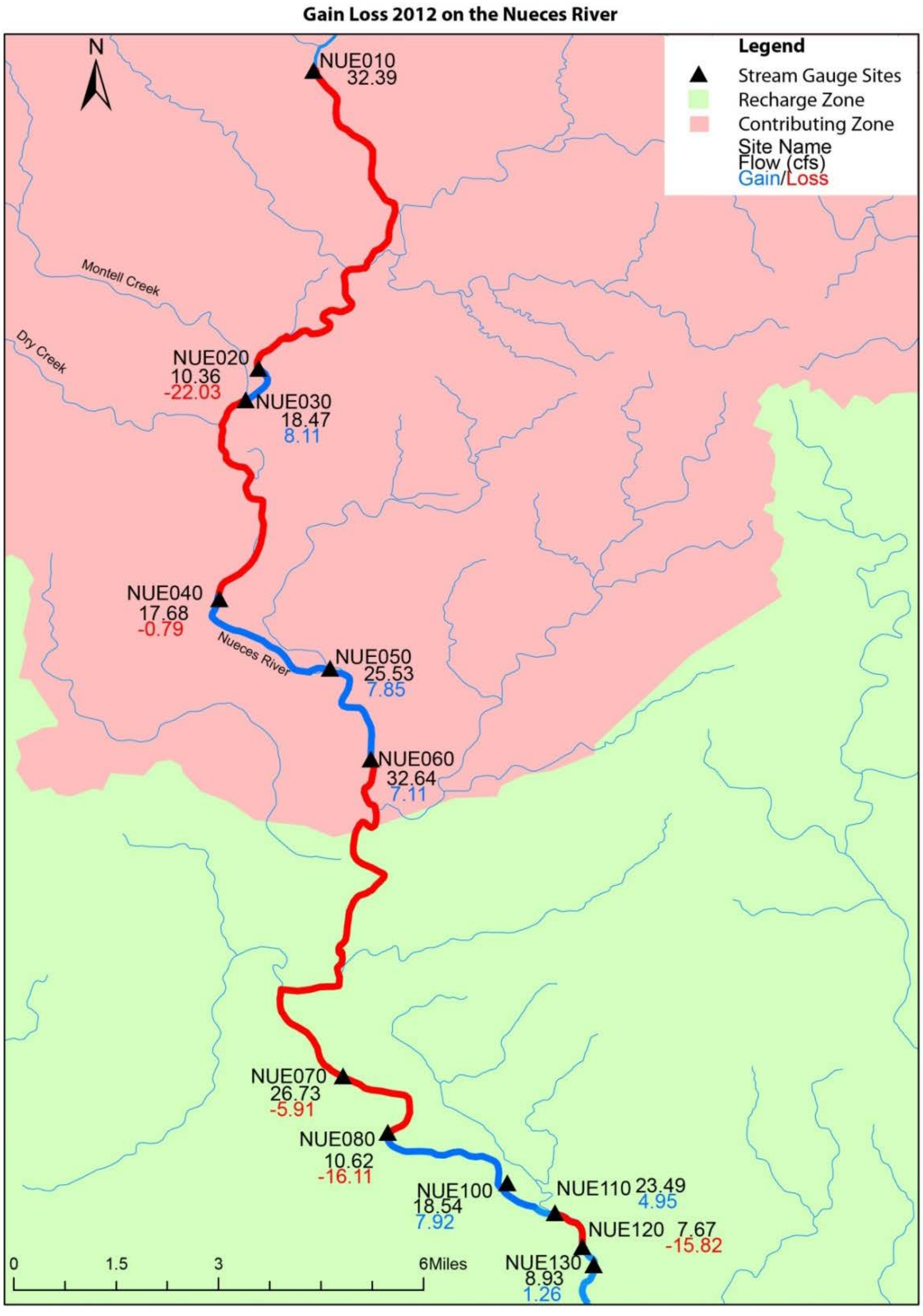

Figure 1.4. Gain/Loss study conducted in January 2012 on the Nueces River over the EACZ and EARZ (EAA and University of Texas at Austin).

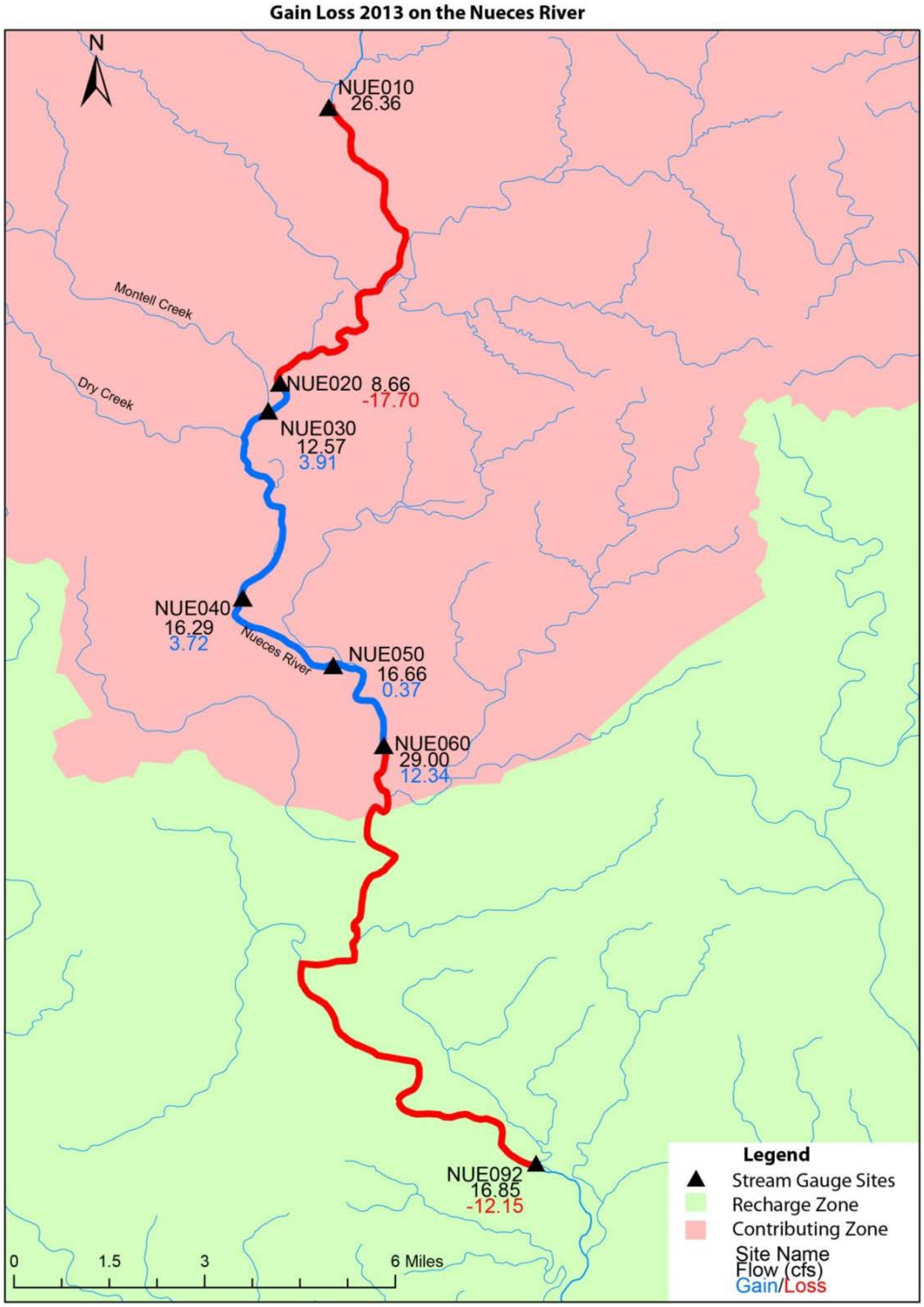

Figure 1.5. Gain/Loss study conducted in March 2013 on the Nueces River over the EACZ and EARZ (EAA).

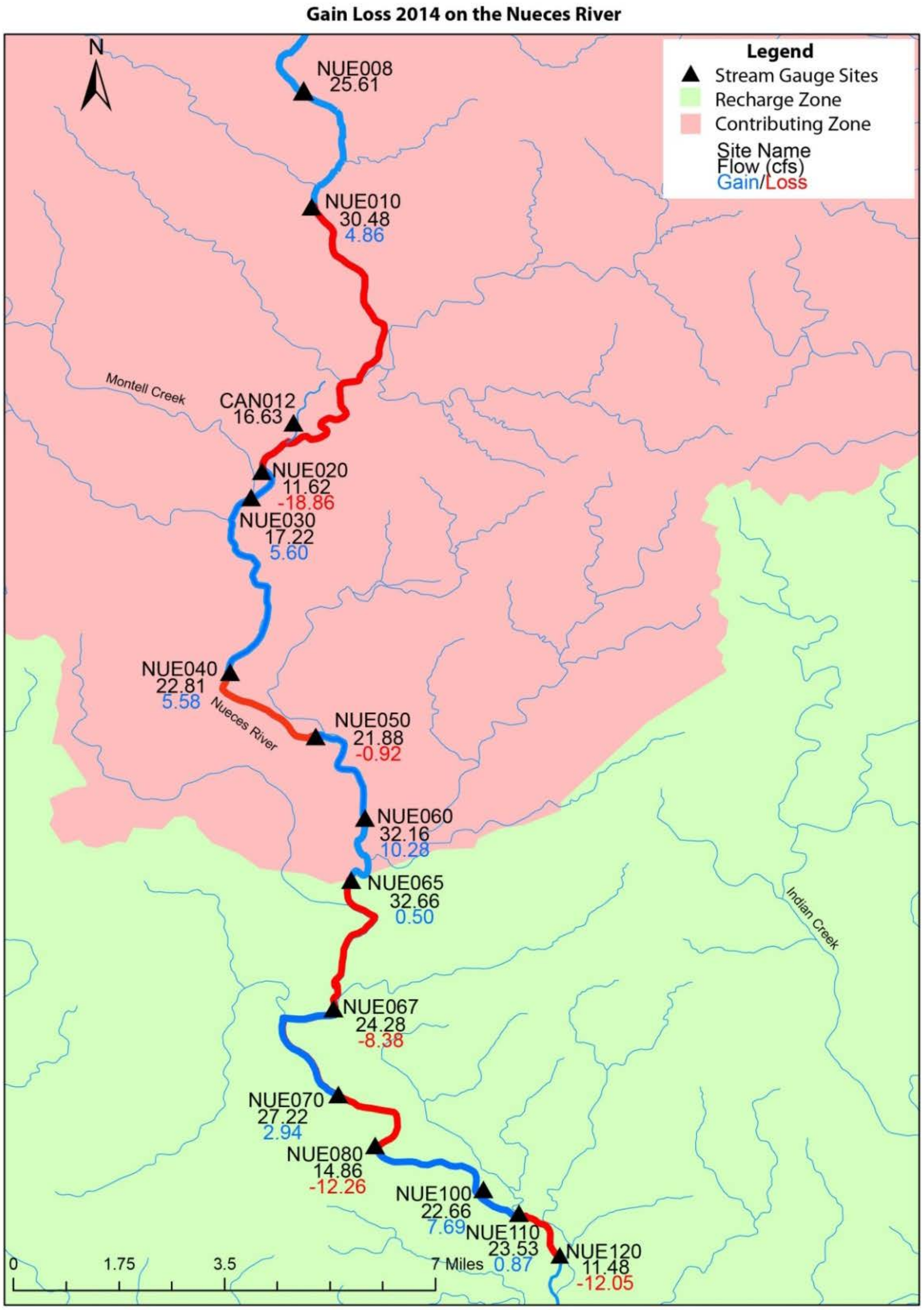

Figure 1.6. Gain/Loss study conducted in March 2014 on the Nueces River over the EACZ and EARZ (EAA).

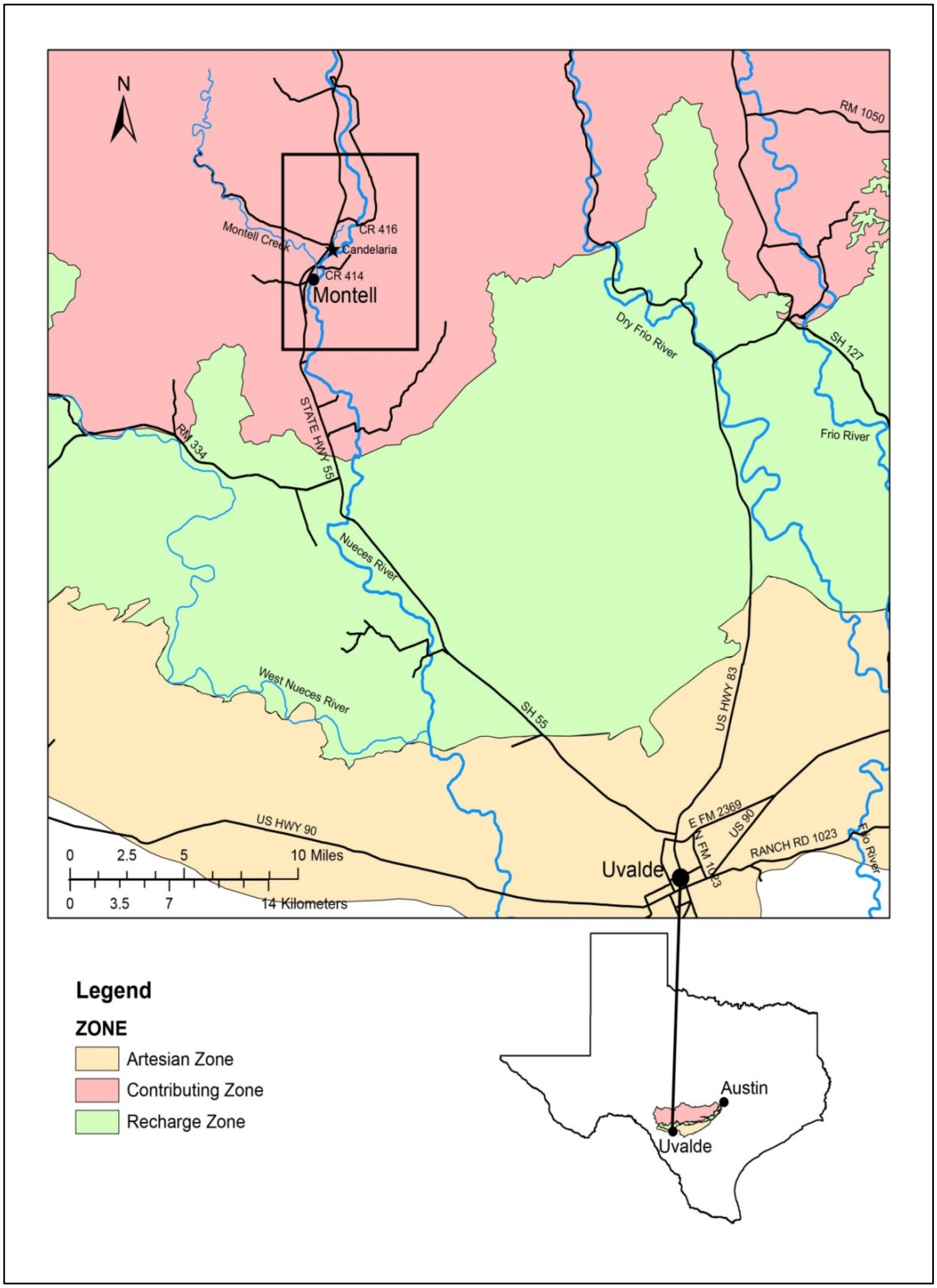

Figure 1.7. The area of study for this thesis near Montell, Texas including Candelaria Creek and part of the Nueces River outlined in the black box.

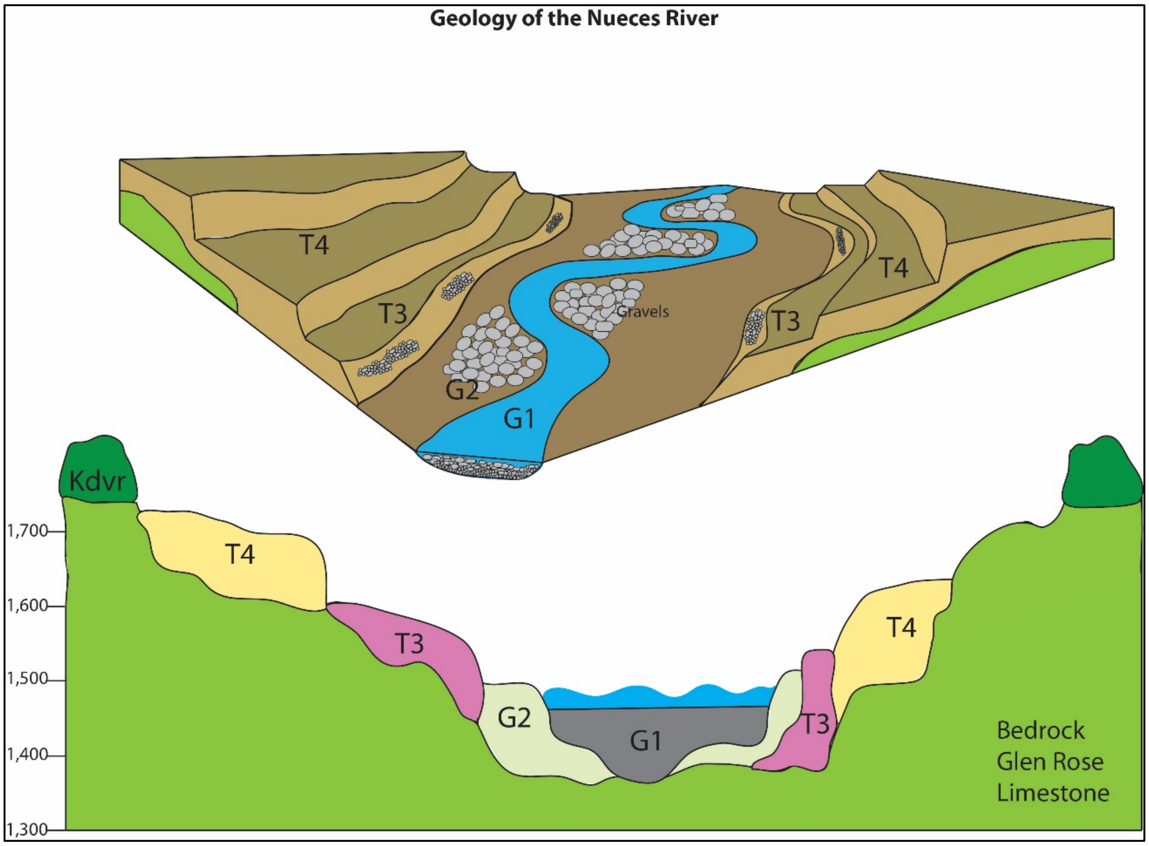

Figure 1.8. Conceptual model of geology near the Nueces River (terrace, gravel deposits, and bedrock).

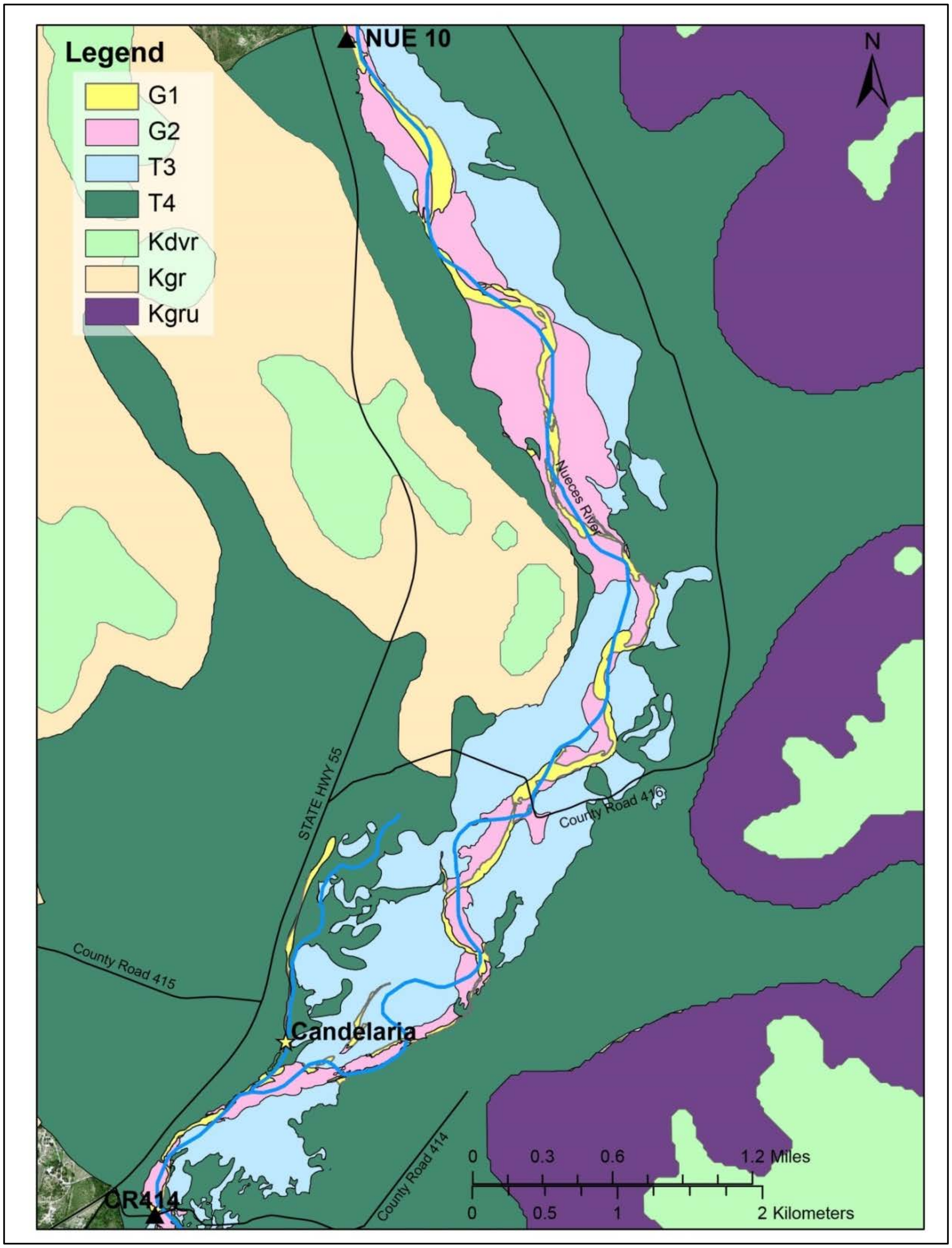

Figure 1.9. Geology near the Nueces River from NUE010 to CR414 modified from Geologic Atlas of Texas (TWDB, 2015b; TNRIS, 2014).

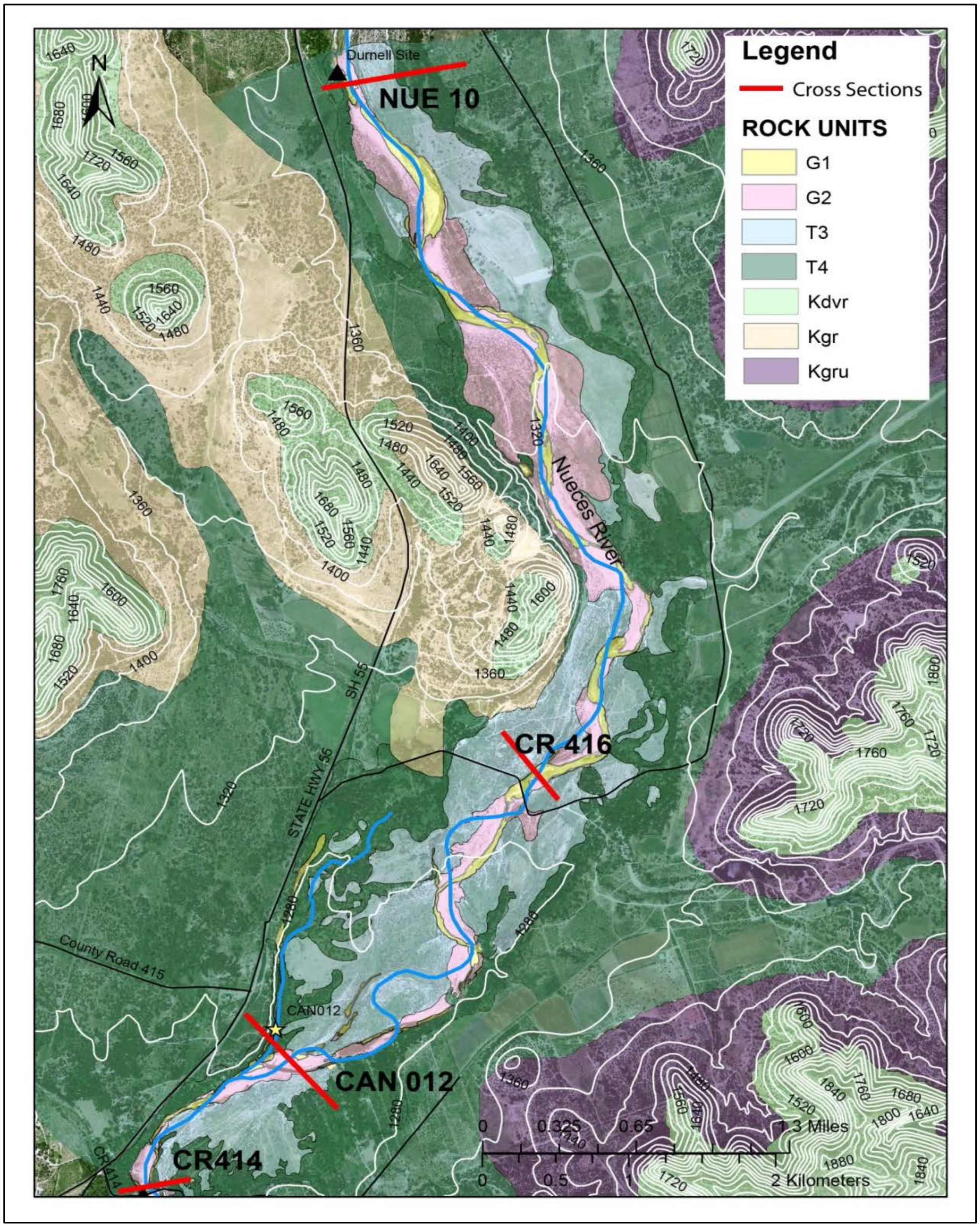

Figure 1.10. Location of cross sections see Figure 1.11 for detailed cross sections. Geology modified from Geologic Atlas of Texas (TWDB, 2015b; TNRIS, 2014)

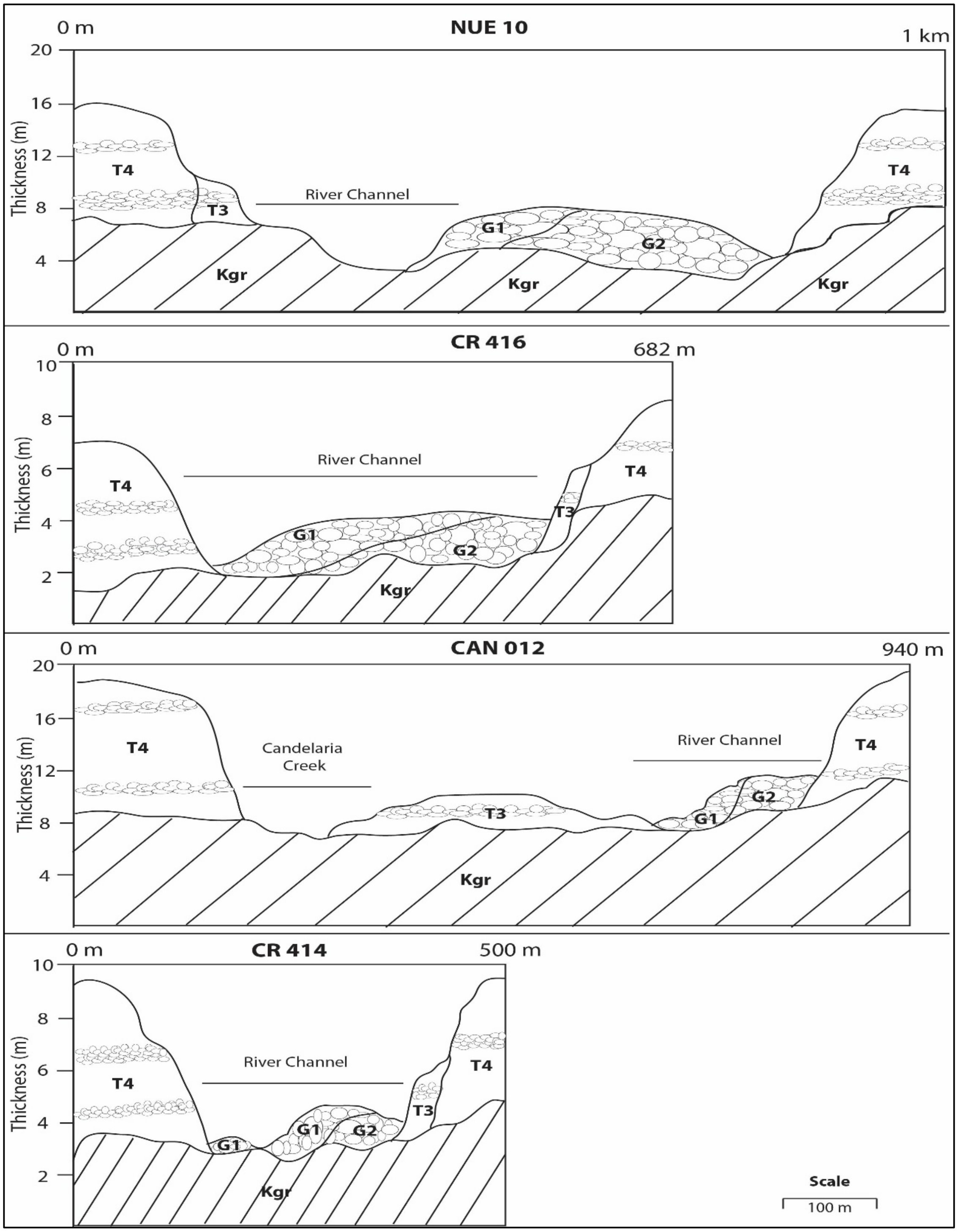

Figure 1.11. Conceptual cross sections from NUE010 to CR 414 depicting terrace, bedrock, and alluvial deposits

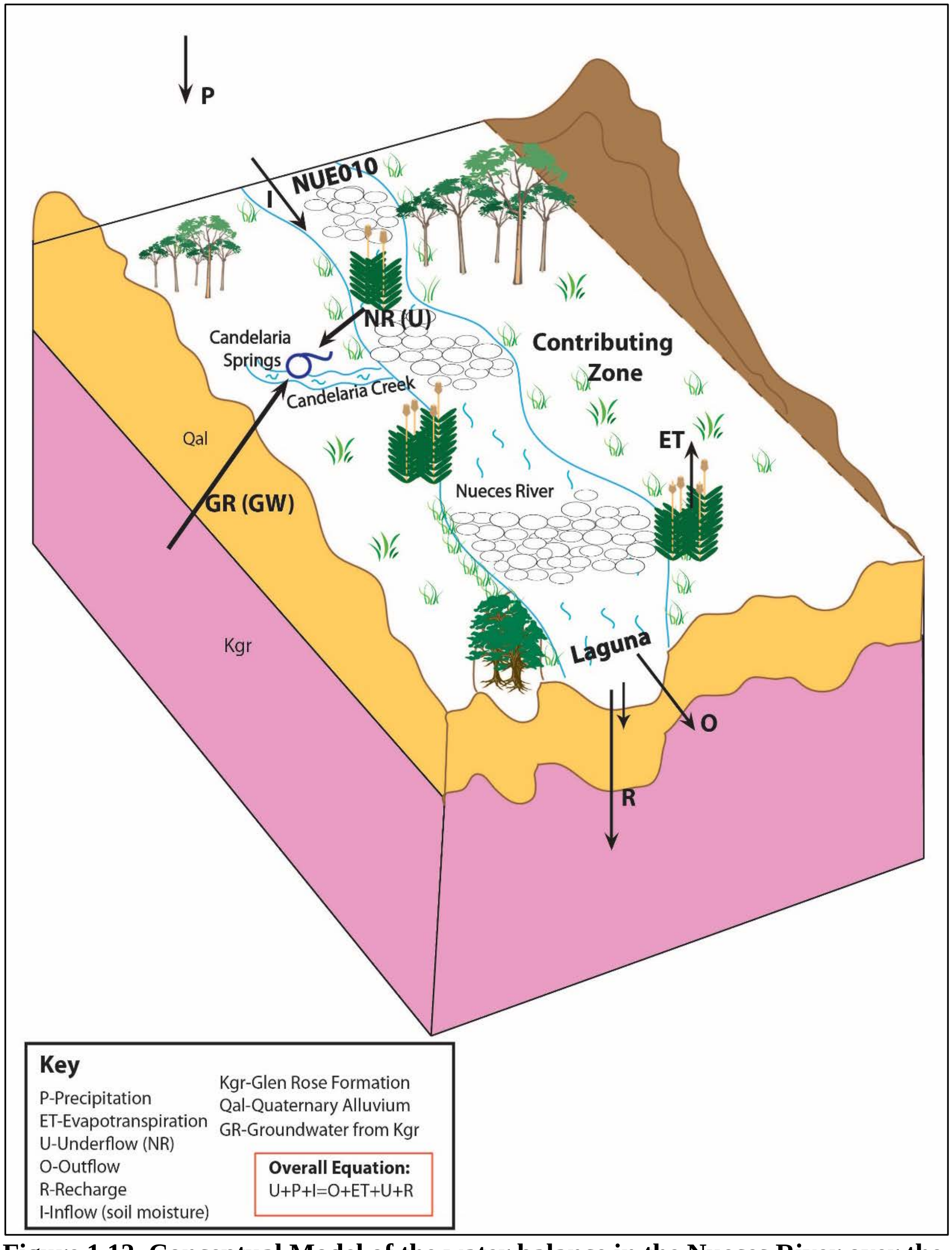

Figure 1.12. Conceptual Model of the water balance in the Nueces River over the Contributing Zone

2. METHODS OF INVESTIGATION

Methods

There were a number of different methods implemented in this study to determine if recharge is occurring over the EACZ. The sites that were studied and the methods used to monitor them are described below. The methods include: 1) geologic mapping, 2) flow gain/loss studies, 3) streamflow hydrograph analysis, 4) potential evapotranspiration analysis, 5) specific conductance, 6) temperature measurements, 7) geochemical analysis, and 8) near surface geophysical measurements. Data collected using these methods were incorporated into a water balance model, flow calculations, and used to calculate the volumetric amount of water moving through the system (discharge multiplied by duration of flood) during high flow conditions.

SITES MONITORED

Five main sites were monitored along the Nueces River and Candelaria Creek: Durnell, Candelaria, CR414, CR416, and Laguna (Figure 2.1; Table 2.1). Sites were selected based on hydrogeologic significance and ease of access. Data collected include: flow, specific conductance, temperature, weather and geophysical data (Table 2.1). Geologic mapping and cross sections were created for CR414, CR416, Candelaria Creek, and NUE010 (Figure 1.8-Figure 1.11).

Flow was monitored continuously at four sites: NUE010, CAN012, CR414 and Laguna. CAN012 and NUE010 are both operated by the Edwards Aquifer Authority (EAA). CR414 (08189998) and Laguna (08190000) are operated by the USGS. At

CAN012 and NUE010, manual flow measurements were taken at various hydrologic conditions. Pressure transducers were placed permanently at CAN012 in March and NUE010 in July 2013. A barometer was installed at NUE010 in July 2013. Data from the pressure transducers and barometer were used to create a continuous flow record CAN012 and NUE010. A discharge rating curve was produced using manual stage readings and flow measurements (Figure 2.2, Figure 2.3). The flow ranges for each site were: 0.48-14 m^3/s (17-503 cfs) at NUE010, 0.06-0.68 m^3/s (2-24 cfs) at CAN012, 0-1.3 m^3/s (0-47 cfs) at CR414, and 0.17-170 m^3/s (6-6,000 cfs) at Laguna.

Continuous temperature and specific conductance sensors (Onset HOBO U24-001 Conductivity Data Logger) were placed at Candelaria Springs, Candelaria Headwater Springs A and B, and Durnell Springs. The objective for installing the sensors was to measure spring and river fluctuations in temperature and specific conductance during precipitation and high-flow events. Synoptic specific conductance and temperature measurements were taken at each site near the logging probe. The Nueces River specific conductance ranged from 369-452 µS/cm and the springs ranged from 383-448 µS/cm. Additional temperature probes (n=10) were installed in various places along the Nueces River and at low-flow springs (n=2) (Table 2.1).

A weather station was set up by the EAA in the Contributing Zone of the Edwards Aquifer. The weather station was deployed at Durnell near NUE010, in the Contributing Zone. The weather station recorded: temperature, precipitation, wind speed, soil moisture, wind direction, solar radiation, pressure, relative humidity, and dew point. The weather station data were used to calculate potential evapotranspiration (PET).

Synoptic near surface geophysical and aqueous geochemistry data were collected at the sites along the Nueces River, Candelaria Creek, and Montell Creek (Figure 2.1, Table 2.1). Geochemistry data were collected from springs, wells, and surface water sources in the summer of 2013 and 2014. Chemical analysis on the various water samples aided in determining the water sources for springs contributing to Candelaria Creek. In October, 2013, geophysical data were collected near Candelaria Creek and Candelaria Springs. Geophysical methods included electrical resistivity (ER) and electromagnetism (EM). Each method that was used in this study is described below.

Table 2.1. Sites monitored on the Nueces River and Candelaria Creek

Site Name	Location	Continuous Flow	Synoptic Streamflow	Weather Station	Conductivity	Temperature	Chemistry	Geophysical Data
Durnell (ET 1)	Nueces River			✓				
NUE10	Nueces River	✓	✓		✓	✓	✓	
Durnell Springs	Pool flowing to Nueces River				✓	✓	✓	
Durnell Pool	Nueces River					✓		
Durnell Nueces River	Nueces River					✓		
Nueces River near Durnell Springs							✓	
Candelaria	Candelaria Creek							✓
Candelaria Springs	Candelaria Creek				✓	✓	✓	
Candelaria Headwater Springs (A&B)	Candelaria Creek				✓	✓	✓	
CAN012	Candelaria Creek	✓	✓					
Candelaria Bridge	Candelaria Creek					✓		
Candelaria Confluence	Candelaria Creek merges w/ Nueces					✓	✓	
Upstream Candelaria Creek	Candelaria Creek						✓	
Downstream Candelaria Creek	Candelaria Creek						✓	
Alluvial Well-Willies	Candelaria Creek						✓	
CR414	Nueces River	✓	✓				✓	
Laguna Gauge	Nueces River	✓	✓					
CR 416	Nueces River		✓				✓	
Nueces River bl Uvalde, TX	Nueces River	✓						
Bird (ET 2)				✓				
Bird Creek	Bird Creek	✓	✓					
Bird Springs	Bird Creek feeds Nueces				✓	✓	✓	
Nueces River near Bird Springs							✓	
Archies Spring	Tributary feeds to Nueces					✓	✓	
Trinity Well-Headquarters	near Montell Creek						✓	
Trinity Well-Hunting-Grandmas	near Montell Creek						✓	
Orchard Springs	near Montell Creek						✓	
NUE008	Nueces River		✓					
NUE020	Nueces River		✓			✓		
NUE030	Nueces River		✓					
NUE40	Nueces River		✓			✓		
NUE050	Nueces River		✓					
NUE060	Nueces River		✓					
NUE070	Nueces River		✓					
NUE080	Nueces River		✓					
NUE090	Nueces River		✓					
NUE092	Nueces River		✓					
NUE100	Nueces River		✓					
NUE110	Nueces River		✓					
NUE120	Nueces River		✓					
NUE130	Nueces River		✓					

GEOLOGIC MAPPING

Information about the geology near the Nueces River was gathered from Clark, 2003 and from the Geologic Atlas of Texas (TWDB, 2014; TRNIS, 2014). Utilizing ArcGIS, Lidar and GoogleMaps a more detailed geologic map was created to determine the extent of terrace and gravel deposits near the Nueces River and Candelaria Creek (Figure 1.9). Utilizing the detailed geologic map, the areal extent of terrace and gravel deposits could be estimated, which is important when performing calculations to estimate hydraulic conductivity and the ability of different geologic units to transport flow (Figure 1.8, Figure 1.9).

The stratigraphic units near the river were classified into two different terrace and two different gravel units. The Quaternary terraces are classified by age into two different deposits, denoted T4 to T3, oldest to youngest, respectively. The Holocene gravels are classified into two different groups by age, denoted as G1 the youngest and G2 the oldest (Figure 1.8, Figure 1.9). I used detailed field observations and analysis of four cross sections at CR414, Candelaria, CR416, and the Durnell site (NUE010) to construct this classification scheme (Figure 1.10, Figure 1.11).

FLOW GAIN/LOSS STUDY

To understand how much flow the springs were contributing to Candelaria Creek, a detailed gain/loss study was conducted in May 2014. Flow measurements were taken using a SonTek Flowtracker Handheld Acoustic Doppler Velocity Meter (ADV) at various locations upstream and downstream of spring input. Data accuracy was verified by completing evaluation checks before gathering data. Data evaluation was also completed to ensure that the correct spacing was used for the stream channel cross section used to measure flow (i.e., if it was flowing more rapidly in one area smaller sections were used). This device is also equipped with SmartQC that is a built in quality control feature to ensure the velocity is not out of range, the sensor is not blocked and is measuring velocity accurately. These gain/loss data were used to determine if there were any other sources of gain/loss in the study area near Candelaria Creek.

STREAMFLOW HYDROGRAPHS

Pressure measurements (translated to flow) were taken continually at the following gauging locations: NUE010, CAN012, CR414 (08189998) and Laguna (08190000) using In-Situ Rugged Trolls. The flow was calculated at NUE010 and CAN012 using the rating curves (Figure 2.2, Figure 2.3). Before the pressure transducer data was translated to discharge, atmospheric pressure was removed. After the atmospheric pressure is removed from the pressure transducer readings, the readings are solely water pressure. Water pressures were then converted to stages, and then these stages are related to discharge using the rating curves (Figure 2.2, Figure 2.3). When developing the rating curves, it was difficult to estimate the flood flows at NUE010, because no stage readings and flows were taken during a storm event. Therefore, after a storm the height and width of the debris in the stream channel were measured. Flood flow was calculated based on this area and an estimated velocity. Stream velocity was estimated by applying a slower velocity on the edge of the stream channel to account for roughness (0.305m/s; 1 ft/sec), and a faster velocity in the center area of the main channel (0.61-0.91 m/s; 2-3 ft./sec) from observation of floating debris during the peak of the storm. Then velocity was estimated using the length divided by the estimated time. A range of velocities were used to calculate flow estimated between 432 to 553 cfs and the average was selected (500 cfs). These velocity ranges showed that the flow is affected more by cross-sectional area, which was measured more precisely, than the velocity value. Adding a flood point (stage and flow) helped in creating a more accurate hydrograph and rating curve that captured flood events. CAN012 is located in Candelaria Creek, so flood flow in this location is buffered, as it is a small tributary to the Nueces River. No high flow point was added to this rating curve (Figure 2.3).

POTENTIAL EVAPOTRANSPIRATION AND WEATHER STATIONS

Methods to calculate potential evapotranspiration (PET) have improved in recent years. A robust and common way to calculate potential evapotranspiration is by the Penman-Monteith equation (Allen et al., 1998; FAO, 2014; Monteith, 1981; Penman, 1948). This method can be used if stomatal resistance values are known for plants in the area where PET is being estimated and if common weather data are available (temperature, precipitation, wind speed, soil moisture, solar radiation, pressure, relative humidity, and dew point). Goodrich et al. (2010) estimated riparian evapotranspiration using remote sensing and field measurements in the semi-arid San Pedro Basin in Arizona. They used these data to create a Penman-Monteith-based model that estimated evapotranspiration for mesquite, cottonwoods, and grasses. In Australia, Doody et al.

(2013) estimated evapotranspiration using the Penman-Monteith method from *Salix*, an invasive high water user. They estimated the amount of water that might return to the environment if the *Salix* were removed. In south-central Texas, evapotranspiration has been calculated by examining the impact of shrub removal, water uptake by riparian-zone plants, and the role of transpiration in the water cycle (Hauwert and Sharp, 2014; Wilcox and Huang, 2010; Moore et al., 2012; Moore et al., 2011; Moore and Owens, 2011). Potential evapotranspiration (PET) in the riparian zone is estimated in this thesis and incorporated into the water balance of this system.

Weather station data collected in the EACZ were utilized for conducting potential evapotranspiration (PET) calculations using the Penman-Monteith method (Equation 2-1). The weather station used was an Onset HOBO U30 and data were collected by the EAA (EAA, 2015b). To use the Penman-Monteith method an estimation of stomatal resistance for the vegetation in the riparian zone is required. In summer of 2013, stomatal resistance estimates were gathered for numerous riparian vegetation species within the Nueces River basin. Stomatal resistance was measured using a leaf porometer (Table 2.2). Multiple measurements were taken over a 12-hr daylight period from various native and invasive riparian plants including: shrubs (buttonbush *Cephalanthus occidentalis*), grasses (giant cane *Arundo donax*, eastern gammagrass *Tripsacum dactyloides*), typical grass (sawgrass *Cladium mariscus*, switchgrass *Panicum virgatum*) and trees (chinaberry *Melia azedarach*, elm *Ulmus crassifolia*, mesquite *Prosopis glandulosa*, pecan *Carya illinoinensis*, and sycamore *Platanus occidentalis*). With the collected data, a program was created in Matlab to calculate the potential evapotranspiration in the riparian zone of the Nueces River (Table 2.2; Appendix D). For PET calculations, an average stomatal resistance for riparian plants of 180 s/m was used. Potential evapotranspiration data were also used to estimate the evaporative losses in the riparian zone of the Nueces River and Candelaria Creek. PET data are used in creating a water balance of the system to calculate how much water is lost in the system by potential evapotranspiration.

The following equations were used in conducting PET calculations for the riparian zone of the Nueces River using the Penman-Monteith equation:

$$\lambda E = \frac{A\Delta r_a + \rho_a c_a (e^*(T_a) - e_a)}{\Delta r_a + \gamma(r_a + r_s)} \qquad \textbf{(2-1)}$$

Where:

λ=latent heat of evaporation ($2.47*10^6$ J/kg); E=potential evapotranspiration [L/t];

A=available energy (A=Rn); Rn=incoming solar radiation [W/m^2]; $r_a=\frac{1}{C_a}$;

ρ_a=atmospheric pressure [kPa]; $c_{a=}$heat capacity of air (1005 J/kg-K);

e*=saturation vapor pressure at the temperature of the water surface (T_s) [kPa];

T_a=the air temperature [K]; e_a=vapor pressure of the overlying air column [Pa];

γ=psychometric constant (66 Pa/K); r_s=stomatal resistance [s/m]

To evaluate the amount of PET in the riparian zone of the Nueces River Equation 2-2 was used. I assumed an average PET of 2.93 mm/day, a width of the riparian and zone of 100 m (0.06 mi.), length of the stream channel of 22 km (14 mi.), and a stomatal resistance of 180 s/m.

$$APET \ = A * Avg_{PET} \tag{2-2}$$

$$PET\ from\ Nueces\ River = 220{,}000m^2 * 2.93\frac{mm}{day} * \frac{10^{-3}\, m}{mm} = 6{,}446\frac{m^3}{days}$$

$$1cfs = 24{,}470\frac{m^3}{days}$$

$$6{,}446\frac{m^3}{days} = 2.6\ cfs$$

Where:

A= riparian zone area [L^2]; APET=estimated PET from the riparian area near the Nueces River [L/t]; Avg_{PET}=the average PET [L/t]

The PET estimated in the riparian zone was used in the water balance of this system.

Table 2.2. Average leaf porometer readings gathered with a Decagon SC-1 Leaf Porometer

Species	Native	Type	Average Porometer Readings (s/m)
Arundo Donax	No, invasive	Grass	152
Eastern Gamma	Yes	Grass	201
Grass	Yes	Grass	146
Switch Grass	Yes	Grass	373
Saw Grass	Yes	Sedges/Rushes	202
Button Bush	Yes	Woody	105
China Berry	No	Woody	56
Elm	Yes	Woody	66
Mesquite	Yes	Woody	308
Pecan Tree	Yes	Woody	164
Sycamore	Yes	Woody	89

SPECIFIC CONDUCTANCE MEASUREMENTS

Temperature and specific conductance data have been used in to analyze spring sources, temporal variations of temperature and specific conductance, and to understand the responses of temperature and specific conductance to hydrologic fluxes in karst aquifer systems. Ozyurt et al. (2014) conducted a study in Croatia on the Gacka River where they analyzed three major springs to determine their water sources using temperature and specific conductance. They found that all three springs are fed from similar aquifers based on similar temperature and specific conductance data. Larocque et al. (1998) used spatio-temporal data to analyze a large regional karst aquifer in France. Using time-series flow-rate, specific conductance, temperature, and precipitation data, they established hydrodynamic links between rivers and springs. Both of these studies analyzed spring characteristics and source water by using temporal temperature and specific conductance data. Similar to the studies conducted in karst systems, temperature and specific conductance are analyzed at springs and surface water sources in this thesis to aid in determining the source water for the springs that feed Candelaria Creek.

Synoptic specific conductance measurements were taken in the river, springs, and creek to indicate water chemistry (fresh or saline), source water, and locate springs. These specific conductance measurements were taken synoptically in March of 2013, and in April and May of 2014. Continuous specific conductance measurements were taken in three springs (Candelaria, and Candelaria Headwaters Springs A and B) and in the Nueces River (at Durnell near NUE010). The continuous specific conductance measurements were recorded on Hobo Specific conductance Data Logger for freshwater; data from the loggers were downloaded approximately every two months. Manual measurements of specific conductance were taken near the loggers to insure their accuracy and to compare manual measurements to continuous measurements. Continuous measurements were used to determine if specific conductance changed temporally or in response to different precipitation or high flow events.

TEMPERATURE MEASUREMENTS

Hobo TidBit temperature sensors were deployed in springs (n=2) and along the Nueces River (n=10). Temperature was also measured simultaneously with specific conductance on the Onset Hobo Specific Conductance Data Logger at Candelaria Springs, Nueces River at Durnell near NUE010, Headwater Springs A and B. The resulting data were used to infer how springs and river temperature changed temporally and in response to high flow or precipitation events. If the springs stayed a constant temperature, this would indicate a groundwater sourced spring. If the spring temperature fluctuated significantly with seasons, the spring may be sourced from the Nueces River or another surface water source.

CHEMICAL ANALYSIS

Major anion and cations can be used to describe water chemistry and to identify different sources. For example, Han and Liu (2004) used major ions and Sr isotopes to characterize the chemistry of two major rivers (Wujiang River and Yuanjiang River) in a karst region in China. They found that lithology and topography characterized the rivers, carbonic and sulfuric acid controlled carbonate dissolution, and the sulfuric acid was anthropogenic. Price and Swart (2006), used major cations and anions along with stable isotopes to identify sources recharging an aquifer system in the Everglades. Stable isotopes and major ion chemistry were used to determine if rainfall or surface water recharges the aquifer. Major cations and anions are used in this thesis to assess the major constituents present in the springs and surface water, and to determine source water for springs that feed Candelaria Creek.

Oxygen isotopes have been used to detect evaporative signatures that are indicative of surface water or groundwater. Studies have been conducted using oxygen isotopes to analyze hydrochemical processes and to determine source water in karst systems. Katz et al. (1997) used the $^{87}Sr/^{86}Sr$ ratio and stable isotopes, D, ^{18}O, and ^{13}C to trace hydrochemical processes, in mantled karst in Florida, to create mixing models, and to locate recharge mechanisms. Katz (1998) used $\delta^{18}O$ and δD to determine the amount of surface water and groundwater mixing in three different karst systems in northern Florida. Kanduč et al. (2014) evaluated groundwater/surface-water interaction in the Velenje Basin, Slovenia using $\delta^{18}O$, DIC, and Sr isotopes; using these isotopes they were able to determine recharge time, recharge rates, and chemical evolution in the basin. Similar to the studies above, isotopes (dissolved inorganic carbon (DIC), δ18O, δD, and $^{87/86}Sr$) are used in this study to distinguish source water location for springs feeding Candelaria Creek.

Various studies have used major ion chemistry and isotopes in the Edwards Aquifer region to evaluate recharge, mixing, and source water location. Strontium isotopes have been used in numerous studies, BSEACD, 2011-2012; Christian et al., 2011; Koepnick, 1985; Musgrove and Banner, 2004; Oetting et al., 1996; Wong et al., 2013; and Wong et al., 2012, on the Edwards and Trinity Aquifers to trace geologic units, to analyze mixing between aquifers, and to identify source waters. Musgrove et al. (2010) analyzed the relationship between hydrogen isotopes and chloride to identify geochemical processes that impact groundwater: mixing with saline groundwater, mixing with storm-water recharge, and mixing with recharge water that has evaporated. Pape et al. (2010) conducted a study in central Texas analyzing oxygen isotopes to determine variability in precipitation and cave-drip waters. These researchers analyzed data from 1999 to 2007 to develop a Local Meteoric Water Line for central Texas. Similar to these studies, isotopes are used in this thesis to distinguish source water location for springs feeding Candelaria Creek.

Samples were taken from Candelaria Creek, the Nueces River, wells, and springs near Candelaria Creek and the Nueces River for chemical analysis (Table 2.1). The chemical analysis of these sources is used to determine if there is any significant difference and to locate the source water for springs feeding Candelaria Creek. Water samples were collected close to the spring's orifice or in the thalweg of a surface water body in June 2013, July 2013, and July 2014 (n=31). Samples were collected using gloves that were changed at each sample site. Samples taken for cations, anions, and strontium (Sr) analysis were all filtered using a 0.25 micron in-line filter syringe. For obtaining water from a well, purging to parameter stabilization was conducted prior to sample collection. Method and field blanks were utilized to ensure sample collection and sampling methods were accurate and quality assured. Field parameters were tested when gathering the sample including: pH, specific conductance, temperature, and alkalinity using either an YSI Pro556 or Myron Ultrameter II. Alkalinity was measured in the lab using titration methods.

The samples from springs, wells, and surface water sources were all analyzed for cations and anions. Some of the samples were analyzed for dissolved inorganic carbon (DIC), δ18O, δD and $^{87/86}$Sr. Cations were analyzed using the Agilent 7500ce ICP-MS and anions were analyzed using an Ion Chromatography, DIC (DIC), δ18O and δD were analyzed using ThermoElectron MAT 253 (Gas Bench and TCEA). Strontium isotopes were analyzed with a Finnigan-MAT 261 thermal ionization mass spectrometer. All analyses were conducted at The University of Texas Jackson School of Geosciences laboratories.

NEAR SURFACE GEOPHYSICAL METHODS

Electrical resistivity (ER) has been applied in karst settings to find caves, sinkholes, and other karst features. For example, a study by Zhou et al. (2000) characterized bedrock geology and located sinkholes using a dipole-dipole array in a karst area in Indiana. Sumanovac and Weisser (2010) used seismic data and ER to characterize local geology in a karst area in Croatia. They located fractured zones and delineated water-saturated areas. ER has also been used in south-central Texas within the Edwards Aquifer to evaluate the extent of Leona River deposits. Green et al. (2008) used a dipole-dipole array to estimate the thickness of the Leona Gravel deposits and was able to delineate the vertical extent of these deposits. Electrical resistivity and electromagnetics (EM) were used in this thesis to characterize the near subsurface geology and determine the depth to bedrock. Characterizing the bedrock geology aided in determining if flow could be transported through the shallow subsurface.

Electrical resistivity (ER) and two different electromagnetic instruments (EM-31 and EM-34) were used in October 2013 to understand the subsurface geology near Candelaria Creek. The AGI Supersting 8 Channel instrument was set up to collect ER data using a command file at four different sites near Candelaria Creek utilizing Inverse Schlumberger and dipole-dipole electrode arrays (Figure 3.20). The dipole-dipole array is useful in distinguishing layers in the subsurface, whereas the Inverse Schlumberger array is useful in describing geology at depth, which is why these arrays were chosen. ER data were processed using AGI EarthImager 2D, this software uses forward modeling to deduce resistivity models from ER transects; iterations of the data were run until there was a root mean square error (RMS) less than 5 percent (ER 3, ER 1) or less than 6 percent (ER 4). Only one ER cross section had an RMS less than 15 percent due to complicated topography of this cross section (ER End). Geonics EM-31 and EM-34 were utilized at various locations throughout the site to understand the shallow subsurface near

Candelaria Creek and the Nueces River. The data gathered from geophysics were used to estimate the thickness of different subsurface units and depth to bedrock.

VOLUMETRIC FLOW CALCULATIONS AND HYDROGRAPH ANALYSIS

Hydrograph analysis and the calculated stream discharge during a flood moving through this system were used to examine the response of streamflow to precipitation events and high-flow events. Data were used from four stream gauges (upstream to downstream: NUE010, CAN012, CR414, and Laguna) that recorded three high-flow (flood) events (May 2013, May 2014, and September 2014). The discharge during high flow was calculated using the methods below. This calculation was performed to investigate if recharge could be occurring from NUE010 to CR414. The volumetric amounts of water during high flow were calculated using different segments (refer to Figure 1.2 for locations):

- NUE010 and CR414 (Segment 1)
- NUE010 and CAN012 (Segment 2)
- CAN012 and USGS CR414 (Segment 3)
- USGS CR414 and USGS Laguna (Segment 4)

The volumetric amount of flow was calculated using the flood flow hydrographs. The area under the hydrograph was calculated from the rising limb to the falling limb by using the following equation:

$$V = \Delta Q * \Delta t \qquad \textbf{(2-3)}$$

Where:

V=volumetric amount of water during flood pulse [L^3]; ΔQ= change between peak flow and baseflow (flow prior to rising limb of hydrography) [L^3/t]; Δt=total time of flood [t]

These calculations were performed for three storms at four different stream gauges. Then the volumetric amount of flow between different gauging stations (different segments) were calculated using the following equations for three different storms:

$$\Delta V\ Segment\ 1 = \Delta V\ at\ NUE010 - \Delta V\ at\ USGS\ CR414 \quad \textbf{(2-4.1)}$$

$$\Delta V\ Segment\ 2 = \Delta V\ at\ NUE010 - \Delta V\ at\ CAN012 \quad \textbf{(2-4.2)}$$

$$\Delta V\ Segment\ 3 = \Delta V\ at\ CAN012 - \Delta V\ at\ USGS\ CR414 \quad \textbf{(2-4.3)}$$

$$\Delta V\ Segment\ 4 = \Delta V\ at\ USGS\ CR414 - \Delta V\ at\ Laguna \quad \textbf{(2-4.4)}$$

Where:

ΔV of a segment number=volumetric change between two different stream gauges [L^3]; ΔV at *gauge*=volumetric change calculated using Equation 2-3 [L^3]

The volumetric change calculated between different stream gauges (segments) was then used to calculate the volumetric change at CAN012:

$$\Delta V\ at\ CAN012 = \Delta V\ Segment\ 1 - \Delta V\ Segment\ 2 \quad \textbf{(2-5)}$$

Where:

ΔV at CAN012=the volumetric flow at CAN012 calculated as the difference between two segments [L^3]; ΔV of a segment number=volumetric change between two different stream gauges (Equation 2-4) [L^3]

The volumetric amount of water at Candelaria Creek during a flood was calculated as the difference between segment 1 and 2, this was compared to the average volumetric amount of water during flood-flow in Candelaria Creek. The difference between the volumetric amount of water calculated between segments and the volumetric amount at high-flow conditions in Candelaria Creek was used to assess possible contributions of recharge from NUE010 to CR414.

Hydrograph analysis compared response times to precipitation events, the length of flood flows, and how high-flow events propagate through the system. In hydrograph analysis, the lag time between precipitation and peak flow was calculated to determine how different gauges were influenced by precipitation. Next, the response of different stream gauge hydrographs to precipitation events was investigated to determine the amount of precipitation that was required to increase streamflow. The investigation of response times to precipitation determined how locality and intensity of storms impacted peak flows and propagation of floods in the system from NUE010 to Laguna. The propagation of floods through the system is important, as it influences the amount of recharge estimated over the Contributing Zone, if flood flow never makes it to Laguna (recharge index gauge) there may be unaccounted recharge.

WATER BALANCE CALCULATIONS

A water balance was created for the Nueces River and Candelaria Creek between NUE010 and Laguna to understand recharge and the impact of different hydrologic components to this system (area of study for water balance (NUE010 to Laguna) is larger than volumetric calculations (NUE010 to CR414)). The water balance method was used to test the hypothesis that recharge could be occurring over the EACZ. The main inputs to this water balance were inflow from NUE010 gauge and precipitation. The main outputs were outflow at the Laguna gauge, PET, and some underflow. Recharge was calculated as inputs subtracted from outputs. Daily volumetric amounts were calculated using the following equations:

$$P\ (Volume\ of\ Precipitation) = Pa * A * \mathrm{t} \quad \textbf{(2-6.1)}$$

$$I\ (Volume\ of\ Inflow)\ = Q_{NUE010} * t \quad \textbf{(2-6.2)}$$

$$ET\ (Volume\ of\ ET) = ET * A * t \quad \textbf{(2-6.3)}$$

$$U\ (Volume\ of\ Underflow) = Q_{springs} * t \quad \textbf{(2-6.4)}$$

$$O\ (Volume\ of\ Outflow) = Q_{Laguna} * t \quad \textbf{(2-6.5)}$$

Where:

Volume of Precipitation/Inflow/PET/Underflow/Outflow=volumetric amount of water in a day in the Contributing Zone of the Edwards Aquifer [L^3]; Pa=daily average precipitation over the Nueces River basin [L/t]; A=area of the Nueces River basin [L^2]; Q_{NUE010}=average flow at NUE010 gauge [L^3/t]; $Q_{springs}$=average flow at Candelaria Headwater Springs A and B [L^3/t]; Q_{Laguna}=average flow at USGS Laguna gauge [L^3/t]; t=amount of time in a day [t]

After these daily volumes were calculated, recharge to the system was calculating using the following equation:

$$R = (P + I) - (O + ET + U^{*}) \quad \textbf{(2-7)}$$

Where:

R=average daily recharge [L^3]; P=average daily volumetric precipitation [L^3]; I= average daily volumetric inflow [L^3]; O= average daily volumetric stream discharge [L^3]; ET= average daily volumetric potential evapotranspiration [L^3]; U*= average daily volumetric underflow, only includes estimated flow contribution from the Upper Glen Rose [L^3]

Average daily recharge was calculated for the area from NUE010 to Laguna to test the hypothesis that recharge occurs over the Contributing Zone. This average daily recharge estimate could also be compared to the daily recharge estimates made through volumetric calculations using flood hydrographs and the flow calculations.

FLOW CALCULATION

To estimate the hydraulic conductivity of different geologic units in the study area flow calculations were conducted to test the hypotheses that: 1) Candelaria Springs is sourced from the Nueces River through underflow and 2) recharge is occurring over the EACZ. The main equations, based on Darcy's law, used in this model are:

$$Q = KiA = Aq \quad \textbf{(2-8.1)}$$

$$K = \frac{q}{i} \quad \textbf{(2-8.2)}$$

$$v = \frac{d}{t} \quad \textbf{(2-8.3)}$$

$$v = \frac{q}{\emptyset_{eff}} \quad \textbf{(2-8.4)}$$

Where:

Q=flow [L^3/t]; q=Darcian velocity or specific discharge [L/t]; A=cross sectional area [L^2]; K=hydraulic conductivity [L/t]; v=average linear velocity [L/t]; i=hydraulic gradient [-]; d=distance from one streamflow gauge to another [L]; t=time (length of time from high flow or peak precipitation to lower specific conductance values) [t]; $\emptyset_{eff}$=effective porosity [%]

Average linear velocity was estimated by using the distance from NUE010 to: Durnell, Candelaria Springs, CR414, Candelaria Headwater Springs A and B; these distances were estimated using GIS, Google Earth, and USGS topographic maps. The time input parameter was calculated by examining how flood pulses propagated though the system, specifically looking at floods in July, May, September, and October 2014. Time was estimated by calculating the amount of time between peak flow at NUE010 and a lower specific conductance signature in the source water being investigated (in the Hobo continuous specific conductance sensors in the springs and Nueces River). The time was also calculated in a different way for to NUE010-Nueces River, Candelaria Springs, Candelaria Headwater Springs A and B and for NUE010, Candelaria Creek, CR414, and Laguna by estimating the time lag from peak precipitation to peak flow. The average linear velocity was calculated by dividing the distance by the time. This velocity was then multiplied by the effective porosity to get the specific discharge. Hydraulic conductivity was then calculated by dividing the specific discharge by the hydraulic gradient. The vertical elevation and horizontal distances were measured in Google Earth and GIS (with LIDAR data).

These flow calculations were used in two ways: (1) to estimate hydraulic conductivity of the subsurface between different sites along the Nueces from NUE010 to CR414 and (2) to estimate the flow in the sub surface NUE010 to CR414. These flow calculations aided in determining if there is a large amount of flow through the subsurface and if recharge could occur in the EACZ.

Ch. 2 Figures

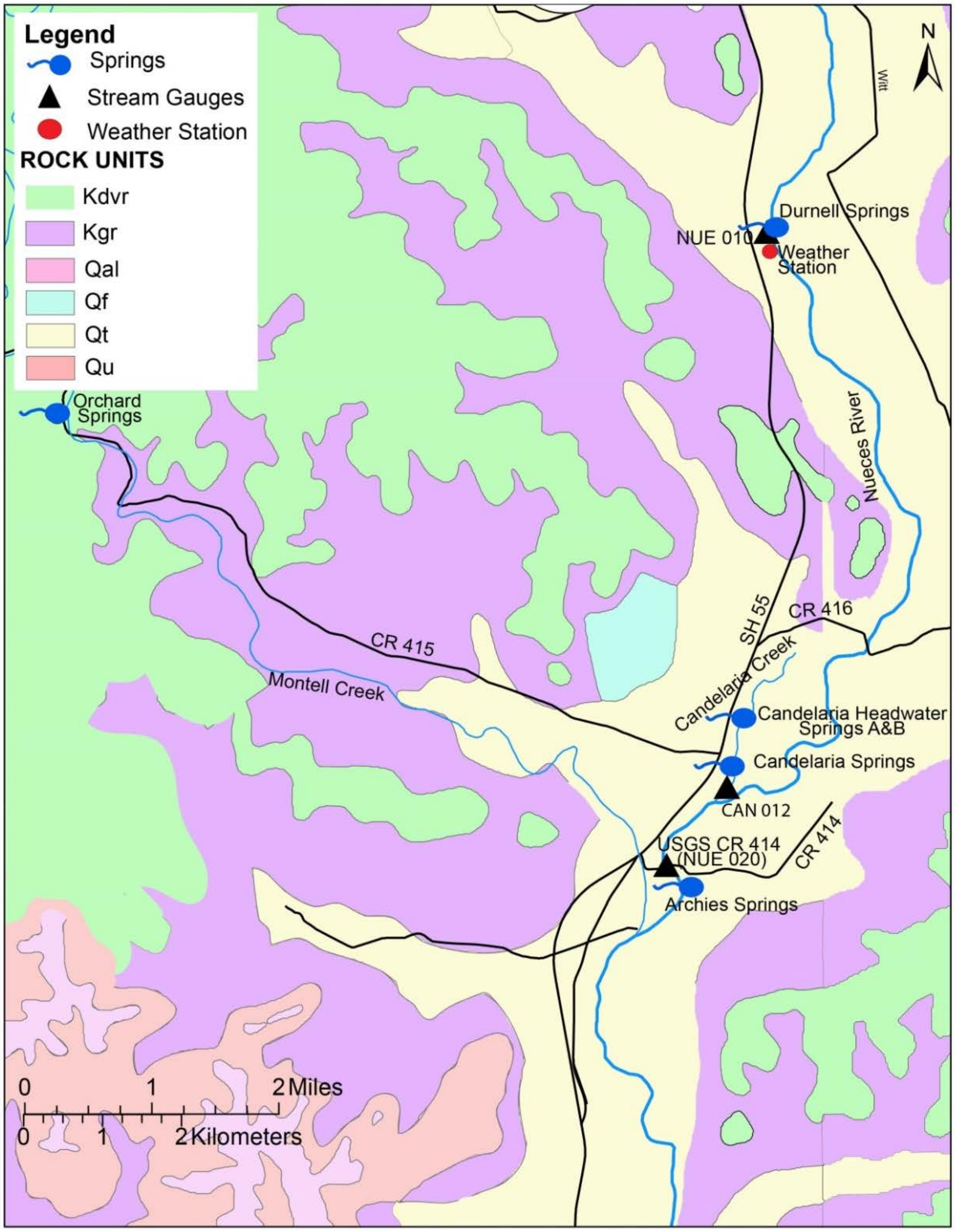

Figure 2.1. Spring and gauge site locations near Candelaria Creek and the Nueces River used as part of this study.

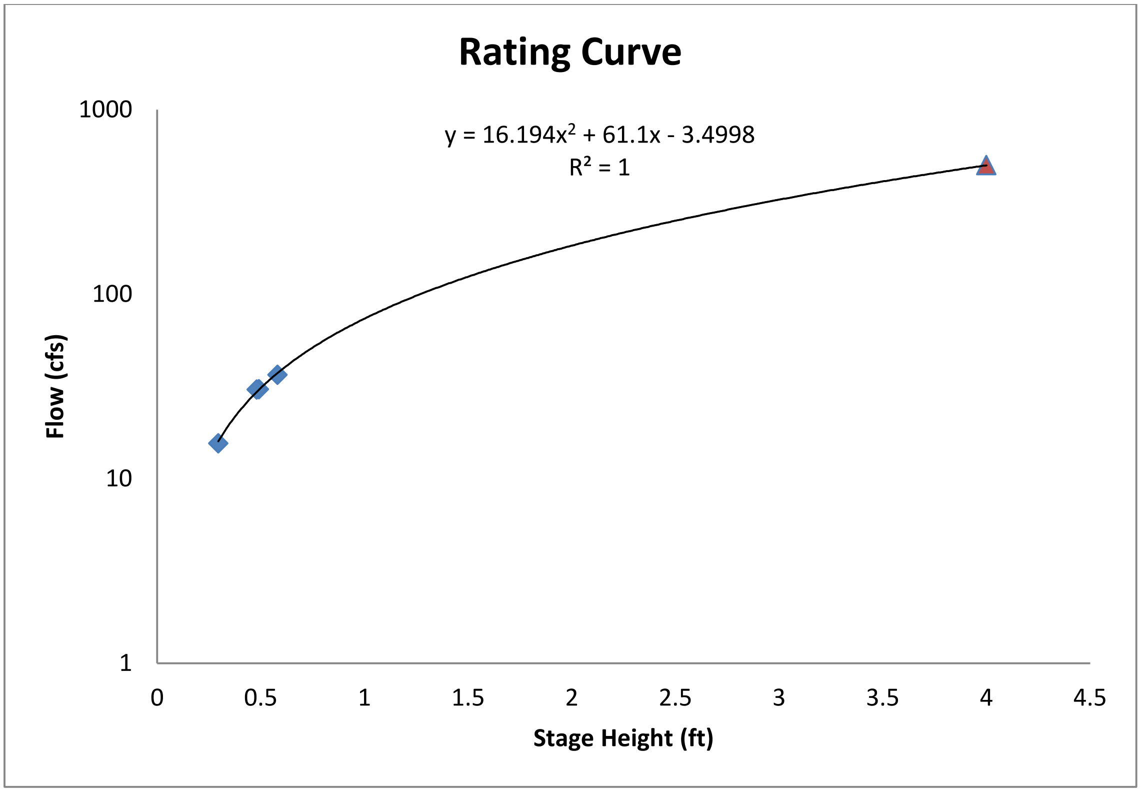

Figure 2.2. Rating Curve NUE010, equation and R^2 value seen in graph. Flood flow in the Nueces River near NUE010 was estimated using indirect measurement techniques (see red triangle).

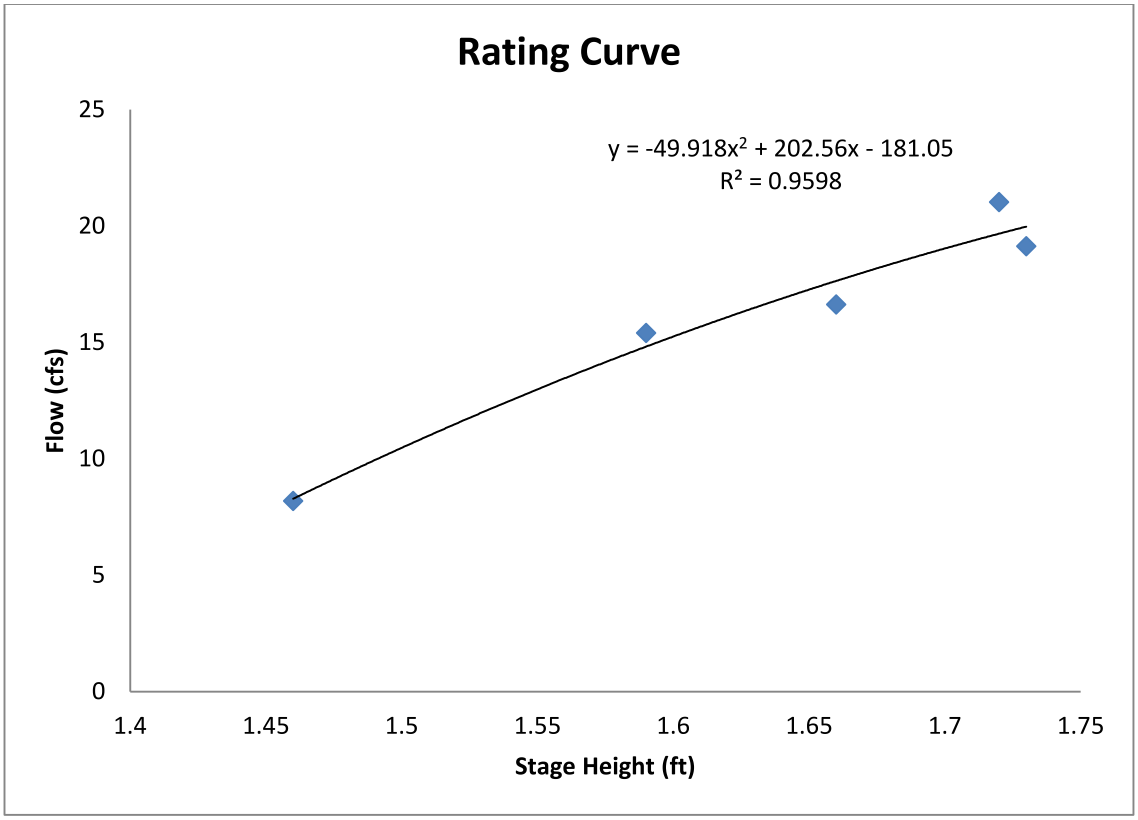

Figure 2.3. Rating Curve CAN012, equation and R^2 value seen in graph.

3. RESULTS AND DISSCUSSION

Results

FLOW GAIN/LOSS STUDIES

The results from gain/loss studies in the Nueces River show that: 1) recharge is difficult to estimate without multiple gauges; 2) recharge occurs in both the Recharge and Contributing zones; and 3) the behavior of some reaches alternates between gaining or losing over time (Figure 1.4, Figure 1.5, Figure 1.6). Based on these results, this thesis focused on a small segment of the Nueces River and Candelaria Creek, where a significant amount of flow 0.48-0.62 m^3/s (17-22 cfs.) is lost over the Contributing Zone (Figure 1.4, Figure 1.5, Figure 1.6; Appendix B).

A gain/loss study of Candelaria Creek revealed it to be a gaining creek that has major inputs from three significant springs, Candelaria Springs and Candelaria Headwater Springs A and B (Figure 3.1). The creek continues to gain until its convergence with the Nueces River. Downstream of the convergence, the Nueces is a losing stream over (0.35 km; 0.22 mi.) until it receives spring input that causes it to revert to a gaining reach (Figure 3.1; Appendix B). In the segment's losing portion, the Nueces River decreases by approximately 0.14 m^3/s (5 cfs.; 10 ac-ft./12,335m^3); in the segment affected by spring input, the river gains 0.17 m^3/s (6 cfs.; 12 ac-ft./ 14,802 m^3). Candelaria Creek contributes an estimated 52-64% of the flow measured at the USGS recharge index gauge (Laguna), which makes it a significant hydrologic feature to understand the water balance of this system.

POTENTIAL EVAPOTRANSPIRATION RESULTS

Potential evapotranspiration measurements and calculations show that potential evapotranspiration (PET) from the Nueces River riparian zone ranges from 0.0074 to 0.015 m^3/s (0.26-0.54 cfs) with a 100 m riparian zone and 0.028 to 0.057 m^3/s (1-2 cfs) with a 500 m riparian zone along the river. Average PET in the riparian zone of the Nueces River and Candelaria Creek is 2.93 mm/day (0.12 in./day), with a maximum of 6 mm/day (0.24 in./day) during the summer and 1 to 1.5 mm/day (0.039 to 0.059 in./day) during the winter (Figure 3.2). The calculated potential evapotranspiration measurements were compared to PET values from the Texas A&M AgriLife Extension in Uvalde, Texas and the evaporation calculated by the TWDB in Region 808 (TWDB, 2013 and Texas A&M AgriLife Extension, 2013). In general, the PET values from the TWDB and the Texas A&M AgriLife Extension were higher than the calculated values in the study area. This could be due to sensor error (low incoming solar radiation or RH too high or variable wind speed and pressure) or different environmental conditions (well watered reference grass vs. riparian stream channel variable stages) or different stomatal resistance values (Figure 3.2; Appendix H).

Stomatal resistance in plants is an important potential evapotranspiration component; stomatal resistance values for crops in this area ranged from 56 to 373 s/m. Native vegetation along the Nueces River, compared to invasive species, did not exhibit a significant difference in stomatal resistivity. Grasses on average had higher stomatal resistance values than woody vegetation, except for mesquite trees (Table 2.2).

SPECIFIC CONDUCTANCE RESULTS

Continuous and synoptic specific conductance measurements were taken in the Nueces River, in Candelaria Creek, and at numerous springs feeding the river and creek. The specific conductance measurements showed an average specific conductance of Nueces River 388 µS/cm, Candelaria Springs 383 µS/cm, Candelaria Headwater Springs A 455 µS/cm and Candelaria Headwater Springs B 421 µS/cm (Figure 3.32). The continuous specific conductance measurements showed lower specific conductance during large precipitation and high-flow events; these lower specific conductance values are prevalent in Headwater Springs B and the Nueces River near NUE010 (Figure 3.3, Figure 3.4). A lower specific conductance signature occurs occasionally at Candelaria Springs and Headwater Springs A due to high-flow and significant precipitation events (Figure 3.5, Figure 3.6, Figure 3.7). The following describes how the sources (Candelaria Springs, the Nueces River near NUE010, Candelaria Headwater Springs A and B) respond to large precipitation, high-flow events, and how floods propagate through the system noted by the response in the specific conductance measurements.

The specific conductance of Candelaria Springs fluctuates between 370 to 420 µS/cm, but during high-flow events the specific conductance drops to 270 µS/cm. Candelaria Headwater Springs A has a lower specific conductance signature during high-flow events; specific conductance fluctuates between 450 and 500 µS/cm, and can get as low as 422 µS/cm during high-flow events (Figure 3.32). Candelaria Headwater Springs B is strongly correlated to the lower specific conductance values measured on the Nueces

River near Durnell; it fluctuates between 375 to 490 µS/cm and can get as low as 286 µS/cm (Figure 3.32). The probe in the Nueces River near Durnell shows decreases in specific conductance during peak flow events greater than 0.85 m^3/s (30 cfs). The specific conductance signature in the Nueces River fluctuates between 390 to 450 µS/cm and during peak flow can get as low as 150 µS/cm. Specific conductance in the Nueces River displays a daily cyclic pattern of increasing and decreasing specific conductance values (Figure 3.4).

High-flow events recorded at flow gauges NUE010 and CAN012 create lower specific conductance signatures at springs that feed the Nueces River and Candelaria Creek (Figure 3.5-Figure 3.10). The specific conductance of Candelaria Headwater Springs A, Candelaria Headwater Springs B, Candelaria Springs, and the Nueces River decrease during large flow events (5.69-14.24m^3/s; 201-503 cfs) (Figure 3.3). In the storm of May 2014, at Candelaria Springs, there was a short lag time between peak flow and precipitation to lower specific conductance signature (Figure 3.5). During the September 2014 storm Candelaria Headwater Springs A and B showed a short lag time between peak flow and a longer lag time from peak precipitation and lower specific conductance (Figure 3.6, Figure 3.7). During the May 2014 storm the Nueces River showed a short lag time between peak flow and peak precipitation and lower specific conductance (Figure 3.8). An example of how floods propagate through the system and associated time lags from peak precipitation and flow, to lower specific conductance signature is seen in Figure 3.9 and Figure 3.10 for the May 2014 storm.

The time lags associated with peak flow and lower specific conductance signatures were investigated during four different peak flow events in May, July, August and September 2014. The lag time between peak flow at NUE010 and a lower specific conductance signature for these four water bodies (Candelaria Headwater Springs A, Candelaria Headwater Springs B, Candelaria Springs, and the Nueces River) ranges from 6,420 to 30,240 minutes, 1,097 to 10,080 minutes, 3,551 to 21,600 minutes, and 64 to 821 minutes, respectively (Table 3.3; Figure 3.5-Figure 3.10). The lag times provide information about how floods propagate through the system. During high-flow events and large precipitation events specific conductance typically decreases first at NUE010, Candelaria Springs B, occasionally at Candelaria Headwater Springs A, and later at Candelaria Springs (Figure 3.5-Figure 3.9). Candelaria Springs does not always obtain a lower specific conductance signature due to peak flow; this may be related to the locality of precipitation (eg. September 2014 storm).

After a storm in July 2014, the time lag between peak flow at NUE010 and decreased specific conductance signatures was 3 hours to reach NUE010, 6 days to reach Candelaria Headwater Springs A and B, and 15 days to reach Candelaria Springs (Table 3.2; Figure 3.4). The May 2014 flood event showed how specific conductance freshening can propagate through the system. The lag time from peak precipitation to a decrease in specific conductance is 76 minutes for NUE010, 5,802 minutes for Candelaria Headwater Springs B, and 76 minutes for Candelaria Springs (no data for Candelaria Headwater Springs A) (Table 3.2; Figure 3.9, Figure 3.10).

There is a stronger correlation between precipitation and lower specific conductance values in the Nueces River and springs, than high-flow events and lower specific conductance values. In general, compared to the time lag between peak flow and lower specific conductance, a shorter lag time occurs between peak precipitation and lower specific conductance (Table 3.2; Figure 3.3, Figure 3.4). Large precipitation events (7.62 mm to 20.32 mm; 0.3 to 0.8 in) lead to a lower specific conductance signature in Candelaria Headwater Springs A, Candelaria Headwater Springs B, Candelaria Springs, and the Nueces River. The lag time between peak precipitation at NUE010 and a lower specific conductance signature at Candelaria Headwater Springs A, Candelaria Headwater Springs B, Candelaria Springs, and the Nueces River ranges from 6,563 minutes, 287 to 5,802 minutes, 76 to 12,878 minutes, and 64 to 821 minutes, respectively (Table 3.2; Figure 3.4). The time lags were investigated during four different large precipitation events in May, July, August, and September 2014 (Figure 3.4).

Synoptic specific conductance events were conducted over the Contributing Zone in March 2013 and April and May 2014. The synoptic event over the Contributing Zone in March 2013 indicated that specific conductance becomes more saline further from the spring source. Water was fresh near spring input, increased in specific conductance at the confluence with the Nueces River, and then decreased downstream of the Nueces River. During the April and May 2014 synoptic event, specific conductance of the headwater springs was high (414-420 and 448-455 µS/cm, 380 µS/cm) near Candelaria Springs, and the river's specific conductance signature ranged from 370 to 400 µS/cm, upstream to downstream respectively (Figure 3.11, Figure 3.12, Figure 3.13).

Table 3.1 Specific conductance statistics from four different sites in the Nueces River and springs feeding Candelaria Creek at various high and low flow conditions over the period of record most from June 2013 to January 2015.

Specific conductance (µS/cm)				
Site (n=number of samples)	**Minimum**	**Maximum**	**Median**	**Mean**
Nueces River (n=25,885)	150	498	402	388
Candelaria Springs (n=51,579)	270	497	384	383
Candelaria Headwater Springs A (n=18,202)	422	529	449	455
Candelaria Headwater Springs B (n= 20,860)	286	497	422	421

Table 3.2. Time lag associated with peak flow or peak precipitation events and lower specific conductance values.

Floods	Site	Time from Peak Flow	Time (min.)	Time (sec.)
July 2014	NUE10	3 hrs	180	10800
	CANH_A	7 days	10080	604800
	CANH_B	7 days	10080	604800
	CAN	15 days	21600	1296000
May 2014	NUE_DUR	2-7 hrs	120 to 420	7200 to 25200
	CANH_A	19-21 day	27360 to 30240	1641600 to 1814400
	CANH_B	2 days 19 hrs 42 min	4062	243720
	CAN	2 days 19 hrs 1 min	4021	241260
Sept 2014	NUE_DUR	19 min	19	1140
	CANH_A	4 days 11 hrs	6420	385200
	CANH_B	22hrs 17min	1337	80220
	CAN	9 days 18 min	12978	778680
Aug 2014	NUE_DUR	1hr 4 min	64	3840
	CANH_A	no lowering in EC		
	CANH_B	18 hrs 17 min	1097	65820
	CAN	no lowering in EC		
Floods	**Site**	**Time from Peak Precip.**	**Time (min.)**	**Time (sec.)**
July 2014	NUE_DUR	13 hrs 41min	821	49260
	CANH_A	no lowering in EC		0
	CANH_B	4day 3hrs 17min	5957	357420
	CAN	no lowering in EC		0
May 2014	NUE_DUR	1hr 11 min	71	4260
	CANH_A	no data		0
	CANH_B	1day 10 hrs 42min	2082	124920
	CAN	2hrs 1 min	121	7260
Sept 2014	NUE_DUR	1 hr 4min	64	3840
	CANH_A	4days 13hr 23min	6563	393780
	CANH_B	4hr 47min	287	17220
	CAN	8 day 22hrs 33min	12878	772680

TEMPERATURE RESULTS

Continuous temperature measurements were collected at various springs along the Nueces and in Candelaria Creek. These temperature measurements were used to determine source water. Springs in the area generally remained at a constant temperature of 20-25˚C (68-77F). The temperature in the Nueces River fluctuated seasonally, ranging from 8˚C (46˚F) to 32˚C (90˚F), increasing in the summer and decreasing in the winter. During storm events the temperatures of springs and the Nueces River typically decreased (Figure 3.14). The mean annual surface temperature in the Nueces River Basin ranges from: 20.5˚C (69˚F) with a low of -1.1˚C (30˚F) to a high of 36.1˚C (97˚F) (Diebel and Norda, 2014).

Temperatures near Durnell in the Nueces River, monitored with a continuous probe (Onset logger) displayed daily temperature fluctuations and is impacted by seasonality; the temperature ranges from 19 to 33˚C (72.5-77˚F) and decreases during storm events with precipitation of greater than 15.24 mm (0.6 in.). Temperature near the confluence of Candelaria Creek and the Nueces River does not seem to be impacted greatly by seasonality; it ranges from 18 to 24˚C (66-75˚F) and temperature decreases in response to precipitation events greater than 4.57 mm (0.18 in). The temperature in Candelaria Creek near Candelaria Springs in the shade was not impacted by seasons; the temperature remained between 19 and 22˚C (66-75˚F), and decreased after precipitation events greater than 2.54 mm. (0.1 in.) (Figure 1.2; Appendix E and F). Candelaria

Springs is impacted by seasonality; its temperature ranges from 20 to 26°C (68-79°F) and decreases after precipitation events greater than 17.78 mm. (0.7 in.). Candelaria Headwater Springs A is also impacted by seasonality; its temperature ranges from 21 to 22°C (70-72°F) and its temperature does not decrease in response to large precipitation events. Candelaria Headwater Springs B is likewise impacted by seasonality; its temperature ranges from 20 to 22°C (68-72°F). During precipitation events greater than 13.97 mm. (0.55 in.), its temperature can decrease to 13°C (55°F) (Figure 3.14; Appendix E).

Temperature fluctuates seasonally in most springs and surface water sources near Candelaria Creek and the Nueces River. The continuous data collected within the scope of this project made it possible to examine seasonal fluctuation and average temperatures of springs and the river. Thermal infrared was used to find and search for springs that contribute significant flow to the Nueces River; but due to low resolution this was difficult and ineffective at accomplishing the purpose (Appendix F).

CHEMICAL RESULTS

Springs, wells, and surface water sources in the study area were sampled and tested for major ions over a two year period. The analysis shows that most waters have a strong Ca-HCO_3 signature (Figure 3.15; Appendix I). Major ion data did not aid in distinguishing the source water for the springs that feed Candelaria Creek, so isotopic data was used to assist in determining the source of the spring water. Oxygen isotopes indicated a strong evaporative signature in the springs and surface water. The only spring that did not display this evaporative signature is Orchard Springs (Figure 3.16). Strontium isotopic signatures from springs, surface water, and groundwater sources in the Nueces River and Candelaria Creek were similar to the isotopic signature of Edwards Aquifer springs and rocks, and Trinity Aquifer rocks (Figure 3.17; Figure 3.18). Samples collected from an alluvial well, surface water sources, and springs near Candelaria Creek and NUE010 have similar Sr signatures (Figure 3.17). A detailed strontium-isotope analysis shows that the three main springs that feed Candelaria Creek are similar to the Nueces River surface water and alluvial groundwater ($^{87/86}$Sr: 0.70780 to 070795). The springs differed significantly from signatures of both the Trinity Aquifer (0.70760) and Edwards Aquifer (0.70830), although these are likely endmembers that mixed to create the Sr isotopic signature of Candelaria Springs (Figure 3.19). An Edwards Aquifer signature was obtained from Orchard Springs, which is sourced from the Devils River Formation. Orchard Springs and the Trinity Well are significantly different from the isotopic signatures collected from groundwater, surface water, and spring waters near Candelaria Creek and NUE010. These two endmembers (Trinity Aquifer and Edwards Aquifer) create a strongly correlated mixing line (R^2=0.96) (Figure 3.19).

Isotopic chemistry was an effective way to identify source water locations for the main springs that feed Candelaria Creek. General chemistry did not change significantly with location or from upstream to downstream in the study area over the Contributing Zone.

NEAR SURFACE GEOPHYSICAL RESULTS

Geophysical data were useful in determining the approximate thickness of terraces (1-5 m), alluvial cover (0-3 m), and limestone bedrock (2-10 m). Electrical resistivity (ER) results were used to derive thicknesses of different near surface geologic units near Candelaria Creek and the Nueces River (Figure 3.20-Figure 3.22). Near Candelaria Creek two different terrace units were present and the bedrock was near the surface shown in the creek bed (Figure 3.22; Appendix G). Closer to the Nueces River there were saturated gravel lenses in the subsurface identified, where the gravel in the river bed is dry. A fracture could possibly extend from Candelaria Creek toward the Nueces River. In ER line four, conducted on older terraces elevated above Candelaria Creek, older terrace unit thickness was larger compared to a younger terrace unit near Candelaria Creek and there were possible gravel lenses identified below the terrace deposits, which could conduct flow. Observations of outcrop cross sections show the possibility of gravel lenses intermixed with the terrace deposits (Figure 3.21; Appendix G). The general thicknesses were used in the geologic mapping of the different hydrostratigraphic units (Figure 1.9-Figure 1.11; Appendix G).

FLOW STUDIES/VOLUME CALCULATIONS RESULTS

To examine the volumetric amount of water moving in the Nueces River during a flood pulse (t=length of flood pulse from start of rising to falling limb recession), data were evaluated from four stream gauges (upstream to downstream: NUE010, CAN012, CR414, and Laguna) that recorded three high-flow (flood) events (May 2013, May 2014, and September 2014). To isolate the volumetric amount of water during a flood that was discharged between:

- NUE010 and CR414 (longer segment)
- NUE010 and CAN012 (shorter segment)

The difference between the longer and shorter segment, was a volumetric amount of water from 2,153,659 to 7,078,952 m^3 (1,746 to 5,739 ac-ft.), that was discharged during an average flood pulse (Figure 3.23). The average volumetric amount in Candelaria Creek during the high-flow conditions was 1,370,398 m^3 (1,111ac-ft). The volumetric amount not accounted for by flow in Candelaria Creek was 783,260 to 5,708,553 m^3 (635 to 4,628 ac-ft.); this volume could be recharge (Figure 3.23).

Flood events in the Nueces River peak and decline rapidly whereas flood flow in Candelaria Creek is buffered; flow in the creek rises at a slower rate than in the river (Figure 3.24, Figure 3.25). The duration of peak flood events at all sites is one (1) to four (4) days on average before the flow recedes.

The Nueces River and Candelaria Creek streamflow gauges responded in various ways to precipitation events. The NUE010 gauge responds rapidly to precipitation events of 5.08 to 20.32 mm. (0.2 to 0.8 in.), but it records no change in flow for precipitation events less than 2.54 mm. (0.1 in.) (Figure 3.24). Lag time from peak precipitation events to peak flow at NUE010 ranges from 1 hour and 15 minutes to 9 hours and 30 minutes (Figure 3.24). Compared to other gauges, this response to precipitation events is rapid.

The Candelaria Creek gauge, CAN012, responds rapidly to precipitation events between 15.24 to 20.32 mm. (0.6 to 0.8 in.), but records no rise in flow if precipitation events are less than 5.08 mm (0.2 in.) (Figure 3.24). During dry conditions in 2013 smaller precipitation events, of less than 5.08 mm (0.2 in.), for example, did not increase the flow. Candelaria Creek is buffered from large storm peaks because it is a tributary of the Nueces River. The lag time from peak precipitation events to peak flow at Candelaria Creek ranges from three (3) hours to one (1) day.

The bed of the Nueces River under the County Road (CR) 416 bridge upstream of CAN012 is typically dry with large gravel deposits at the surface, water can flow through the gravels in the riverbed; flow rates through the gravels near the surface can reach 0.57 m^3/s (20 cfs) (Gary, 2013). CR416 is usually dry, but after large precipitation events, water flows over the gravels.

At CR414 on the Nueces River, flow does not respond rapidly to large precipitation events. Flow increases at CR414 only after precipitation events greater than 0.26 in. (6.6 mm.) (Figure 3.24). The lag time from peak precipitation events to peak flow at CR414 ranges from 14 hours to 5 days (Figure 3.24).

The Laguna gauge, a USGS recharge index gauge on the Nueces River, responds rapidly to large precipitation events. The lag time between peak precipitation and peak flow is short, when the precipitation events occur downstream of NUE010 and close to the Laguna gauge. On September 7, 2014, heavy rain fell upstream of NUE010 and initiated a flood event that did not propagate large amounts of flow detected downstream to the Laguna gauge (Figure 3.26, Figure 3.27, Figure 3.28-Figure 3.30). The flow at Laguna increases when precipitation events are between 2.54 to 15.24 mm. (0.1 to 0.6 in.); if a precipitation event measures less than 2.54 mm (0.1 in), the flow does not increase (Figure 3.24). At the Laguna gauge, the lag time between peak precipitation events and peak flow ranges from 45 minutes to six (6) days (Figure 3.24).

Floods propagate through the system in different ways in response to large precipitation events (Figure 3.28-Figure 3.30). During the May 2014 flood, flow peaked first at Laguna; it took an hour and 30 minutes to peak at CAN012 and NUE010, and flow peaked two (2) hours later at CR414. In the May 2013 flood, flow peaked first at NUE010; it took four (4) hours and 30 minutes to peak at Laguna and six (6) hours for flow to peak at CR414. During the last flood in September 2014, flow peaked first at CAN012, 30 minutes later at NUE010, and one (1) day later at CR414, but flow never peaked at Laguna. These hydrographs illustrate how flood pulses propagate through the system and the response of flow to precipitation events (Figure 3.26; Figure 3.27).

WATER BALANCE CALCULATION RESULTS

A water balance calculated for this study area over the EACZ estimated the average daily fluxes that move through the system. The main inputs to the system are precipitation and streamflow measured at the NUE010 gauge and the main outputs are: stream discharge at Laguna, PET, and underflow. The average daily input volumes at NUE010 are 12,335 to 43,172 m^3 (10-35 ac-ft.) from precipitation and 94,978 m^3 (77 ac-ft.) from streamflow (Figure 3.31). The average output volume, and the largest output in this system is streamflow measured at the Laguna gauge 90,044 m^3 (73 ac-ft.). Underflow/input from the Trinity Aquifer is the next largest flux from this system, this is flow from the main Nueces River channel that is diverted to springs that feed Candelaria Creek, this underflow can range from 3,084 to 7,401 m^3 (2.5-6 ac-ft.). Springs that feed Candelaria Creek are approximately 80 percent flow from the river and 20 percent flow from the Upper Glen Rose (Trinity Aquifer). One of the smallest daily losses is from the Trinity Aquifer approximately 617 to 1,480 m^3 (0.5-1.2ac-ft). PET is another loss in this system which is estimated to be 6,167 to 12,334 m^3 (5-10 ac-ft). After estimating the daily losses and gains to this system the daily average estimated recharge ranges from 3,700 to 41,938 m^3 (3-34 ac-ft.) and 1,350,662 to 15,307,509 m^3 (1,095-12,410 ac-ft.) on an annual basis.

FLOW CALCULATION RESULTS

Flow calculations were used to estimate the propensity for underflow in this system. The quantity of loss calculated through gain/loss studies that could be accounted for as underflow and the quantity of loss that could be recharge was estimated using flow calculations. The flow calculations were also used to estimate the hydraulic conductivity of the subsurface near the Nueces River. The underflow or flow through the subsurface between NUE010 and CR416 was estimated at 0.028 to 0.085 m^3/s (1-3 cfs.), between CR416 and CAN012 was estimated at 0.085 to 0.23 m^3/s (3-8 cfs.), and between CAN012 and CR414 was estimated at 0.028 to 0.057 m^3/s (1-2 cfs.). The average loss from NUE10 to CR414 is 0.48 to 0.57 m^3/s (17-20 cfs). Flow calculations show subsurface flow/underflow can account for 0.11 to 0.31 m^3/s (4-11cfs). Between 0.25 and 0.37 m^3/s (9-13cfs) could account for partial flow in Candelaria Creek or recharge. The average flow in Candelaria Creek is 0.056 to 0.68 m^3/s (2-24 cfs), which means 0.2 to 0.31 m^3/s (7-11 cfs) could be recharge (Figure 1.4 - Figure 1.6; Table 3.3; Appendix J).

These flow calculations were also used to determine hydraulic conductivity values of geologic units near the Nueces River in the subsurface and near the riparian zone (Table 3.2, Table 3.3). The hydraulic conductivity values calculated during high-flow events at Candelaria Headwater Spring A and B were 0.12 to 0.55 m/s, at Candelaria Headwater Spring B 0.7 to 1.12 m/s, at Candelaria Springs 0.35 to 2.14, at NUE010 0.26-11 m/s, at Laguna 2-25 m/s, and at CR414 1.78-15.28 m/s (Table 3.3). The estimated hydraulic conductivity values are higher than literature values likely due to large gravel deposits and paleo stream channels near the Nueces River. This model is based on the assumptions that the units have a saturated thickness of 1 m and are relatively horizontal in thickness, these assumptions may impact the hydraulic conductivity estimates.

Table 3.3. Hydraulic conductivity values calculated with flow calculation methods for different sites along the Nueces River and for springs that feed Candelaria Creek. These were estimated from NUE010 to the site found in the column "Site Name". See Table 1.4 for a comparison of hydraulic conductivity values from literature and estimated effective porosity of different geologic units in the area.

Site Name	Effective Porosity (%)	Distance (km)	Average Travel Time (min.) (See Table 3.2)	Hydraulic Gradient	Average Linear Velocity (m/s)	K min. (m/s)	K max. (m/s)
CANH_A	5-7	6.3	6,563	0.0154	0.004-0.017	0.12	0.55
CANH_B	5-15	6.3	3,951	0.0154	0.011-0.97	0.7	1.12
Candelaria Springs	5-10	6.5	221	0.0154	0.033-1.2	0.35	2.14
CAN Creek	5-10	7	810	0.0153	0.08-3.62	2.63	21.06
NUE010	15-20	0.2	258	0.00780	0.05-0.005	0.26	11.00
Laguna	5-20	19	4,342	0.00714	0.32-7.2	2.00	25.00
CR414	2-10	11	4,020	0.00712	0.2-2.5	1.78	15.28

COMPARISON OF RECHARGE ESTIMATES

Recharge was: 1) estimated using volumetric calculations in high-flow events from NUE010 to CR414, 2) estimated daily recharge was calculated using a water balance for this system from NUE010 to Laguna, and 3) flow calculations were performed to estimate recharge from NUE010 to CR414. These three different methods provided three different recharge estimates for the area of study (Table 3.3).

Volumetric calculations of recharge were conducted during high-flow conditions, looking at how a volumetric amount of water propagates through the system during a flood. The annual volumetric amount of water was estimated to be 23,811,133 to 102,753,970 m^3 (19,304 to 83,304 ac-ft, 512-1,390 cfs) in the Nueces River Basin over the EACZ. These calculations indicated that between 3 and 14% of total recharge to the Edwards Aquifer/Trinity Aquifer (17 to 77% of recharge in the Nueces Basin) may be unaccounted for as loss over the EACZ. This estimate is higher than other recharge estimates, because it was calculated during high-flow conditions. The other two methods estimate recharge over dry-average flow conditions.

The average daily water balance model of inflows and outflows to the system were used to estimate recharge. Using the water balance model annual and daily recharge was estimated to be: 3,700 to 41,938 m^3 (3-34 ac-ft.) average daily and 1,350,662 to 15,307,509 m^3 (1,095-12,410 ac-ft.; 17.3 cfs) average annual. This showed that between 0.5 to 2% of total recharge (1 to 13% of Nueces Basin) may be unaccounted for over the

EACZ. This estimation was completed for average daily conditions and may be more reflective of actual recharge estimations during dry to average annual flow conditions.

Flow calculations (gain/loss studies) were used to estimate the quantity of loss that could be recharge and/or underflow. Using this model annual recharge was estimated to range from 6,213,048 to 9,814,814 m^3 (5,037 to 7,957 ac-ft., 562-889 cfs). This recharge estimates shows that 0.9 to 1.3% of total recharge (4.7 to 7.4% of Nueces Basin) may be unaccounted for currently over the EACZ. These flow calculations were conducted for a smaller area (NUE010 to CR414) than the water balance model, which is why the recharge numbers may be more accurate. The calculations were also performed for dry to average hydrologic conditions.

Each method used gave a different estimate of recharge over the EACZ, the best estimate was made using the flow calculations, which was for a smaller area and falls within the recharge range calculated for a larger area using the Water Balance model. Overall, each method illustrated that there is a significant amount of recharge occurring in the EACZ. There are assumptions made for each calculation, these assumptions may cause errors, but in order to account for the errors associated with the calculations a range from low to high flow conditions was created.

Table 3.4. Table showing the average recharge estimates calculated in three different ways and the percentage of total recharge and recharge in the Nueces River Basin.

Recharge Method	**Estimated Annual Recharge**	**Estimated Annual Recharge (cfs)**	**Percentage of Total Recharge**	**Percentage of Recharge in Nueces River Basin**
Volumetric/Flow Studies (During High Flow Conditions)	23,811,133-102,753,970 m^3 (19,304- 83,304 ac-ft.)	512-1,390	3-14%	17-77%
Water Balance	15,307,509 m^3 (1,095-12,410 ac-ft.)	17.3	0.5-2%	1-13 %
Flow Calculations (Darcy's Law)	6,213,048-9,814,814 m^3 (5,037 -7,957 ac-ft.)	562-889	0.9-1.3%	4.7-7.4 %

Discussion

Results from gain/loss studies, streamflow analysis, PET, geologic investigation, volumetric, and water balance calculations show that there is a significant amount of water that could recharge to the EACZ/Trinity Aquifer. The results from temperature and specific conductance data, chemical analyses, near surface geophysical studies, and flow calculations support the hypothesis that the main springs that feed Candelaria Creek are sustained through underflow from the Nueces River with a small addition from the Trinity Aquifer.

RECHARGE IS OCCURRING IN THE EACZ

Gain/loss studies identified that there is significant loss, 17-22 cfs over the EACZ from NUE010 to CR414, and this loss could be recharge (Figure 1.4-Figure 1.6). Geologic investigation of different terrace and gravel units near the Nueces River and Candelaria Creek suggest the propensity for underflow, but based on volumetric and water balance calculations not all of the flow lost can be accounted for as underflow. Volumetric and water balance calculations estimated that a significant amount of recharge could be occurring over the EACZ during high and normal flow conditions. Based on the amount of recharge calculated moving through the system during a flood pulse, volumetric calculations indicate that a large amount of water could be recharged during high-flow conditions. Water balance calculations were useful in identifying the quantity of recharge occurring in the EACZ during average daily conditions. Overall gain/loss studies, water balance, flow, and volumetric calculations all support the hypothesis that recharge is occurring in the EACZ.

Currently, it is assumed that little to no recharge occurs over the EACZ and models used to estimate recharge in the Edwards Aquifer assume recharge is only occurring over the EARZ (Puente, 1978; USGS, 2014). Some recharge may be unaccounted for based on current methods used to calculate recharge. For example, in September 2014, a high-flow event at NUE010 was not recorded at the Laguna gauge, the main recharge index gauge. In this system the storm dissipated as recharge, storage or underflow; this high flow event may have provided a significant amount of recharge that was never taken into account based on current methods. This suggests the need for multiple gauges to estimate recharge in the Contributing Zone and Recharge Zone, as gains and losses can vary temporally and spatially. The recharge occurring over the EACZ (Trinity Aquifer) may contribute to the Edwards Aquifer through interformational flow. Further study is needed to determine if the Trinity Aquifer is recharging the Edwards Aquifer. Studies to examine the interaction between the Edwards and Trinity Aquifers may include multiple dye trace tests at various locations, installing monitoring wells in the EACZ and EARZ, and further assessments similar to this thesis in other surface water basins. Recharge in the EACZ is significant as it may impact the way the aquifers are managed, especially if the Trinity Aquifer is recharging the Edwards Aquifer.

CANDELARIA SPRINGS IS SOURCED FROM THE NUECES RIVER AND TRINITY AQUIFER

Flow analysis on the Nueces River and Candelaria Creek revealed that there is a significant amount of flow at NUE010, but it disappears near CR416 on the Nueces River. The water that is lost near CR416 may be transported as underflow and reappear in Candelaria Creek as springs. The Nueces River runs parallel to Candelaria Creek but is dry until the convergence with Candelaria Creek downstream (Figure 2.1). A study on Candelaria Creek identified that the springs provide a significant amount of water to the creek. These springs are important as Candelaria Creek contributes a significant amount of flow to the Laguna gauge, the USGS recharge index gauge. The source water of these springs was estimated to be 80% from the Nueces River and 20% from Trinity Aquifer based on isotopic, specific conductance, and temperature data. The analyses support the hypothesis that the springs that feed Candelaria Creek are primarily sourced from underflow and secondarily from the Trinity Aquifer.

The results from continuous and synoptic specific conductance measurements in the Nueces River, springs, and Candelaria Creek provided information on source location and flow propagation in this system. Candelaria Headwater Springs A, Candelaria Headwater Springs B, and Candelaria Springs all had lower specific conductance values in response to high-flow and large precipitation events. The response of specific conductance to high flow and precipitation events at Candelaria Headwater Springs B is very similar to the gauge on the Nueces River near Durnell. This spring, Candelaria Headwater Springs B, is closer to the Nueces River and is more likely to receive flow from the river than Candelaria Headwater Springs A (Figure 3.32). Candelaria Headwater Springs A does not always respond to high-flow events; this spring is located farther from the Nueces River and as a result the source water may be different than Candelaria Headwater Springs B. Candelaria Headwater Springs A and B both have different specific conductance signatures, which indicates that one spring may receive more water from the Nueces River or Trinity Aquifer. Candelaria Springs shows a longer lag time between peak flow and lower specific conductance than the two headwater springs, but it does appear to be sourced from surface water from the Nueces River because it has a lower specific conductance signature in response to large precipitation and high-flow events (Figure 3.32) . Overall specific conductance was useful in determining source location, and travel times associated with large volumes of water. The specific conductance showed that springs that feed Candelaria Creek are sourced primarily from the Nueces River, with a small amount from the Trinity Aquifer.

The results of continuous temperature measurements show that springs fluctuated seasonally but at smaller amplitude (range) than surface water bodies. Temperature tends to decrease during large storm events in both springs and surface water. Temperature data suggest that springs are sourced from surface water bodies moving through the subsurface. These temperature measurements also provide an estimate of the temperature difference between springs and surface water, which may be useful in detecting springs in future studies (Appendix E).

Water chemistry was useful for determining source water location for the springs that feed Candelaria Creek. Major ion data indicates that the waters have a calcium bicarbonate signature attributed to limestone in the area. The strontium and oxygen isotopic data suggests that Candelaria Springs and Candelaria Headwaters Springs A and B are sourced from surface water from the Nueces River. The springs may also be sourced partially from the Trinity Aquifer suggested by strontium isotopic data and the hydrogeologic placement of the springs. The springs fall within the strontium isotopic range for surface water sources in the area and along the evaporative signature in oxygen isotopes indicating a surface water source is contributing to spring flow (Figure 3.16, Figure 3.18). Sr isotopic signature suggests mixing from the Trinity Aquifer signature and the Nueces River. The springs that feed the Nueces River originate in the Edwards Aquifer and this signature evolves as the waters come into contact with the Upper Glen Rose (Trinity Aquifer). This signature evolution is evident in the surface waters of the Nueces River (Figure 3.17-Figure 3.19). Mixing between the Edwards and Trinity Aquifers to obtain the surface and spring water Sr isotopic signature is also suggested by the mixing line where the R^2 value is 0.96, suggesting that the Edwards and Trinity are two end-members mixing (Figure 3.19). One spring, Orchard Springs, has a higher strontium and oxygen isotopic signature due to: elevation (higher elevation), a possible difference in recharge temperature, and a different geologic unit, an Edwards Aquifer unit (Devils River Formation). Overall, isotopic data suggest that the springs that feed Candelaria Creek are sourced from the Nueces River (80%) and Trinity Aquifer (20%).

Geophysical data of the near subsurface were useful in estimating the thickness of units near Candelaria Creek and the Nueces River. These thicknesses were used in modeling the amount of flow that could be transported through each unit. Geophysics was also helpful in determining depth to bedrock so that the alluvial cover above the bedrock could be estimated. Results from flow calculations and geologic mapping, showed a greater hydraulic conductivity for units near CAN012 and a lower hydraulic conductivity near CR414. This illustrates flow will move preferentially though the subsurface towards Candelaria Creek, instead of flowing towards CR414 (Table 3.3). Geologic mapping and flow calculations indicate that underflow from the Nueces River is possible and that the Nueces River is a major source for the springs feeding Candelaria Creek.

Overall, results from field investigation and recharge calculations suggest that significant recharge is occurring over the EACZ. By determining the source for springs that feed Candelaria Creek, mainly the Nueces River and partially the Trinity Aquifer, it was found that not all loss in the Nueces River can be underflow, some flow loss is recharge. This study also shows that Candelaria Creek contributes a significant amount of flow to the Nueces River over the EACZ.

Ch. 3 Figures

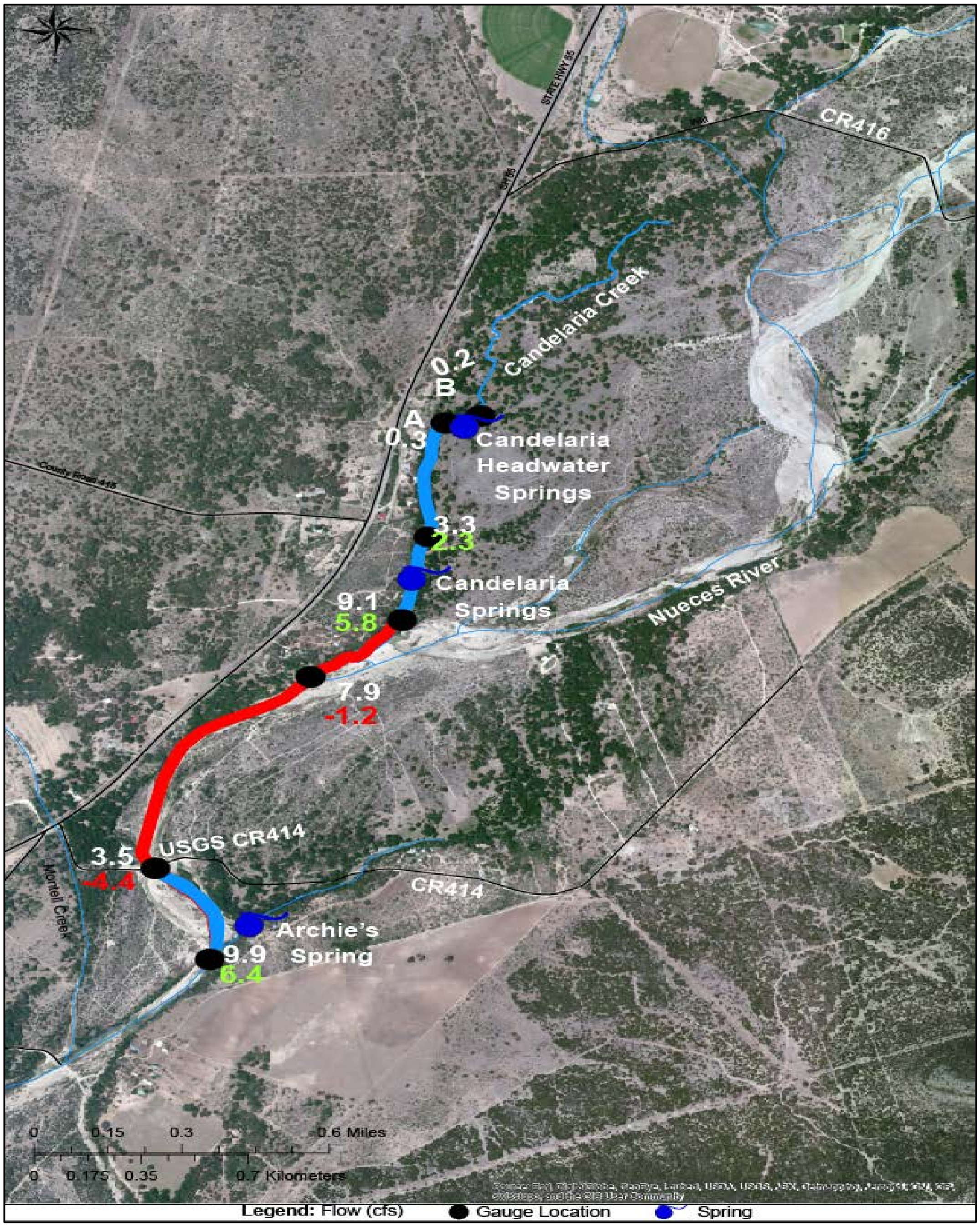

Figure 3.1. Gain/loss study of Candelaria Creek in May 2014, red segments are losing streams and blue segments are gaining streams. The black dots are the gauging locations. Flow is in cfs and the amount of gain (green) or loss (red) is also in cfs.

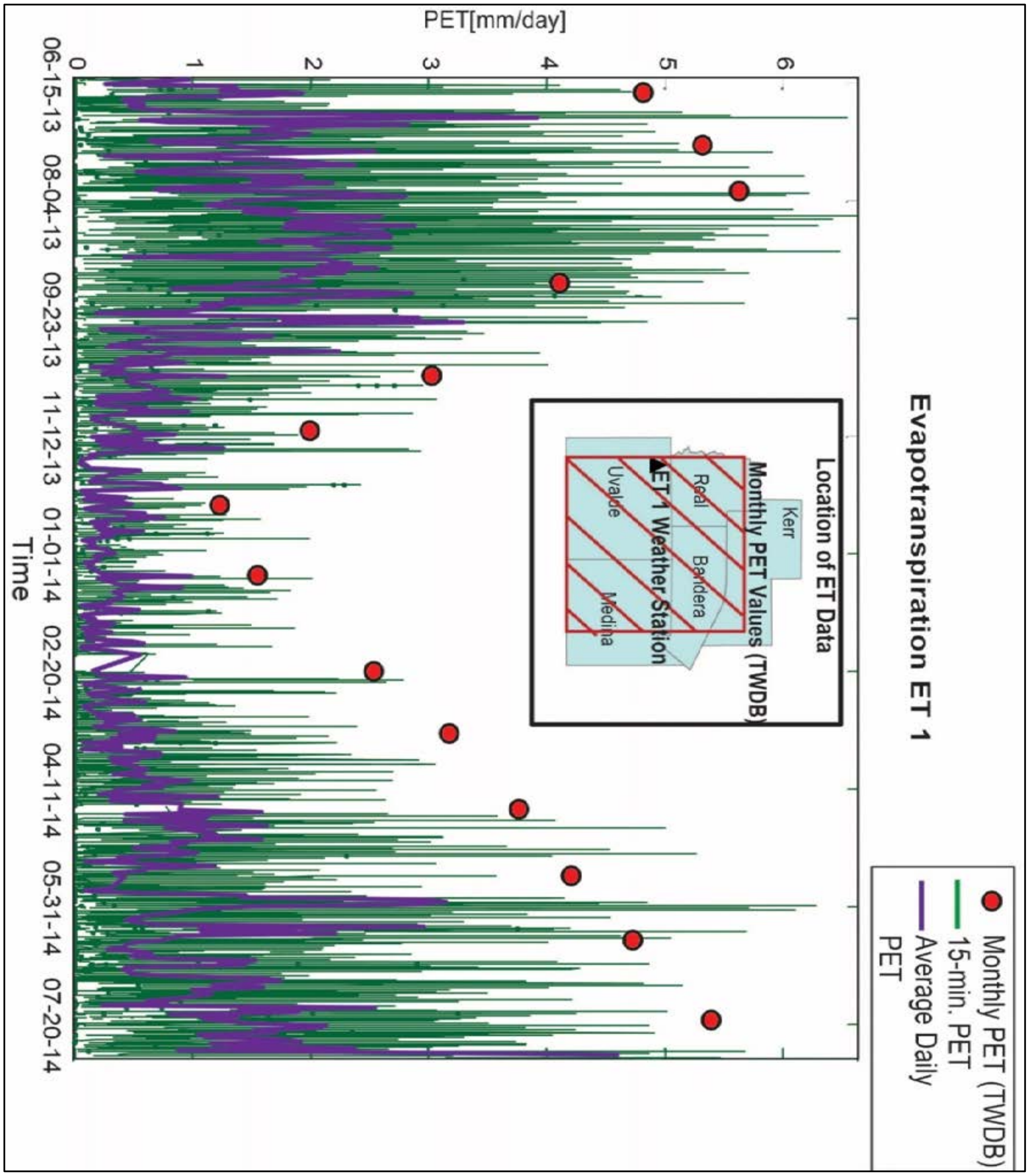

Figure 3.2. Shows the average potential evapotranspiration from the Nueces River near Durnell and NUE010. The fifteen minute data is displayed in green, daily average in purple, and monthly PET from the TWDB for the Uvalde area is displayed with red dots (TWDB, 2013). The black inset box shows where the green and purple PET values were collected at ET 1 Weather Station and the red dots were collected from the larger area cross-hatched in red.

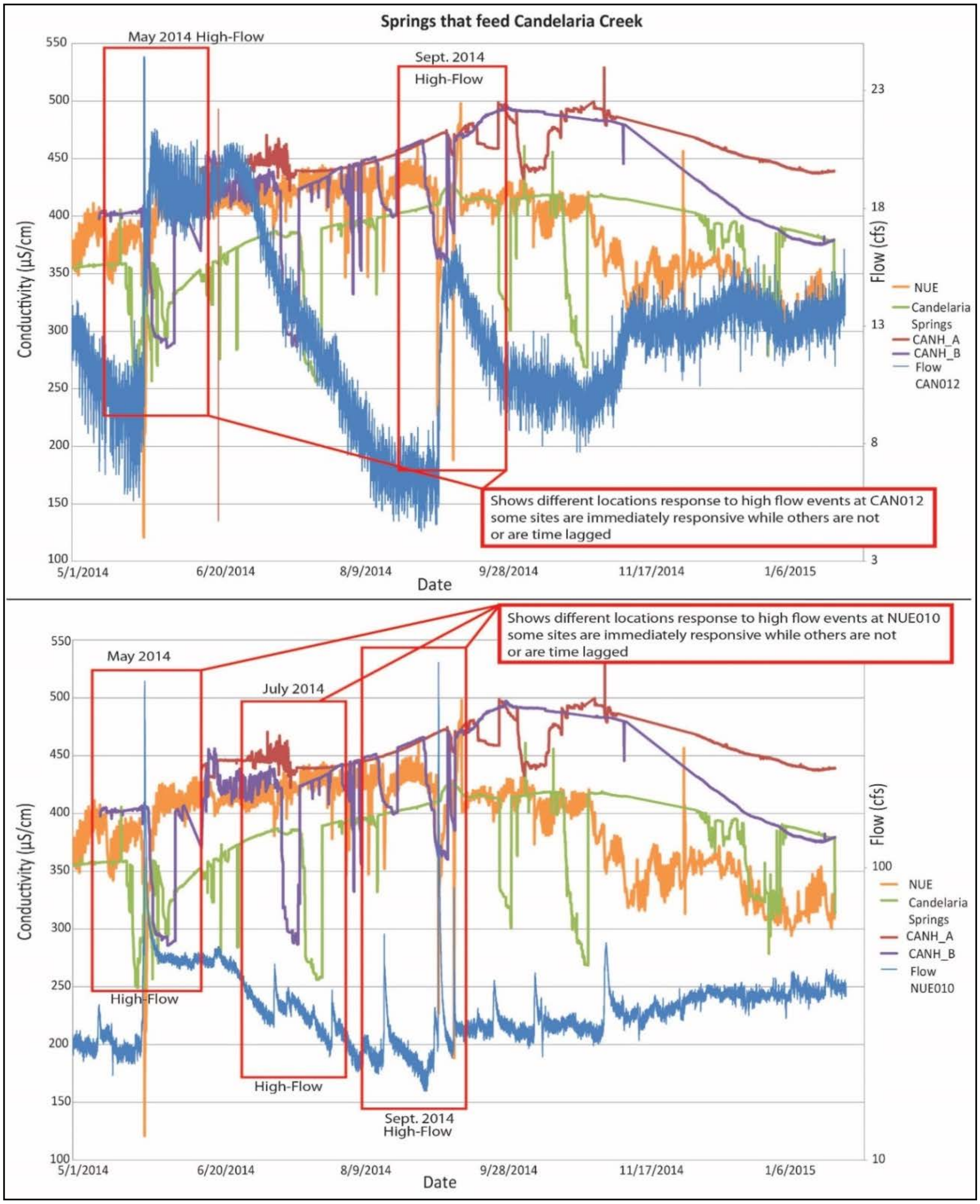

Figure 3.3. Specific conductance measured in the Nueces River near NUE010 and the springs that contribute to Candelaria Creek noted in the graph as orange, green, red, and purple lines. The blue line is flow from CAN012 in the top graph and NUE010 in the bottom graph. The red boxes outline times of high flow.

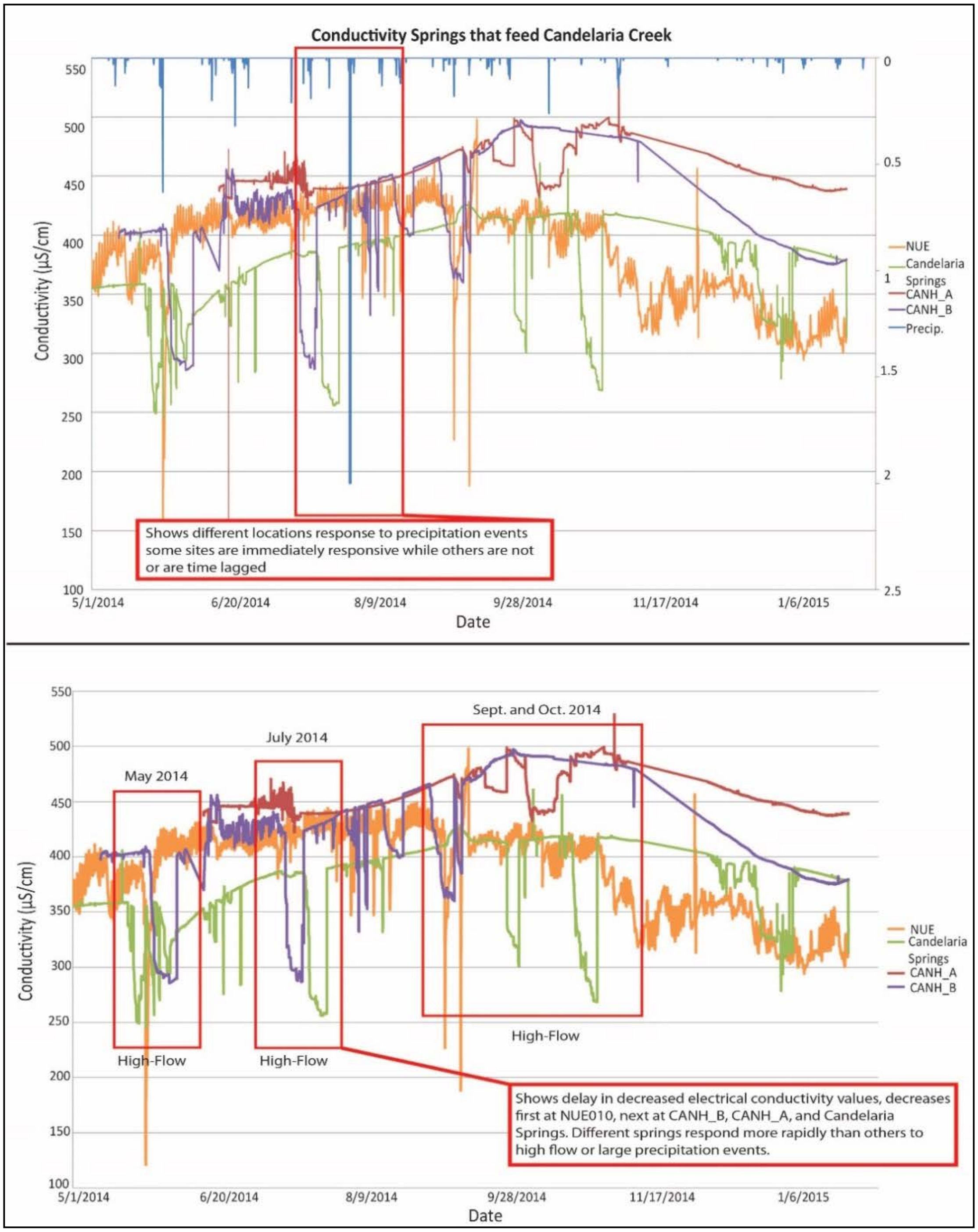

Figure 3.4. Specific conductance measured in the Nueces River near NUE010 and springs that contribute to Candelaria Creek noted in the graph as orange, green, red, and purple lines. The blue line is rain near NUE010 in the upper plot and the lower plot shows specific conductance. The red boxes outlines times of high flow.

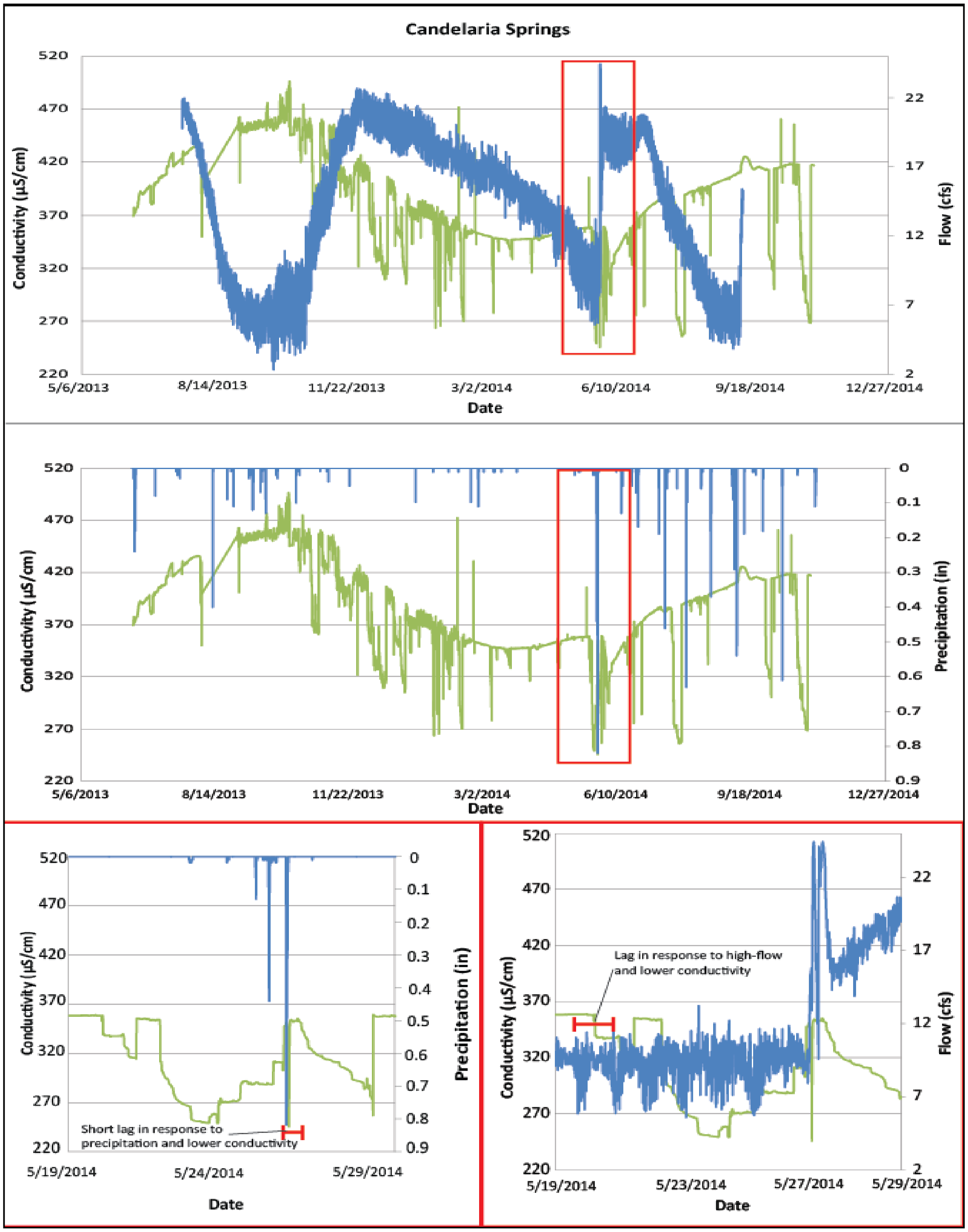

Figure 3.5. Candelaria Springs specific conductance shown with precipitation and flow (blue lines). The red box outlines an event of large precipitation and high flow. More detail on the time periods are shown in the lower two boxes.

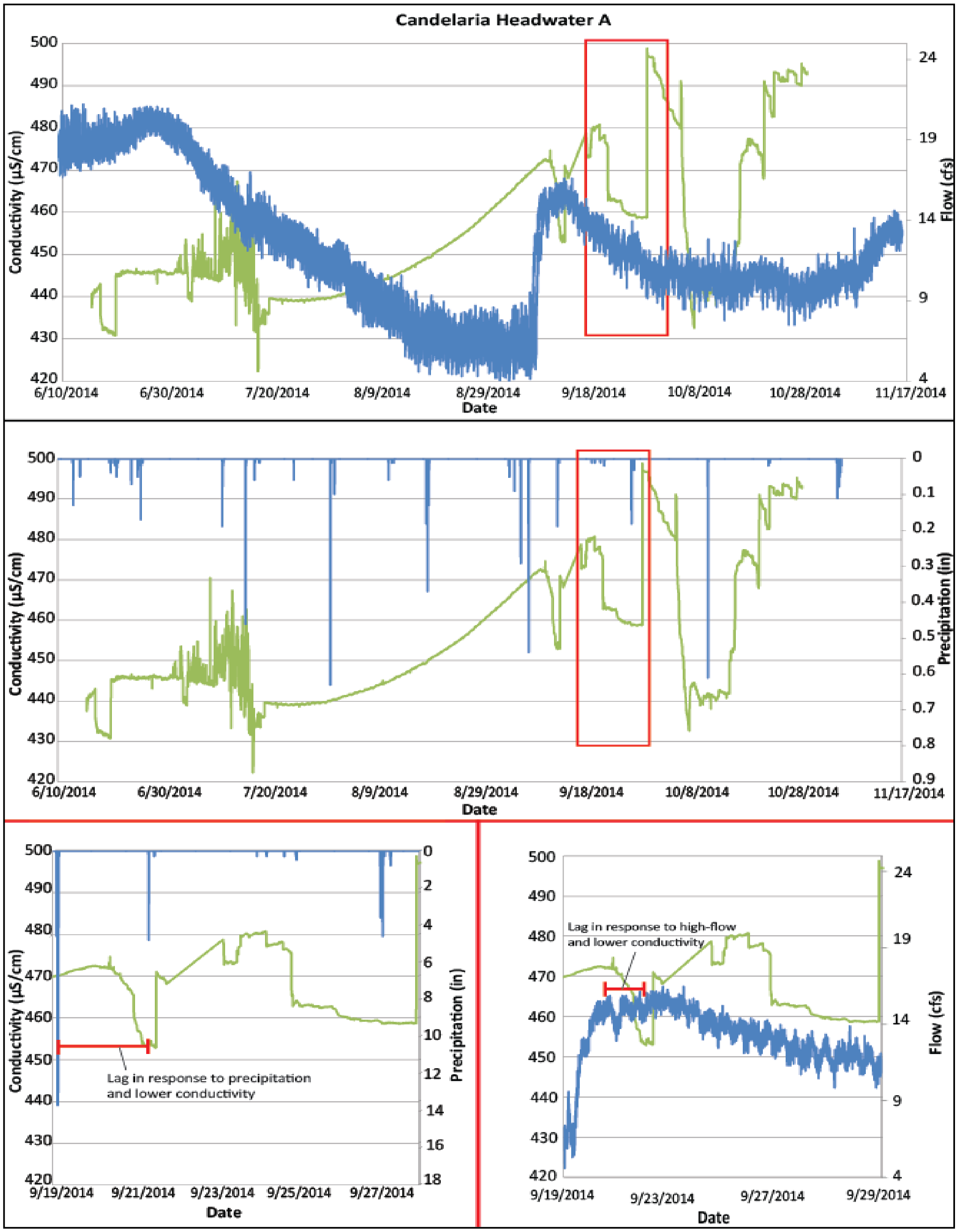

Figure 3.6. Candelaria Headwater Springs A specific conductance shown with precipitation and flow (blue lines). The red box outlines an event of large precipitation and high flow. More detail on the time periods are shown in the lower two boxes.

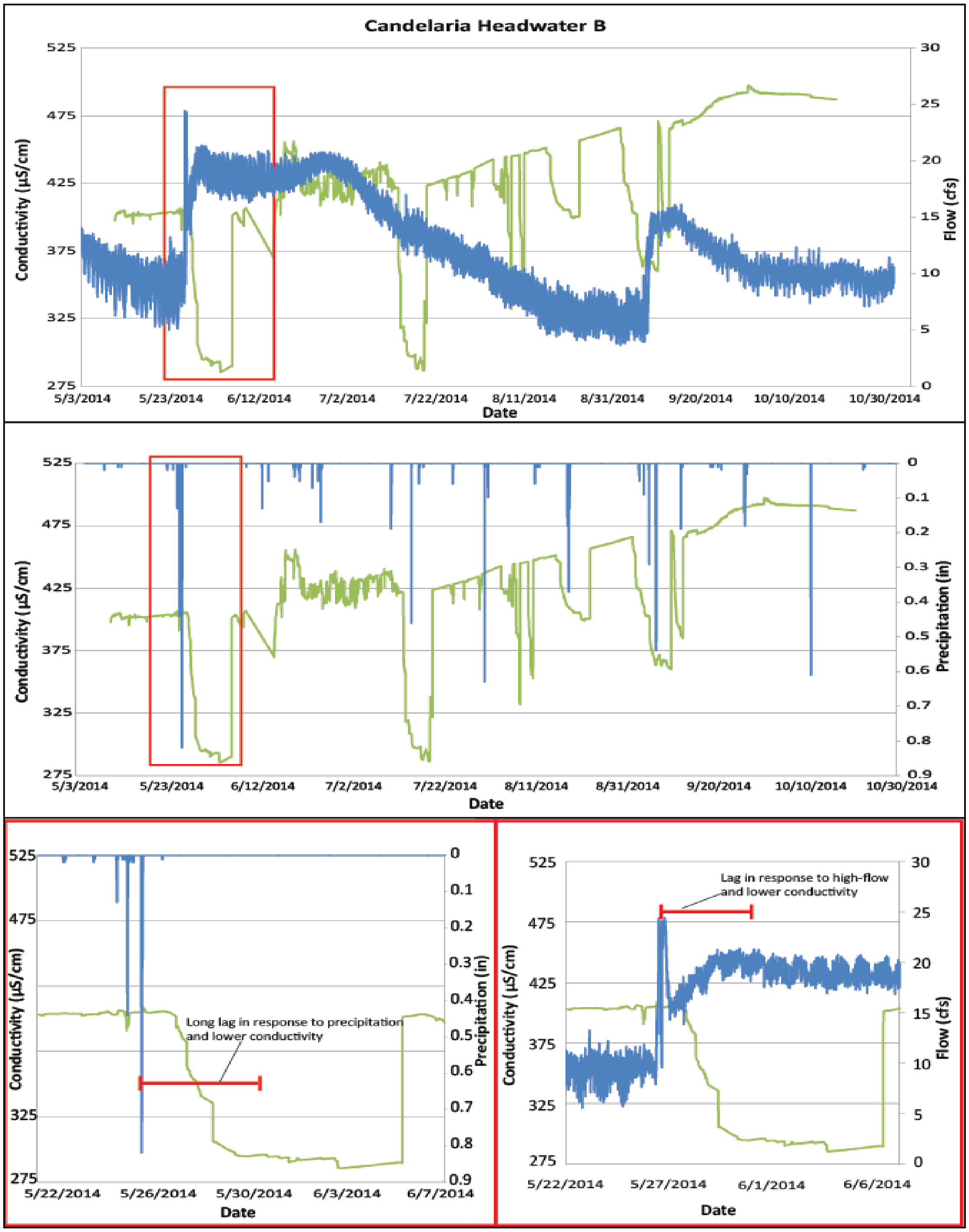

Figure 3.7. Candelaria Headwater Springs B specific conductance shown with precipitation and flow (blue lines). The red box outlines an event of large precipitation and high flow. These time periods are shown in the lower two boxes in more detail.

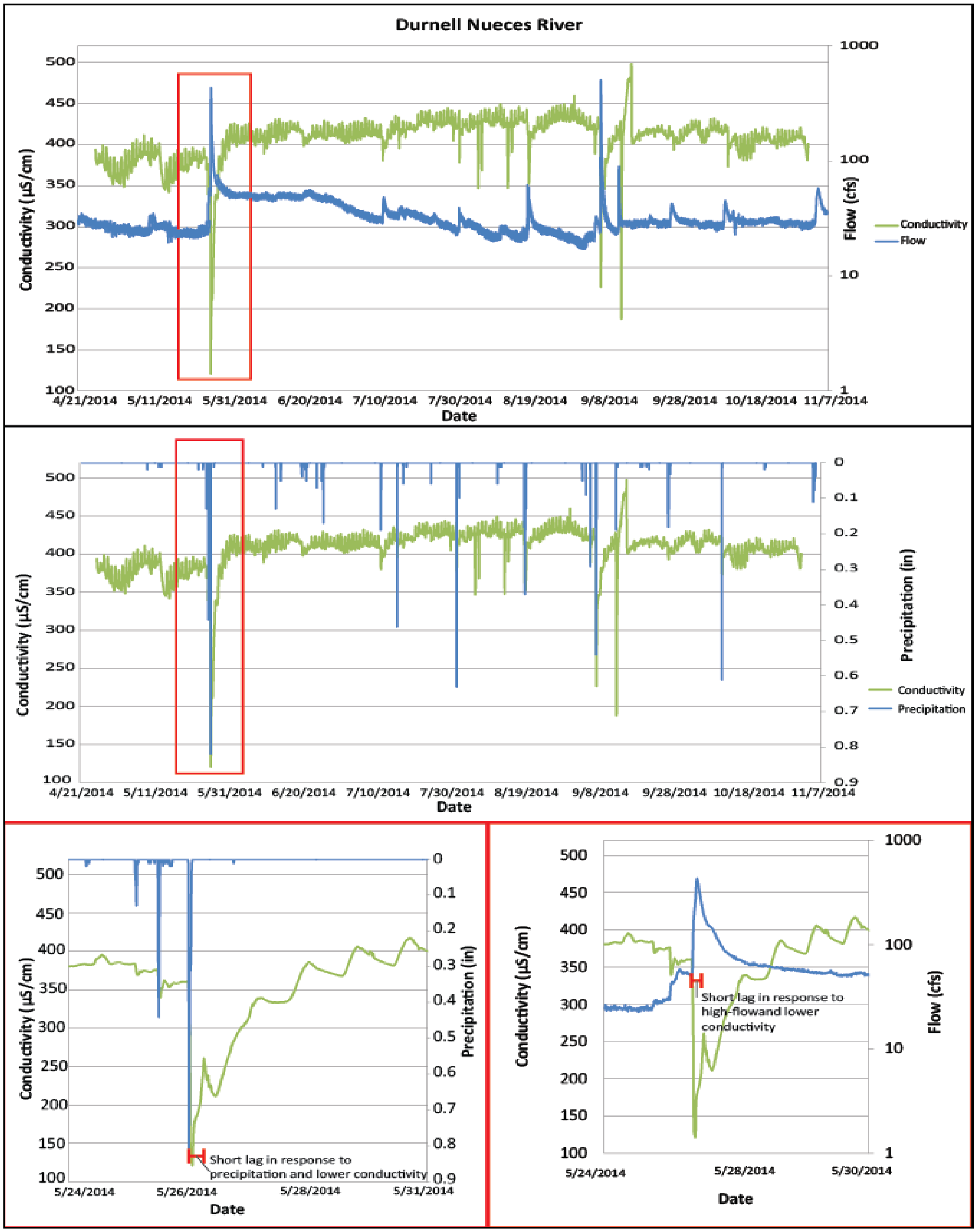

Figure 3.8. Nueces River near NUE010 specific conductance shown with precipitation and flow (blue lines). The red box outlines an event of large precipitation and high flow. More detail on the time periods are shown in the lower two boxes.

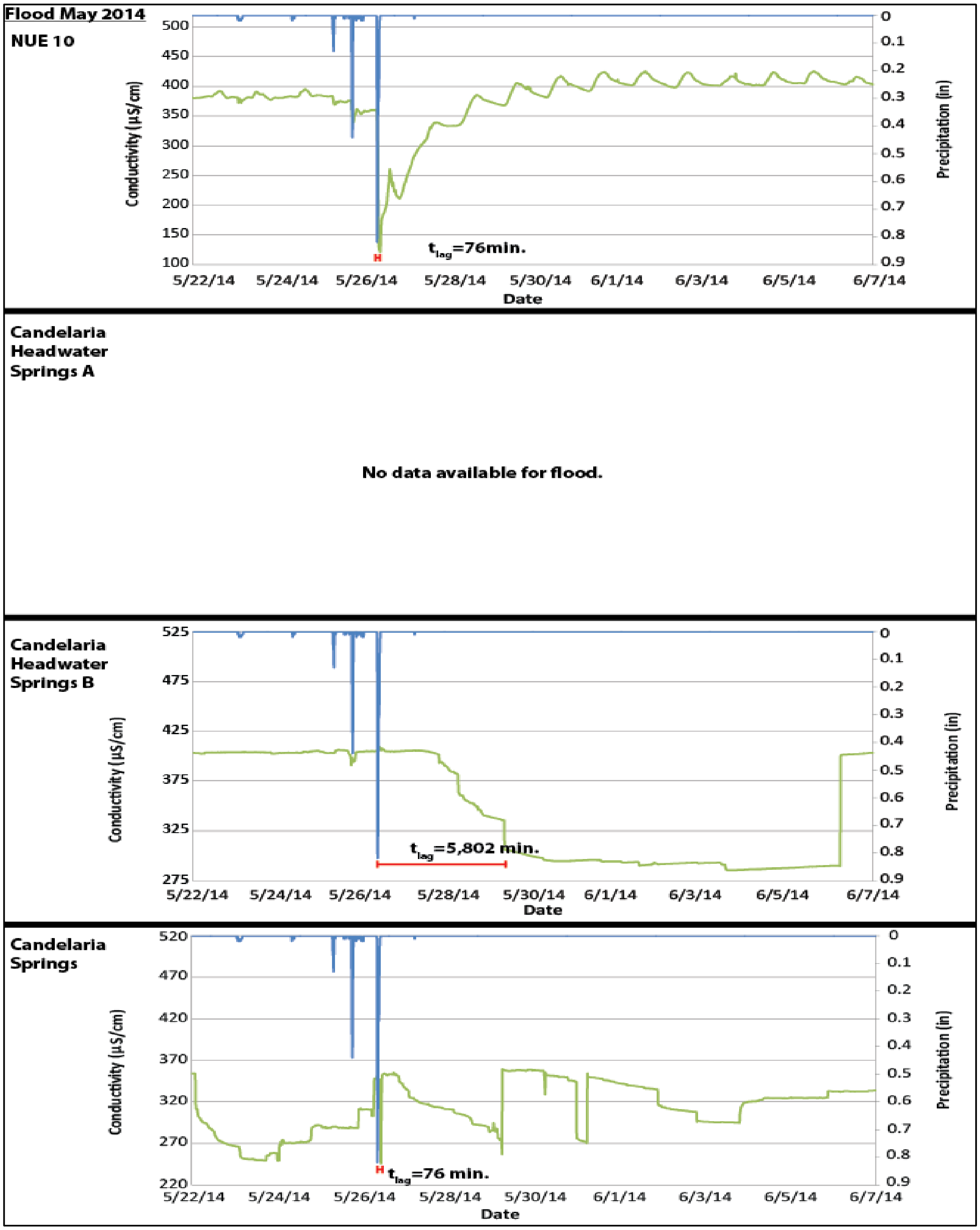

Figure 3.9. The graph shows the response of the Nueces River and springs that contribute flow to Candelaria Creek during a large precipitation event in May 2014 (blue line). This shows the propagation of a flood in this system and associated time lag from upstream to downstream (top to bottom).

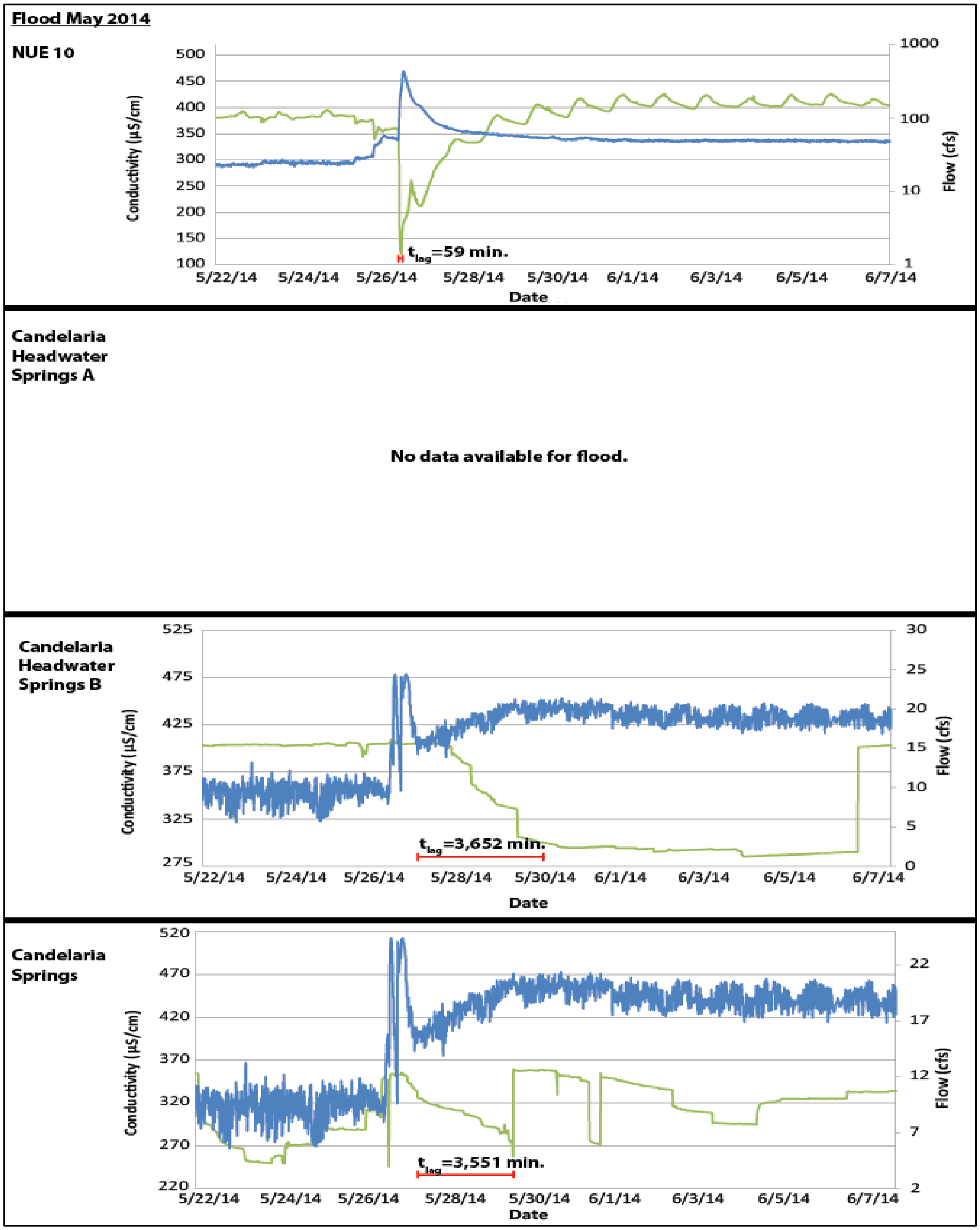

Figure 3.10. The graph shows the response of the Nueces River and springs that contribute flow to Candelaria Creek during a large flow event in May 2014 (blue line). This shows the propagation of a flood in this system and associated time lag from upstream to downstream (top to bottom).

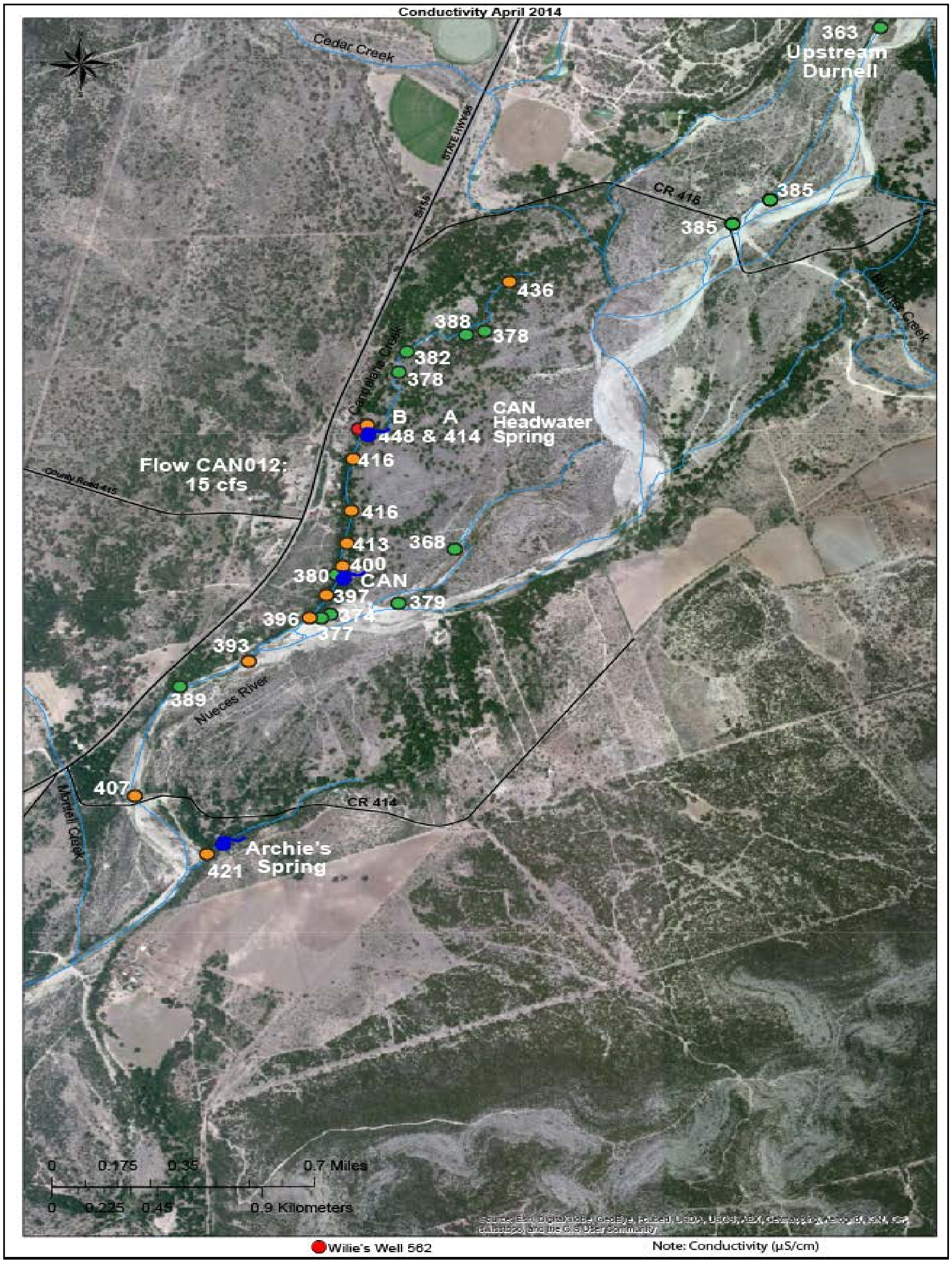

Figure 3.11. Synoptic specific conductance in April 2014. Low specific conductance signature is green, mid-level specific conductance is orange, and high specific conductance signature is red.

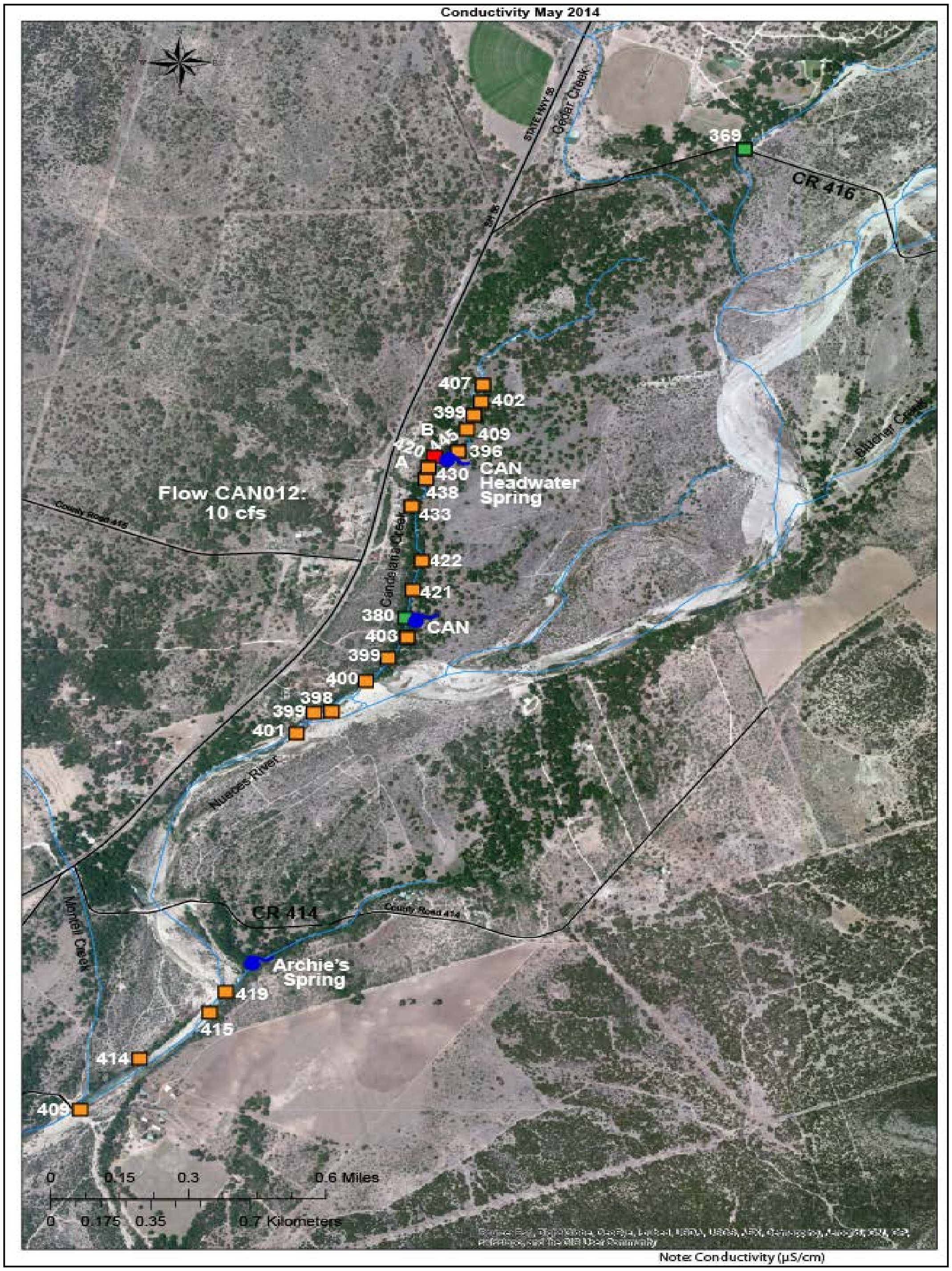

Figure 3.12. Synoptic specific conductance in May 2014. Low specific conductance signature is green, mid-level specific conductance is orange, and high specific conductance signature is red.

Figure 3.13. Synoptic specific conductance in August 2013. Low specific conductance signature is green, mid-level specific conductance is orange, and high specific conductance signature is red.

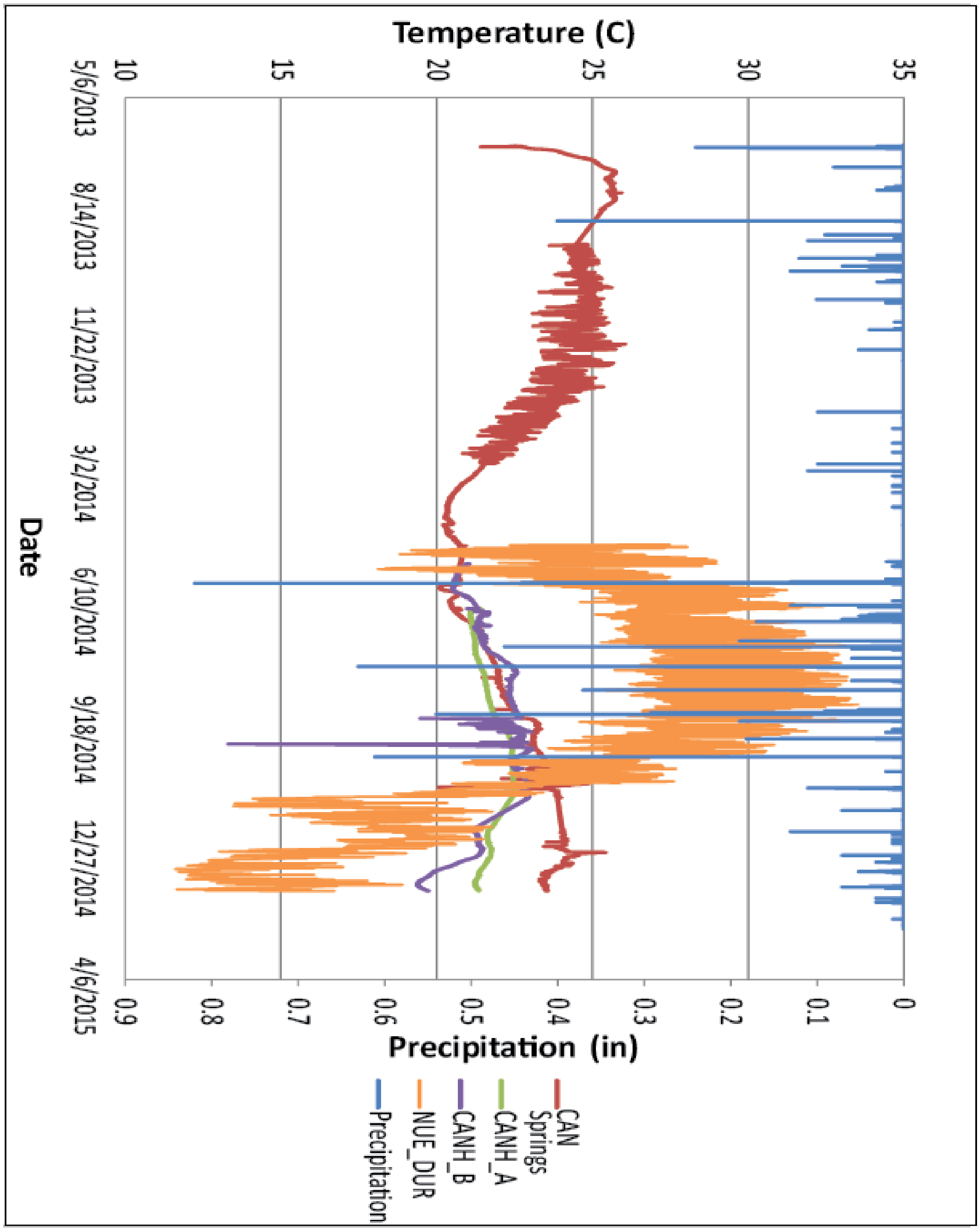

Figure 3.14. Temperature response to precipitation (blue lines) recorded in the springs that contribute flow to Candelaria Creek and the Nueces River near NUE010 (red, green, purple, and orange lines).

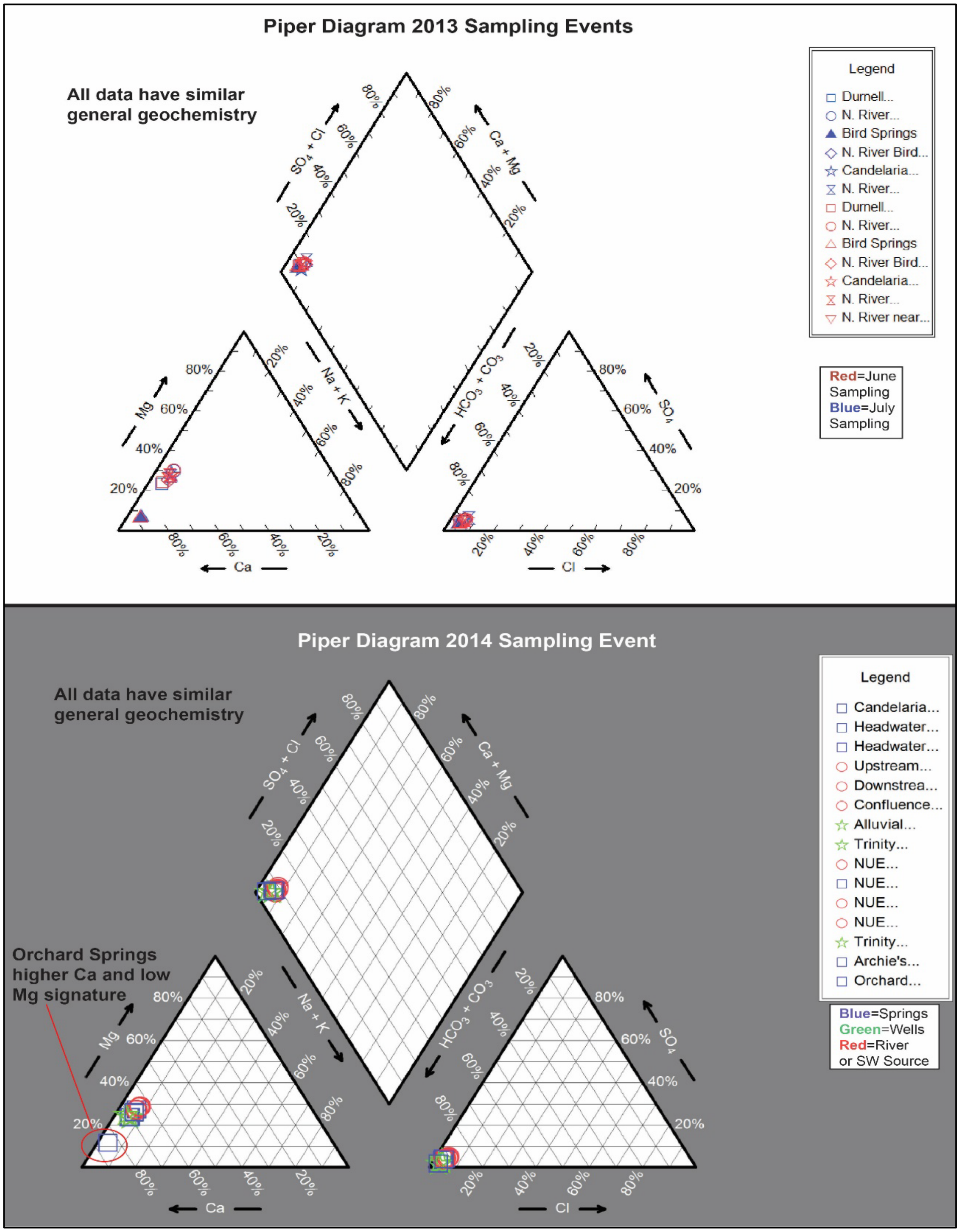

Figure 3.15. Piper diagrams of general water chemistry collected in June and July 2013 and July 2014 of springs, surface water, and wells.

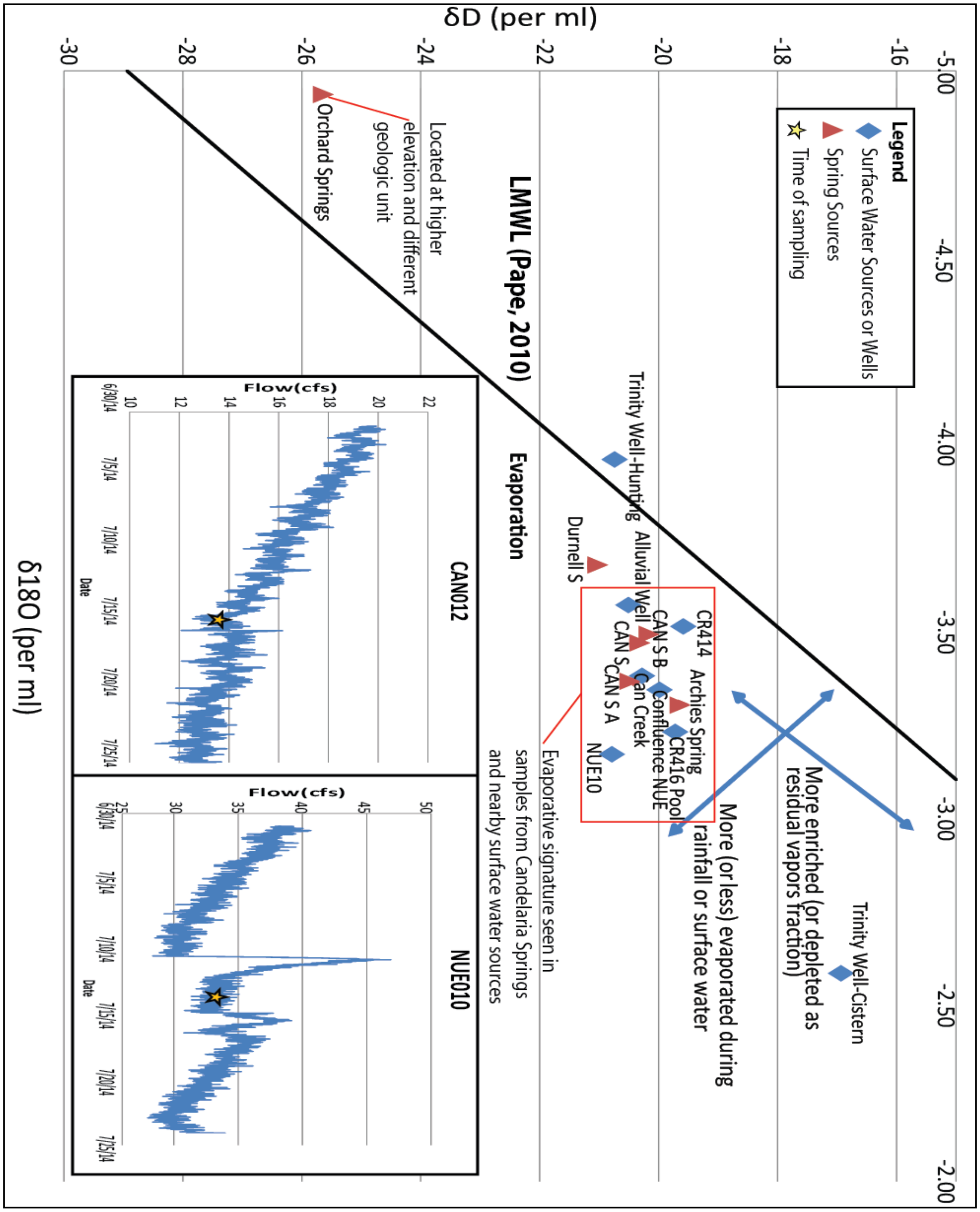

Figure 3.16. Oxygen isotopic chemistry for surface water, wells, and springs collected in July 2014. The inset hydrographs show flow conditions at CAN012 and NUE010 at the sampling time. The black line is the local meteoritic water line from Pape, 2010. The red box denotes where the majority of samples fall.

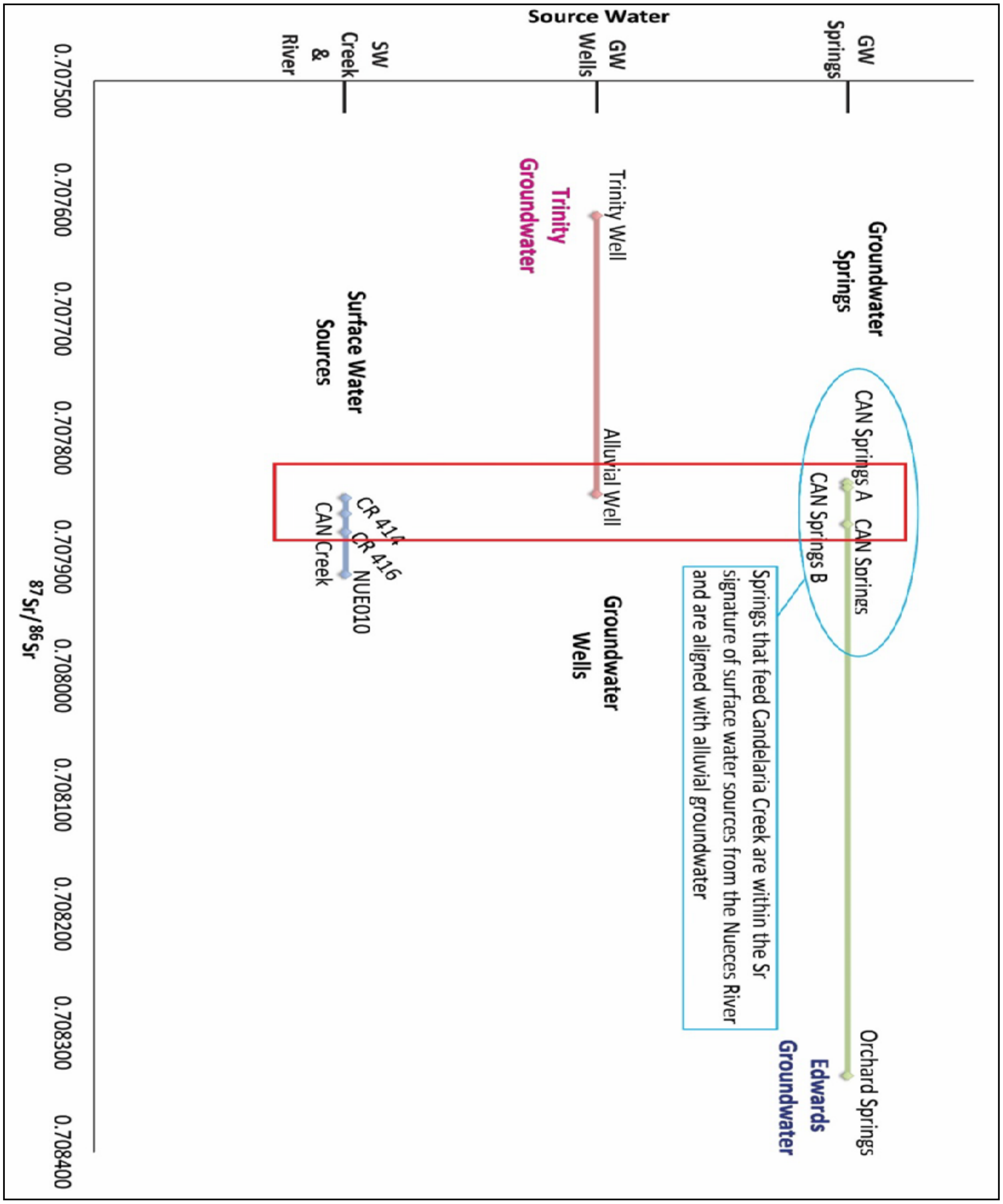

Figure 3.17. Shows the range of isotopic signatures for different source waters groundwater springs, groundwater wells, and surface water sources for samples collected in July 2014. The red box shows that the main springs that feed Candelaria Creek are very similar to the surface water sources. The Edwards and Trinity groundwater are significantly different from the general Sr isotopic signature.

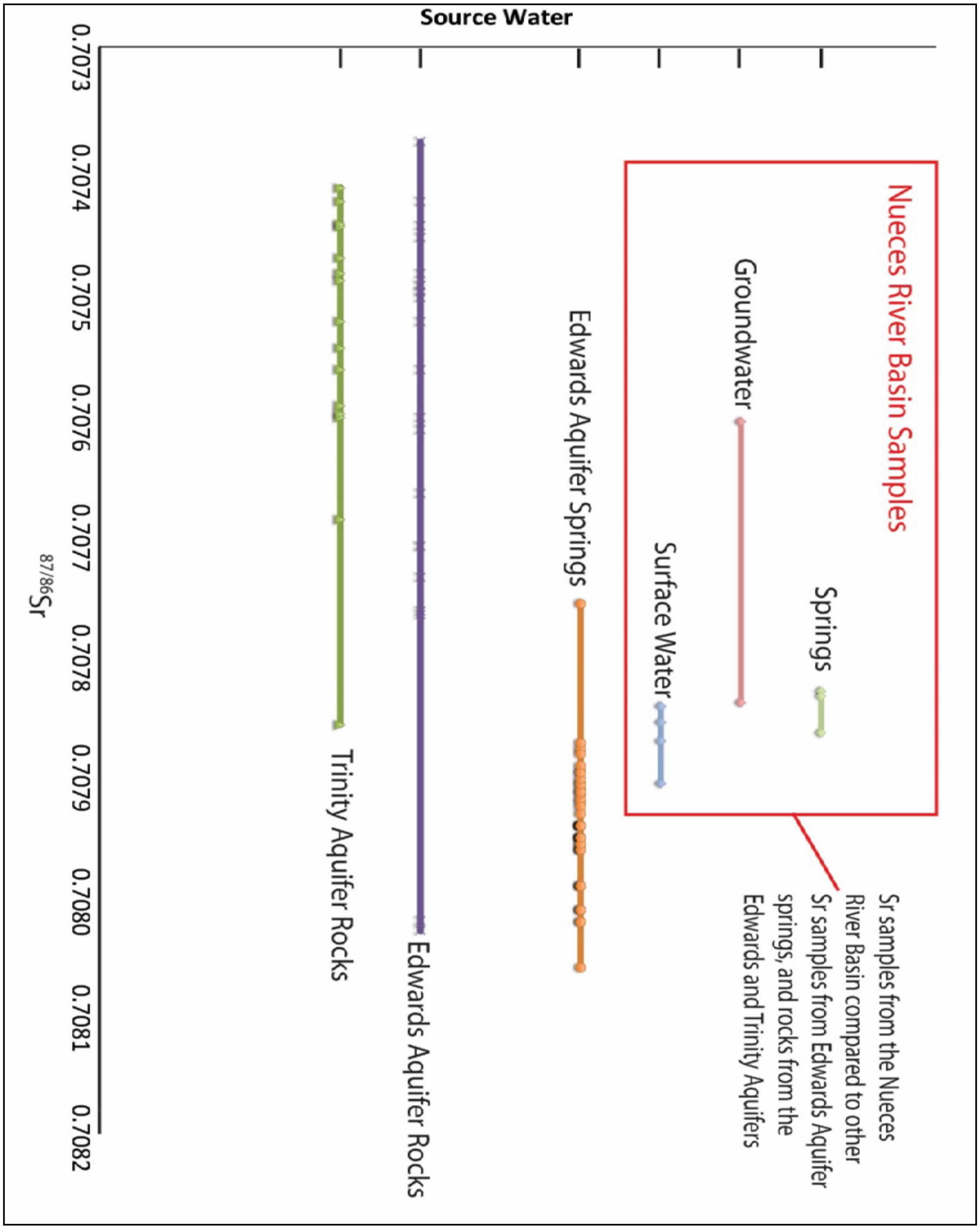

Figure 3.18. Range of Sr isotopic signatures compared to Edwards Aquifer Springs, Rocks, and Trinity Aquifer Rocks (BSEACD, 2011; Musgrove, 2010; Musgrove and Banner, 2004; Oetting, 1996; Christian et al., 2010; Wong, 2012; Koepnick, 1995). The red box highlights where the Nueces River Basin samples fall.

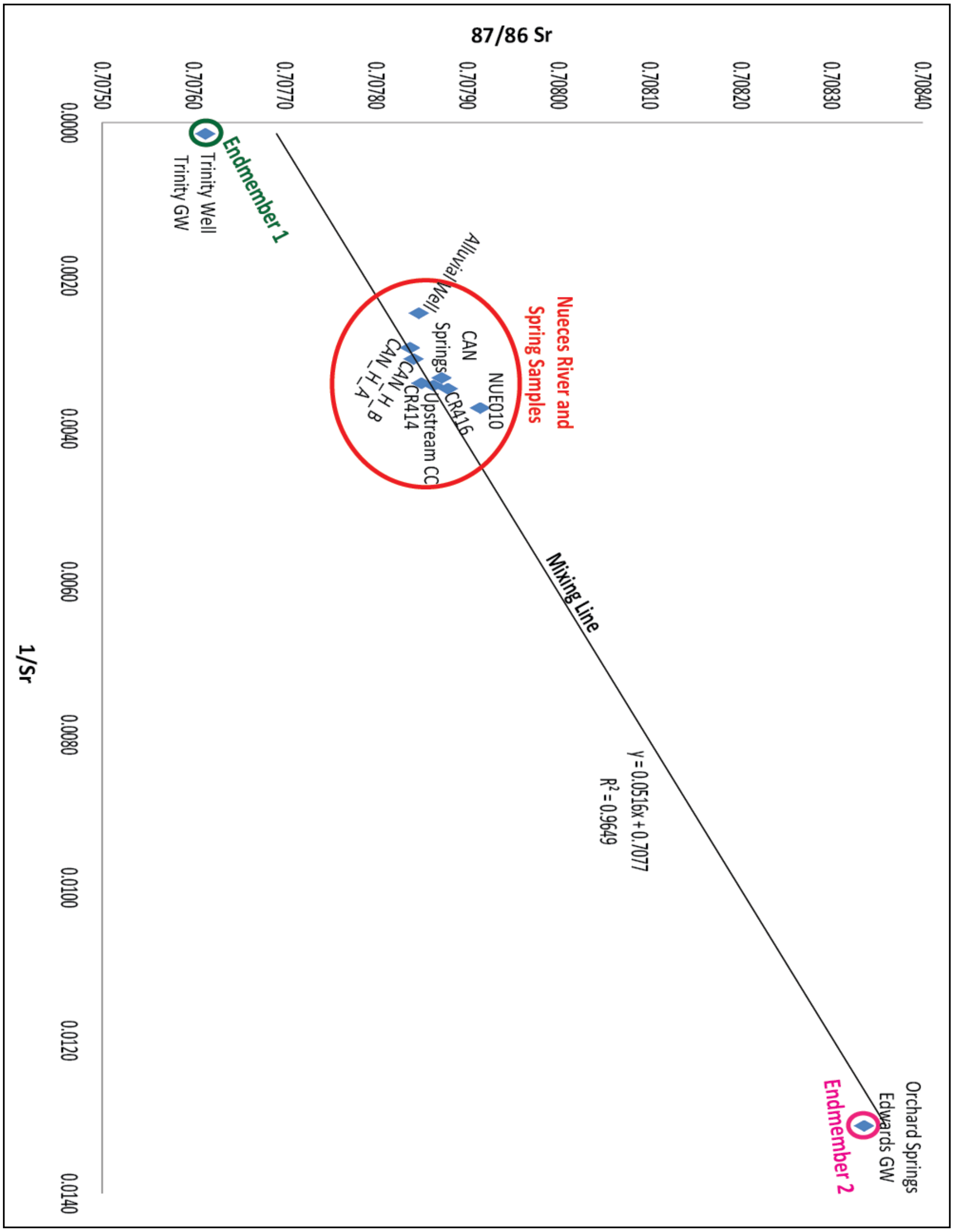

Figure 3.19. Strontium isotopic signature v. 1/Sr concentration. This shows that there are two end members: Trinity Groundwater and Edwards Groundwater. The black line is a linear regression showing a good correlation, which suggests that mixing between these two end members, is occurring.

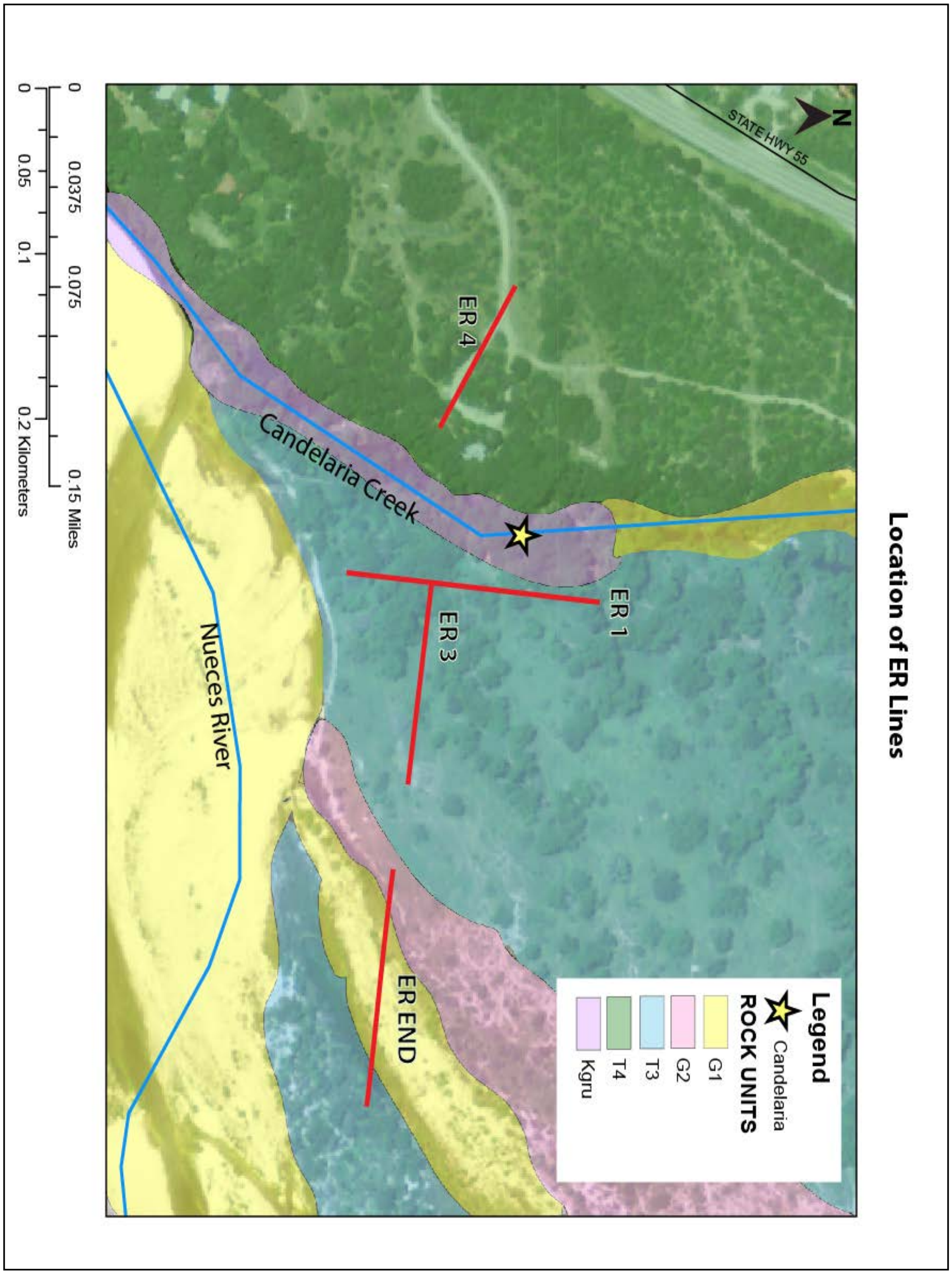

Figure 3.20. Location of ER lines near Candelaria Creek, ER lines depicted as red lines, data were gathered in October 2014.

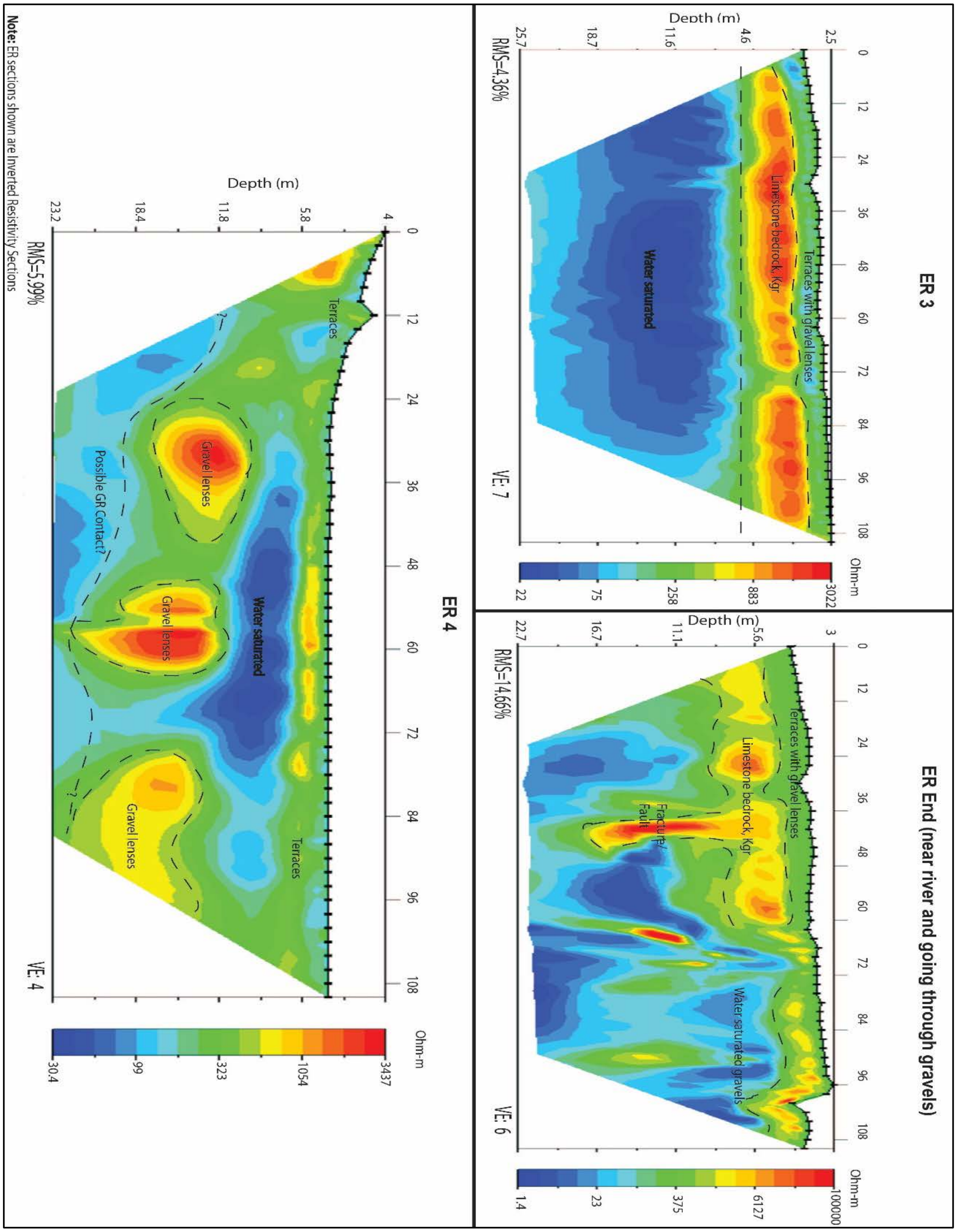

Figure 3.21. Interpreted Inverted Resistivity Sections near Candelaria Creek using the dipole-dipole array. Black dashed lines represent different contacts.

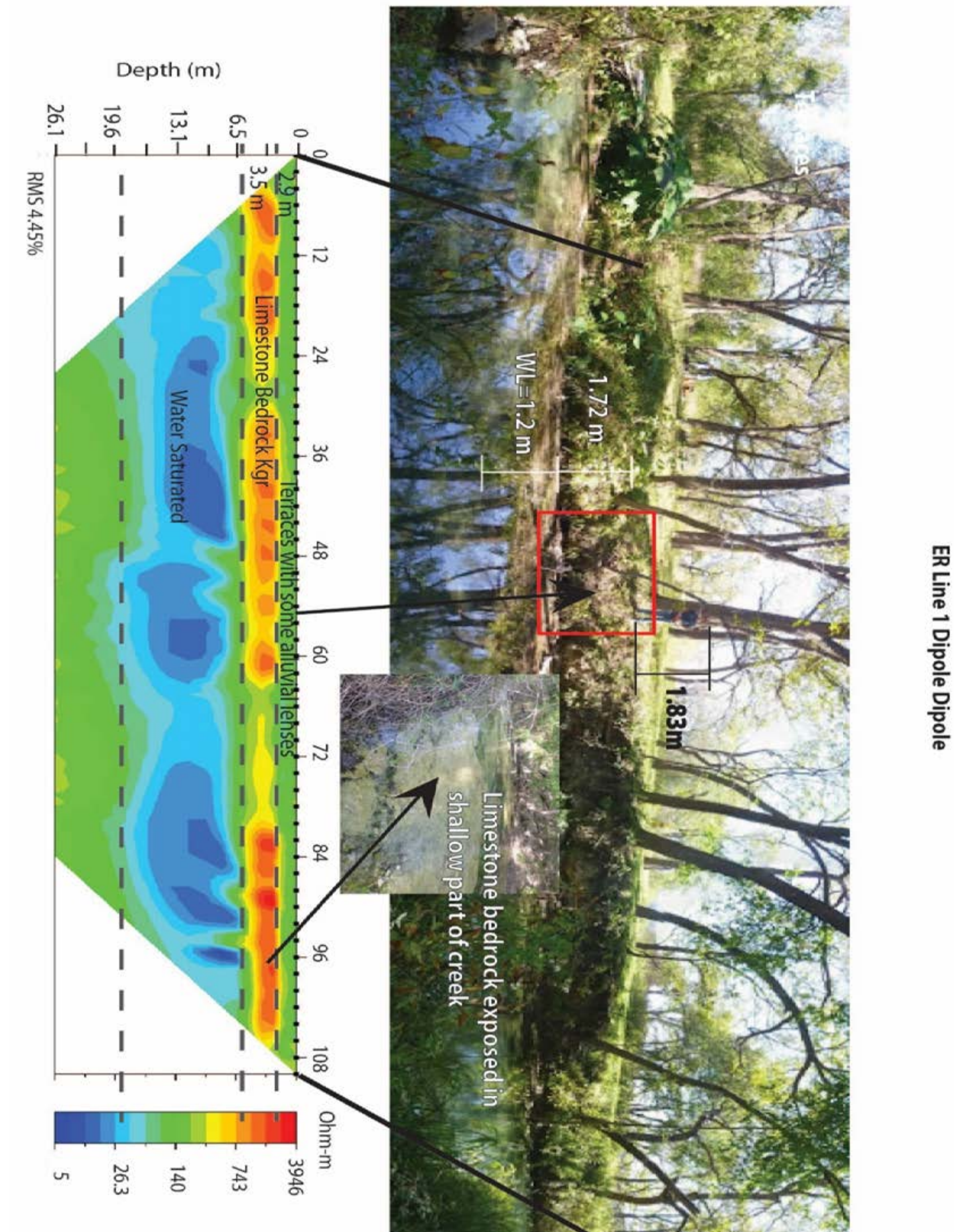

Figure 3.22. ER Line 1 Inverted Resistivity Section shown with an outcrop near where ER Line 1 data was collected, this shows the method used to ground truth the data.

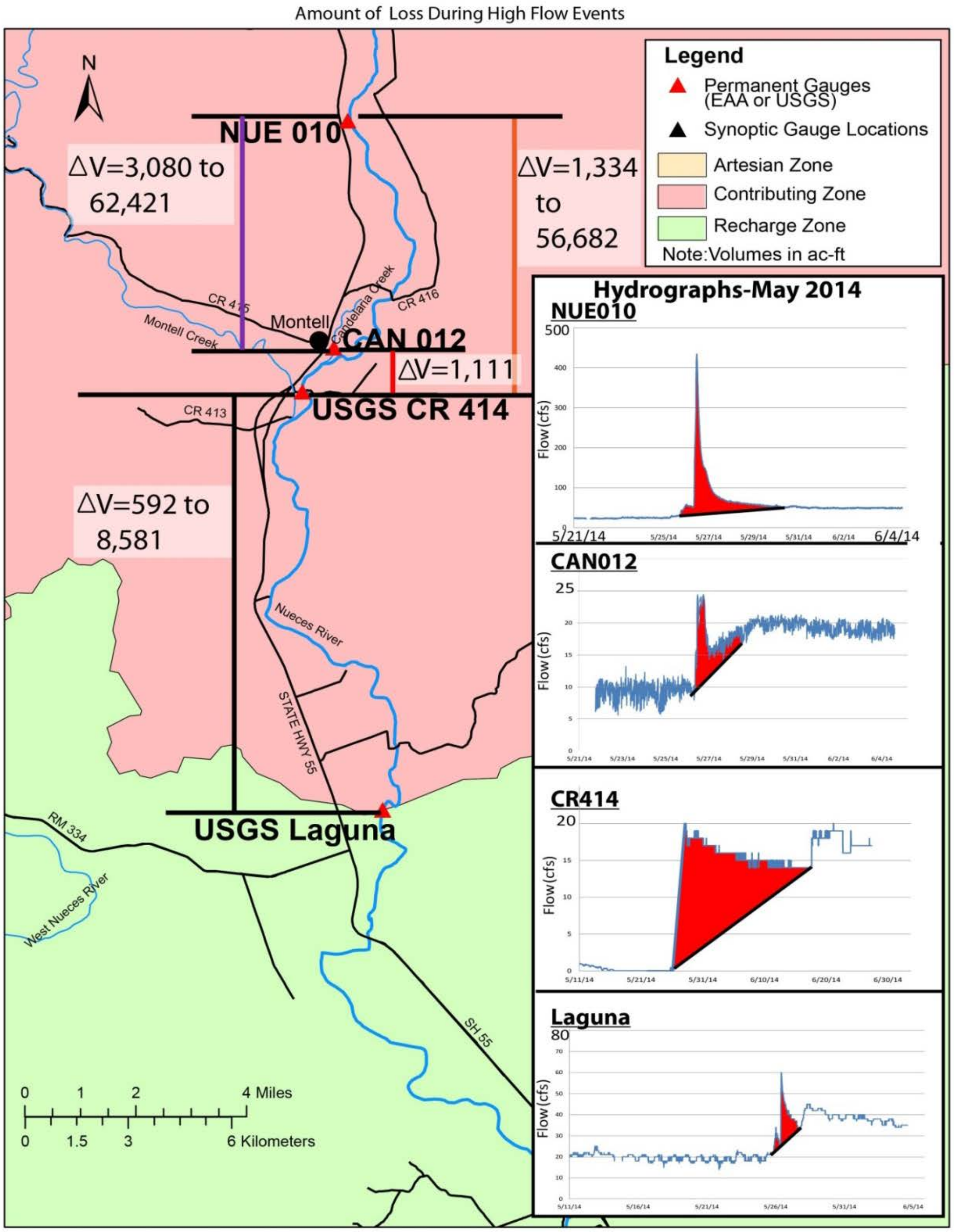

Figure 3.23. Volumetric amount of water moving through the system during high flow conditions noted as ΔV. The hydrographs on the right side of the figure illustrate how the amount of loss (ΔV) is found, as the area under the rising and falling limb (time is not necessarily aligned for each graph, but each graph covers the same time period). For more detailed hydrographs see Appendix J.

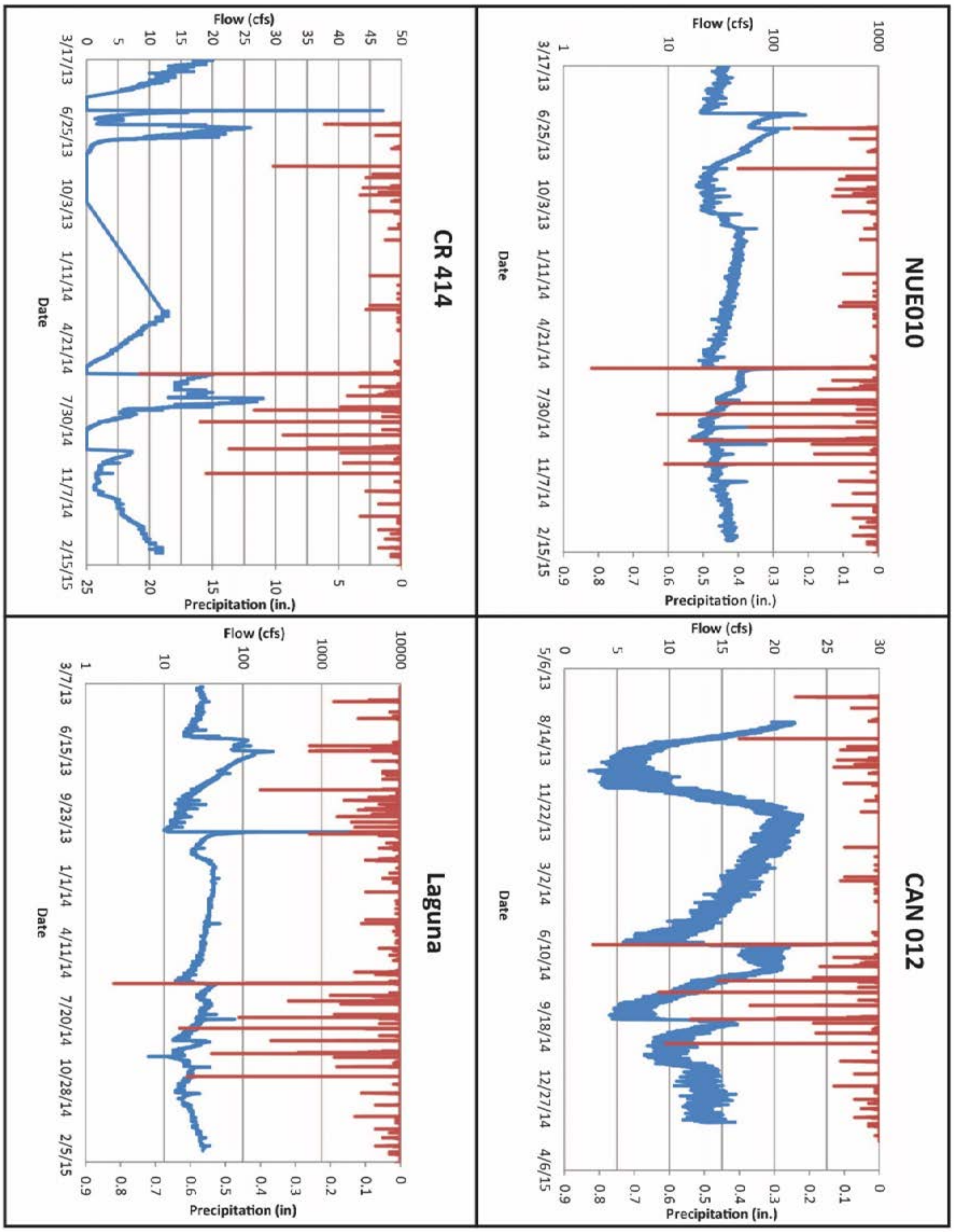

Figure 3.24. Hydrographs from left to right (upstream to downstream) shows response of flow (blue lines) to precipitation events (red lines).

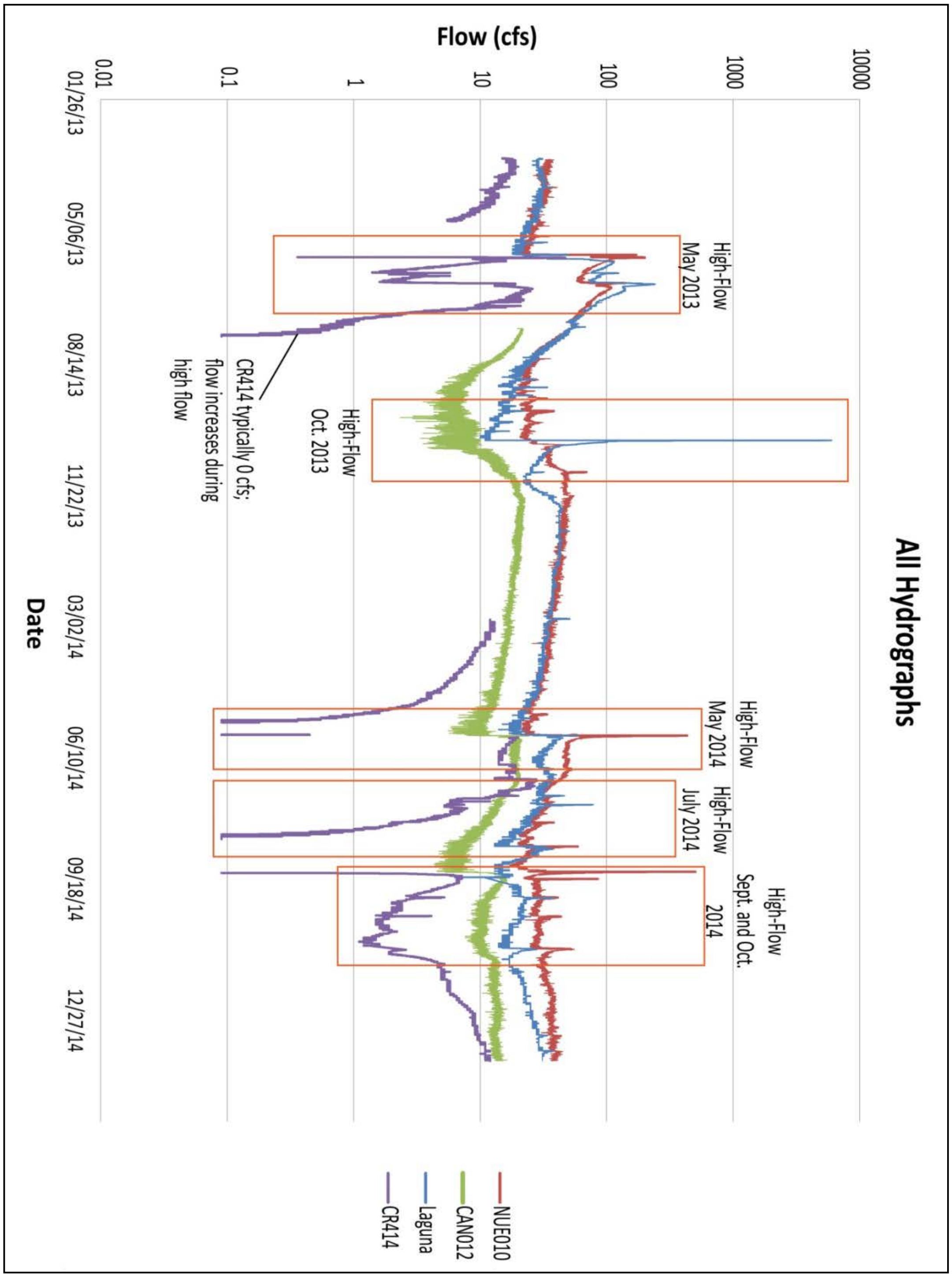

Figure 3.25. Hydrographs from the Nueces River from NUE010 to Laguna. CR414, the purple line, is typically 0 but has increased flow during precipitation or high-flow events. The red boxes outline high flow events.

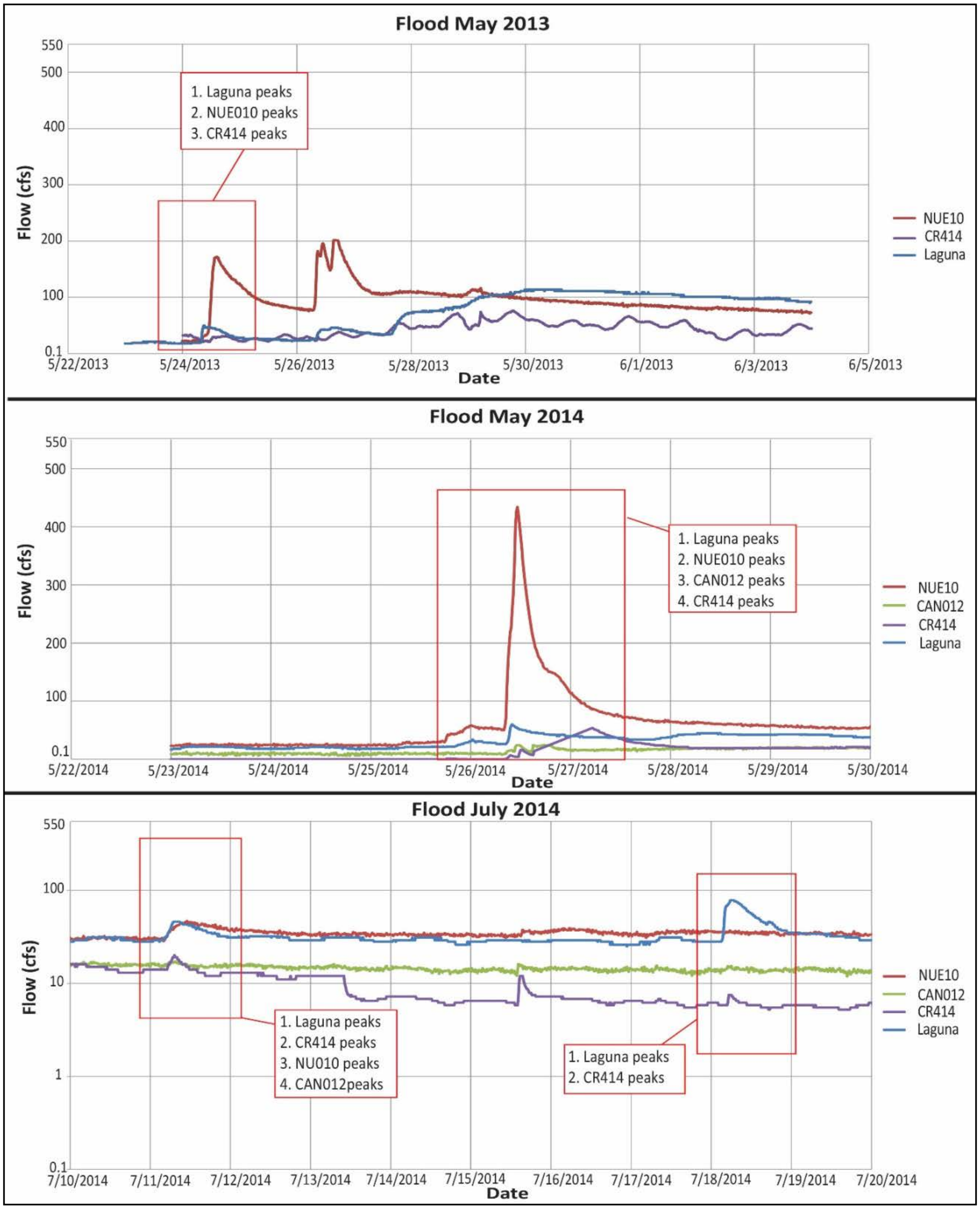

Figure 3.26. More detailed hydrographs of flood events and how they propagate through the system. The red boxes highlight the order of peak flow in the system. (Sometimes there is no peak flow at certain gauges).

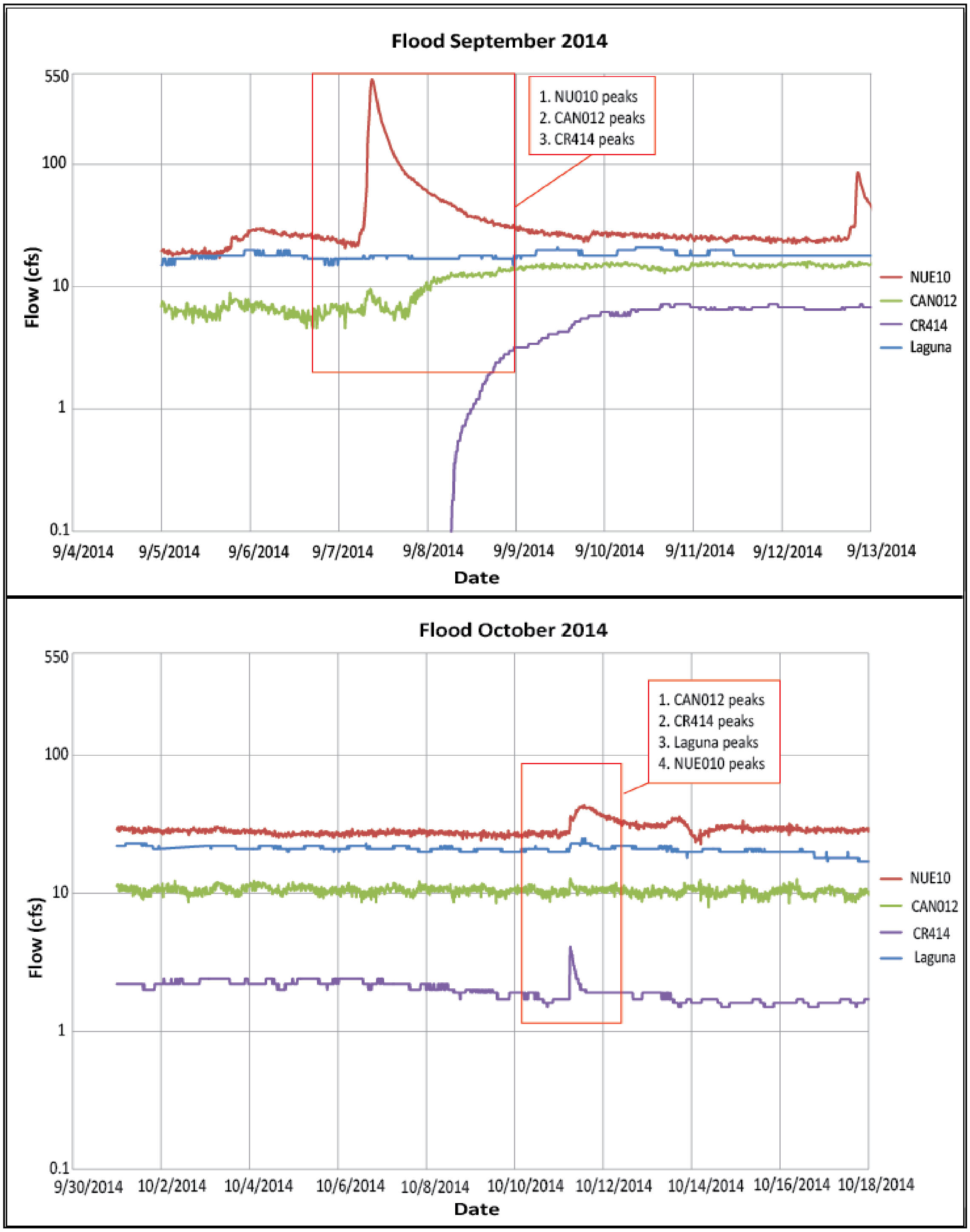

Figure 3.27. More detailed hydrographs of flood events and how they propagate through the system. The red boxes highlight the order of peak flow in the system. (Sometimes there is no peak flow at certain gauges).

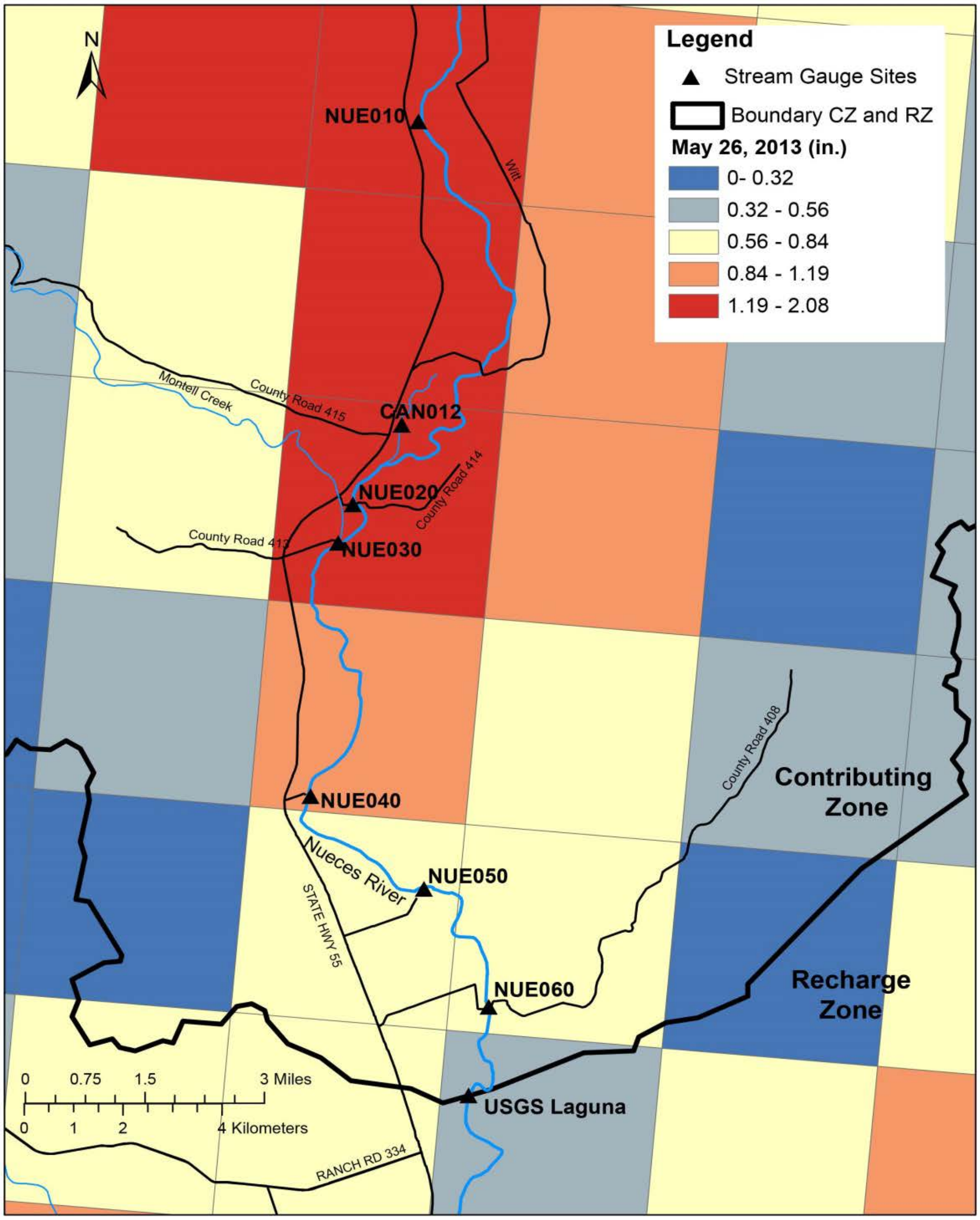

Figure 3.28. Location and intensity of precipitation shown with NexRad data obtained from the EAA in the storm on May 2013. Rain is daily total in inches. The areas that had the most rain are red and the areas with little to no precipitation are blue.

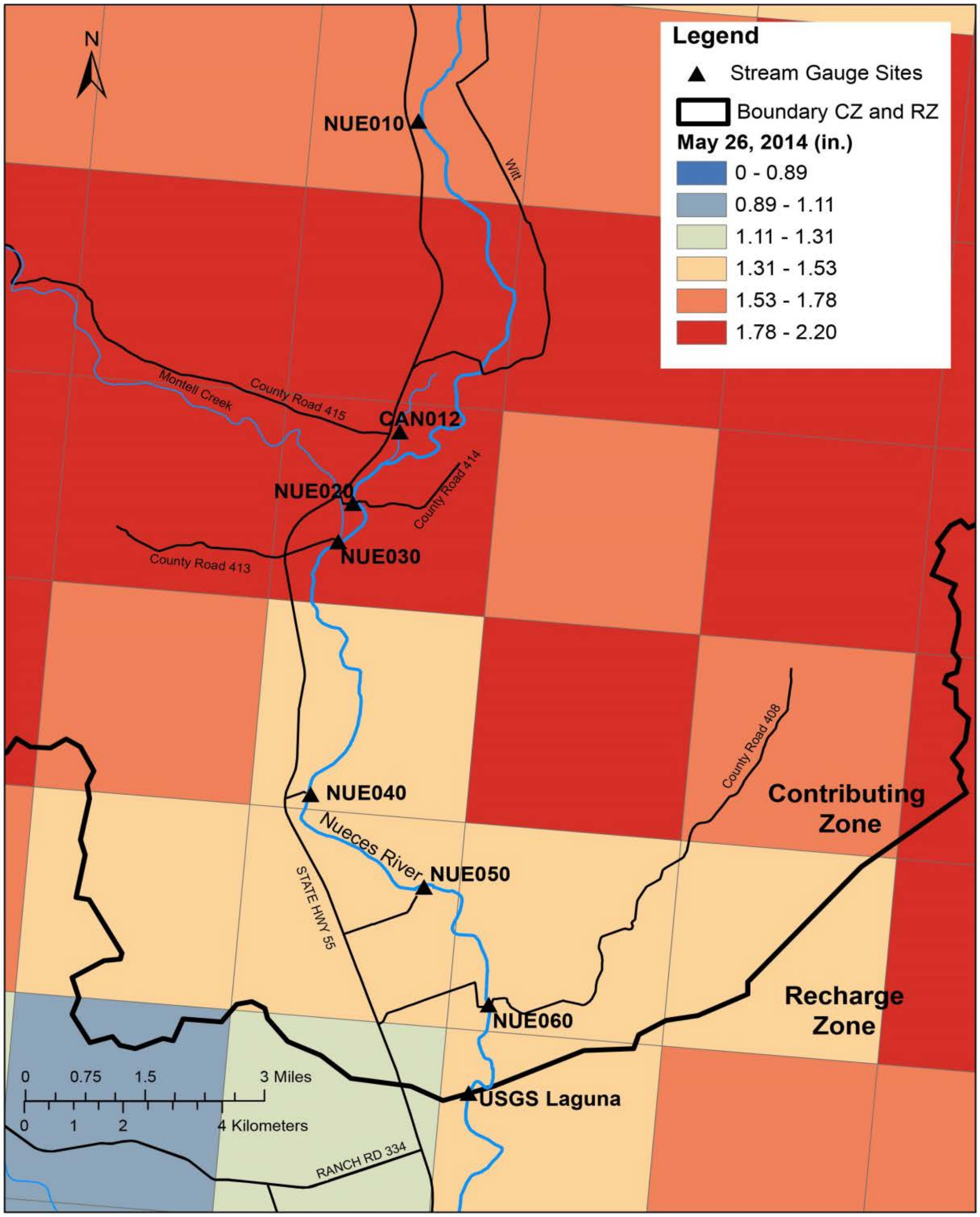

Figure 3.29. Location and intensity of precipitation shown with NexRad data obtained from the EAA in the storm on May 2014. Rain is daily total in inches. The areas that had the most rain are red and the areas with little to no precipitation are blue.

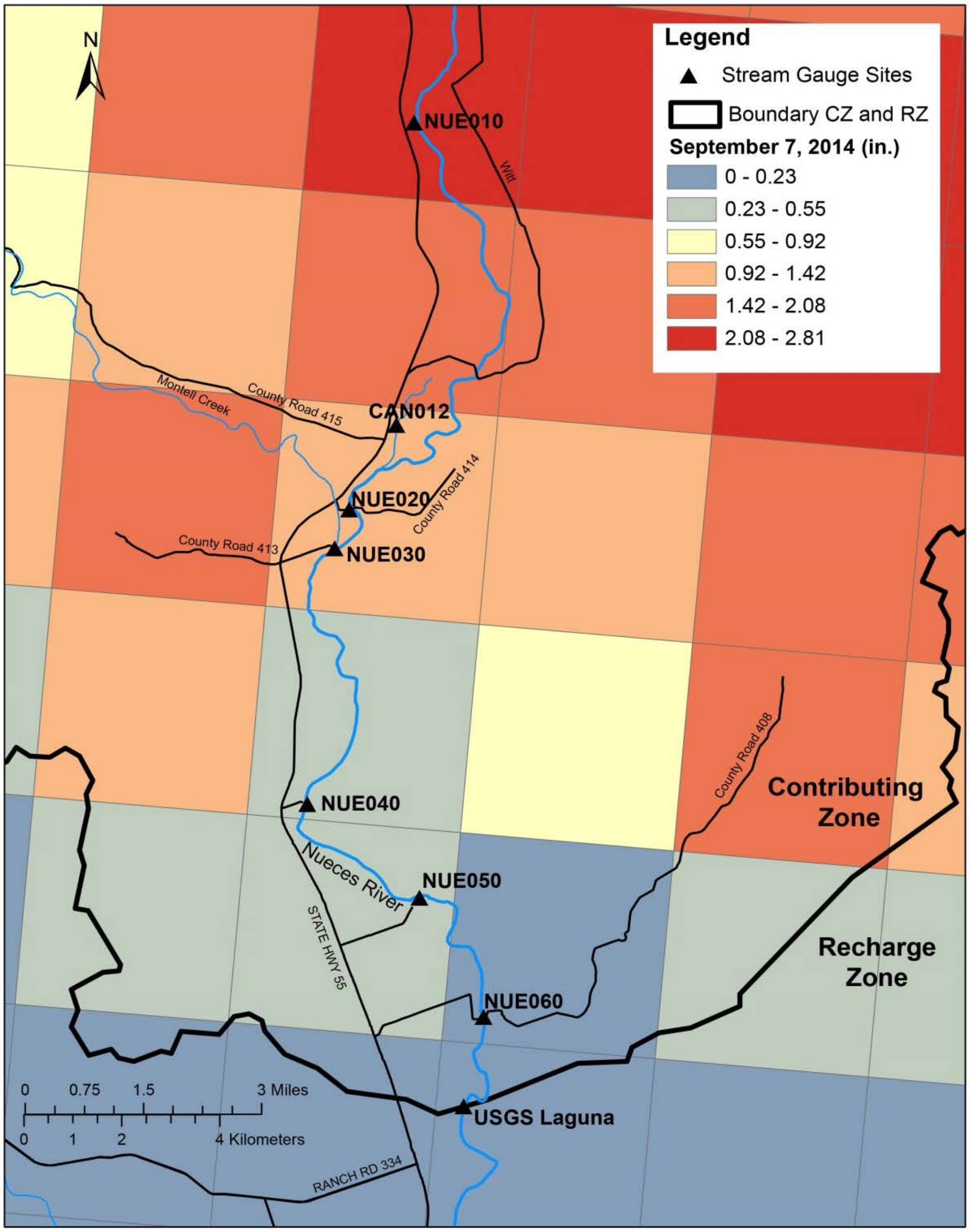

Figure 3.30. Location and intensity of precipitation shown with NexRad data obtained from the EAA in the storm on September 2014. Rain is daily total in inches. The areas that had the most rain are red and the areas with little to no precipitation are blue

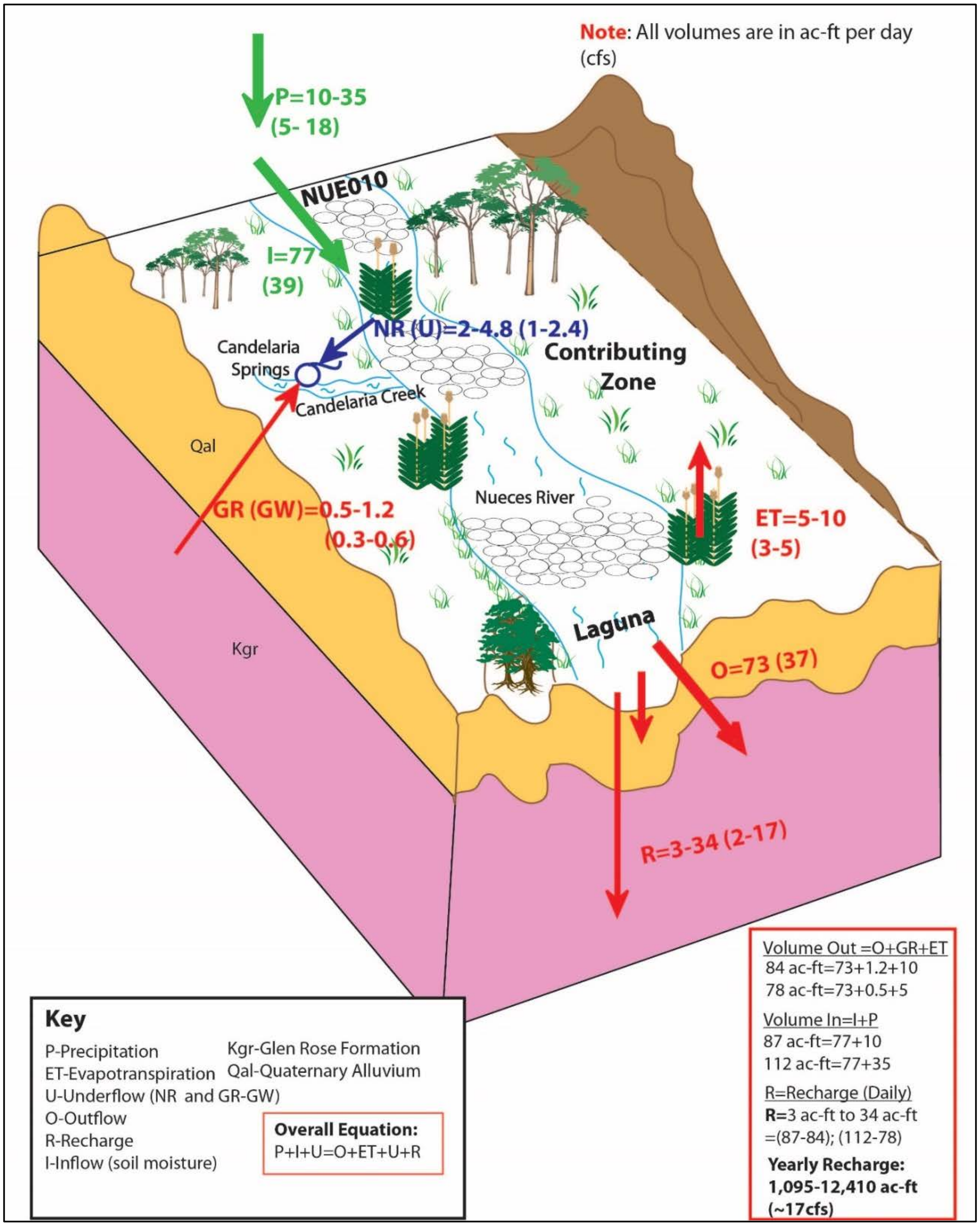

Figure 3.31. Water balance of the Nueces River system in the area of study includes the main outflows and inflows in this system on a daily basis. Note volumes are estimated daily averages in ac-ft. and cfs in parentheses. The annual amount of recharge is outlined in the red box.

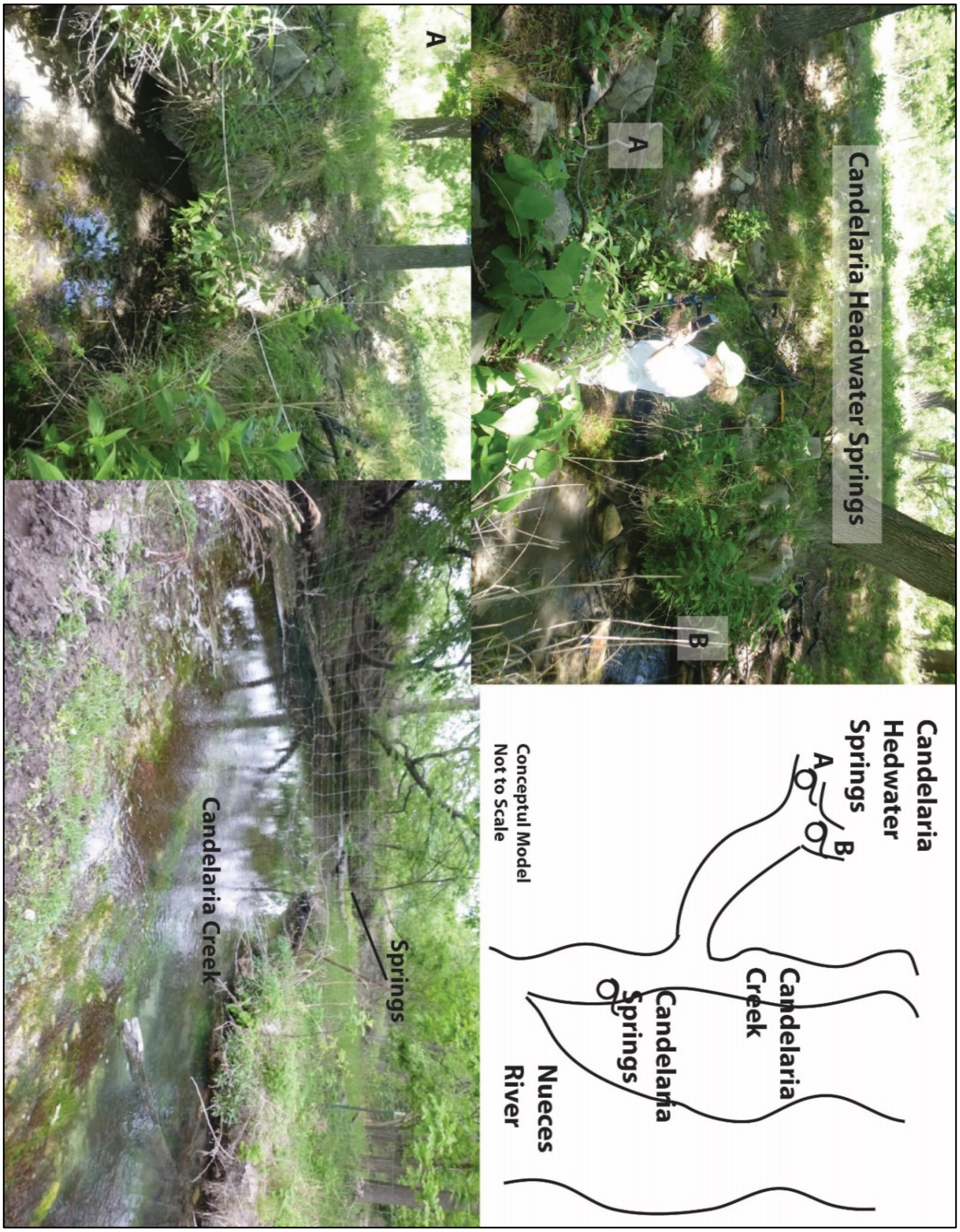

Figure 3.32. This figure shows the location of Candelaria Springs, Candelaria Headwater Springs, and a conceptual model of the springs and their location relative to the Nueces River.

4. CONCLUSIONS

The goal of this study is to evaluate the water balance in the Nueces River by delineating spatial recharge over the EACZ. Limited research had been conducted previously on the interactions between a river, alluvium, and aquifers in a karst system. The knowledge gained from this study can be applied to other karst aquifer systems that are recharged by surface water inputs. This study provides knowledge and increased understanding of flow systems and recharge in the Nueces River EACZ. The results can be used to characterize the spatial variability of recharge in a karst system and evaluate gauging requirements for estimating recharge. The findings of this research suggest that recharge is occurring in the EACZ and may be unaccounted for currently.

The results from gain/loss studies, volumetric analysis, water balance, and flow calculations suggest that significant recharge occurs over the Contributing Zone. Recharge in the Contributing Zone that may currently be unaccounted for is between 0.9 to 2% of the total recharge and 4 to 11% of recharge in the Nueces River Basin. The locations of the boundaries between the Recharge Zone and Contributing Zone may need to be relocated or the spatial dimensions of the Recharge Zone and Contributing Zone may need to be redefined.

Overall, this research supported the hypotheses that: (a) recharge is occurring over the Contributing Zone of the Edwards Aquifer and some recharge may currently be unaccounted for and (b) the main source of water for springs that feed Candelaria Creek is underflow from the Nueces River with a small amount from the Trinity Aquifer.

Determining the water source is also significant because the springs that feed Candelaria Creek provide 52-64% of flow measured at the USGS Laguna gauge. This is important if the recharge over the EACZ (Trinity Aquifer) is contributing to the Edwards Aquifer. Further research should be conducted to determine if and how much recharge over the EACZ (Trinity Aquifer) flows to the Edwards Aquifer via interformational flow. If the Trinity Aquifer is recharging the Edwards Aquifer, this may also have implications for how both aquifers are managed.

Methods used in this thesis could be applied to a larger portion of the Nueces River over the EARZ. Utilizing gain/loss studies the temporal and spatial variability of loss can be captured more readily over the EARZ, especially with multiple gauging locations along the river. The gain/loss studies may show the need for continuous gauges in a specific location or the need for multiple gauges to estimate recharge over the EARZ. Streamflow analysis, PET, water temperature, and specific conductance, water chemistry, and near surface geophysics can assess the storage and underflow in the system over the EARZ, and can aid in estimating the amount of recharge more accurately.

Further studies could include: using similar methods in other karst systems to estimate and understand recharge processes, conducting further investigations to determine if the Trinity Aquifer is recharging the Edwards Aquifer, and similar methods can be applied to other watershed in the San Antonio Segment of the Edwards Aquifer to understand and estimate recharge more accurately. Some methods that could be used in future studies may include: dye tracing tests, drilling nest piezometer wells near the river, and collecting groundwater data (levels, hydraulic conductivity, etc.).

A. APPENDIX: ENDANGERED SPECIES

A.1. LIST OF ENDANGERED & THREATENED SPECIES COVERED BY EAA-HCP

The EAA-HCP regulates pumping of the Edwards Aquifer, to ensure that these species do not lose their habitat.
Species found at: http://www.eahcp.org/index.php/about_eahcp/covered_species

Comal Springs Dryopid Beetle
Strygoparhus Comalensis

Comal Springs Riffle Beetle
Heterelmis Comalensis

Fountain Darter
Etheostoma Fonticola

Peck's Cave Amphipod
Stygobromus Pecki

San Marcos Salamander
Eurycea Nana

San Marcos Gambusia
Gambusia Georgei

Texas Blind Salamander
Eurycea Rathbuni

Texas Wild Rice
Zizania Texana

Edwards Aquifer Diving Beetle
Haideoporus texanus

Comal Springs Salamander
Eurycea sp.

Texas Troglobitic Water Slater
Lirceolus smithii

B. APPENDIX: GAIN/LOSS STUDY

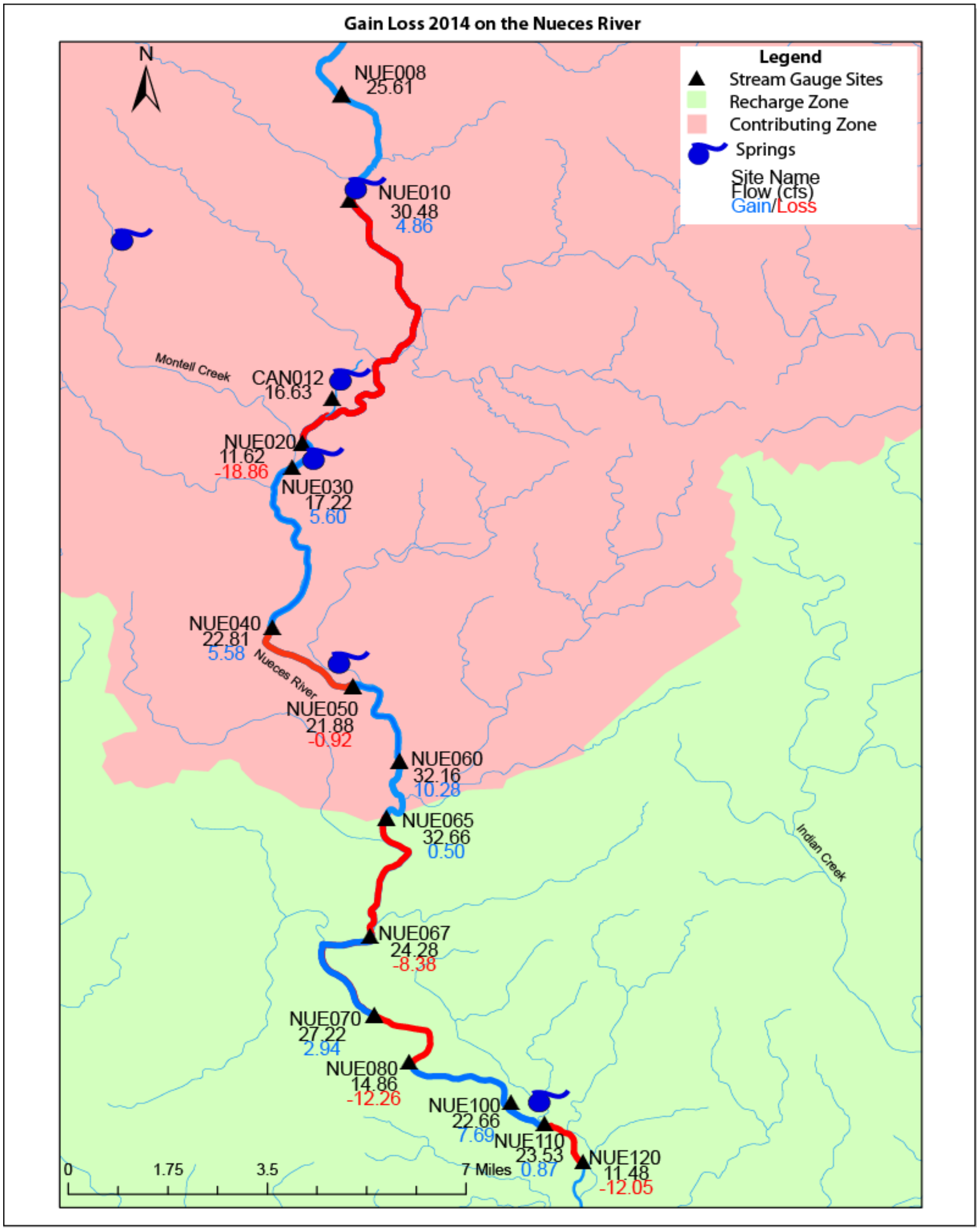

Figure B.1. The gain/loss study conducted in 2014 was the most comprehensive gain loss study. Gains are in blue, loss in red. Also shown are the locations of springs known or found in the area. There is some correlation between the location of springs and gaining streams. In general there is likely a spring source in the gaining segment of the river or some source of underflow.

C. APPENDIX: STRATIGRAPHY OF UVALDE COUNTY

Table C.1. Stratigraphy of Uvalde county modeled after Clark, 2003

Series	MAVIRICK BASIN	DEVILS RIVER TREND	Aquifer	Porosity
	Alluvium	Alluvium		
Pleistocene	Leona Formation	Leona Formation	Leona Aquifer	Fabric selective interparticle
Pliocene	Uvalde Gravel	Uvalde Gravel	none	Fabric selective interparticle
Eocene	Wilcox Group		Confining unit	Low porosity/low permeability
Upper Cretaceous	Navarro Group	Navarro Group	Confining unit	Low porosity/low permeability
	Taylor Group	Taylor Group	Confining unit	Low porosity/low permeability
	Austin Group	Austin Group	Confining unit	Low to moderate porosity and permeability
	Eagle Ford Group	Eagle Ford Group	Confining unit	Primary porosity lost/low permeability
	Buda Limestone	Buda Limestone	Confining unit	Low porosity/low permeability
	Del Rio Clay	Del Rio Clay	Confining unit	Negligible
Lower Cretaceous	Salmon Peak Formation	Devils River Formation	Edwards Aquifer	Low to high porosity and permeability
	McKnight Formation			Low to high porosity and permeability
	West Nueces Formation			Low to high porosity and permeability
	Upper Glen Rose Limestone	Upper Glen Rose Limestone	Trinity Aquifer	Low permeability

D. APPENDIX: METHODOLOGIES USED

Table D.1. Instrumentation used at various sites in performing the research for this thesis.

Instrument	Method	Data	Image of Instrument	Source
	Acoustic doppler velocity	Flow		http://www.sontek.com/productsdetail.php?FlowTracker-Handheld-ADV-1
Sontek River Surveyor Smart Pulse HD	Acoustic doppler velocity	Flow		http://www.sontek.com/productsdetail.php?SonTek-SL-8
TidBit Hobo temperature sensors	--	Temperature		http://www.onsetcomp.com/products/data-loggers/utbi-001
Onset HOBO U30 weather stations	--	PET		http://www.onsetcomp.com/products/data-loggers/u30-nrc

Decagon SC-1 Leaf Porometer	--	Stomatal Resistance		http://www.decagon.com/assets/Images/Product-Images/Canopy/Leaf-Porometer1.jpg
YSI Pro556	--	Synoptic specific conduct-ance		https://www.ysi.com/556
Onset HOBO U24-001 Conductivity Data Logger	--	Continuous specific conductance		http://www.onsetcomp.com/products/data-loggers/u24-001
In-Situ Rugged Trolls	--	Pressure		https://in-situ.com/products/level-temp-data-loggers/rugged-troll-100/

Myron Ultrameter II	--	pH, Specific conductance (field parameters)		http://www.myronlmeters.com/v/vspfiles/photos/DH-UMII-6PII-2.jpg

D.2. Matlab Code

This code was used to calculate potential evapotranspiration using the Penman-Monteith equation with an average stomatal resistivity of 180 s/m.

```
%----------------------------------------------------------------------
% ET Calcs for Riparian Zone
% By Jenna Kromann
% University of Texas at Austin
% This program calculates evapotranspition using Penman-Monteith
equation
% Estimates Net Radiation from measured Solar Radiation
% Last modified 09/16/2013 by JK
%----------------------------------------------------------------------



% clear all
% clc
%
% load('Time1.mat')
% load('Pressure1.mat')
% load('Rain1.mat')
% load('RH1.mat')
% load('SolarRad1.mat')
% load('Temp1.mat')
% load('WindSpeed1.mat')
%
% t=Time;
% Zm = 2.92;          %height of temperature and velocity measurement
[m]
% Ta = Temp;          %air temperature [oC]
% r = RH/100;         %relative humidity
% va = WindSpeed;     %wind speed [m/s]
% P = Pressure;        %atm pressure [mb]
% Sr = SolarRad;      %solar radiation [W/m2]
% G = 0;              %ground heat flux [W/m2]
% Zveg = 1;           %vegetation height [m]
% rs = 180;            % need to convert mmol/m2s to [s/m]   %total
plant stomatal resistance [s/m] *average of values of Riparian Veg
% WDen = 1000;        %Water Density [Kg/m3]
% lambdaV = 2495000-(2.36*10^-3).*Ta*10^6;  %Latent heat of
vaporization [J/Kg]
%
% esat = 6.11*exp(lambdaV./463.*((1/273.15)-(1./(Ta+273.15)))); %sat
vapor pressure [mb]
% e = r.*esat;                                 %vapor presssure [mb]
%
% %Estimating Net Radiation - Rs and Rso assumed to be equal (FAO)
% alpha = 0.23;       %albedo = 0.23 for the hypothetical grass
reference crop FAO
```

```
% Rns = (1-alpha)*Sr; %net shortwave radiation [W/m2]
% sigma = 5.670*10^-8;%Stefan-Boltzmann constant [W m?2 K?4]
% Rnl = sigma.*(Ta.^4./2).*(0.34-(0.13*sqrt(e))).*(1.35-0.35); %net
outgoing longwave radiation [W/m2]
% Rn = Rns - Rnl;     %net radiation [W/m2]
%
% A = Rn-G;           %Available energy [W/m2]
% Zd = 0.7*Zveg;      %Zero place displacement [m]
% Z0 = 0.1*Zveg;      %Roughness height [m]
% Ra = 288;           %dry air constant [J/(K*Kg)]
% ADen = (P/100)./((Ta+273.15).*Ra);    %Air density [Kg/m3]
%
% delta = 2508.3./(Ta+237.3).^2.*exp(17.3*Ta./(Ta+237.3)); %[kpa]
% ca = va/(6.25*(log((Zm-Zd)/Z0))^2);     %atmospheric conductance
[m/s]
% ra = 1./ca;                             %atmospheric resistance
% gamma = 1005.*P./(lambdaV.*0.622);        %gamma
%
% %ET
% E = (A.*delta.*ra+(ADen.*ca.*((esat-
e)./10)))./(delta.*ra+gamma.*(ra+rs));  % ET[W/m2]
% Em = E./(lambdaV.*WDen);                 %ET [m/s]
% Emm = Em*1000*60*60*24                   %ET [mm/day]
% AvEmm = nanmean(Emm)
%
% plot(t,Emm);
% datetick ('x', 'mm-dd-yy', 'keepticks')
% xlabel('Time');
% ylabel('ET[mm/day]');
% title('Evapotranspiration ET 1');
% axis tight
```

E. APPENDIX: TEMPERATURE AND RAIN

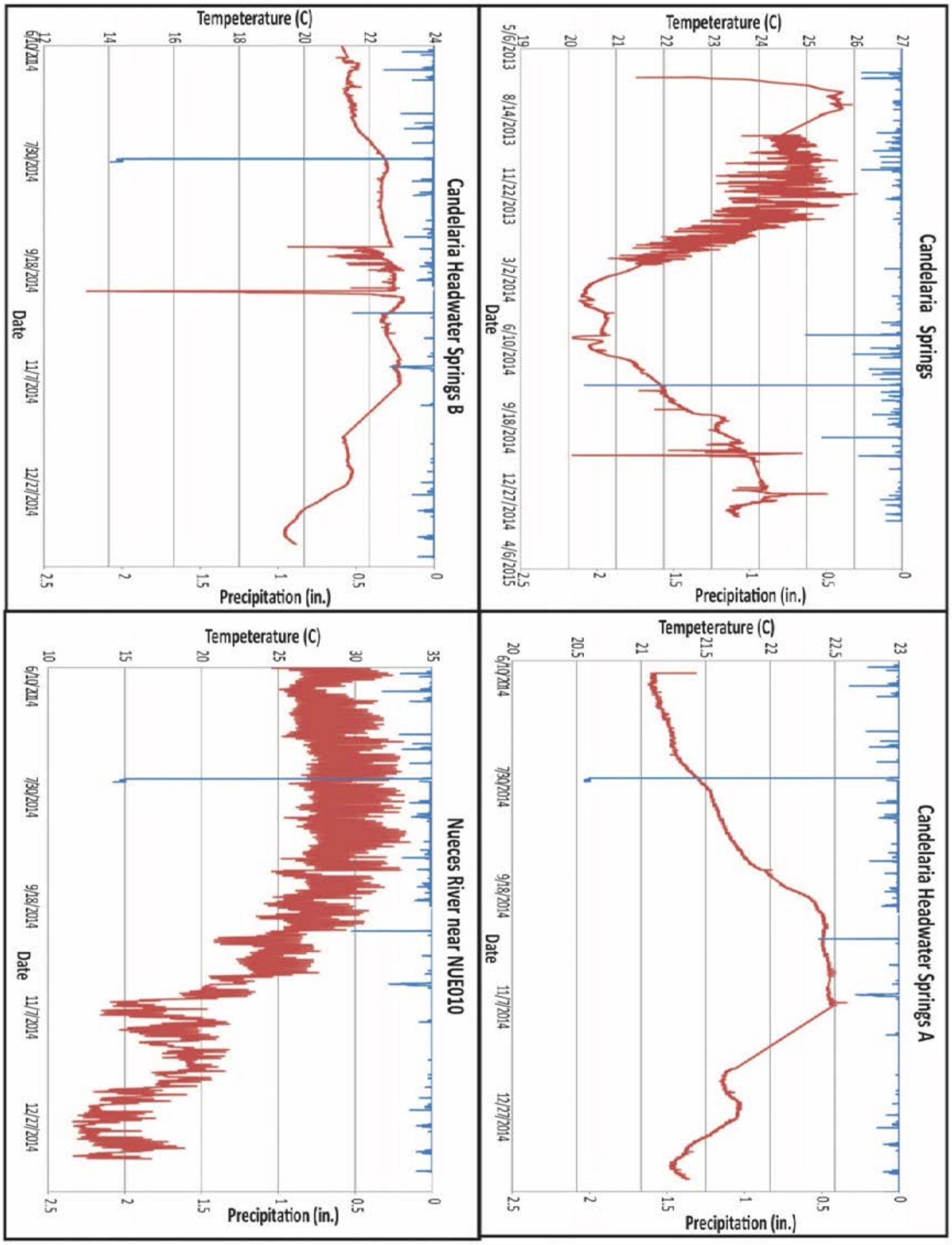

Figure E.1. Temperature response to rain at springs that feed Candelaria Creek and at the Nueces River, temperature measurements gathered with Hobo probes displayed as red lines and rain data from PET 1 displayed as blue lines.

TIDBIT PROBES

The following figures displayed below are temperature (green line) and precipitation (blue lines) graphs at a specific field location. The temperature measurements were taken with a different probe a Tidbit probe (instead of the Hoboware probes). These temperature probes were placed at various locations along the Nueces River and Candelaria Creek. These graphs were used to understand the response in temperature to different precipitation events

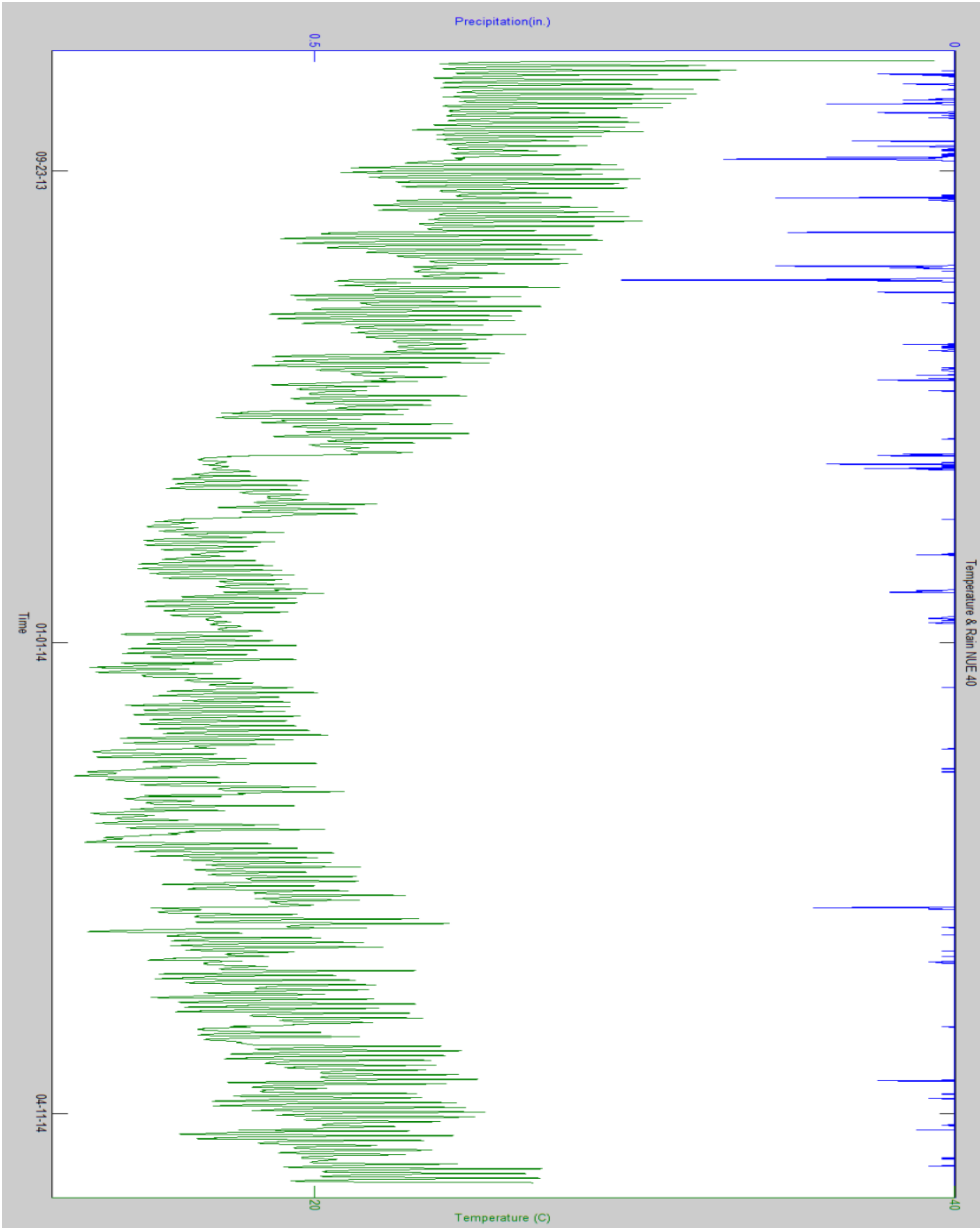

Figure E.2. Temperature in green at NUE040 compared to precipitation events in blue from ET 1.

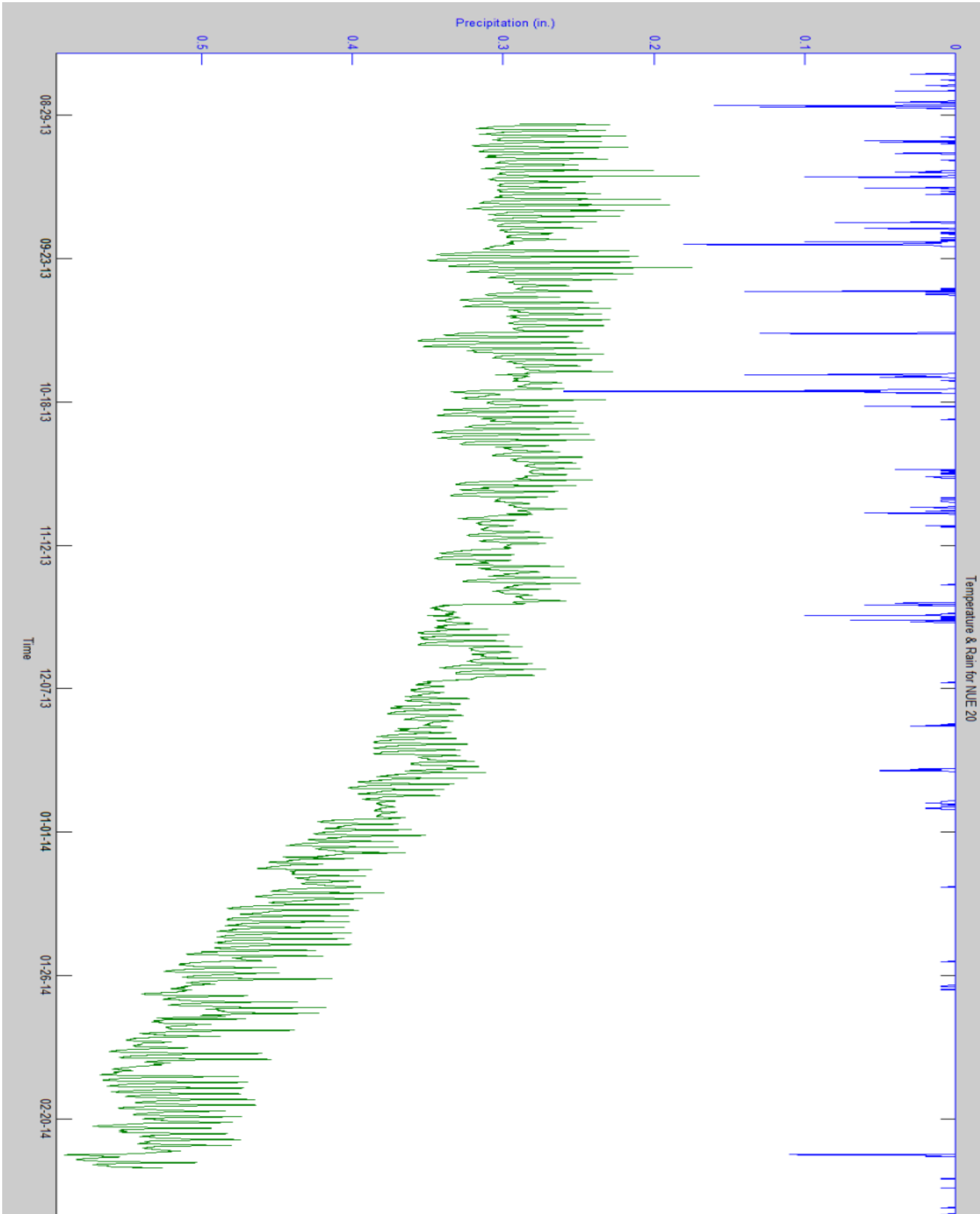

Figure E.3. Temperature in green at NUE020 compared to precipitation events in blue from PET 1.

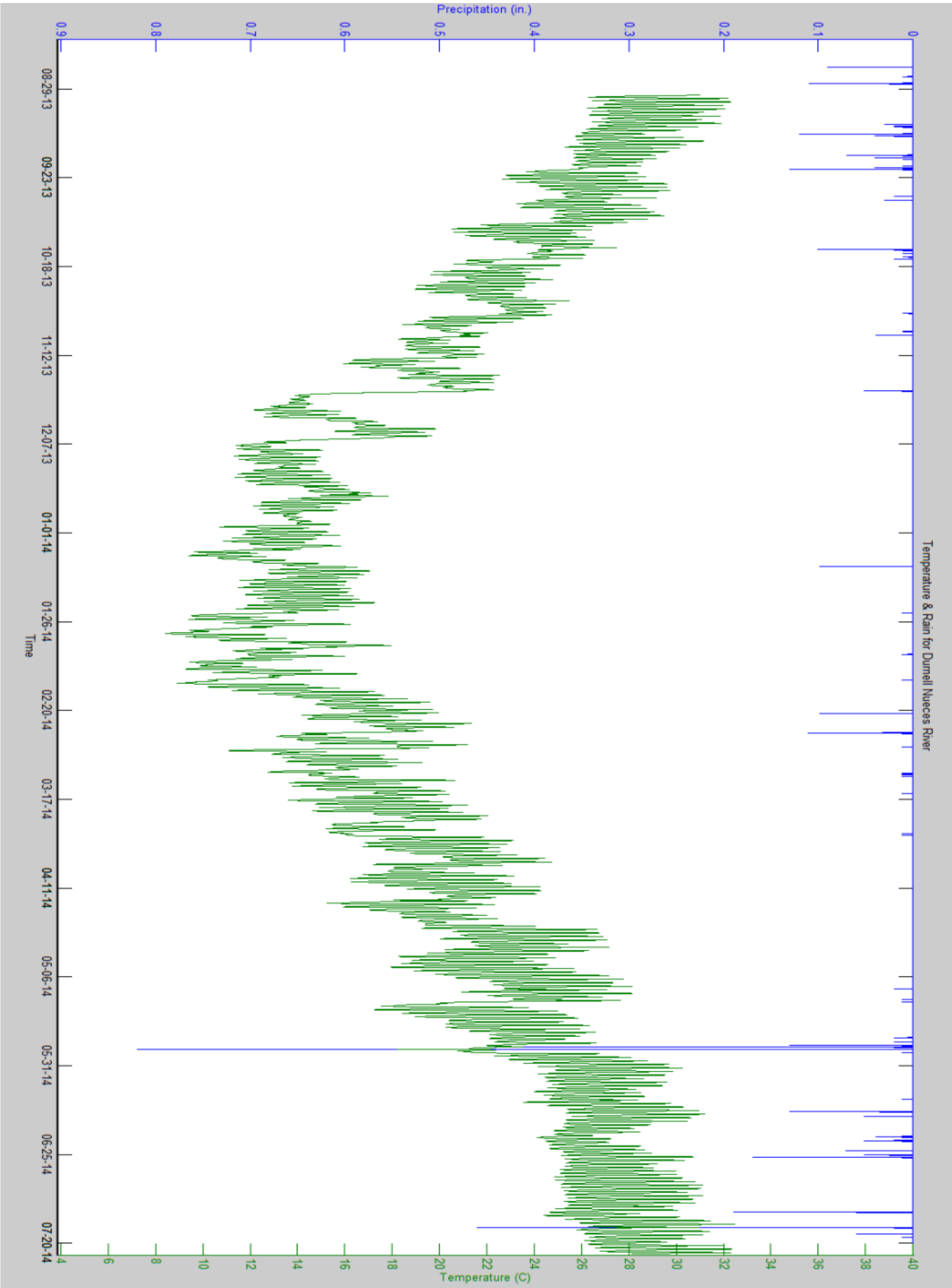

Figure E.4. Temperature in green on the Nueces River near Durnell compared to precipitation events in blue from PET 1

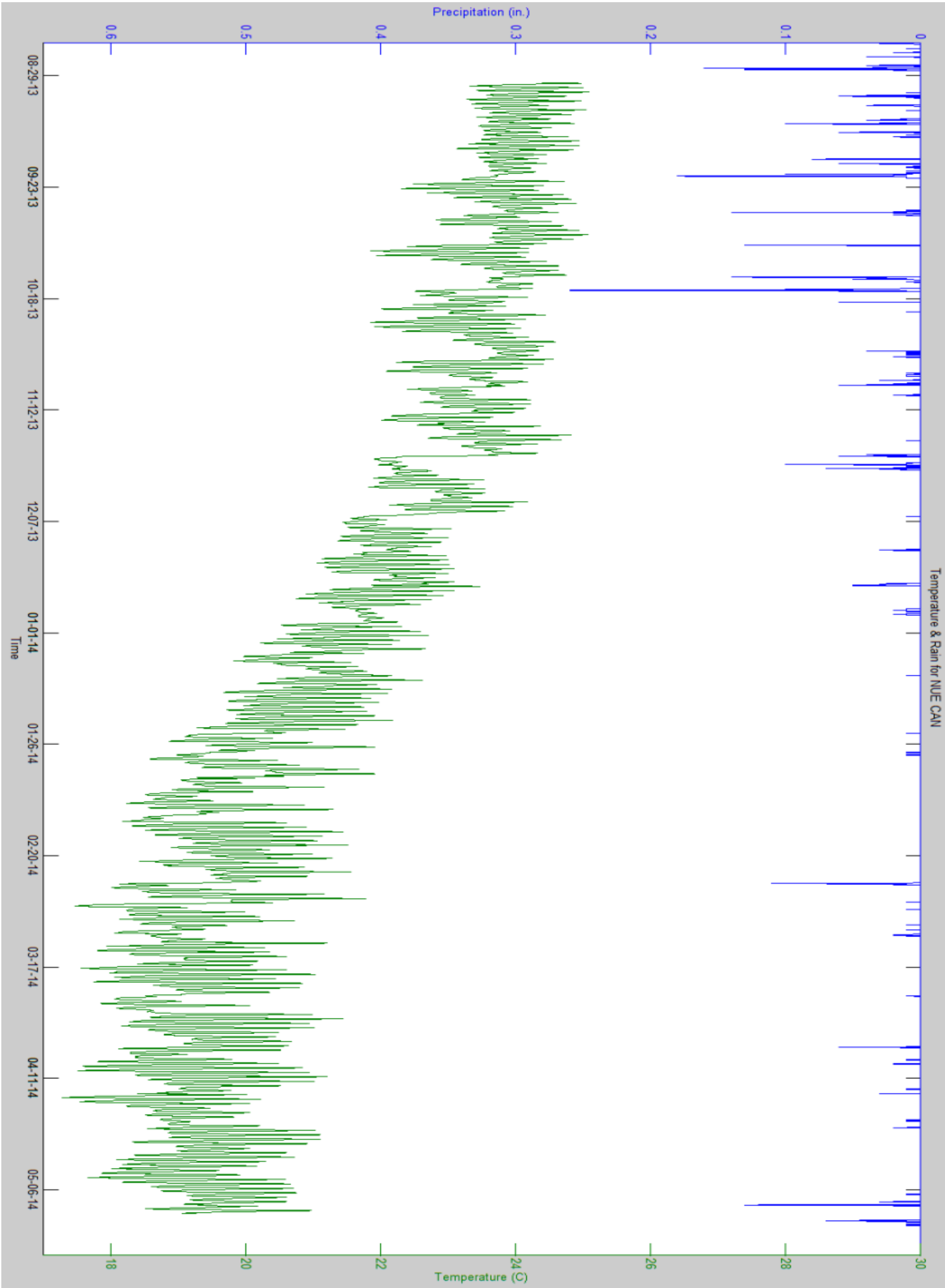

Figure E.5. Temperature in green on the Nueces River near Candelaria Springs compared to precipitation events in blue from PET 1.

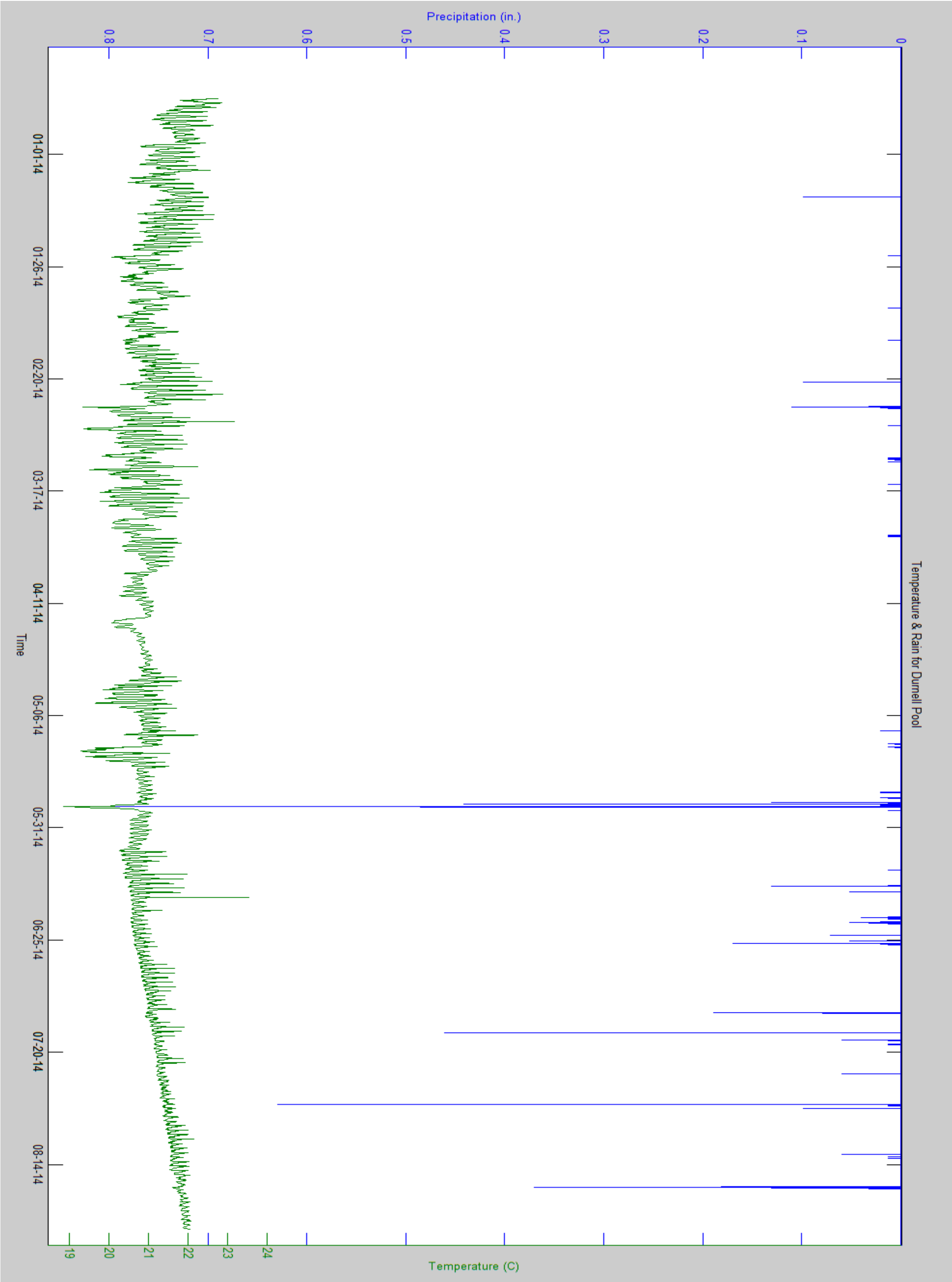

Figure E.6. Temperature in green in Durnell Pool near Durnell Springs compared to precipitation events in blue from PET 1.

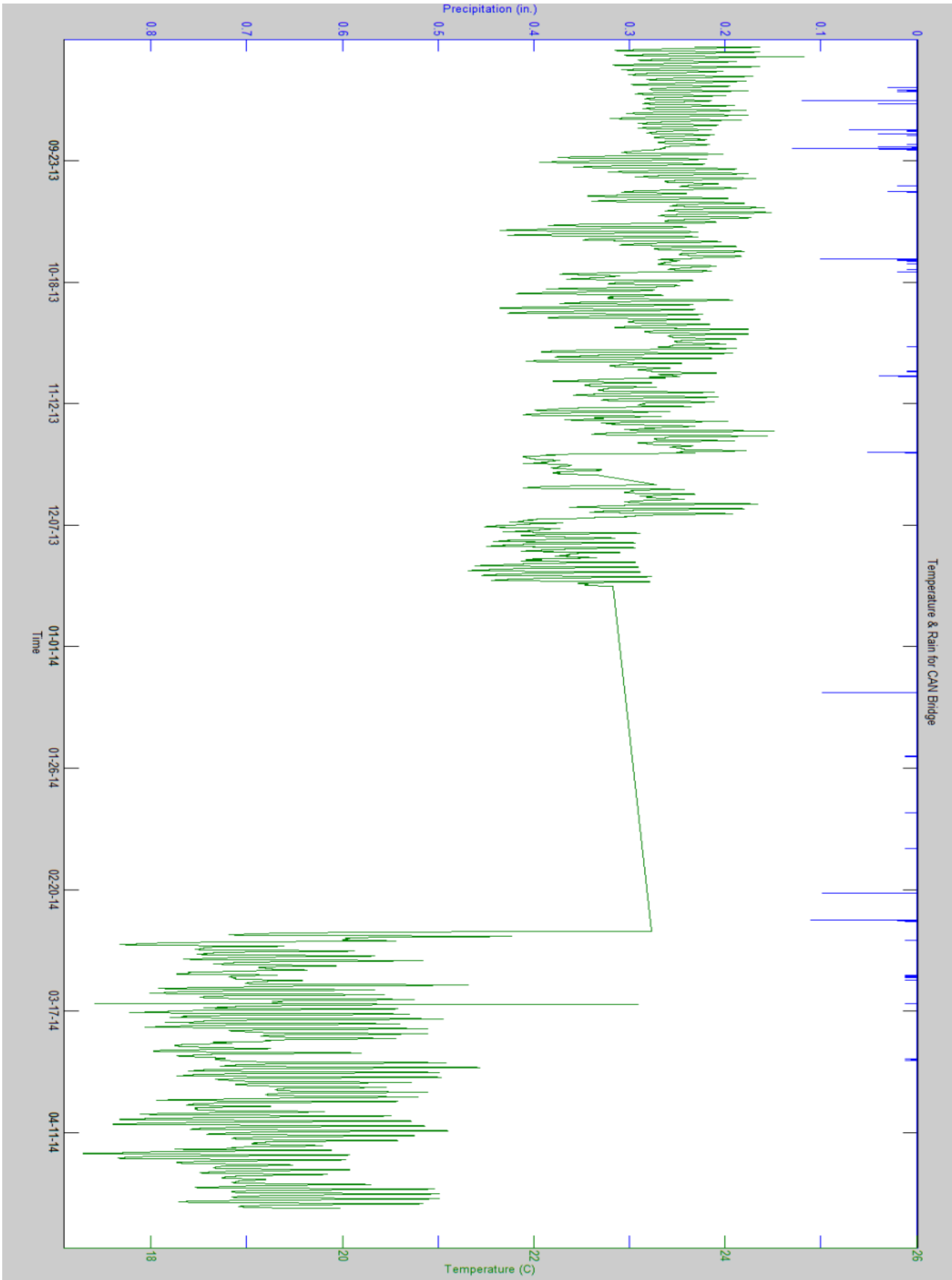

Figure E.7. Temperature in green in Candelaria Creek near Candelaria Springs compared to precipitation events in blue from PET 1.

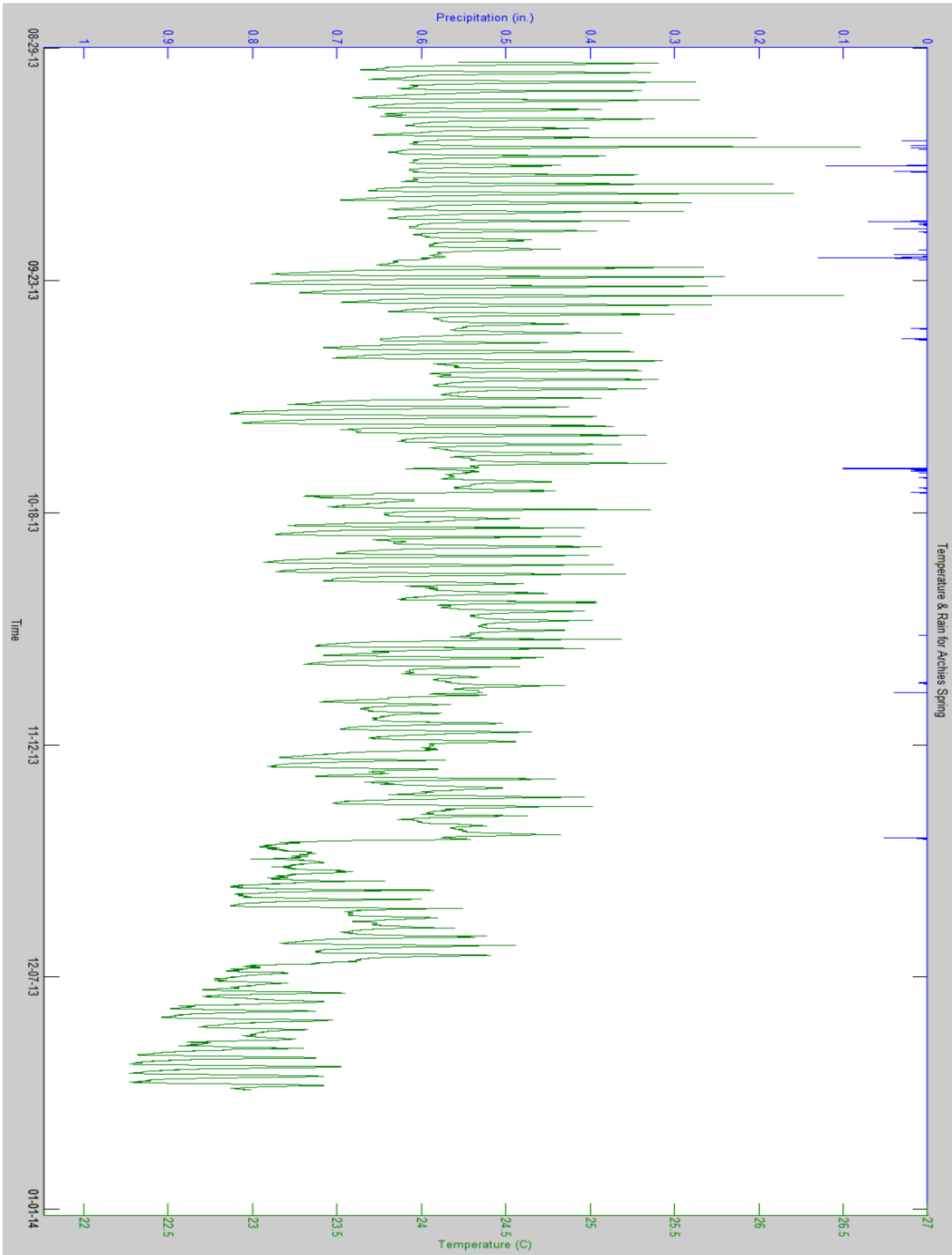

Figure E.8. Temperature in green on the Nueces River near Archies Spring compared to precipitation events in blue from PET 1.

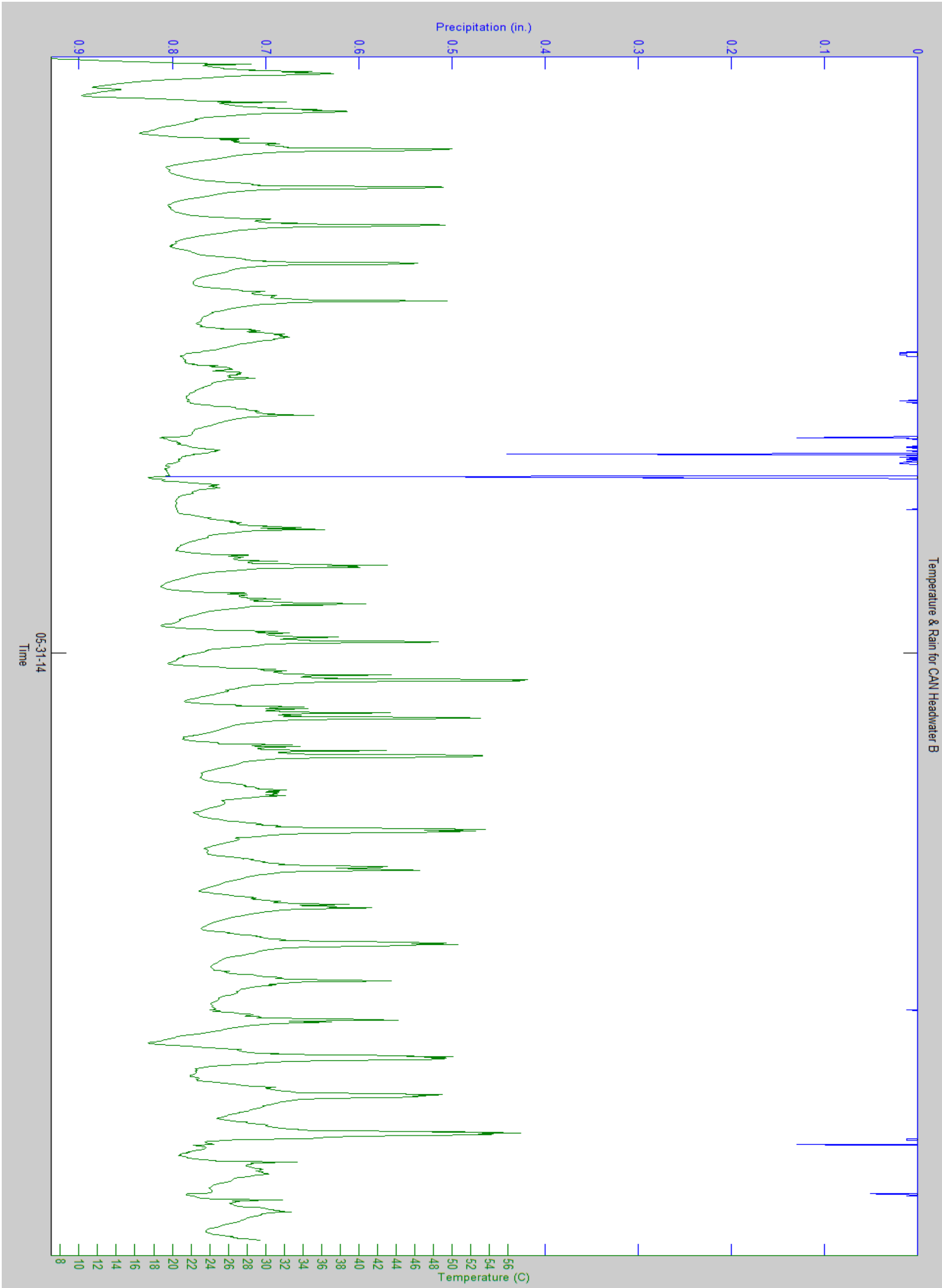

Figure E.9. Temperature in green at Candelaria Headwater Springs B compared to precipitation events in blue from PET 1.

COMPARISON OF HOBO TEMPERATURE TO TIDBIT

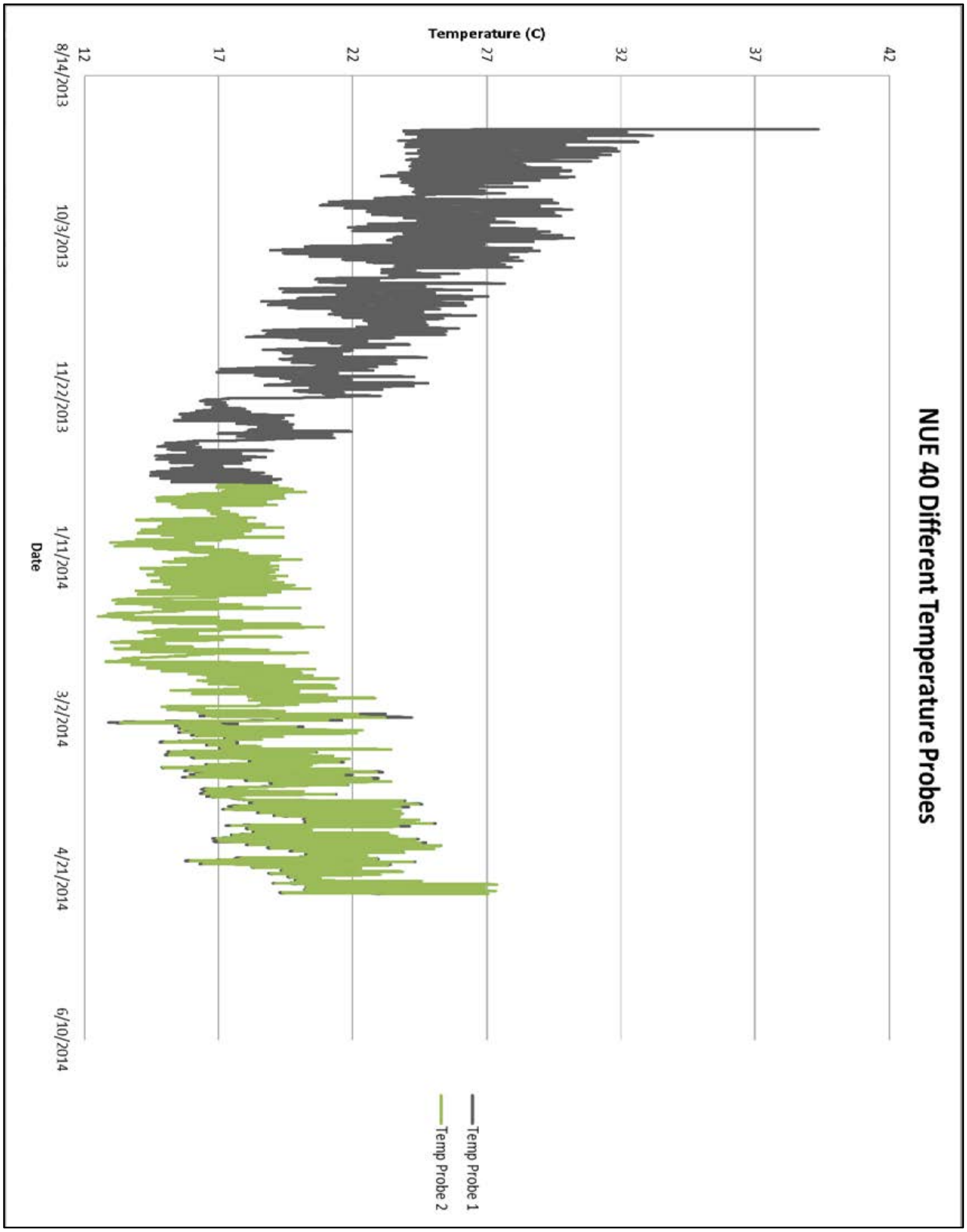

Figure E.10. Two different Tidbit probes were used at each site; the figure shows a comparison of the different probes at NUE040. This comparison was completed for each site to make sure the temperature readings were accurate.

HOBO PROBES

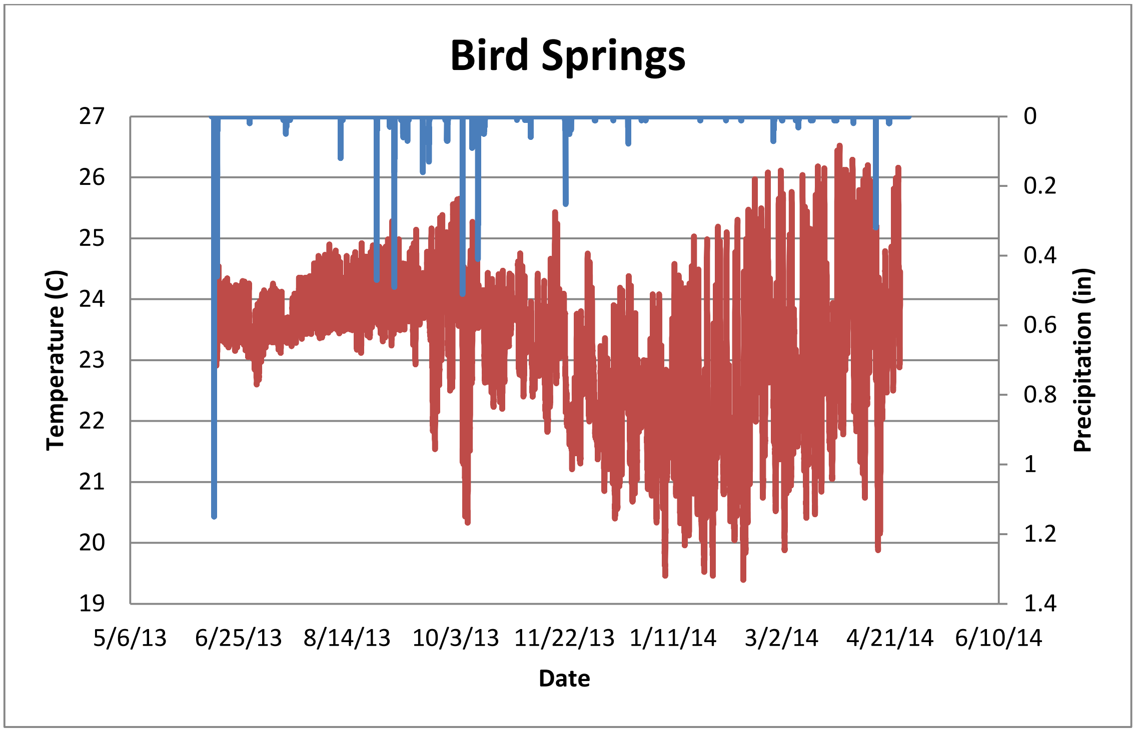

Figure E.11. Temperature data collected for Bird Springs (red) a spring over the EARZ. The blue is precipitation from PET 1.

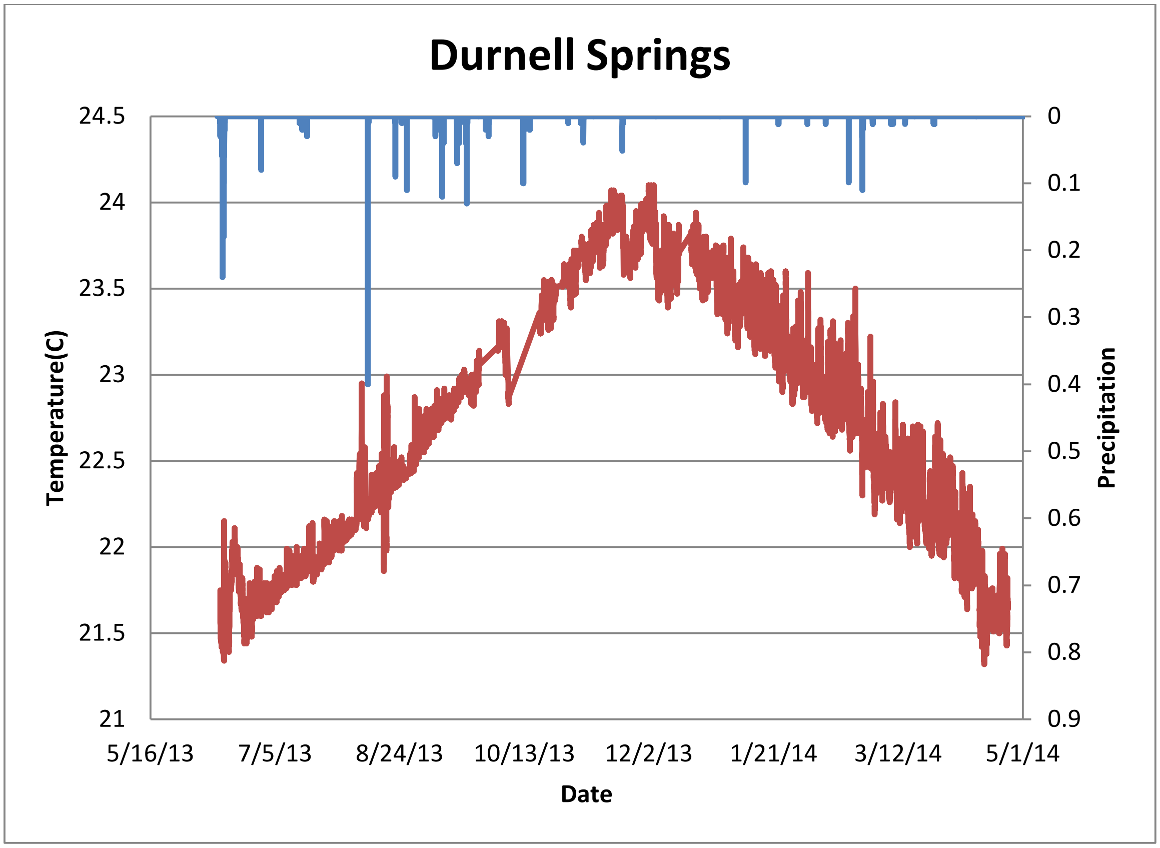

Figure E.12. Temperature data collected for Durnell Springs (red) near NUE010 and Durnell Pool. The blue is precipitation data from PET 1.

F. APPENDIX: THERMAL INFRARED

This method was used to search for springs in the Nueces River. The resolution is not broad enough to search for springs, but is good for determining how spring water mixes with surface water (there has to be a significant temperature difference).

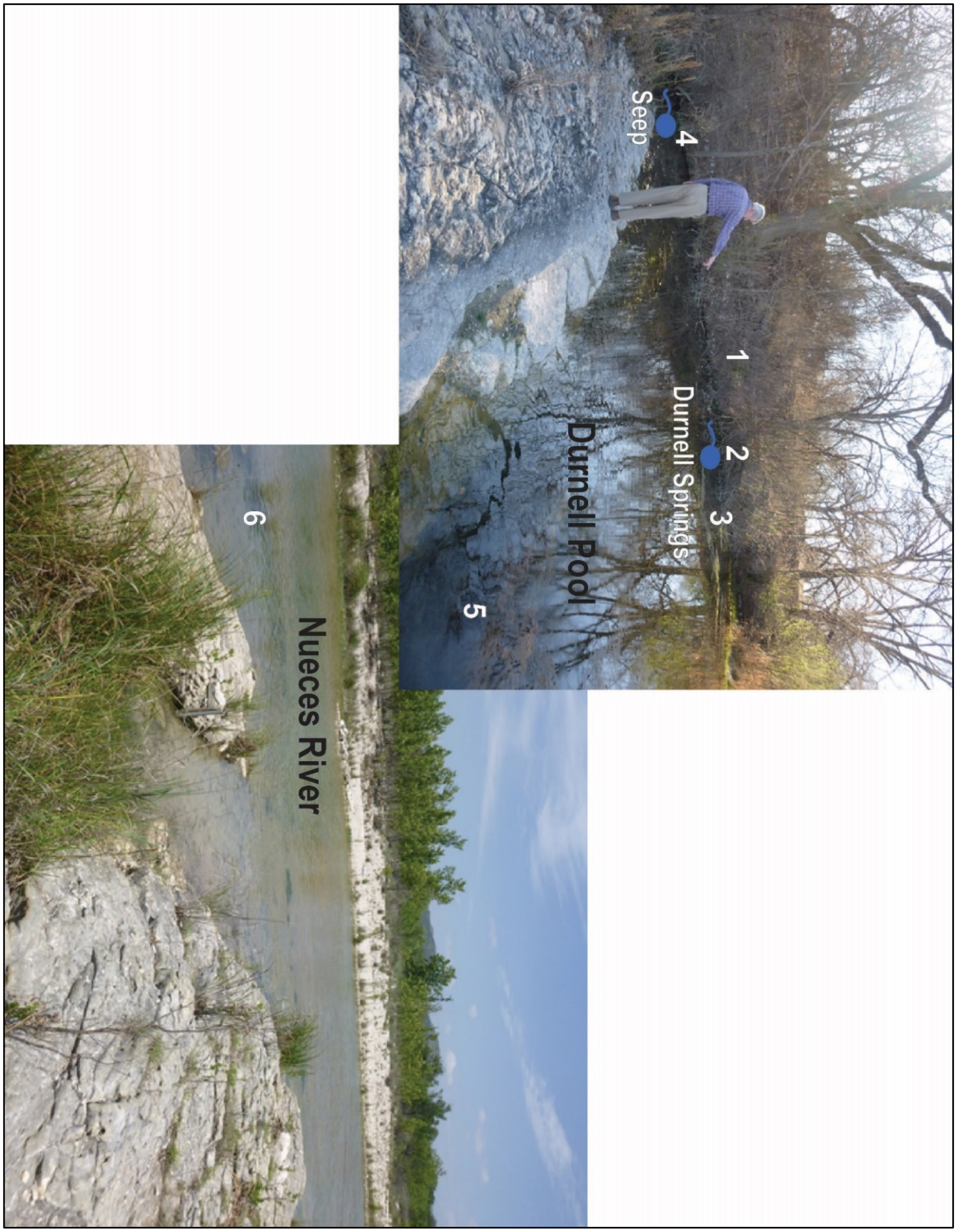

Figure F.1. Locations of thermal infrared shot near Nueces River by NUE010, numbers correspond to sites where thermal infrared images were taken. See Figure F.2 for thermal infrared images.

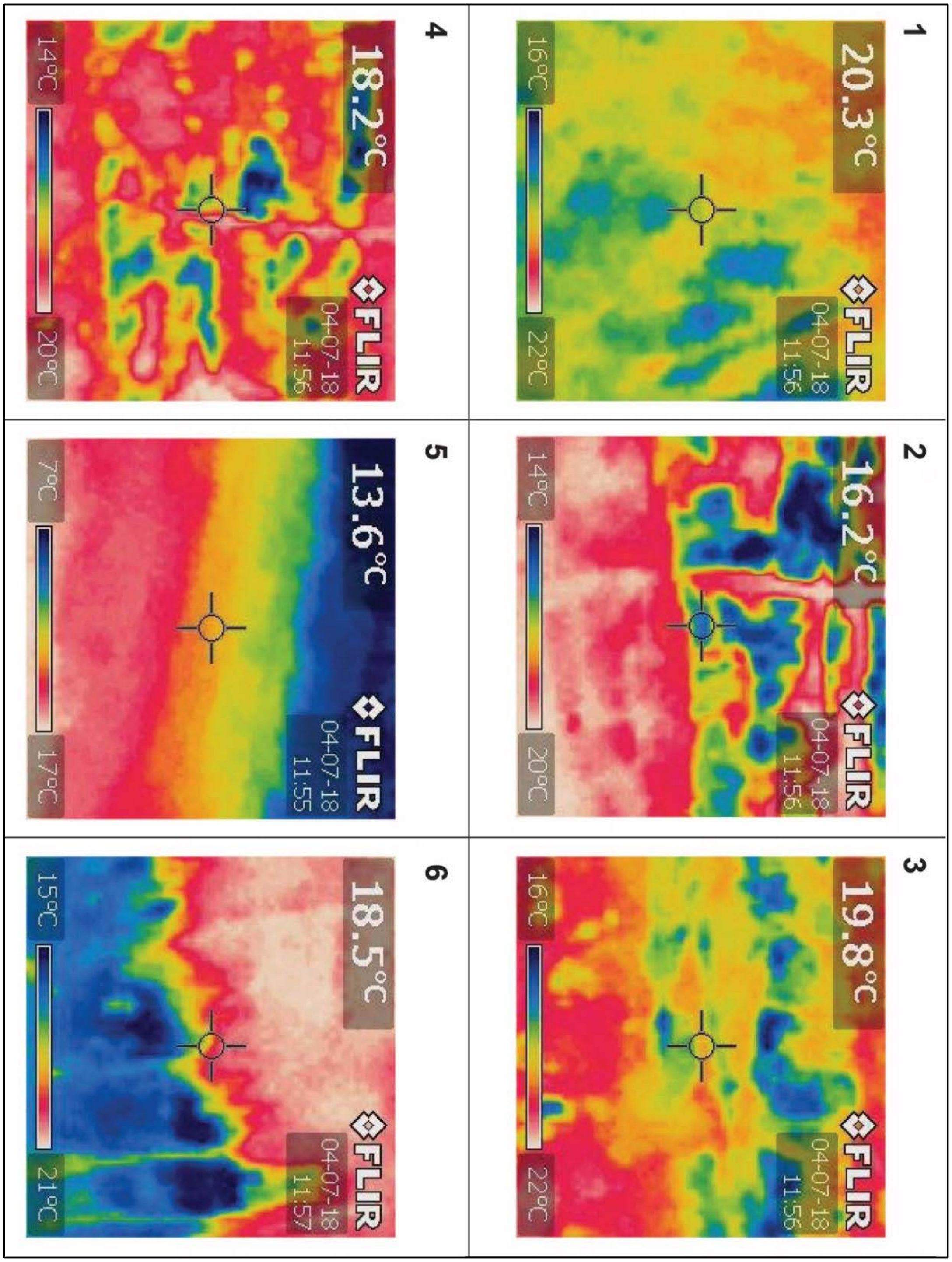

Figure F.2. Thermal infrared images, numbers correspond to the figure above showing the location of the image.

G. APPENDIX: GEOPHYSICAL STUDIES-EM

The following figures show data collected using to different EM instruments: EM 31 and EM 34 in vertical and horizontal orientations (measuring different depths in the subsurface). These measurements were gathered near Candelaria Creek and the Nueces River, either along ER lines or near Candelaria Creek of the Nueces River.

EM 34 40m Vertical

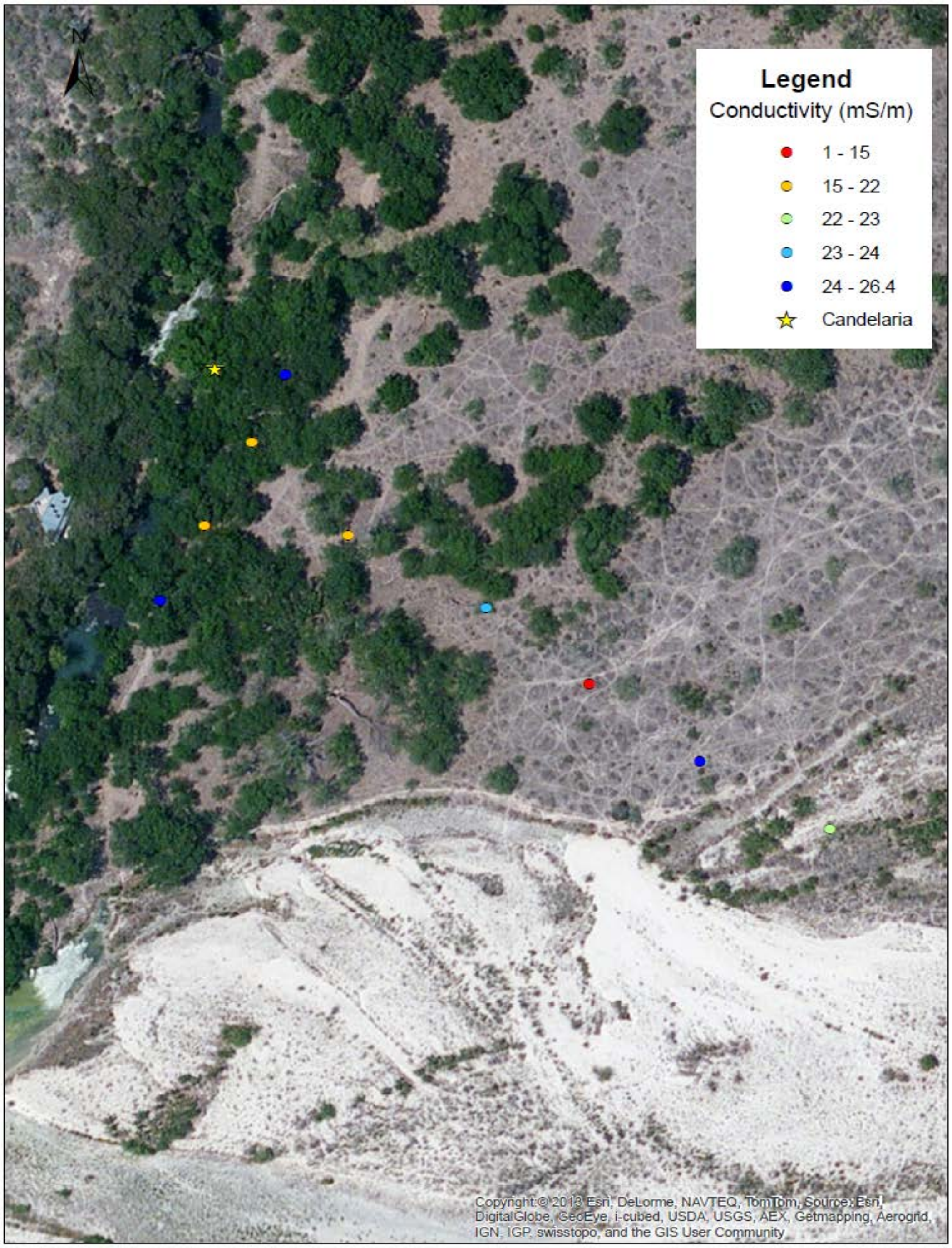

Figure G.1. Results from EM 34 spaced 40 m measured in the vertical orientation. These measurements were gathered along ER lines near Candelaria Creek and the Nueces River. Colored points shown represent the range of conductivity in the subsurface.

EM 34 40m Horizontal

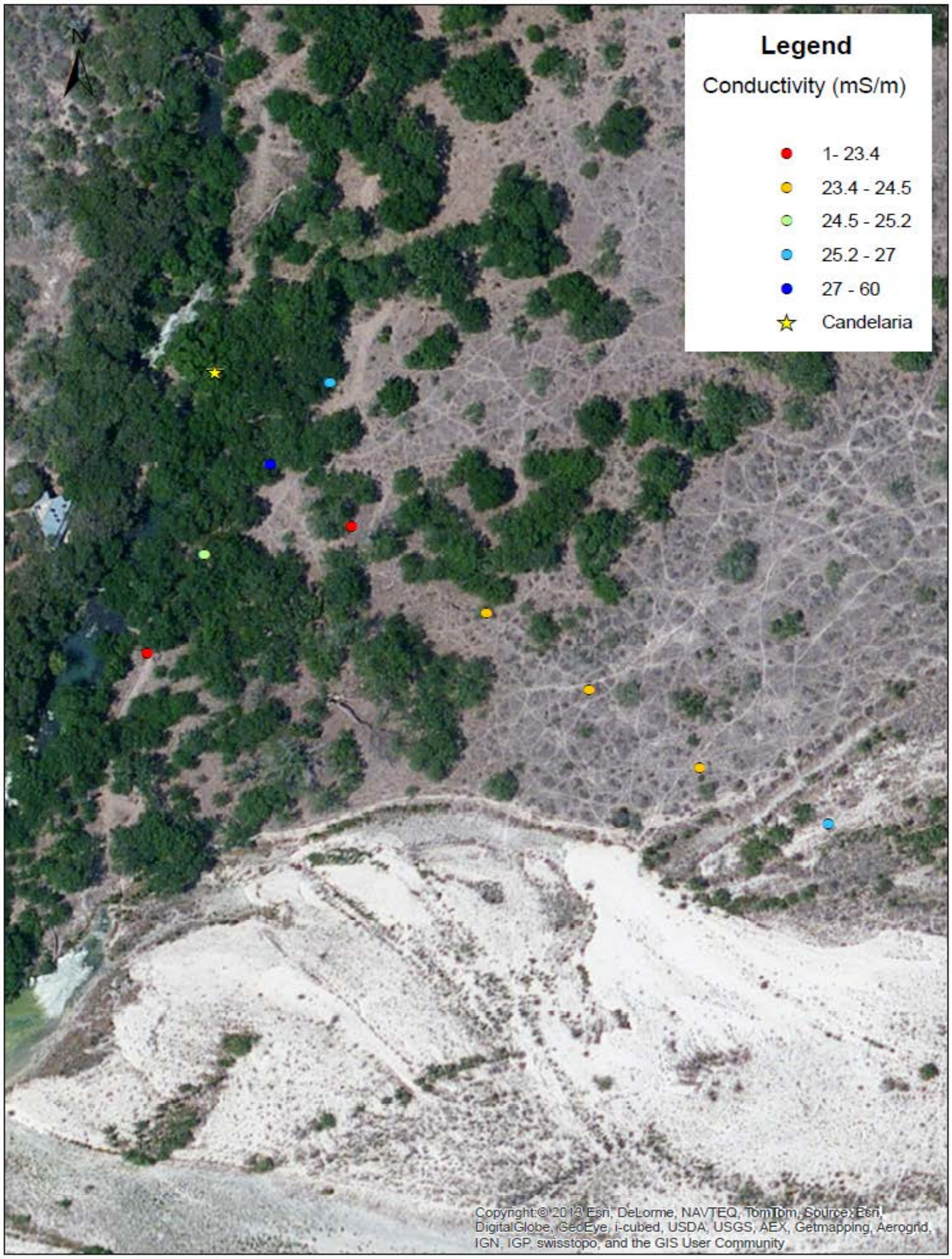

Figure G.2. Results from EM 34 spaced 40 m measured in the horizontal orientation. These measurements were gathered along ER lines near Candelaria Creek and the Nueces River. Colored points shown represent the range of conductivity in the subsurface.

EM 34 20m Vertical

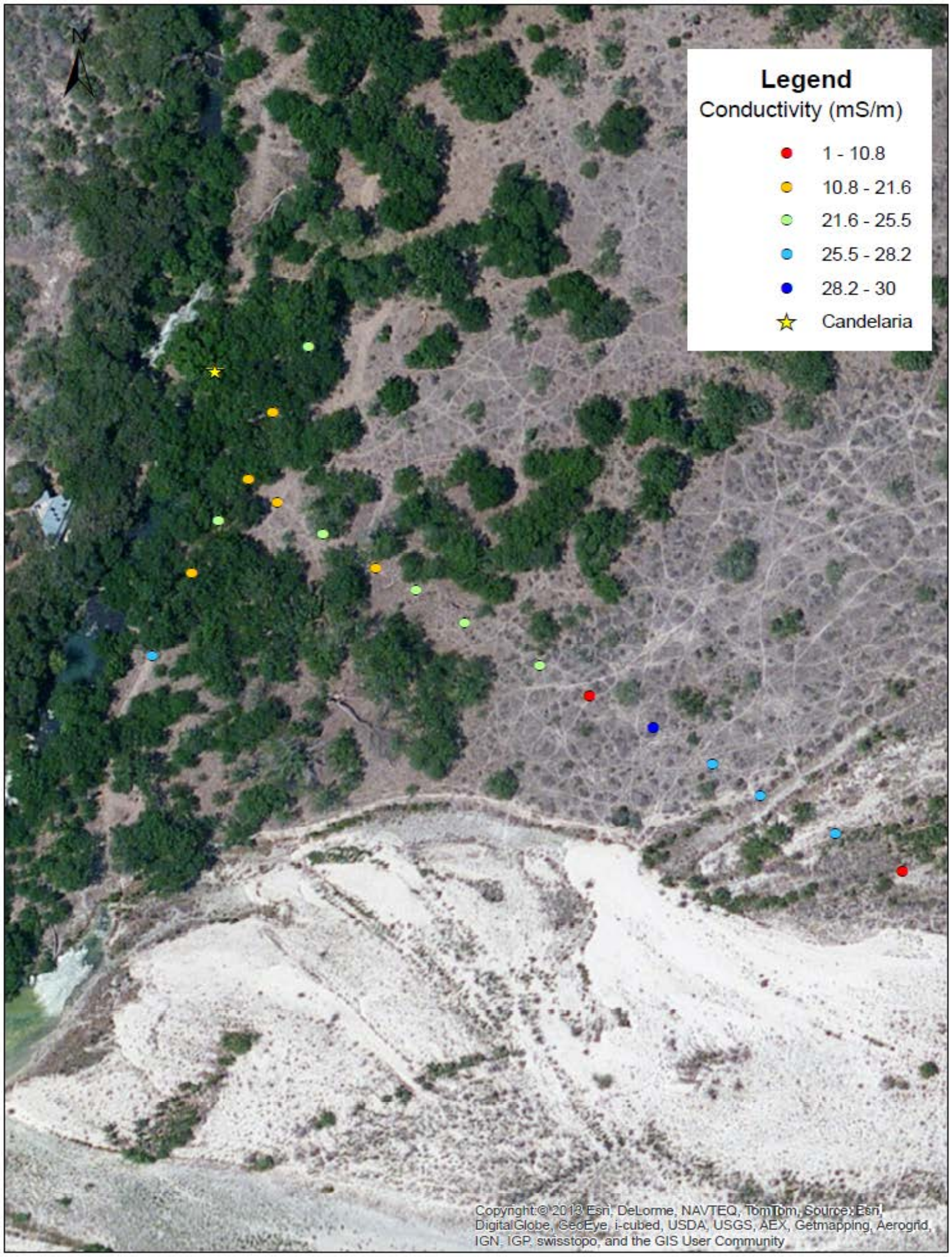

Figure G.3. Results from EM 34 spaced 20 m measured in the vertical orientation. These measurements were gathered along ER lines near Candelaria Creek and the Nueces River. Colored points shown represent the range of conductivity in the subsurface.

EM 34 20m Horizontal

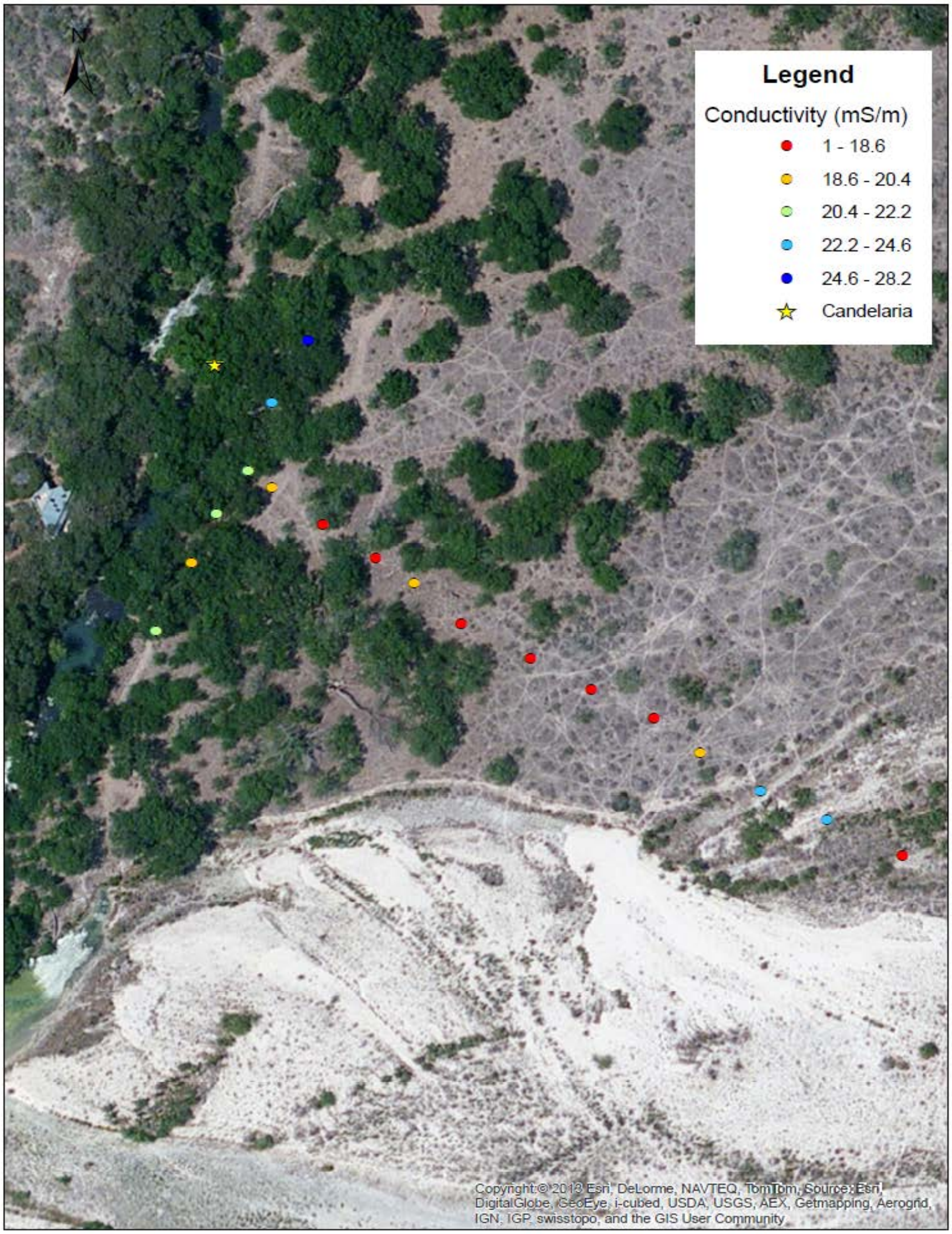

Figure G.4. Results from EM 34 spaced 20 m measured in the horizontal orientation. These measurements were gathered along ER lines near Candelaria Creek and the Nueces River. Colored points shown represent the range of conductivity in the subsurface.

EM 34 10m Vertical

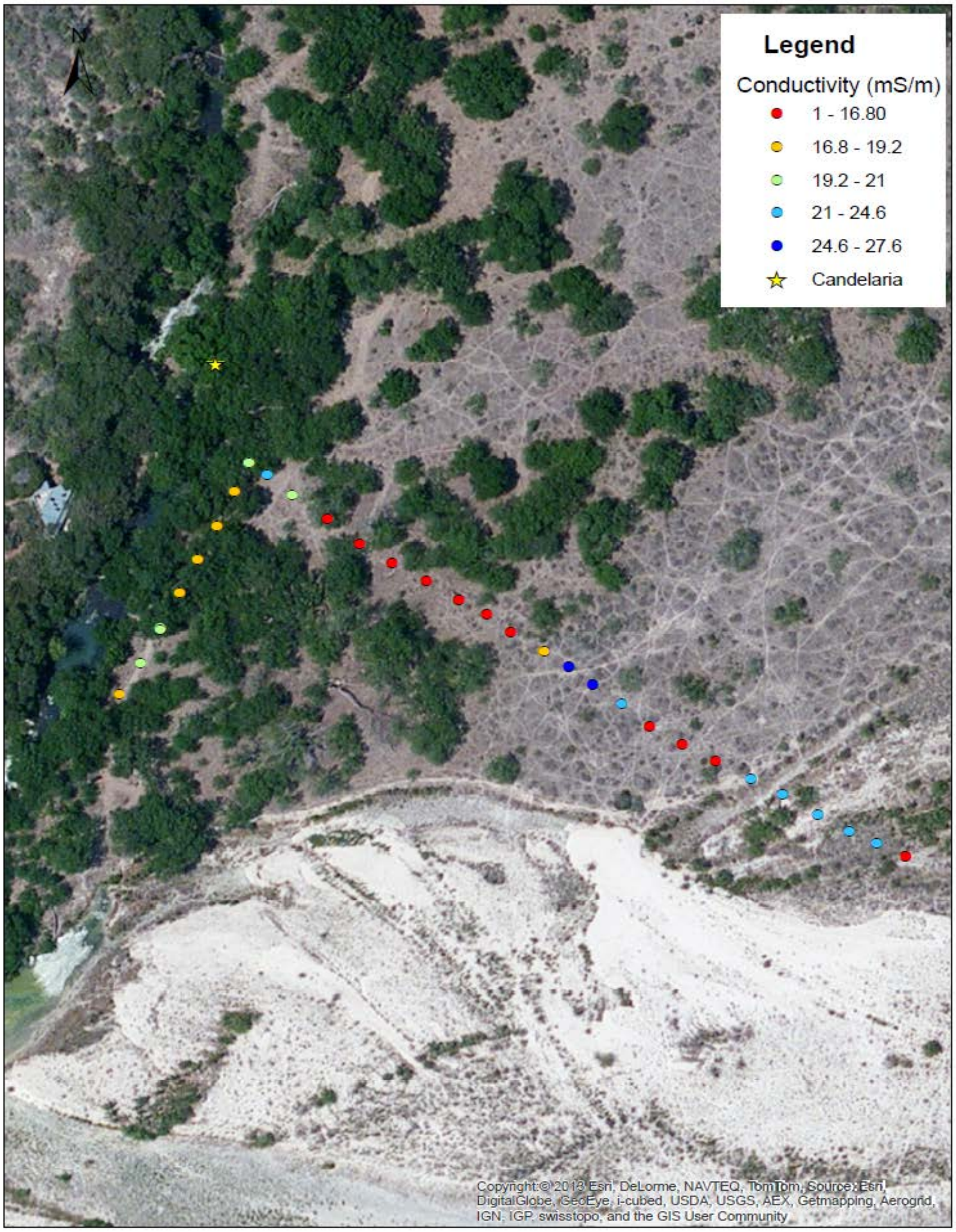

Figure G.5. Results from EM 34 spaced 10 m measured in the vertical orientation. These measurements were gathered along ER lines near Candelaria Creek and the Nueces River. Colored points shown represent the range of conductivity in the subsurface.

EM 34 10m Horizontal

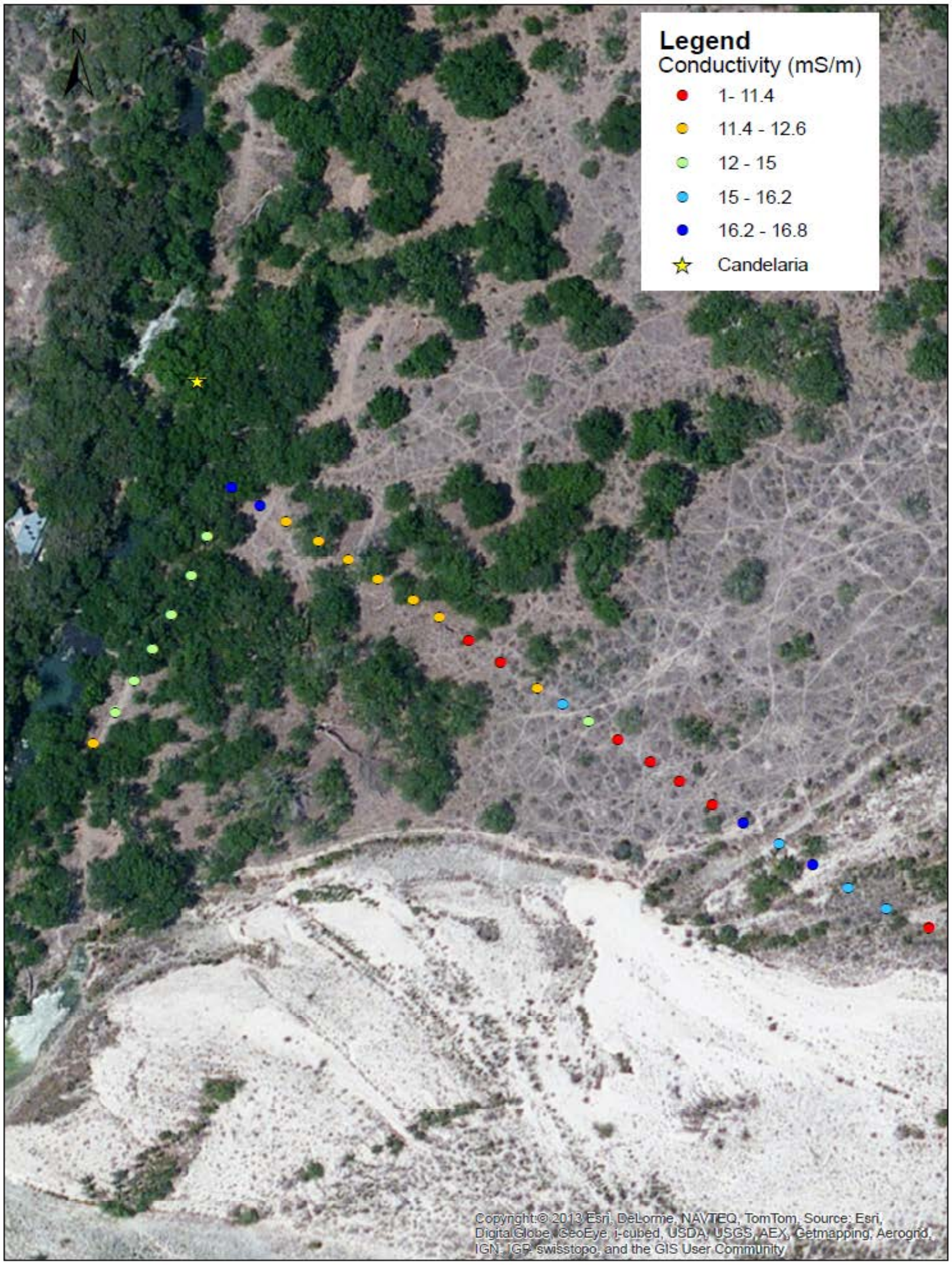

Figure G.6. Results from EM 34 spaced 10 m measured in the horizontal orientation. These measurements were gathered along ER lines near Candelaria Creek and the Nueces River. Colored points shown represent the range of conductivity in the subsurface.

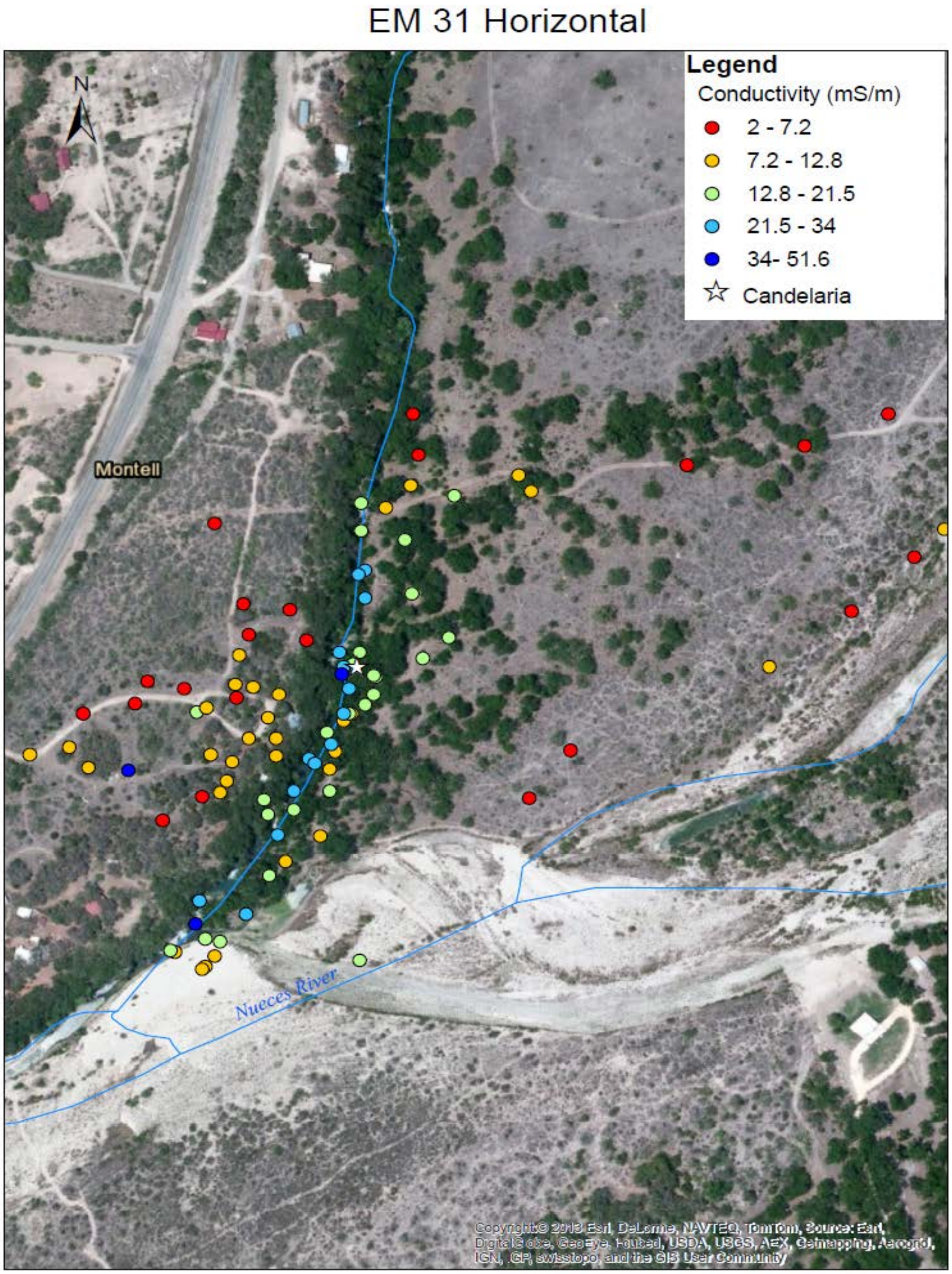

Figure G.7. Results from EM 31 gathered in the horizontal orientation near Candelaria Creek and the Nueces River. Colored points shown represent the range of conductivity in the subsurface.

EM 31 Vertical

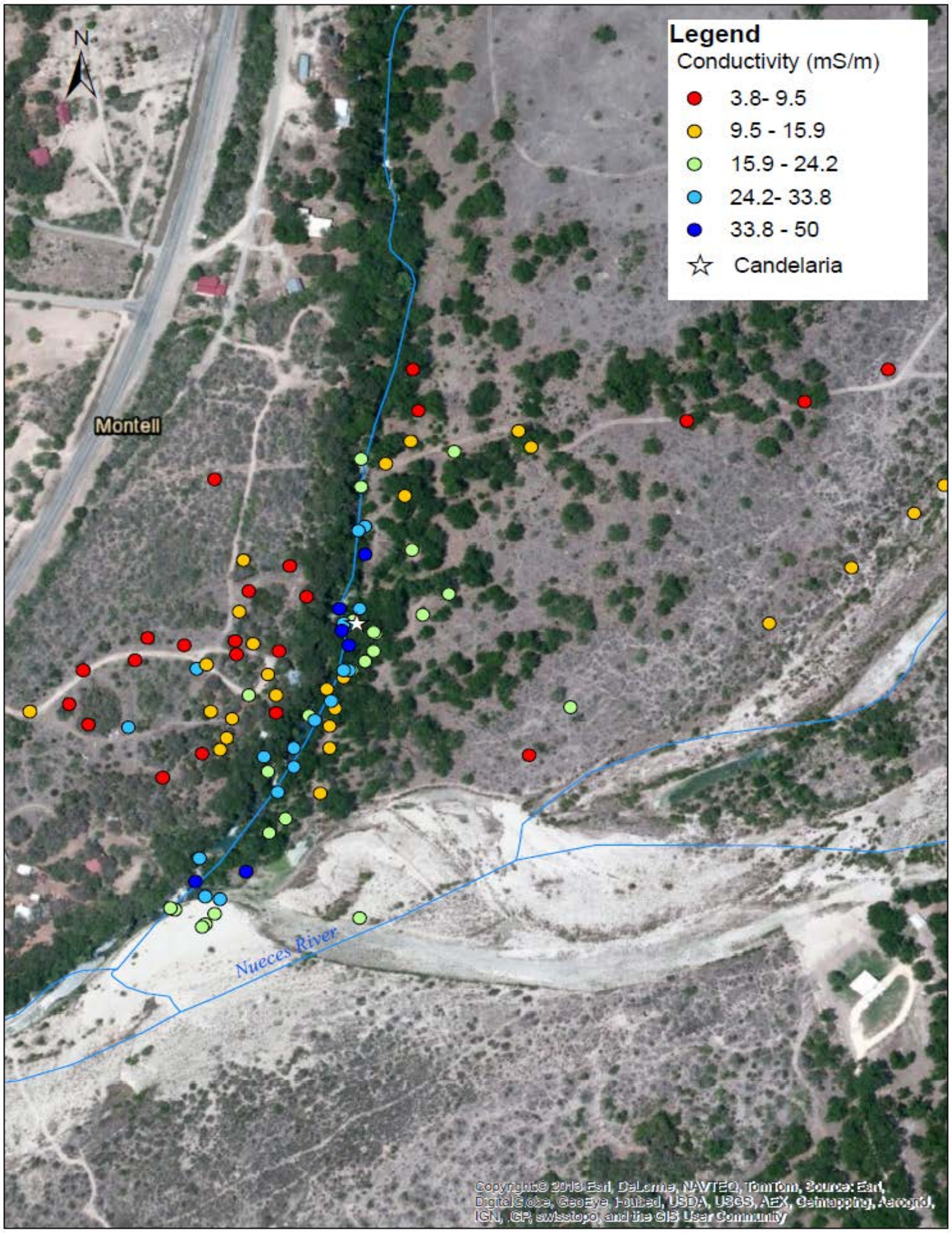

Figure G.8. Results from EM 31 gathered in the vertical orientation near Candelaria Creek and the Nueces River. Colored points shown represent the range of conductivity in the subsurface.

H. APPENDIX: PET

Table H.1. Monthly estimated PET values, converted to mm/day to compare PET values estimated on the Nueces River to values from Texas A&M Agrilife Extension and TWDB in Quad 808 (Texas A&M AgriLife Extension, 2013 and TWDB, 2013).

PET	Uvalde (in/month)	mm/month	days in month	mm/day
Jan	2.44	61.98	31	2.00
Feb	2.95	74.93	28	2.68
Mar	4.62	117.35	31	3.79
Apr	5.85	148.59	30	4.95
May	6.7	170.18	31	5.49
Jun	7.21	183.13	30	6.10
Jul	7.5	190.50	31	6.15
Aug	7.31	185.67	31	5.99
Sep	5.7	144.78	30	4.83
Oct	4.4	111.76	31	3.61
Nov	2.89	73.41	30	2.45
Dec	2.36	59.94	31	1.93
Total	**59.93**	1522.22		4.17
PET	**Quad 808 (in/month)**	in/month	days in month	mm/day
Jan	1.87	47.50	31	1.53
Feb	2.89	73.41	28	2.62
Mar	4.02	102.11	31	3.29
Apr	4.63	117.60	30	3.92
May	4.91	124.71	31	4.02
Jun	5.79	147.07	30	4.90
Jul	6.49	164.85	31	5.32
Aug	6.84	173.74	31	5.60
Sep	4.83	122.68	30	4.09
Oct	3.93	99.82	31	3.22
Nov	2.36	59.94	30	2.00
Dec	1.61	40.89	31	1.32
Total	50.17	1274.32		3.49

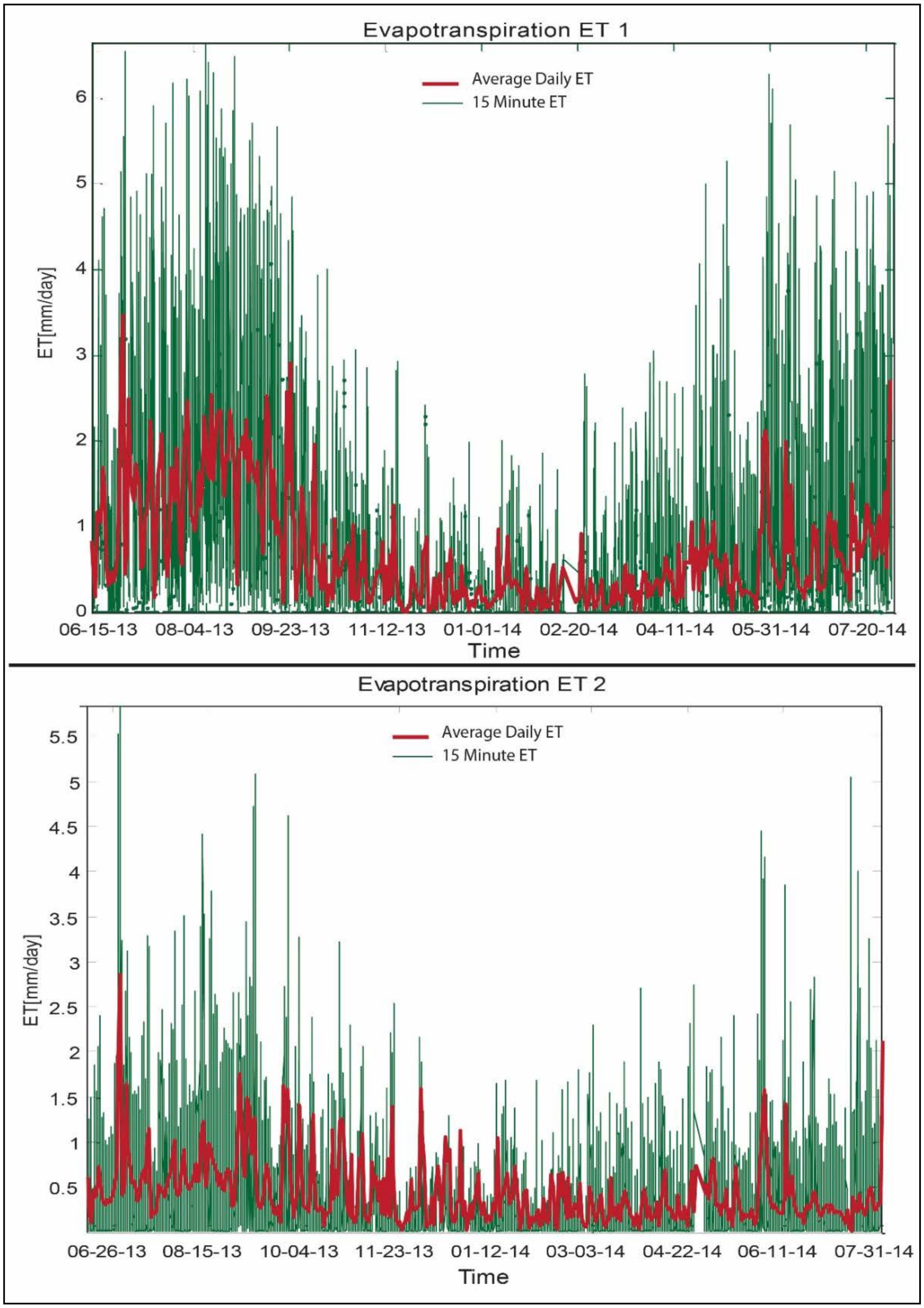

Figure H.1. Comparison of PET values for two different PET stations near the Nueces River , 15 minute in green and daily averaged values in red.

PET and Hydrologic Fluctuations:
The following graphs show the PET values (PET 1) in purple converted to cfs, along with flow averaged over 1 hour in green, 5 hours in red, and 3 hours in blue. These graphs below are examples at NUE010 or CAN012. The graphs were made to compare fluxes in hydrographs to see if PET could account for the cyclic fluxes displayed in the hydrographs.

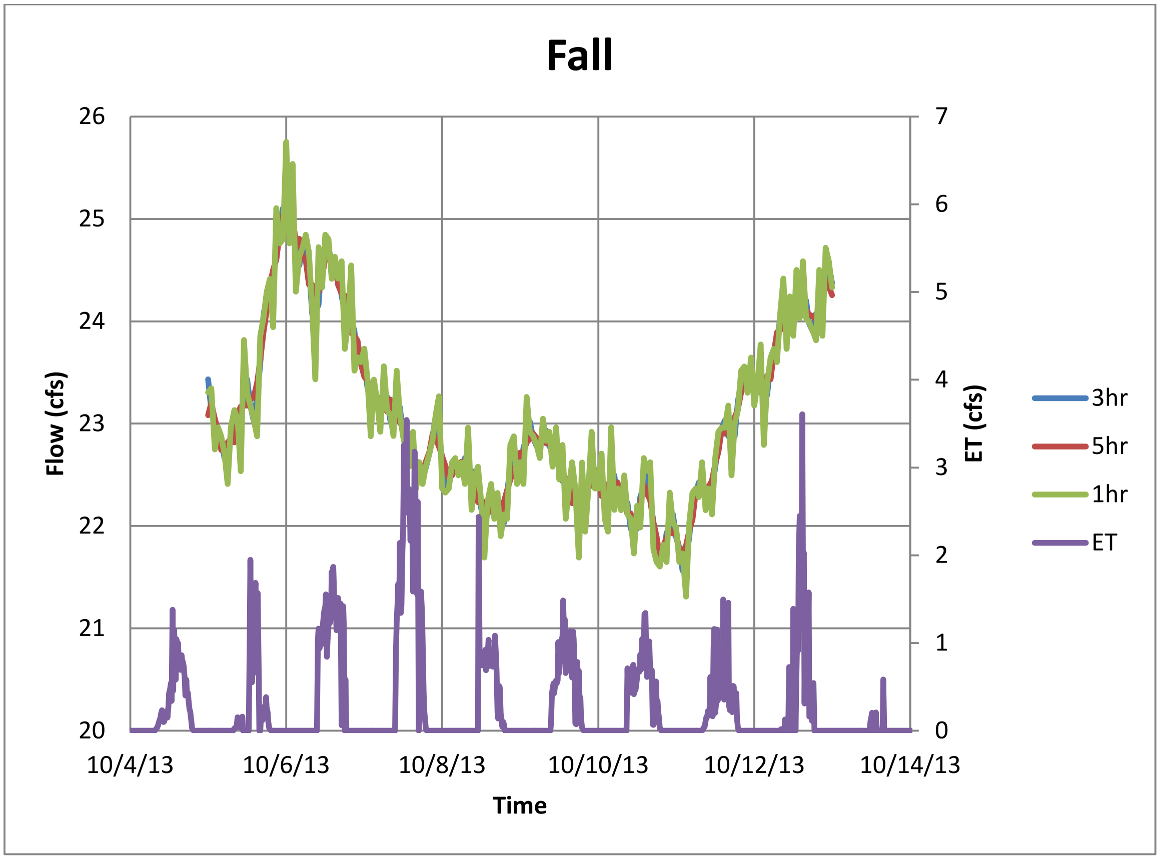

Figure H.2. PET and flow at NUE010 in the fall.

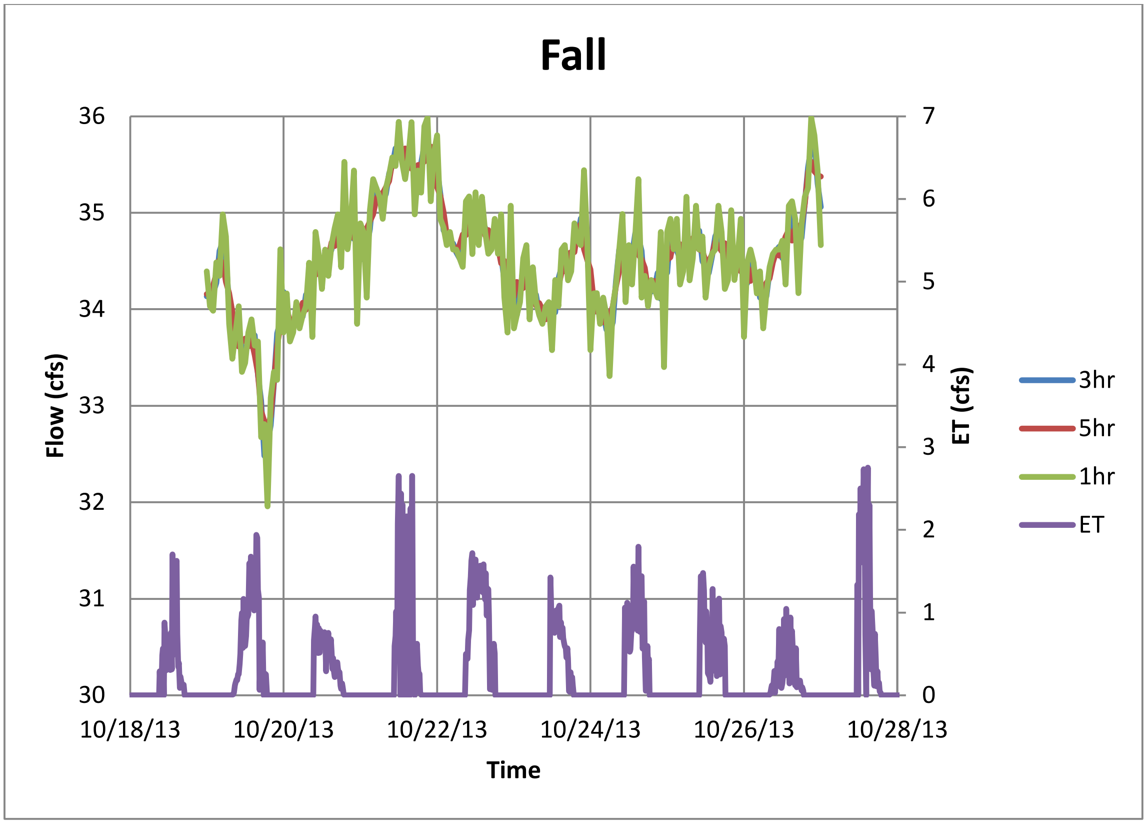

Figure H.3. PET and flow at NUE010 in the late fall.

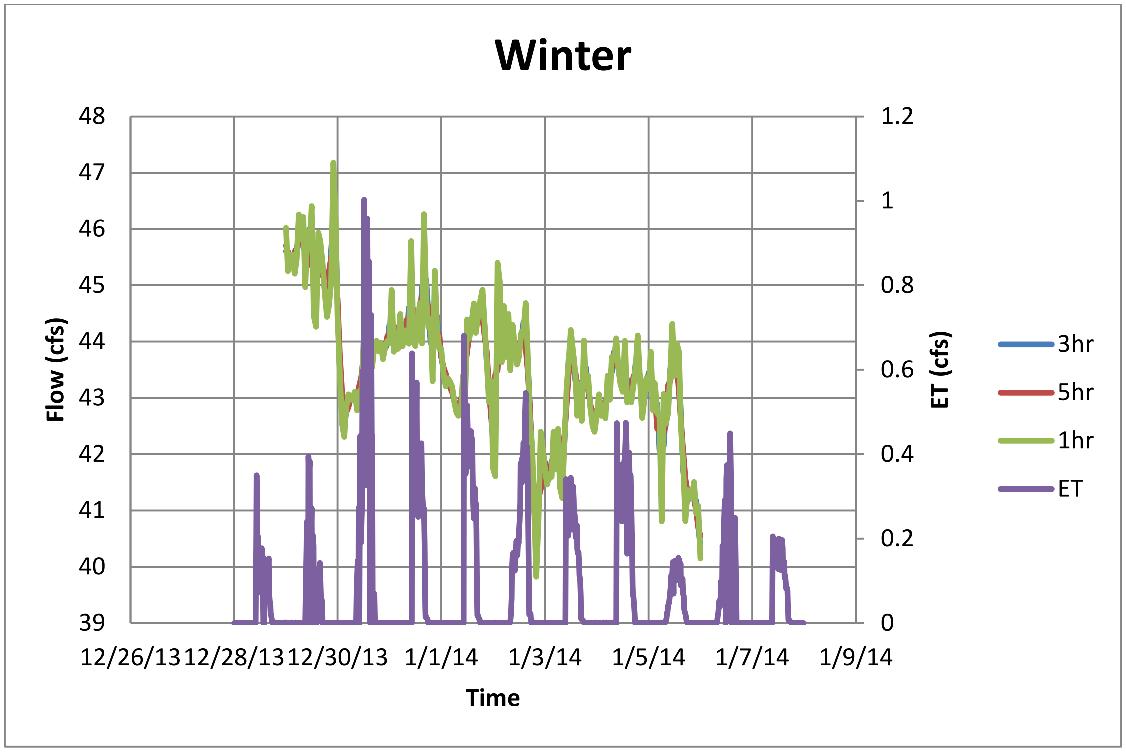

Figure H.4. PET and flow at NUE010 in the winter.

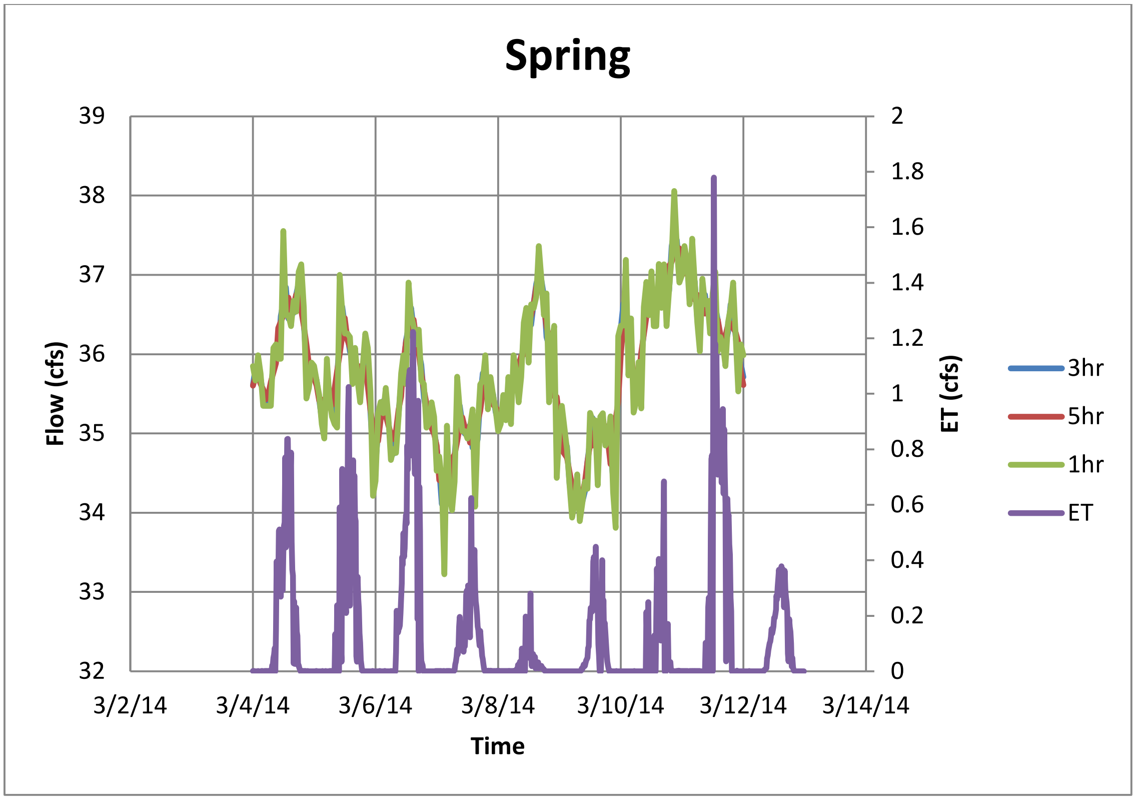

Figure H.5. PET and flow at NUE010 in the spring.

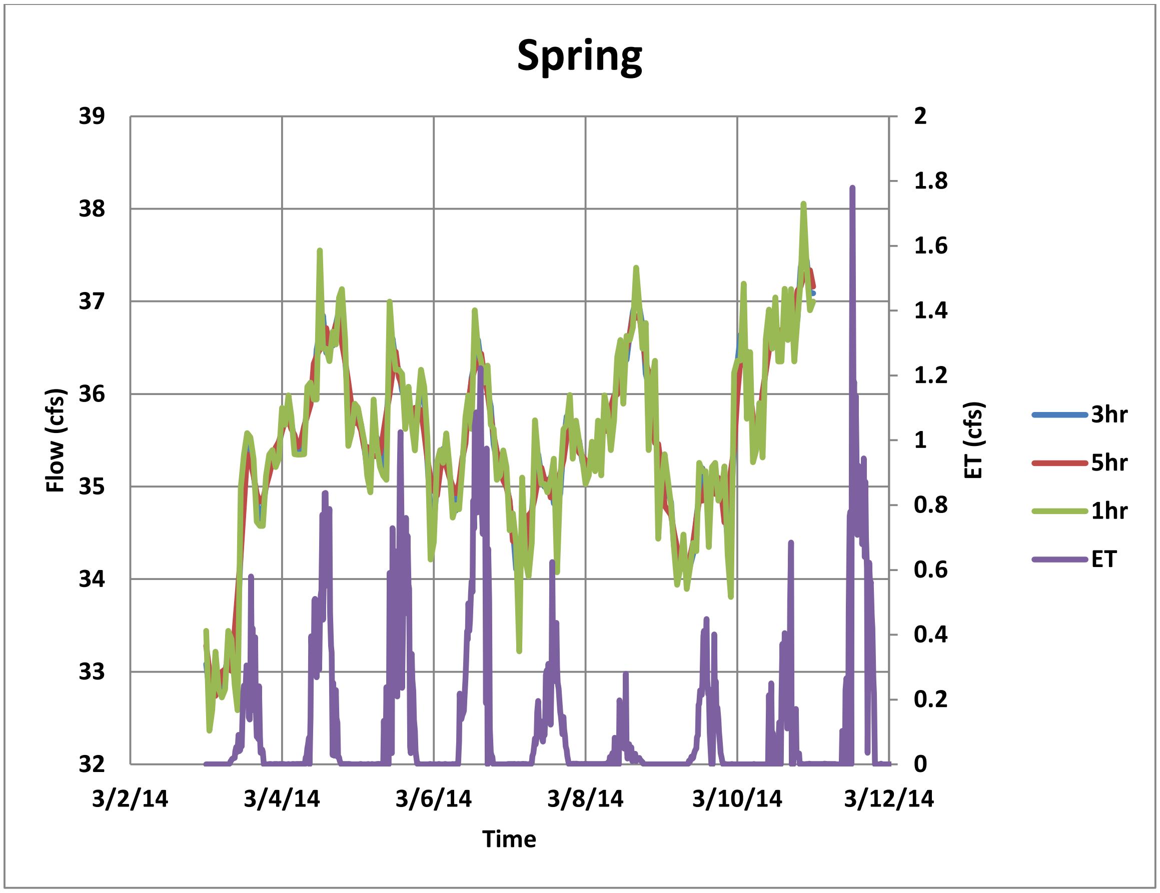

Figure H.6. PET and flow at NUE010 in the spring during a shorter time period.

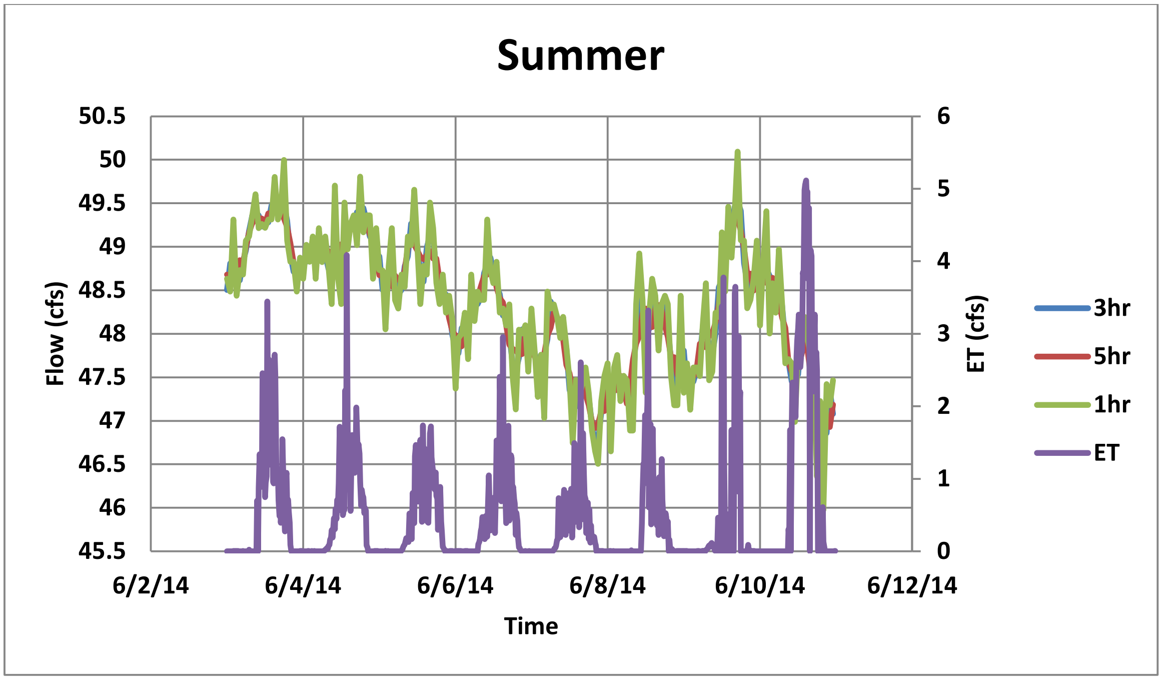

Figure H.7. PET and flow at NUE010 in the summer.

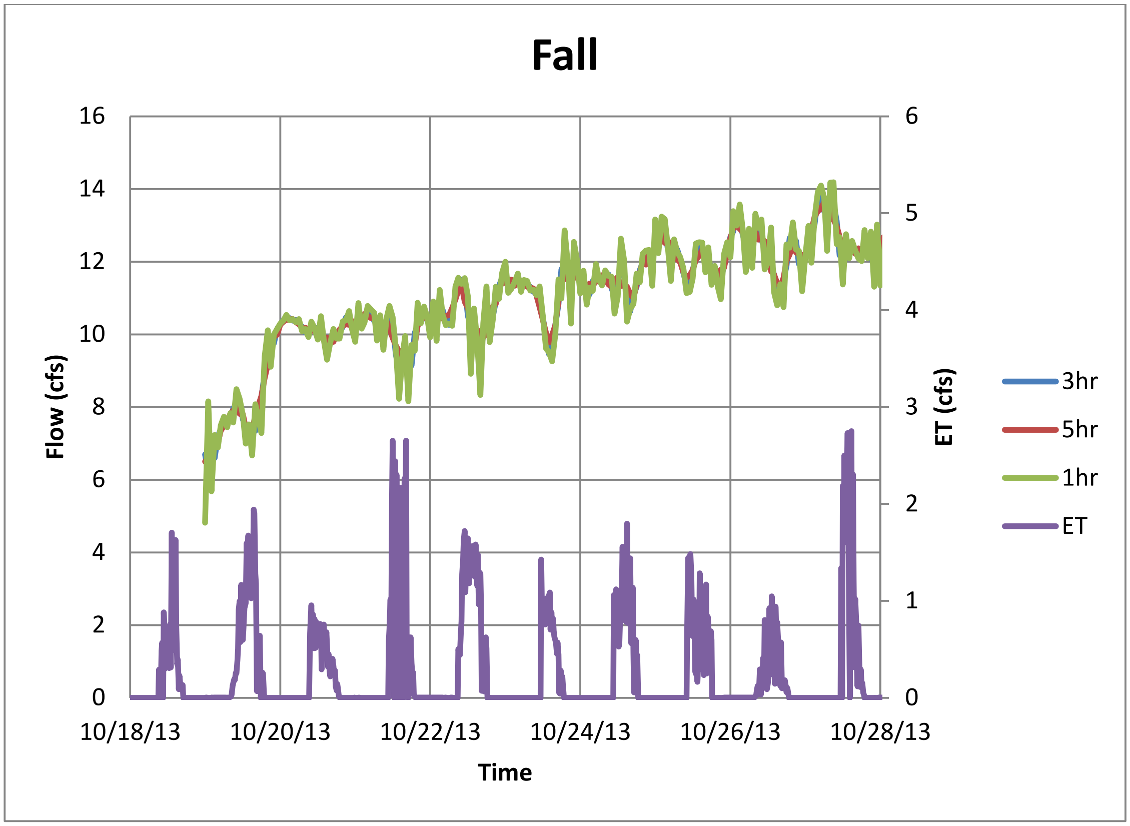

Figure H.8. PET and flow at CAN012 in the late fall.

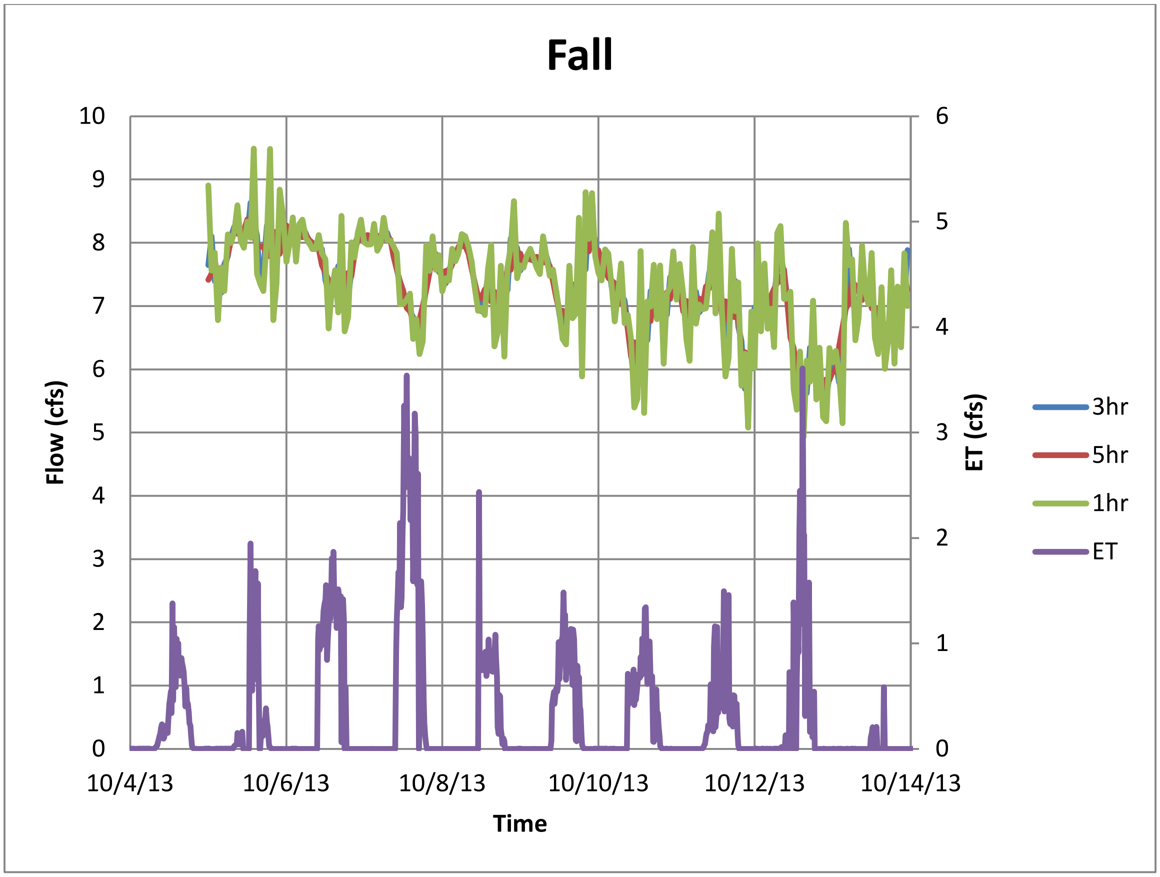

Figure H.9. PET and flow at CAN012 in the early fall.

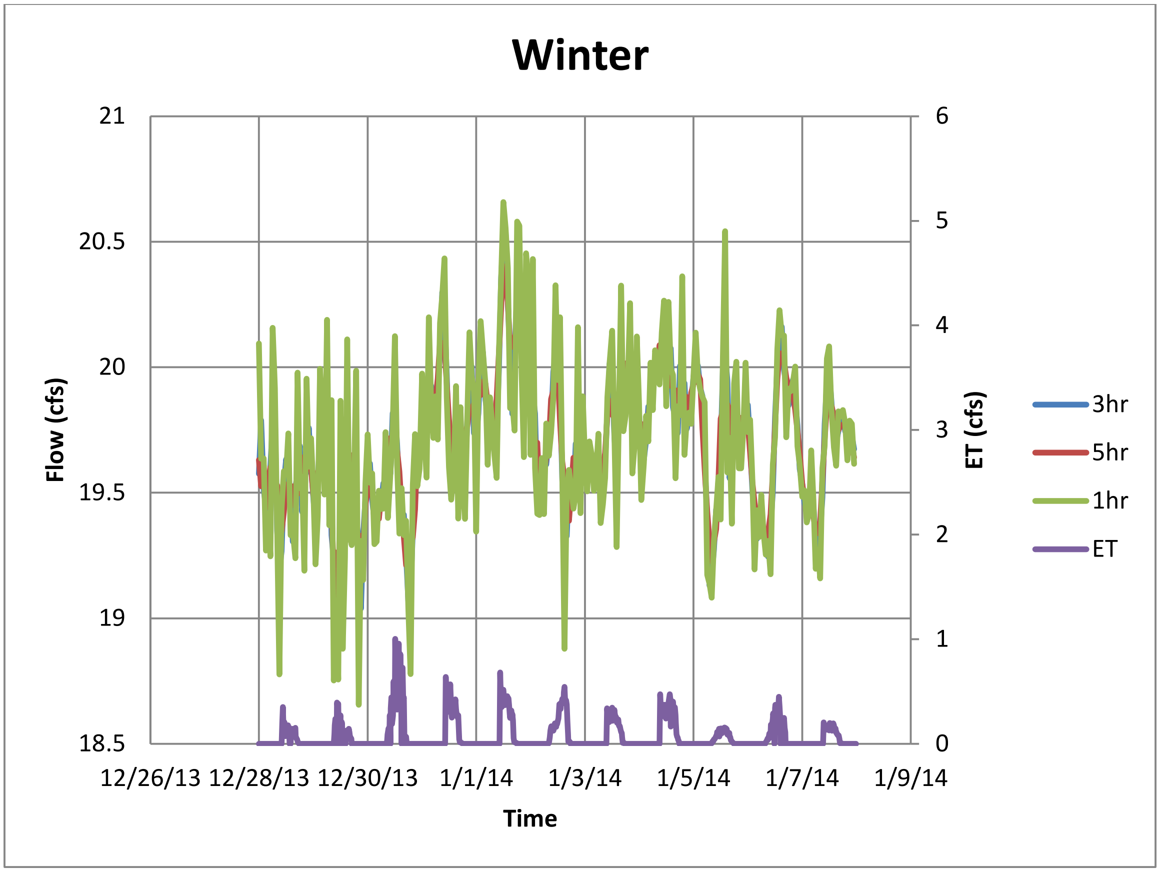

Figure H.10. PET and flow at CAN012 in the winter.

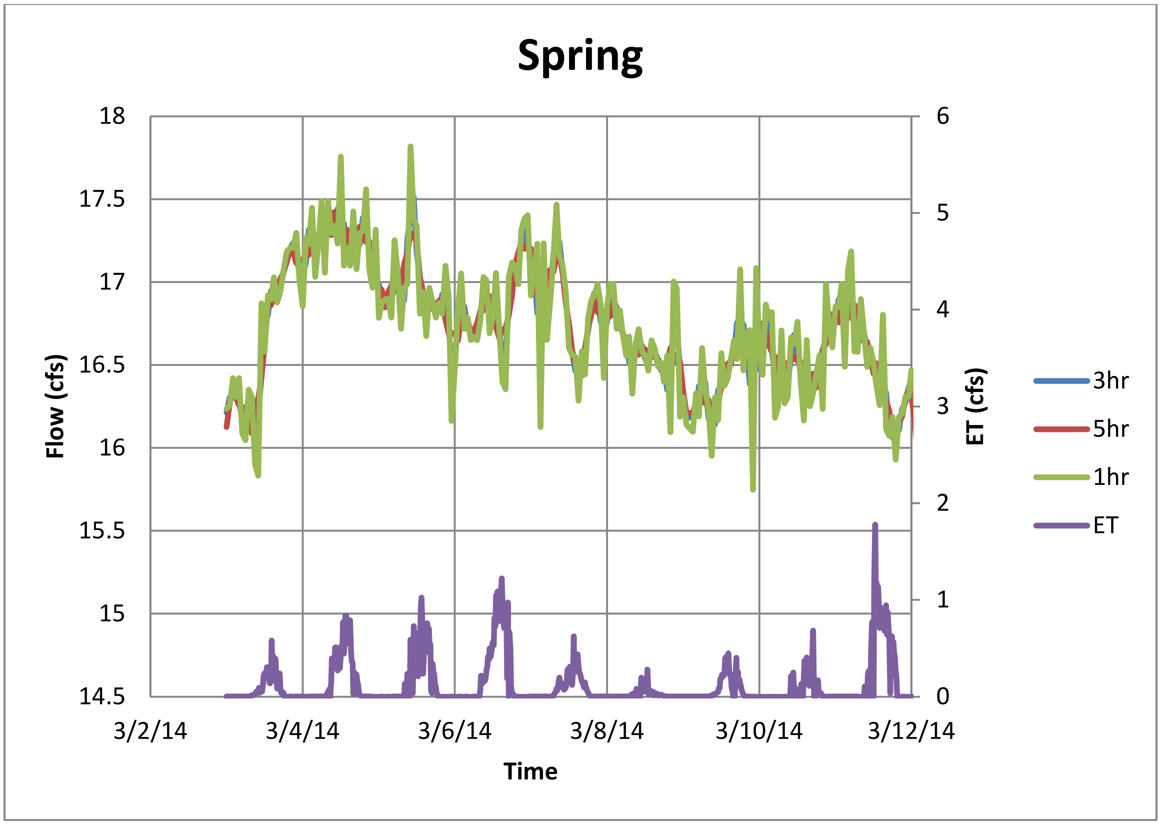

Figure H.11. PET and flow at CAN012 in the spring.

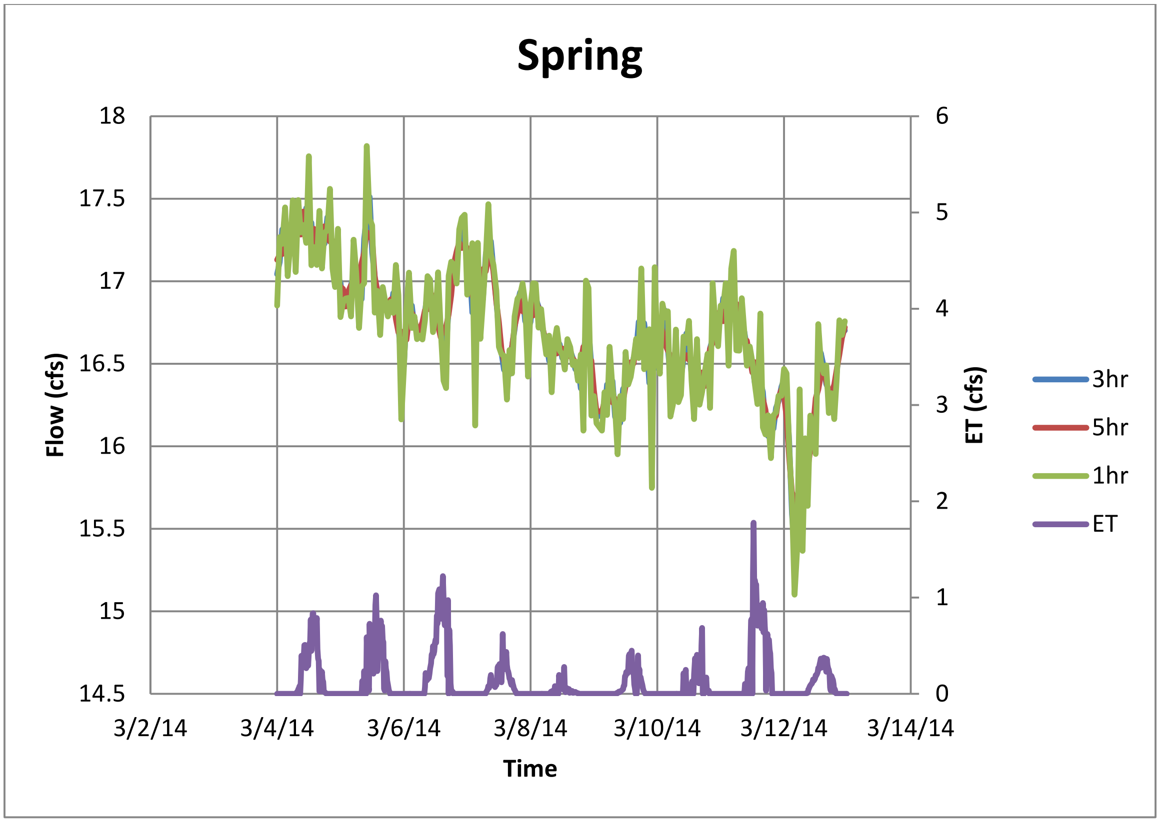

Figure H.12. PET and flow at CAN012 in the spring during a shorter time period.

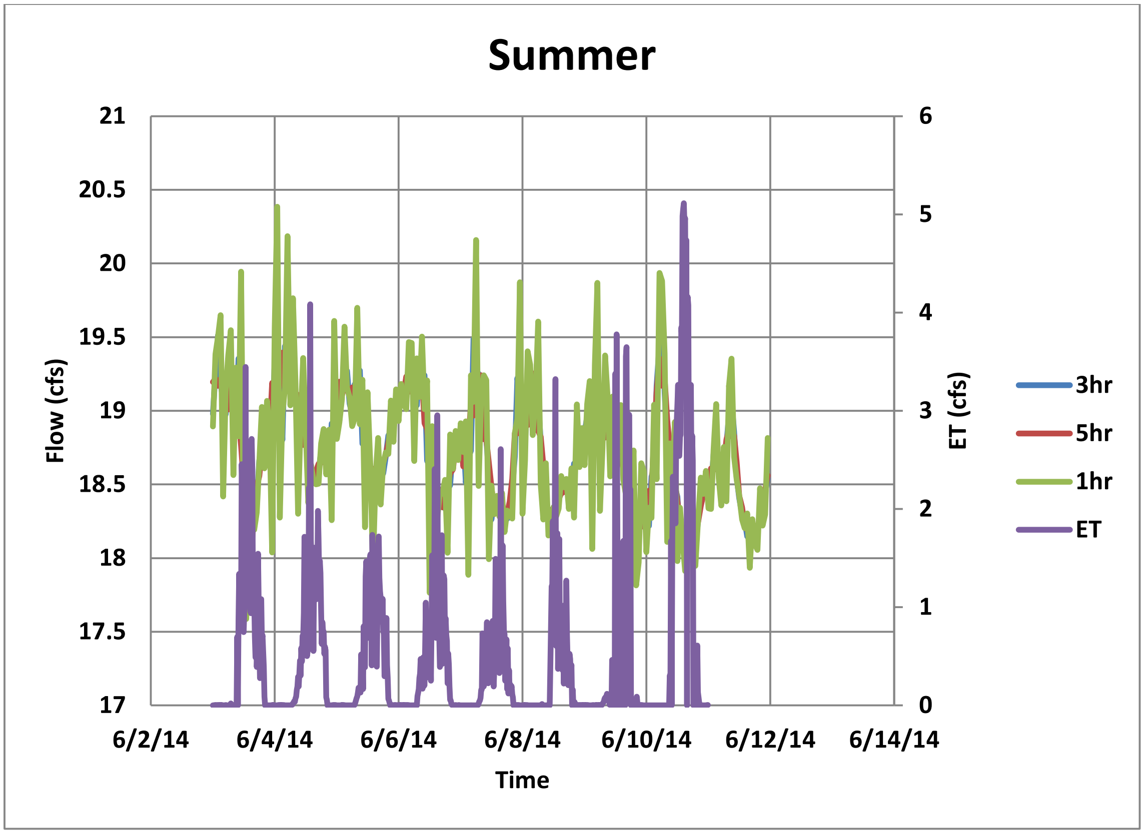

Figure H.13. PET and flow at CAN012 in the summer.

I. WATER CHEMISTRY

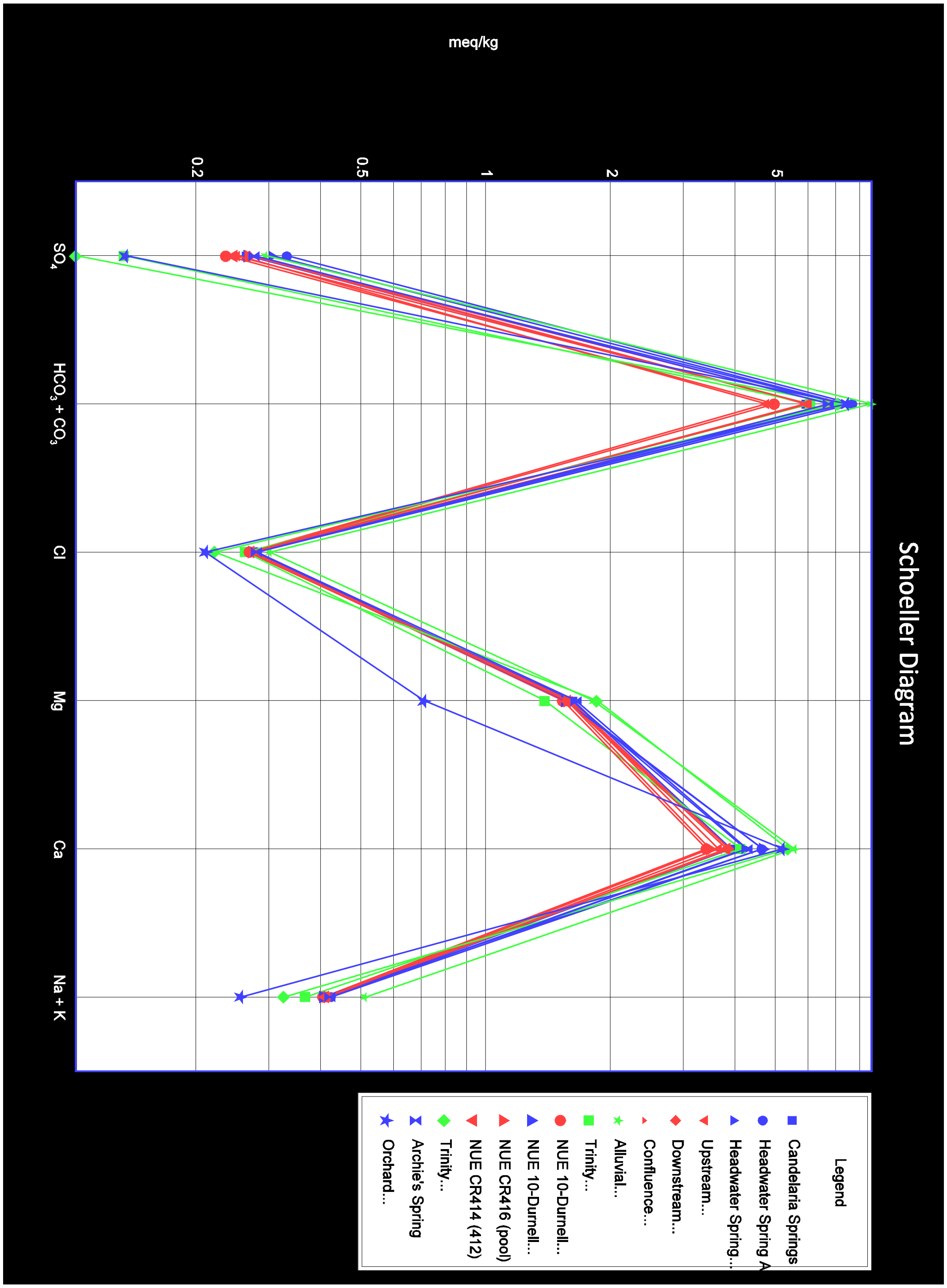

Figure I.1. Schoeller Diagram for general chemistry of samples collected in July 2014. The springs are in blue, the surface water sources are in red, and the groundwater sources are in green. This diagram shows sulfate, magnesium and Na+K vary the most at each site.

J. HYDROGRAPHS

The following hydrographs for NUE010, CAN012, CR414, and Laguna are shown below. The mean daily average was taken in each hydrograph and is displayed below. A peridogram analysis was performed in Matlab to evaluate the daily cyclic fluctuations seen in the hydrographs at each site; the results from each analysis are seen below (frequency and magnitude of the fluctuations).

NUE010

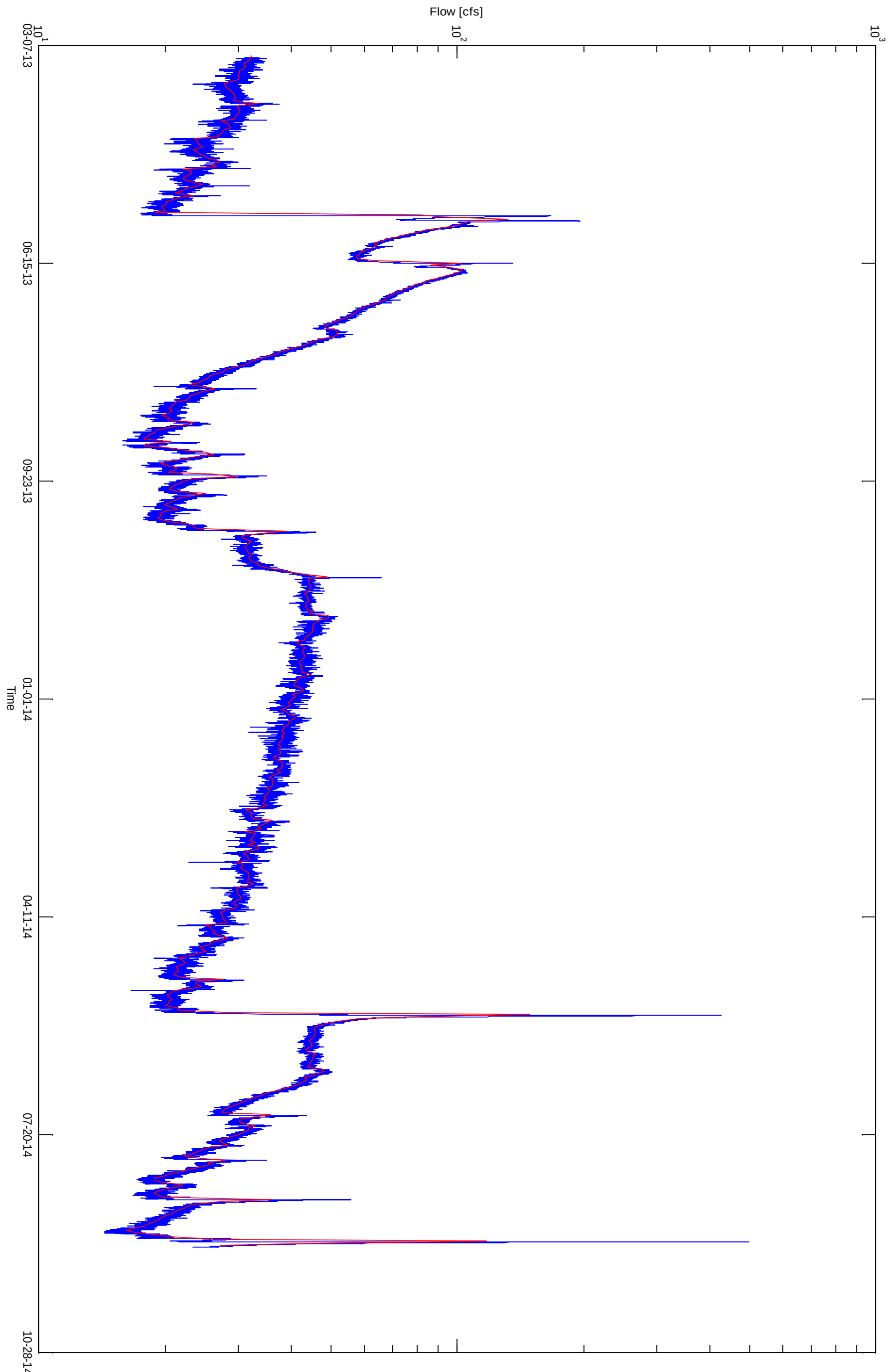

Figure J.1. Flow at NUE010 in blue and daily mean flow values in red.

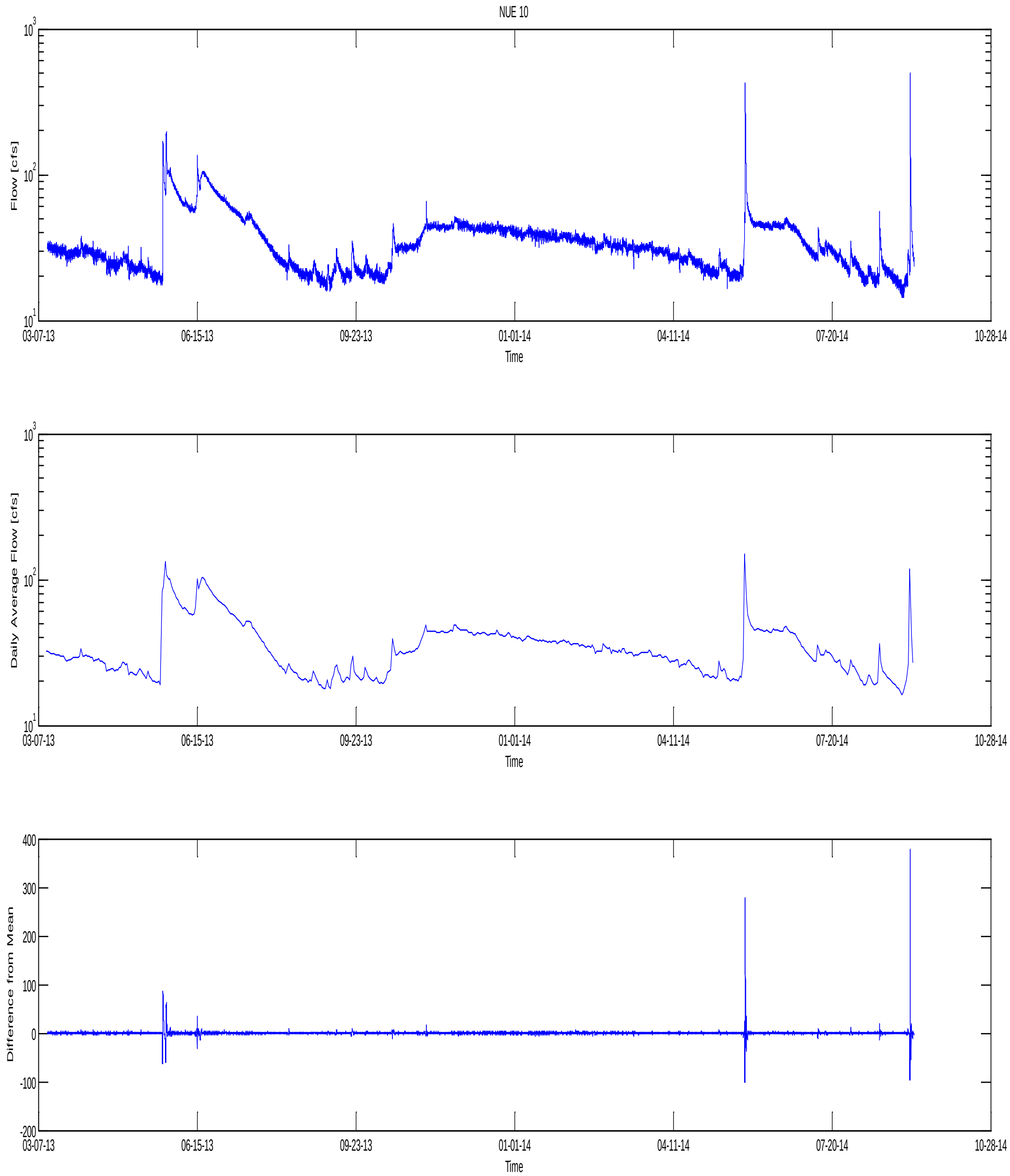

Figure J.2. The top graph shows 15 minute flow data for NUE010, the middle graph shows the daily average flow, and the bottom graph shows the difference from the mean (15 minute flow data subtracted from the daily average flow). These graphs display the amplitude of cyclic fluctuations.

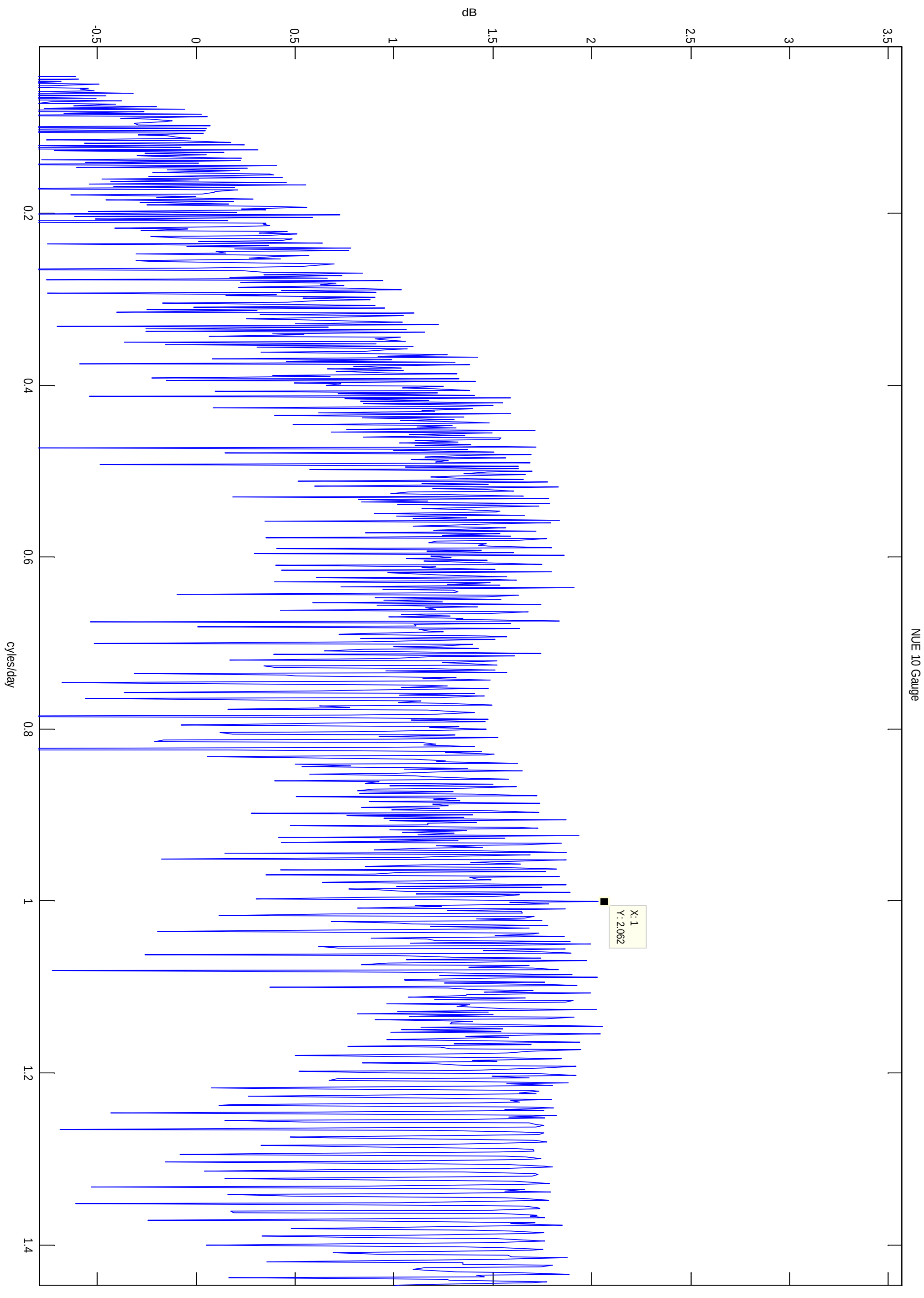

Figure J.3. Peridogram analysis results for NUE010. The peak shows a daily reoccurrence in cyclic fluctuations at NUE010.

CAN012

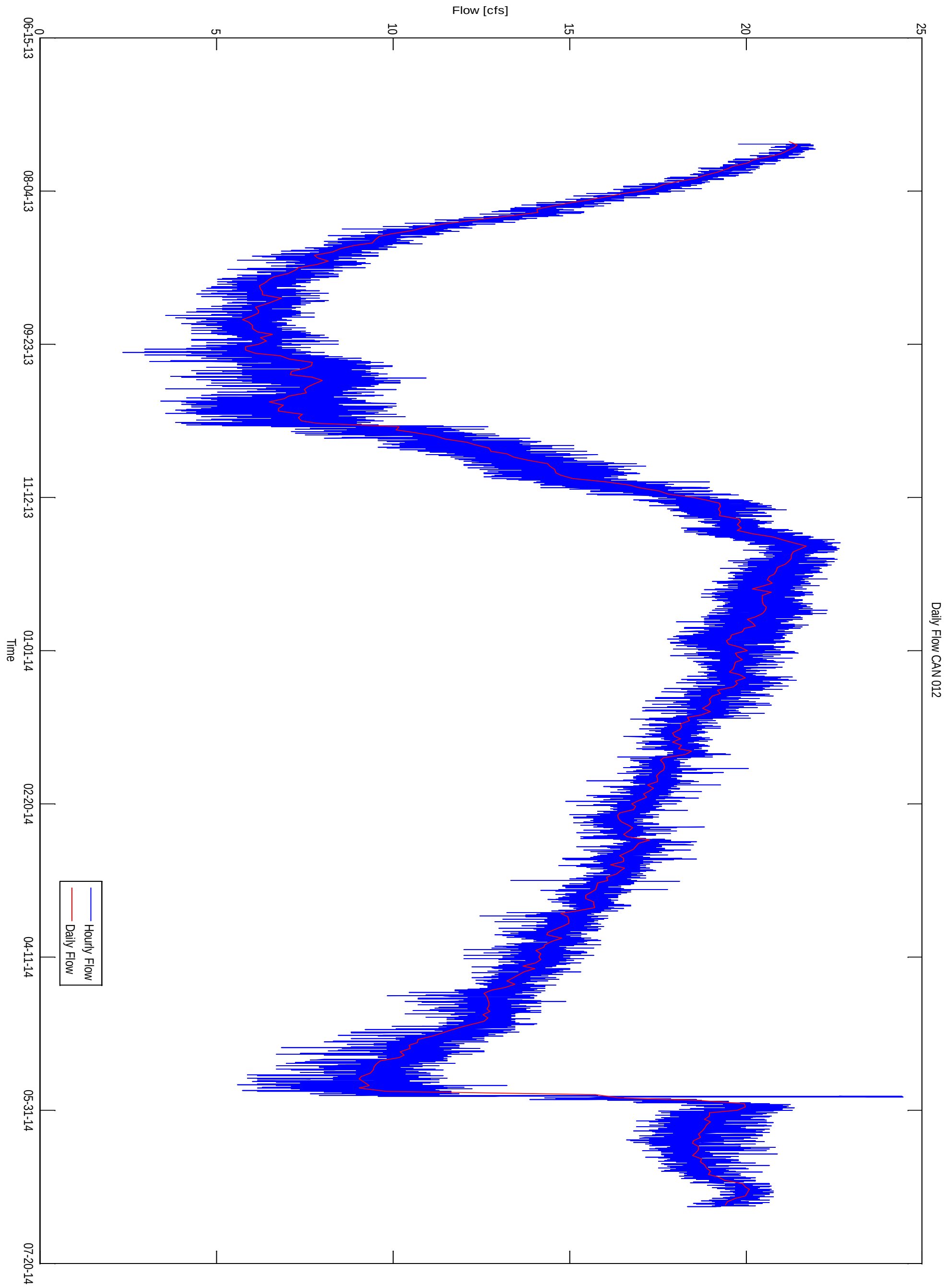

Figure J.4. Flow at CAN012 in blue and daily mean flow values in red.

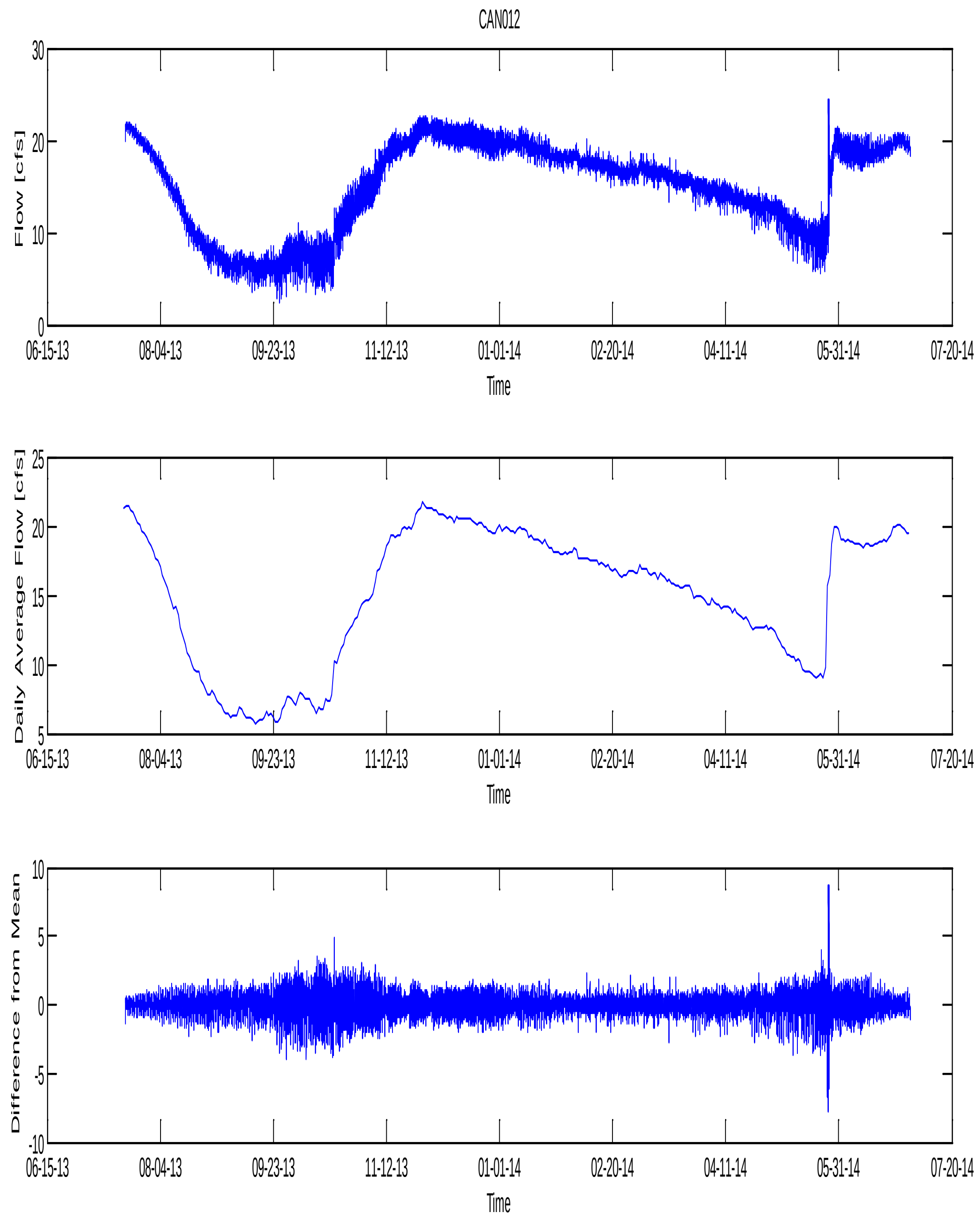

Figure J.5. The top graph shows 15 minute flow data for CAN012, the middle graph shows the daily average flow, and the bottom graph shows the difference from the mean (15 minute flow data subtracted from the daily average flow). These graphs display the amplitude of cyclic fluctuations.

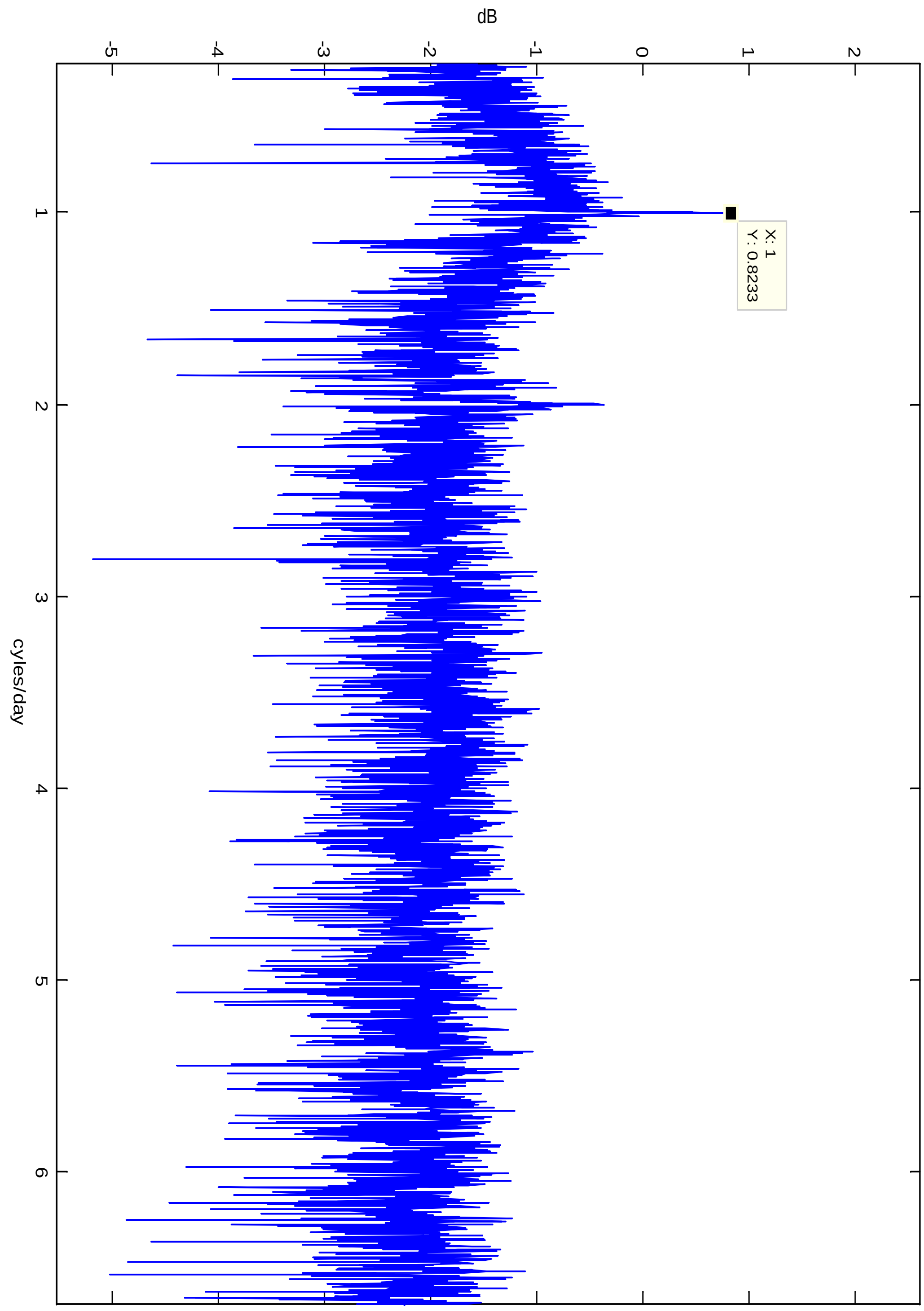

Figure J.6. Peridogram analysis performed for CAN012. This shows daily cyclic fluctuations

LAGUNA

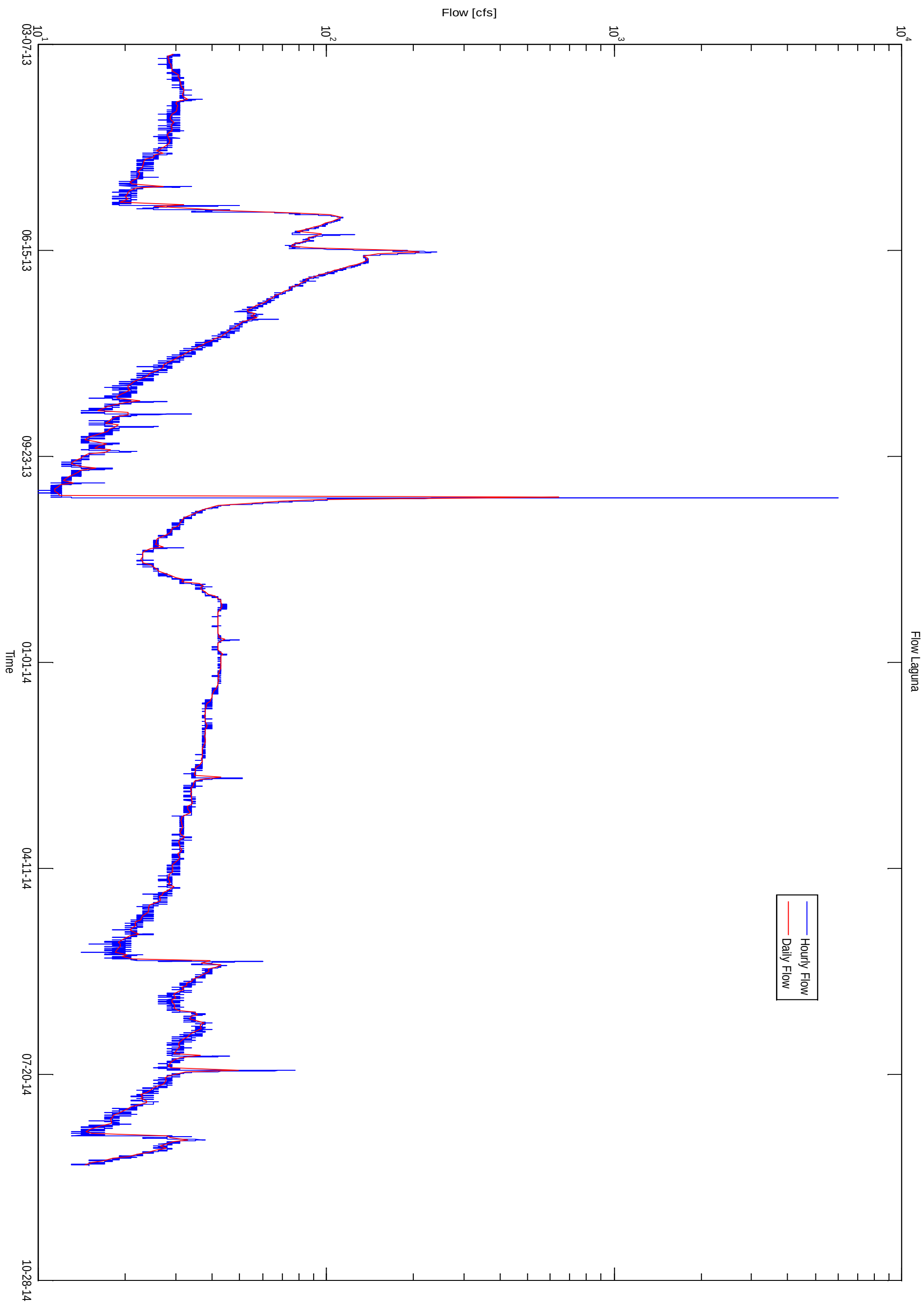

Figure J.7. Flow at Laguna in blue and daily mean flow values in red.

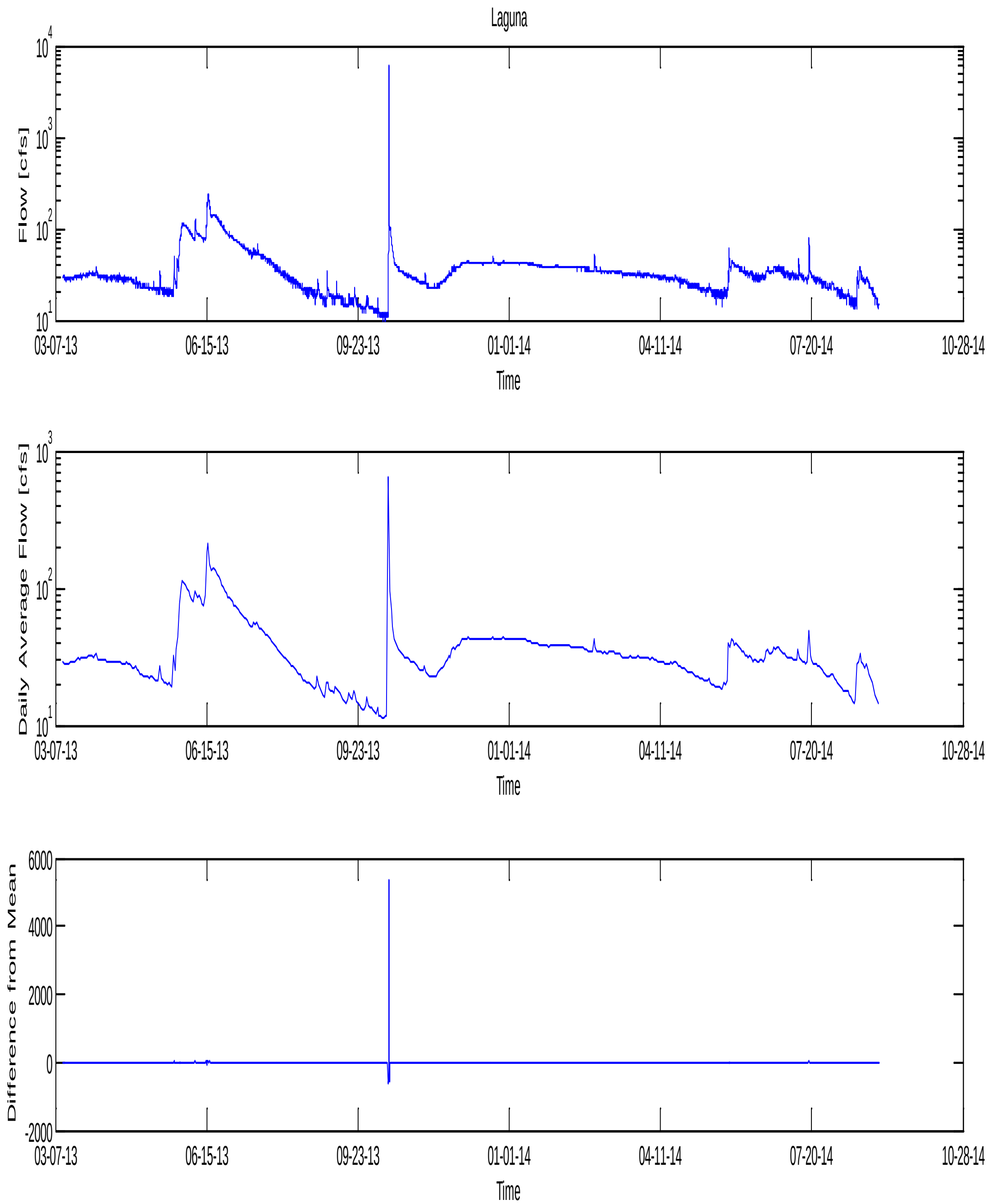

Figure J.8. The top graph shows 15 minute flow data for Laguna, the middle graph shows the daily average flow, and the bottom graph shows the difference from the mean (15 minute flow data subtracted from the daily average flow). These graphs display the amplitude of cyclic fluctuations.

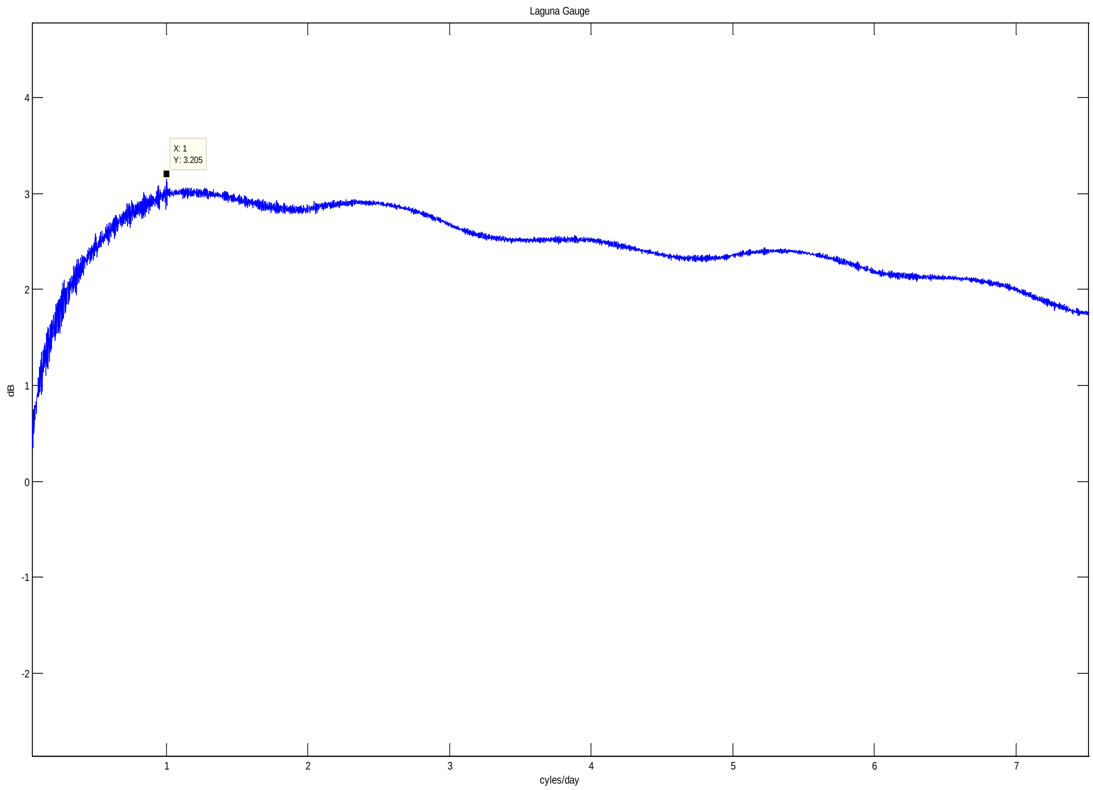

Figure J.9. Peridogram analysis results for Laguna gauge. The peak shows a daily reoccurrence in cyclic fluctuations at Laguna gauge.

CR414

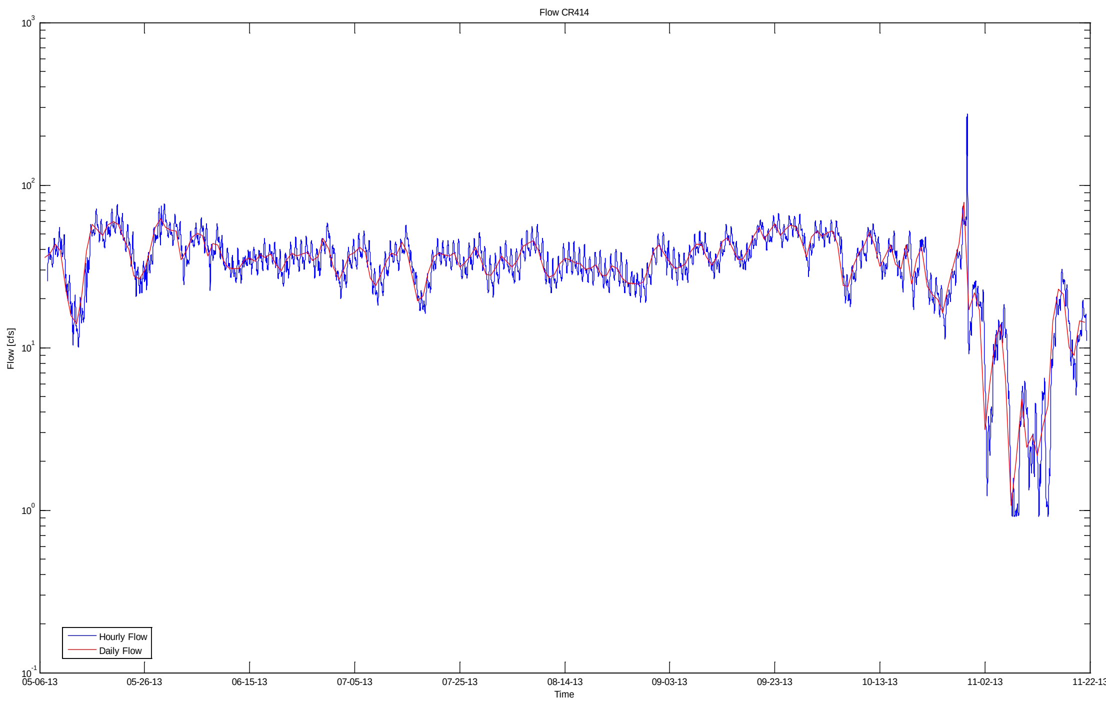

Figure J.10. Flow at CR414 in blue and daily mean flow values in red.

Peridogram analysis was not performed due to lack of data and this gauge typically reads 0 cfs.

REFERENCES

Allen, R., Pereira, L., Raes, D., and Smith, M., 1998, Chapter 2 - FAO Penman-Monteith equation: http://www.fao.org/docrep/x0490e/x0490e06.htm.

Banta, J.R., Lambert, R.B., Slattery, R.N., and Ockerman, D.J., 2012, Streamflow gain and loss and water quality in the upper Nueces River Basin, south-central Texas, 2008–10: U.S. Geological Survey Scientific Investigations Report 2012–5181, 40 p., http://pubs.usgs.gov/sir/2012/5181.

Barker, R. A., and Ardis, A. F., and Geological Survey (U.S.), 1994, Geologic history and hydrogeologic setting of the Edwards-Trinity aquifer system, west-central Texas: Austin, Tex. : Denver, CO, U.S. Dept. of the Interior, U.S. Geological Survey ; Earth Science Information Center, Open-File Reports Section iv, 51 p.

Barton Springs Edwards Aquifer Conservation District (BSEACD), 2011-2012, Scientific Reports: http://www.bseacd.org/publications/reports.

Burkholder, B. K., Grant, G. E., Haggerty, R., Khangaonkar, T., and Wampler, P. J., 2008, Influence of hyporheic flow and geomorphology on temperature of a large, gravel-bed river, Clackamas River, Oregon, USA: Hydrological Processes, v. 22, p. 941–953, doi: 10.1002/hyp.6984.

Cardenas, M. B., and M. N. Gooseff, 2008, Comparison of hyporheic exchange under covered and uncovered channels based on linked surface and groundwater flow simulations: Water Resour. Res., 44, W03418, doi:10.1029/2007WR006506.

Cardenas, M. B. Cardenas, M.B., 2009, Stream-aquifer interactions and hyporheic exchange in gaining and losing sinuous streams: Water Resources Research, v. 45, doi: 10.1029/2008WR007651.

Cardenas, M.B., Lagmay, A. M. F., Andrews, B. J., Rodolfo, R. S., Cabria, H. B., Zamora, P. B., and Lapus, M. R., 2012, Terrestrial smokers: Thermal springs due to hydrothermal convection of groundwater connected to surface water: Geophysical Research Letters, v. 39, p. n/a–n/a, doi: 10.1029/2011GL050475.

Christian, L. N., Banner, J. L., Mack, L. E., 2011, Sr isotopes as tracers of anthropogenic influences on stream water in the Austin, Texas, area: Chemical Geology 282, 84-97.

Clark, A.K., Edwards Aquifer Authority (Tex.), and Geological Survey (U.S.), 2003, Geologic framework and hydrogeologic characteristics of the Edwards Aquifer, Uvalde County, Texas: U.S. Dept. of the Interior, U.S. Geological Survey ; U.S. Geological Survey Information Services, Austin, Tex. : Denver, CO.

Diebel, J., and Norda, J., 2014, WeatherSpark: https://weatherspark.com/averages/31871/Uvalde-Texas-United-States.

Edwards Aquifer Authority, 2007, Hydrologic Data Report: Edwards Aquifer Authority, p. 94.

Edwards Aquifer Authority, 2013, Hydrologic Data Report: Edwards Aquifer Authority, p. 22, http://www.edwardsaquifer.org/documents/2014_Tramallo-etal_2013HydrologicData.pdf.

Edwards Aquifer Authority, 2014, Hydrologic Data Report: Edwards Aquifer Authority, http://www.edwardsaquifer.org (unpublished currently)

Edwards Aquifer Authority, 2015a, About the EAHCP, http://eahcp.org/index.php/about_eahcp.

Edwards Aquifer Authority, 2015b, Weather Stations, http://www.edwardsaquifer.org/aquifer-data-and-maps/weather-stations

EPA, 2003, Ecoregions of Texas: ftp://ftp.epa.gov/wed/ecoregions/tx/tx_front.pdf.

FAO, 2014, Ch. 2 FAO Penman-Monteith equation: http://www.fao.org/docrep/x0490e/x0490e06.htm.

Ford, D.C., and Williams, P., 2007, Karst Hydrogeology and Geomorphology: Wiley, Chicester, p. 40.

Freeze, R.A. and Cherry, J. A., 1979, Groundwater: Englewood Cliffs, N.J, Prentice-Hall, 604 p.

Gary, M. and Kromann, J., 2013, Evaluation of Riparian Water Flux Patterns in the Upper Nueces, Sabinal, Frio, and Dry Frio Rivers, Texas in Relation to the Control of Arundo Donax: EAA, p. 1-28.

Gary, M., Gary, R., and Hunt, B., 2011 Interconnection of the Trinity (Glen Rose) and Edwards Aquifers along the Balcones Fault Zone and Related Topics, Karst Conservation Initiative Meeting: http://www.bseacd.org/uploads/AquiferScience/Proceedings_Edwards_Trinity_final.pdf.

Goodrich, D.C., Scott, R., Qi, J., Goff, B., Unkrich, C.L., Moran, M.S., Williams D., Schaeffer, S.,Snyder, K., Mac Nish, R., Maddock III, T., Pool,D., Chehbouni, A., Cooper, D.I., Eichinger, W.E., Shuttleworth, W.J., Kerr, Y., Marsett, R., Ni, W, 2000, Seasonal estimates of riparian evapotranspiration using remote and in situ measurements: J. Ag. and For. Meteorol,. 105(1-3):281-309.

Green, P., Bertetti, P., and McGinnis, R., 2009, Investigating the Secondary Aquifers of the Uvalde County Underground Water Conservation District Final Report: Geosciences and Engineering Division Southwest Research Institute, p. 1-74.

Green, T. R., Winterle, R. J., and Prikryl, D. J., 2008, Discharge From the Edwards Aquifer through the Leona River Floodplain, Uvalde, Texas: JAWRA, V. 44, No.4, p. 887-901.

Han, G. L., and Liu, C. Q., 2004, Water geochemistry controlled by carbonate dissolution: a study of the river waters draining karst-dominated terrain, Guizhou Province, China: Chemical Geology, v. 204, p. 1-21.

Hauwert, N.,M., and Sharp, J., M., 2014, Measuring Autogenic Recharge over a Karst Aquifer Utilizing Eddy Covariance Evapotranspiration: Journal of Water Resource and Protection, 6, p. 869-879.

Johnson, S., Schindel, G., and Veni, G., 2010, Tracing Groundwater Flowpaths in the Edwards Aquifer Recharge Zone, Panther Springs Creek Basin, Northern Bexar County, Texas: Edwards Aquifer Authority, http://www.edwardsaquifer.org/documents/2010_Johnsonetal_PantherSpringsCreekBasinFlowpaths.pdf.

Jones, I., R. Anaya, and S. Wade. 2011. Groundwater availability model: Hill Country portion of the Trinity aquifer of Texas: Texas Water Development Board, Report 377,160. http://www.twdb.state.tx.us/publications/reports/numbered_reports/doc/R377_HillCountryGAM.pdf.

Jordan, M. A., 1977, Ch. 3: The Balcones Fault Zone of Austin: http://www.lib.utexas.edu/geo/ggtc/toc.html.

Kanduč, T., Grassa F., McIntosh, J., Stibilj, V., Ulrich-Supovec, M., Supovec, I., Jamnikar, S., 2014, A geochemical and stable isotope investigation of groundwater/surface-water interactions in the Velenje Basin, Slovenia: Hydrogeology Journal, DOI 10.1007/s10040-014-1103-7.

Katz, B. G., Coplen, T. B., Bullen, T. D. and Davis, J. H., 1997, Use of Chemical and Isotopic Tracers to Characterize the Interactions between Ground Water and Surface Water in Mantled Karst: Groundwater, 35: 1014–1028. doi: 10.1111/j.1745-6584.1997.tb00174.x.

Katz, B. G., 1998, Using δ 18O and δ D to Quantify Ground-Water/ Surface-Water Interactions in Karst Systems of Florida, USGS: AWCI Monitoring Papers. http://acwi.gov/monitoring/nwqmc.org/98proceedings/Papers/19-KATZ.html.

Koepnick, R. B., Denison, R. E., Burke, W. H., Hetherington, E. A., Nelson, H. F.,Otto, J. B., and Waite, L. E., 1985, Construction of the seawater 87/86Sr curve for the Cenozoic and Cretaceous: Supporting data: Chemical Geology, v. 58, p. 55-81.

Larocque, M., Mangin, A., Razack, M., Banton, O.,1998, Contribution of correlation and spectral analysis to the regional study of a large karst aquifer (Charente, France): Journal of Hydrology, 205, pp. 217–231

Lewelling, B.R., Tihansky, A. B., and Kindinger, J. L., 1998, Assessment of the Hydraulic Connection Between Groundwater and the Peace River, West-Central Florida: USGS, Report 97-4211, p.1-102

McClay, R.W., and Small, T.A., 1976, Progress report on geology of the Edwards aquifer, San Antonio area, Texas, and preliminary interpretation of borehole geophysical and laboratory data on carbonate rocks: U.S. Geological Survey Open-File Report 76–627, 65 p.

Moore, G.W. and Owens, M.K., 2012, Transpirational water loss in invaded and restored riparian forests of the Rio Grande: Restoration Ecology, 20(3): 346–351.

Moore, G. W., Jones, J. A., and Bond, B. J., 2011, The role of transpiration in predicting stream flow at hourly to interannual scales in a forested catchment: Hydrological Processes. DOI: 10.1002/hyp.8095.

Moore G.W. and M.K. Owens, 2011, Transpirational water loss in invaded and restored riparian forests of the Rio Grande: Restoration Ecology, DOI: 10.1111/j.1526-100X.2011.00774.

Monteith, J. L, 1981, Evaporation and surface temperature: Meteorolgical. Society, 107: 1-27.

Musgrove, M., Fahlquist, L., Houston, N., Lindgren, R., and Ging, P., 2010, Geochemical Evolution Processes and Water Quality Observations Based on Results of the National Water Quality Assessment Program in the San Antonio Segment of the Edwards Aquifer, Texas, 1996-2006: USGS, Scientific Investigations Report 2010–5129.

Musgrove, M. and Banner, J. L., 2004, Controls on the spatial and temporal variability of vadose dripwater geochemistry: Edwards Aquifer, central Texas: Geochimica et Cosmochimica Acta 68, 1007-1020.

Oetting, G. C., Banner, J. L., and Sharp, J. M. Jr., 1996, Regional controls on the geochemical evolution of saline groundwaters in the Edwards aquifer, central Texas: Journal of Hydrology 181, 251-283.

Ozyurt, N.N., Lutz , H.O., Hunjak, T., Mance, D., Roller-Lutz, Z., 2014, Characterization of the Gacka River basin karst aquifer (Croatia): Hydrochemistry, stable isotopes and tritium-based mean residence times, Science of The Total Environment 487, 245-254.

Pape, J. R., Banner, J. L., Lawrence, E. M., Musgrove, M., Guifoyle, A., 2010, Controls on oxygen isotope variability in precipitation and cave drip waters, central Texas, USA: Journal of Hydrology, v. 385, p. 203-215.

Penman, H. L., 1948, Natural evaporation from open water, bare soil and grass: Proc. Roy. Soc. London, A193, 120-146.

Price, R. M., and Swart, P. K., 2006, Geochemical indicators of groundwater recharge in the surficial aquifer system, Everglades National Park, Florida, USA: Perspectives on Karst Geomorphology, Hydrology, and Geochemistry, v.404, p. 251-256

Puente, C., 1978, Method of estimating natural recharge to the Edwards Aquifer in the San Antonio area, Texas: U.S. Geological Survey Water-Resources Investigations Report,78-10.

Rose, P.R., 1972, Edwards Group, surface and subsurface, central Texas: Austin, University of Texas, Bureau of Economic Geology Report of Investigations 74, 198 p.

Slade, R., Bentley, T., and Michaud, D., 2002, Results of streamflow gain-loss studies in Texas, with emphasis on gains from and losses to major and minor aquifers: U.S. Geological Survey Open-File Report 02–068, 131 p.

Sumanovac, F., and Weisser, M., 2001, Evaluation of resistivity and seismic methods for hydrogeological mapping in karst terrains: Journal of Applied Geophysics, v. 47, p. 13–28.

Texas Water Development Board (TWDB), 2011b, Desired future conditions for the Blossom, Brazos River Alluvium, Edwards (Balcones Fault Zone), Ellenburger-San Saba, Hickory, Marble Falls, Nacatoch, Trinity, and Woodbine aquifers: TWDB, http://www.twdb.texas.gov/groundwater/docs/DFC/GMA8_DFC_Adopted_2011-0427.pdf.

Texas Water Development Board (TWDB), 2012, 2012 Water for Texas: Texas Water Development Board, p.1-314.

Texas Water Development Board (TWDB), 2013, Precipitation & Lake Evaporation (Quadrangle Number 808): TWDB, http://www.twdb.texas.gov/surfacewater/conditions/evaporation.

Texas Water Development Board (TWDB), 2015a, Trinity Aquifer: http://www.twdb.texas.gov/groundwater/aquifer/majors/trinity.asp

Texas Water Development Board, 2015b, Geologic Atlas of Texas (GAT): http://www.twdb.texas.gov/groundwater/aquifer/GAT/

Texas A&M AgriLife Extension, 2013, Average Montly ETo (PET): http://texaset.tamu.edu/pet.php

TNRIS, 2014, Geologic Atlas of Texas (GAT): http://www.tnris.org/get-data#geology

USGS, 2014, Hydrological Simulation Program—Fortran: http://water.usgs.gov/software/HSPF.

Wilcox, B.P., and Huang, Yun, 2010, Woody plant encroachment paradox: Rivers rebound as degraded grasslands convert to woodlands: Geophysical Research Letters. 37:1-5.

Wong, C.I., Kromann, J.S., Hunt, B.B., Smith, B.A., and Banner, J.L., 2013, Investigating Groundwater Flow Between Edwards and Trinity Aquifers, Central Texas: Groundwater, Vol. 52, No. 4, pg. 624-639, DOI: 10.1111/gwat.12106.

Wong, C., Mahler, B. J., Musgrove, M., and Banner, J. L., 2012, Changes in sources and storage in a karst aquifer during a transition from drought to wet conditions: Journal of Hydrology.

Zhou, W., Beck, B.F., and Stephenson, J.B., 2000, Reliability of dipole-dipole electrical resistivity tomography for defining depth to bedrock in covered karst terranes: Environmental Geology, v. 39.